

**DEPOSITIONAL ENVIRONMENT AND TECTONIC  
PROVENANCE OF PALAEOGENE SEDIMENTS IN AND  
AROUND BOTSA, KOHIMA DISTRICT, NAGALAND**



Aienla Ozukum

Submitted  
In partial fulfillment of the requirement of the Degree  
of Doctor of Philosophy in Geology  
Nagaland University  
2022

# **NAGALAND UNIVERSITY**

November 2022

## **DECLARATION**

I, Aienla Ozukum, hereby declare that the subject matter of this thesis is the record of work done by me, during the period May 2014 to May 2022. That the content of this thesis has not provided the basis for the award of any previous degree to me, or to the best of my knowledge, to anybody else, and that the thesis has not been submitted by me for any research degree in any other University/Institute.

This thesis is submitted to the Nagaland University in partial fulfilment for the degree of Doctorate in Philosophy in Geology under the supervision of Dr. S.K. Srivastava of Nagaland University.

Date:

Place: Department of Geology  
Nagaland University  
Kohima Campus, Meriema

AIENLA OZUKUM

Ph.D. Scholar

Department of Geology  
Reg. No. 564/2014 (20<sup>th</sup> May, 2014)

Head

Prof. S. K. Singh  
Department of Geology  
Nagaland University  
Kohima Campus, Meriema

Supervisor

Dr. S.K. Srivastava  
Department of Geology  
Nagaland University  
Kohima Campus, Meriema

# NAGALAND



# UNIVERSITY

Dr. S.K. Srivastava  
Associate Professor  
Department of Geology

Email: [sksrivastava@nagalanduniversity.ac.in](mailto:sksrivastava@nagalanduniversity.ac.in)  
[sanjaikohima@yahoo.co.in](mailto:sanjaikohima@yahoo.co.in)

## CERTIFICATE

The thesis presented by Mrs. Aienla Ozukum, M.Sc., bearing registration No. 564/2014 dated 20<sup>th</sup> May, 2014 embodies the results of investigations carried by her under my supervision and guidance.

I certify that this work has not been presented for any degree elsewhere and that the candidate has fulfilled all conditions laid down by the University.

Date:

(S.K. SRIVASTAVA)

Supervisor



# नागालैण्ड विश्वविद्यालय

## NAGALAND UNIVERSITY

(संसद द्वारा पारित अधिनियम 1989, क्रमांक 35 के अंतर्गत स्थापित केंद्रीय विश्वविद्यालय)

(A Central University established by the Act of Parliament No.35 of 1989)

मुख्यालय: तुमामी, जुन्हेबोटो (नागालैण्ड), पिन कोड-798627

Headquarters: Lumami, Dist: Zunheboto, (Nagaland), Pin Code-798 627

### PLAGIARISM-FREE UNDERTAKING

Name of Research Scholar	Aienla Ozukum
Ph.D. Registration Number	No. 564/2014
Title of Ph.D. thesis	Depositional environment and tectonic provenance of Palaeogene sediments in and around Botsa, Kohima District, Nagaland
Name & Institutional Address of the Supervisor / Co-Supervisor	Dr. S. K. Srivastava Associate Professor Department of Geology, Nagaland University Kohima Campus, Meriema
Name of the Department & School	Department of Geology / School of Sciences
Date of submission	
Date of plagiarism check	17.09.2022
Percentage of similarity detected by the <b>URKUND</b> software	6%

I hereby declare / certify that the Ph.D. thesis submitted by me is complete in all respects, as per the guidelines of the Nagaland University for this purpose. I also certify that the thesis (soft copy) has been checked for plagiarism using URKUND similarity-check software. It is also certified that the contents of the electronic version of the thesis are the same as the final hard copy of the thesis. A copy of the report generated by the URKUND software is also enclosed.

(Name & Signature of the Scholar)

Date:

Place:

Name & Signature of the Supervisor with seal:



## *Acknowledgement*

*I would like to express my deepest gratitude to Dr. S. K. Srivastava for giving me the opportunity to work under his supervision. His valuable advice, motivation, immense knowledge and expertise has encouraged me throughout the time of research and writing of this thesis. His patience inspired me to accomplish the work and I am extremely privileged and grateful.*

*I would like to extend my gratitude to the Dean, School of Sciences, Nagaland University. I extend my sincere thanks to the Head of Department, Geology, Nagaland University, for all the necessary provisions and cooperation rendered during my research period. I am also thankful to the faculty and staff of this Department for their valuable assistance and suggestions that benefitted me in completing my study.*

*I could not have completed this endeavor without the support and help rendered endlessly by Dr. A. Moalong Kichu. Right from the beginning, to being a helpful and resourceful field partner till the end in helping with the compilation, our partnership will always be cherished and valued. Forever thankful and indebted.*

*Special thanks to my fellow scholars Mrs. Anettsüingla and Dr. J.N. Moiya for the continuous encouragement, valuable inputs and suggestions during the course of my study.*

*I am highly obliged to Dr. Jayanta Jivan Lashkar, Gauhati University for his help during the course of study and the Department of Geological Sciences, Gauhati University, Assam for XRD analysis and SEM photography.*

*I am also thankful to Dr. Maibam and his Research Scholars in the Department of Earth Sciences, Manipur University for the help rendered in pulverization of the samples. I would also like to acknowledge the Wadia Institute of Himalayan Geology, Dehradun for XRF analysis.*

*My friends 'Chocolates Daisies Diamonds', may we always uplift each other through words and prayers.*

*My parents and siblings are worthy of all the gratitude, without whom I would not have made it through. I owe what I am, to you all. Thank you to my parents, for the sacrifices you've made, your unconditional love and prayers have sustained me this far.*

*The completion of this thesis would not have been possible without the continuous support and motivation from my husband Mr. Zubenthung Ngullie. From the time I embarked this journey, your help and unfailing support has enabled me through. Thank you for being an escort and a comfort and above all, enduring this with me. My dearest daughter Anki, you are such a wonder, you've helped me face and pass through everything with ease. Apo and Oja are beyond blessed to have you.*

*Above all, I thank God for his grace, bountiful showers of blessings and for enabling me to overcome all difficulties and challenges smoothly.*

**(Aienla Ozukum)**

## **PARTICULARS OF THE CANDIDATE**

NAME OF THE CANDIDATE : Aienla Ozukum

DEGREE : Ph.D.

DEPARTMENT : Geology

TITLE OF THE THESIS : **Depositional Environment and Tectonic Provenance of the Palaeogene Sediments in and around Botsa, Kohima District, Nagaland**

DATE OF ADMISSION : 2<sup>nd</sup> September, 2013

APPROVAL OF RESEARCH PROPOSAL : 16<sup>th</sup> June, 2014

REGISTRATION NUMBER & DATE : 564/2014 (20<sup>th</sup> May, 2014)

Head of the Department

## **Biodata of the Candidate**

### **I. PAPERS PUBLISHED**

1. Ozukum, A.; Srivastava, S.K. and Desai, B. (2022): Ichnological study of the Palaeogene sedimentary succession of Botsa, Kohima District, Nagaland, India, *Geological Journal*, Special issue article, **2022**; 1-11.

### **II. ABSTRACT PUBLISHED/ORAL PRESENTATION**

1. Lithofacies and heavy minerals from Palaeogene sediments in and around Botsa, Kohima, Nagaland. National Seminar on Geology, Geochemistry, Tectonics, Energy and Mineral Resources of NE India, Department of Geology, Nagaland University (9<sup>th</sup> – 11<sup>th</sup> November, 2016). Abstract Volume, p. 25.
2. Ichnological study of the Palaeogene sediments in and around Botsa Village, Kohima District, Nagaland. Virtual National Seminar on Sedimentation, Tectonics and Metallogeny of North-East India (21<sup>st</sup> – 23<sup>rd</sup> September, 2020). Abstract Volume, p.13.

### **III. WORKSHOP/TRAINING ATTENDED**

1. Regional workshop for Young Earth Scientists on ‘Tectonics, Sedimentation and Geohazards with special reference to NE India’ organized by the Department of Geology, Nagaland University (16-21 November, 2015).
2. National workshop on ‘Recent advances in Geosciences’ organized by Department of Geosciences, Dr. B. R. Ambedkar University, Etcherla, Srikakulam on 31<sup>st</sup> July, 2020.
3. Online Public Lecture on ‘Landslides along transportation corridor in mountainous region of India’ organized by Department of Geology, K J Somaiya College of Science and Commerce, Mumbai, Maharashtra on 14<sup>th</sup> August, 2020.
4. e-Training on ‘Basic Training Course on Earthquake Geology, Active Fault Mapping and Seismo-tectonic Studies’ conducted by RTD, CR, GSITI, Nagpur from 17<sup>th</sup> -21<sup>st</sup> August, 2020.
5. National Webinar on Landslide susceptibility of Kohima Town, Nagaland Organized by Department of Geology, Model Christian College, Kohima, Nagaland on 26<sup>th</sup> March, 2021.

### **IV. UGC-JRF NET 2013-14**

## Preface

The study has been undertaken to deduce the depositional environment and tectono-provenance of the Palaeogene sediments in and around Botsa, about 40 kms north of Kohima Town. The results of the study are compiled and presented in 7 chapters, each of which deals with different facets of the study.

The compilation begins with the **first chapter** introducing the study area, the objectives and scope of the research and the methodology adopted. The **second chapter** discusses the stratigraphic and tectonic framework of the study area, which includes the regional stratigraphy, geologic setting and the distribution of the lithologic units.

The **third** chapter is devoted to the various lithology and sedimentary structures observed in the study area, the relationship with one another and the utilization of different facies parameters to reconstruct a facies scheme for the study area. **Chapter 4** covers grain size analysis and related parameters to understand the varied sedimentary environments. Textural maturity and palaeocurrent analysis have also been discussed here. **Chapter 5** deals with the petrography, diagenetic features and the geochemical attributes involving the major oxide geochemistry of the sediments. Suitable inferences are drawn from petrographic studies and geochemical analysis.

Reconstruction of palaeoenvironment, depositional history of the area and evidences from ichnological studies are discussed in **Chapter 6**. In this chapter the tectono-provenance of the area, transport mechanism and dispersal of the sediments are discussed. **Chapter 7** summarizes the study and presents the conclusions.

Each of the chapters are arranged with all texts appearing first and the relevant tables, plates and figures following in that order.

An attempt has been made for the first time to apply the facies analysis technique and the trace fossil assemblages for reconstructing the palaeoenvironment in the study area. The study would thus increase in understanding the geodynamic settings as well as the sedimentation history of the region. It is hoped that this thesis will provide a meaningful source of information and offer new insights for further understanding and future research works.

## **List of Tables**

Table 1: Stratigraphic Succession of Nagaland	16
Table 2: Lithofacies scheme for the Palaeogene sediments of the study area	35
Table 3: Grain size data and statistical measures of selected samples	62-65
Table 4: The four discriminant functions of Palaeogene sediments	66-67
Table 5: Values of $V_1$ and $V_2$ for different samples of Barail sediments	68
Table 6: Detrital composition of Palaeogene sediments in the study area	93-94
Table 7: Recalculated percentages of Quartz and Feldspar in Palaeogene sandstones	95-96
Table 8: Percentage of Major Oxides in Palaeogene sediments of the study area	97-98
Table 9: Result of the XRD analysis of the sample No. L2A15	99
Table 10: Summary of the characteristic features of the Palaeogene sediments	134

## List of Plates

Plate 1 : Field photographs	20
Plate 2 : Field photographs	21
Plate 3 : Field photographs	22
Plate 4 : Field photographs	36
Plate 5 : Field photographs	37
Plate 6 : Field photographs	38
Plate 7 : Field photographs	39
Plate 8 : Field photographs	40
Plate 9 : Trace Fossils	41
Plate 10: Trace Fossils	42
Plate 11: Trace Fossils	43
Plate 12: Photomicrographs	100
Plate 13: Photomicrographs	101
Plate 14: Photomicrographs	102
Plate 15: Photomicrographs	103
Plate 16: Photomicrographs	104
Plate 17: Photomicrographs	105
Plate 18: Zircon	106
Plate 19: Tourmaline	107

Plate 20: Rutile, Kyanite & Sillimanite	108
Plate 21: Opaque minerals	109
Plate 22: SEM photographs	109
Plate 23: SEM photographs	110



## List of Figures

Fig. 1 : Location map of the study area	5
Fig. 2 : Tectonic features of North east India	17
Fig. 3 : Geological map of Nagaland	18
Fig. 4 : Geological map of the Study area	19
Fig. 5 : Reference table for symbols used in vertical profile sections	44
Fig. 6 : VPS 1	45
Fig 7 : VPS 2	45
Fig. 8 : VPS 4	45
Fig. 9 : VPS 3	46
Fig. 10: VPS 5	46
Fig. 11: VPS 6	47
Fig. 12: VPS 8	47
Fig. 13: VPS 7	48
Fig. 14: VPS 9	49
Fig. 15: VPS 10	49
Fig. 16: Grain size distribution curves	69-72

Fig. 17: Grain size distribution curves	72-73
Fig. 18: Grain size distribution curves	73
Fig. 19: Grain size distribution curves	74
Fig. 20: Grain size distribution curves	75
Fig. 21: Grain size distribution curves	76
Fig. 22: Inclusive Graphic Skewness plotted against Inclusive Standard Deviation	77
Fig. 23: Graphic Skewness plotted against Inclusive Standard Deviation	77
Fig. 24: Plot of Graphic Skewness plotted against Graphical Mean	78
Fig. 25: Plot of Inclusive Graphic Standard Deviation versus Graphic Kurtosis	78
Fig. 26: C-M diagram plot of Palaeogene sediments	79
Fig. 27: Plot of $V_1$ against $V_2$ of Palaeogene sediments	79
Fig. 28: Sahu log-log plot	80
Fig. 29: Distribution of heavy minerals	110
Fig. 30: XRD curves for samples	111
Fig. 31: Ternary plot (QFR)	112
Fig. 32: Ternary plot ( $Q_pL_vL_s$ )	112

Fig. 33: Ternary plot (Q <sub>t</sub> FL)	112
Fig. 34: Ternary plot (Q <sub>m</sub> FL <sub>t</sub> )	112
Fig. 35: Ternary plot (QFL)	113
Fig. 36: Ternary plot (Q <sub>m</sub> FL <sub>t</sub> )	113
Fig. 37: Ternary plot (Q <sub>m</sub> PK)	113
Fig. 38: Ternary plot (QFL)	113
Fig. 39: Diamond diagrams	114
Fig. 40: Bivariate plot [ $\log (\text{Fe}_2\text{O}_3/\text{K}_2\text{O})$ vs $\log (\text{SiO}_2/\text{Al}_2\text{O}_3)$ ]	115
Fig. 41: Bivariate plot ( $\text{K}_2\text{O}/\text{Na}_2\text{O}$ vs $\text{Fe}_2\text{O}_3/\text{MgO}$ )	115
Fig. 42: Bivariate plot ( $\text{Al}_2\text{O}_3/\text{SiO}_2$ vs $\text{Fe}_2\text{O}_3/\text{MgO}$ )	115
Fig. 43: Bivariate plot ( $\text{TiO}_2$ vs $\text{Fe}_2\text{O}_3/\text{MgO}$ )	115
Fig. 44: Bivariate plot ( $\text{K}_2\text{O}/\text{Na}_2\text{O}_3$ vs $\text{SiO}_2$ )	116
Fig. 45: Bivariate plot ( $\text{SiO}_2$ vs $\text{Al}_2\text{O}_3+\text{K}_2\text{O}+\text{Na}_2\text{O}_3$ )	116
Fig. 46: Ternary plot ( $\text{Fe}_2\text{O}_3\text{-MgO-TiO}_2$ )	116
Fig. 47: Ternary plot ( $\text{CaO-Na}_2\text{O-K}_2\text{O}$ )	116
Fig. 48: Depositional model for the Palaeogene sediments of the study area	128

# Contents

<i>Declaration</i>	i
<i>Certificate of Supervisor</i>	ii
<i>Plagiarism-Free Undertaking</i>	iii
<i>Acknowledgement</i>	iv
<i>Particulars of the candidate</i>	vi
<i>Biodata of the candidate</i>	vii
<i>Preface</i>	viii
<i>List of tables</i>	xi
<i>List of plates</i>	xii
<i>List of figures</i>	xiv
<b>1 INTRODUCTION</b>	<b>1-5</b>
1.1 General	1
1.2 Location of the study area	1
1.3 Geomorphic features	1
1.4 Review of previous literatures	2
1.5 Scope and objectives of the present investigation	3
1.6 Hypothesis	3
1.7 Methodology	4
<b>2 STRATIGRAPHIC AND TECTONIC FRAMEWORK</b>	<b>6-22</b>
2.1 General	6
2.2 Geologic setting	6
2.3 Regional Stratigraphy	8
2.4 Lithologic units, their distribution and field relationships	14
<b>3 LITHOLOGIC DISTRIBUTION, VERTICAL PROFILE SECTIONS AND LITHOFACIES</b>	<b>23-49</b>
3.1 General	23
3.2 Parameters of sedimentary facies	23
3.3 Description of sedimentary structures	25
3.4 Facies Scheme	31
3.5 Description of lithofacies in the study area	31
3.6 Description of Vertical Profile Sections (VPS)	32
<b>4 GRAIN SIZE ANALYSIS</b>	<b>50-80</b>
4.1 General	50
4.2 Grain size analysis	50

4.3	Textural maturity	60
4.4	Palaeocurrent analysis	60
<b>5</b>	<b>PETROGRAPHY AND MAJOR OXIDE GEOCHEMISTRY</b>	<b>81-116</b>
5.1	General	81
5.2	Petrography	82
5.3	Nomenclature, classification and modal analysis	86
5.4	Diagenesis	87
5.5	Geochemical analysis	91
<b>6</b>	<b>DEPOSITIONAL ENVIRONMENT AND TECTONIC PROVENANCE</b>	<b>117-128</b>
6.1	Reconstruction of paleoenvironments	117
6.2	Depositional history	120
6.3	Evidences from ichnological studies	121
6.4	Tectono-provenance	123
6.5	Transportation mechanism and dispersal	126
<b>7</b>	<b>SUMMARY AND CONCLUSION</b>	<b>129-134</b>
	<b>References</b>	<b>135-153</b>
	<b>Published Paper</b>	
	<b>Plagiarism Similarity Index</b>	
	<b>Certificates</b>	

# **CHAPTER 1**

## **INTRODUCTION**

### **1.1 GENERAL**

The Naga Hills characterizes the Western most tract of the Mesozoic-Cenozoic Indo-Sinian collision domain and extends for about 200 km along the Indo-Myanmar border. The Naga Hills, morphotectonically, have been divided into three distinct linear zones (Mathur and Evans, 1964) and have been designated from West to East as Schuppen Belt, the Inner Fold Belt; occupied by two Synclinoria, the Patkai Synclinorium to the North and the Kohima Synclinorium to the South and the Ophiolite Belt. Tectonic evolution of northeastern India is intricately linked with the movement of the Indian plate and its relationship with the tectono-chronology of the Himalayan orogeny. The complicated stratigraphy of the region has been discussed in terms of oblique collision and tectonic wedge model by Naik (1994). Prior to collision, this was certainly a passive margin (Kumar and Naik, 2006) which through time has evolved into an active margin set up where late Palaeogene sediments have been deposited in a foreland basin having a north-east south west trending pattern.

### **1.2 LOCATION OF THE STUDY AREA**

For the purpose of the study, an area, a part of Inner Fold Belt, comprising of well-developed Palaeogene succession in and around Botsa, about 40 km north of Kohima Town, has been identified. It is bounded between latitudes 25°50'00" N and 25°55'00" N and longitudes 94°08'00" E and 94°15'00" E of the topographic map 83 K/1 of the Survey of India. The total area under study covers approximately 50 sq. km (**Fig. 1**).

### **1.3 GEOMORPHIC FEATURES**

The geomorphic features present in the area are the direct manifestations of topographic inversion (Dasgupta, 1977). Having undergone through several cycles of erosion and uplift, the area is essentially occupied by topographically high features. The maximum height encountered in the area is 1735 meters above Mean Sea Level (MSL) and the minimum height being 440 meters

above MSL. The areas with higher altitude constitute the sandstones whereas abundant splintery shales interbedded in thin sandstones observed along the road sections are spread over a large area. No major river flows in the area, however mention has to be made of Nzu River that flows northerly. A number of tributaries, namely Temekhu, Nrarolo, Khwanlo, Shimetelu, Khukhi feeding into Nzu, forms the main drainage system in the area. Rivers like Thuse and Terha Dzupie are flowing westerly and north westerly respectively. A number of streams contribute to the drainage network of the area. Small scale folds, faults and joints are also encountered in the area.

#### **1.4 REVIEW OF PREVIOUS LITERATURES**

The pioneering works of Mallet (1876), Evans (1932), and Mathur and Evans (1964) have laid the foundation of the Northeast Indian geology. Most of the data on Northeast India is from the Upper Assam region, where petroleum exploration is on since 1890 and little is known about the Naga Hills. Since then, useful studies on the stratigraphy, sedimentology, structure, and tectonic framework of the region have come from the works of the Geological survey of India (Chattopadhyay *et al.*, 1983), Oil and natural Gas Corporation (Ganju *et al.*, 1986 ) and the Directorate of Geology and Mining, Government of Nagaland (DGM, 1978) along with contributions made by various workers, including those of Bhandari *et al.* (1973), Dasgupta (1977), Banerjee (1979), Chakravarti and Banerjee (1988), Naik *et al.* (1991), Biswas *et al.* (1994) and Acharyya (2007).

Sarmah (1989), Thong (1993, 2001), Thong and Rao (2006) and Vineetha *et al.* (2008) have worked on the sedimentology and geochemistry of a part of Inner Fold Belt. Srivastava *et al.* (2004) and Srivastava and Pandey (2005) have worked on the tectono-sedimentary evolution and the depositional mechanism of the Palaeogene sediments at Disang-Barail Transitional Sequences (DBTS) of the Kohima district, Nagaland. Imchen *et al.* (2014) has worked on the provenance, tectonic setting and age of the sediments of the Upper Disang Formation in the Phek District of Nagaland. Khalo and Pandey (2018) have worked on the Paleoenvironmental significance of ichnofossil assemblages of the Palaeogene sediments of the Inner-Fold Belt. Recently, Kichu *et al.* (2018) and Srivastava and Kichu (2021) have worked on the paleoenvironmental significance of Trace Fossils and tectono-provenance of the Palaeogene sediments, South of Kohima Town. Most of the workers have related the geological complexities of the region to that of a complex

tectonic regime.

## **1.5 SCOPE AND OBJECTIVES OF THE PRESENT INVESTIGATION**

The proposed study is an attempt to develop a lithofacies scheme which in turn would help in reconstructing the depositional environment for the Palaeogene sediments of the study area. Attempts would also to be made to understand the tectonic provenance of the Palaeogene sediments in the light of the changing tectonic regime. The research work would thus, increase our understanding about the geodynamic settings of the region as well as the sedimentation history.

The study has been carried out with the following objectives:

1. To reconstruct and interpret the depositional environment using facies analysis technique.
2. To characterize the source rock using petrography, heavy minerals and geochemical attributes.

## **1.6 HYPOTHESIS**

Evans (1932) and Mathur and Evans (1964) laid out the Tertiary succession of the Inner Fold Belt in Naga Hills beginning with the argillaceous rocks of Disang Group that are overlain by the arenaceous Barail Group. Sediments of the Naga Hills are highly folded and faulted due to the continuous subduction of the Indian plate below the Myanmar plate where huge quantities of Cenozoic sediments were deposited. Evans (1932) stated that the correlation and subdivision of Disang Group was a most difficult problem in the NE Indian geology. Similar view has also been echoed by Nandi (2017). Nandi (2017) further says that towards the top Disang sediments become sandier and gradually changes to Oligocene Barail sediments, which are dominantly arenaceous in composition. While working with Palaeogene sediments in the southern part of the Kohima Synclinorium, Pandey and Srivastava (1998) have observed that at places it is difficult to delineate the boundary between Disang and Barail Groups of rocks. They suggested that the Disang rocks, being intensely deformed and monotonous, tracing its continuity becomes difficult. The lithostratigraphic boundary between the Disang and the Barail successions is difficult to delineate since the contact is gradational with the development of a mixed lithology i.e., Disang – Barail



Transitional Sequences (DBTS, Srivastava *et al.*, 2004), inferring that the depositional mechanism was largely controlled by tectonic forces. There is not much published sedimentological data available on the proposed study area except those of Thong (1993, 2001) and Thong and Rao (2006).

Through the present work, an attempt has been made for the first time to apply the facies analysis techniques and also to use the trace fossil assemblages for reconstruction of the palaeo-environment. Petrographic and heavy mineral studies in conjugation with geochemical attributes have also been carried out for determining the tectono- provenance of the succession.

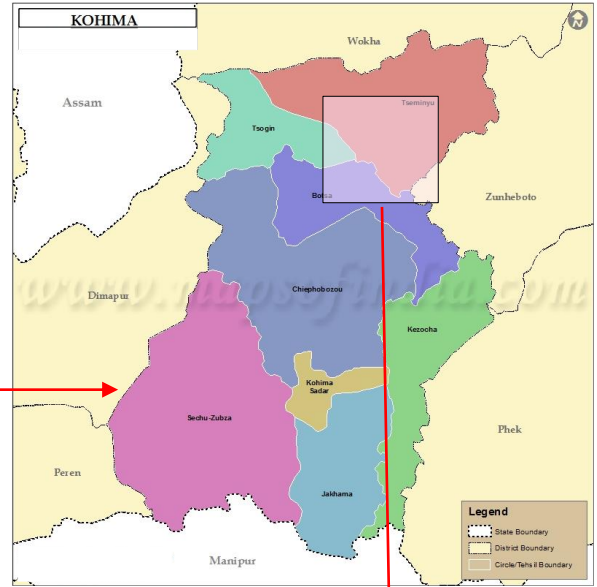
## 1.7 METHODOLOGY

The research methodology involved detailed field work and laboratory investigations. The investigation dealt and advanced along the following direction:

- 1) **Field Studies:** This involved the following:
  - a) Collection of random and oriented samples from suitable rock exposures both in time and space.
  - b) Identification, recording and description of sedimentary structures including biogenic structures.
  - c) Construction of vertical profile sections.
  - d) Recording and identification of lithofacies.
  
- 2) **Laboratory Studies:** The following studies were also performed.
  - a) Petrography including heavy mineral studies.
  - b) Grain size and modal analysis.
  - c) X-ray fluorescence (XRF) of major elemental composition.
  - d) Scanning Electron Microscopic studies.
  - e) X-ray Diffraction (XRD) analysis for clay minerals.



(Not to scale)



(Not to scale)

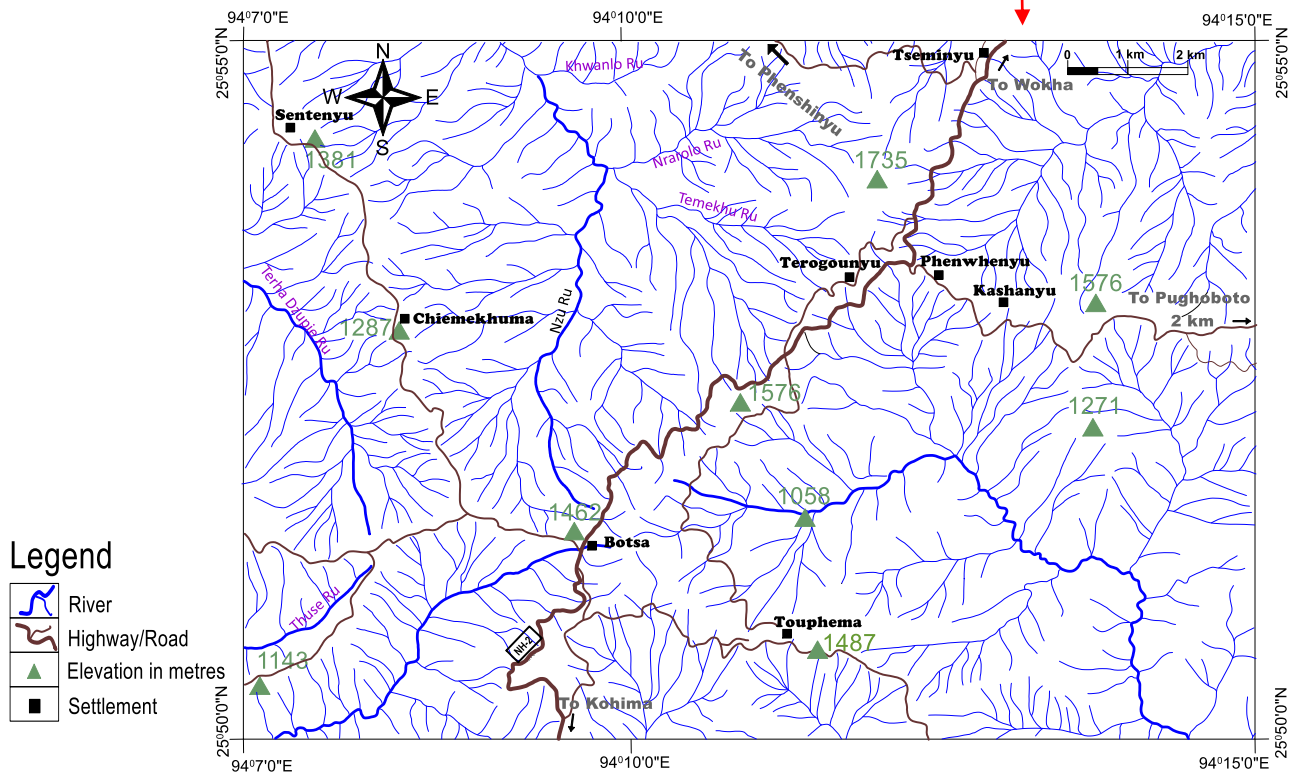


Fig. 1: Location Map of the Study Area

## CHAPTER 2

# STRATIGRAPHIC AND TECTONIC FRAMEWORK

### 2.1 GENERAL

The Naga Hills, trending NE-SW, characterizing the western most tract of the Mesozoic-Cenozoic Indo-Sinian collision, occurs along the eastern margin of North-East India, bordering Myanmar. The Naga Hills, also known as Assam-Arakan Orogenic Belt, which links E-W Himalaya to the N-S Andaman Nicobar Island arc, provides an ideal setting for understanding the geodynamic processes responsible for the evolution of the North East Indian geology through Mesozoic-Cenozoic period.

The Indo-Myanmar Ranges (IMR) is characteristic of orogenic deformations of Cenozoic sediments that resulted due to the convergence of the Indian Plate with the Eurasian Plate in the north and the Myanmar Plate in the east. Subsequent to the break-up of Gondwanaland, the Indian Plate detached itself following its northward drift (Acharyya, 2007). The continuation of north to northeastward movement of the Indian Plate led to its convergence and consequently, the oblique subduction of the Indian plate below the Myanmar Plate in the east and the Eurasian Plate in the north caused overthrusting and obduction of the oceanic crust of the Tethyan Zone which resulted in the emplacement of the Naga Ophiolite (Naik, 1994; **Fig. 2**).

### 2.2 GEOLOGIC SETTING

The Naga Hills constituting the northern extension of the Indo-Myanmar ranges is bounded on the east by the central lowlands of Myanmar, on the west by the Precambrian Karbi-Anglong Massif and the Tertiary Shelf sediments of Assam; and on the north, it continues into the eastern syntaxial bend of the Himalayas. The Naga Hills can be divided into three distinct NE-SW trending morphotectonic units discussed below (**Fig. 3**).

#### 2.2.1 THE BELT OF SCHUPPEN:

According to Mathur and Evans, (1964), NNE-SSW trending Belt of Schuppen, is a narrow linear belt running along the entire western margin of Nagaland for a distance of 350 km.

It is comprised of NE-SW trending over thrusts; along which the Naga Hills has moved north-westward. The Belt of Schuppen, which has an enechelon disposition, is bounded by two marginal thrust on the west by the Naga Thrust and on the east by the Disang Thrust. Oligocene, Miocene and Plio-Pleistocene sediments characterize the Belt of Schuppen. The lithological sequence exposed in this belt comprises of the Barail Group, Surma Group, Tipam Group, Dupitila Group, Dihing Boulder Bed and the alluvium.

### 2.2.2 THE INNER FOLD BELT

Disang Thrust in the west and the Ophio-Disang Thrust in the east define the boundaries of the Inner Fold Belt which occupies the central part of the Naga Hills. Patkai (North) and the Kohima Synclinorium (South) are the two Synclinorium occupy the Inner Fold belt. Dominantly argillaceous Disang sediments, undifferentiated arenaceous Barails and the mixed Disang-Barail Transitional Sequence (Srivastava, 2002) characterize the lithological settings of the Inner Fold Belt. The Inner Fold Belt is represented by folded and thrust pile of thick monotonous splintery shales interbedded with fine grained sandstones, mudstones, siltstones, slates and phyllites with isolated covers of medium to coarse grained sandstones. In Kohima Synclinorium, the younger Surma rocks are developed in its core (DGM, 1978).

### 2.2.3 THE NAGA OPHIOLITE BELT

The Naga Ophiolite Belt occurs as a NNE-SSW trending arcuate belt extending along the eastern margin of Nagaland for nearly 90 km along the border of Myanmar. Consisting of a variety of Mesozoic and Cenozoic magmatic, metamorphic and sedimentary rocks, the Naga Ophiolite Belt originated at the India-Myanmar convergent plate boundary. Tectonically sandwiched between the Naga Metamorphics in the east and the Disang Flysch sediments in the west, the Naga Ophiolite Belt is characterized by dismembered tectonic slices of serpentinites, ultramafic-mafic cumulates, volcanic, plagiogranites and pelagic sediments (GSI, 1989). The Ophiolites are covered by a layer of shales, siltstones and sandy layers recognized as the oceanic pelagic sediments because of the presence of radiolarian chert bands. The associated pelagic sediments include mainly chert and limestone often bedded with the volcanics. Banded radiolarian chert occurs in close association with the ultramafics within the lower part of the Disang Flysch sediments. Harzburgite is the dominant rock type and constitutes more than 80%

of the ultramafics. The Naga Ophiolites are considered an Upper Cretaceous to Lower Eocene age from the fossil assemblages of the limestone inter-bands. During the upliftment of the Ophiolite, submerged areas at intervals in the ophiolite led to the deposition of a different facies of rocks over the ophiolite basement designated as the fourth tectono-stratigraphic unit of post-orogenic molasse known as the Jopi Formation. This is represented by ophiolite derived conglomerate-grit-pebbly and cobble-like sandstone-greywacke-shale/polymictic tuff breccia (Ghose *et. al.*, 2010). Geological Survey of India (GSI, 1975) have named the ophiolite derived volcanoclastics as the Phokphur Formation. These Ophiolite derived volcanoclastics with an open marine to pelagic sedimentary cover unconformably overlies the Ophiolite suites of rocks.

## 2.3 REGIONAL STRATIGRAPHY

The Stratigraphic Succession of Nagaland (**Table 1**, Modified by DGM, Nagaland, 2008, after Ghose *et al.* 1986 and Srivastava *et al.*, 2004) consists of the following litho- units described briefly below.

### 2.3.1 NAGA METAMORPHICS

Brunnschweiler (1966) named a group of mainly low to medium grade Proterozoic metamorphosed rocks exposed along the Indo-Myanmar border as the Naga Metamorphics. Brunnschweiler (1966) has regarded it as unfossiliferous Pre-Mesozoic in age. Recent studies of less deformed members of this formation have not yielded any fossil. The base of this formation though not exposed but it is tectonically juxtaposed against or even overlies the Ophiolites as well as the Phokphur Formation. It is represented by Proterozoic crystalline rocks consisting of quartzite, crystalline limestone/marble, mica schist, phyllites, gneisses, sheared granite with minor serpentinite.

### 2.3.2 NIMI FORMATION:

Nimi Formation is exposed in the eastern fringe of Nagaland and is considered to be a detached part of the Pre- Tertiary Myanmar continental crust. This Formation is represented by a thick sequence of folded metasediments dominantly composed of low grade regionally metamorphosed rocks of phyllite, feldspathic quartzite, limestone and quartz-sericite that is tightly folded in the form of a major NNE trending overturned anticline, representing an

accretionary prism (Agarwal and Ghose, 1986). It stretches over 216 kms, extends in the west of Nimi to Laluri and in the east to Saramati Peak. This Formation is assumed to be of Pre-Mesozoic age.

### 2.3.3 DISANG GROUP:

A large stretch of the Palaeogene Inner fold Belt is occupied by the Disang Group of rocks and considered the oldest exposed sedimentary rock of central Naga Hills. Mallet in 1876 described the Disang Group from the type section of the Disang river. The Disang Group does not display significant lithofacies variation but rather it exhibits a monotonous lithological sequence of shale-siltstone succession. The thickness varying between 2000 to over 3000 m, the Disang Group of rocks is sub-divided into Lower Disang Formation and Upper Disang Formation, wherein the lower units are characterized by dark grey, finely laminated splintery grey shales and dark to black carbonaceous shales with mudstone interbands and intercalated with very thin beds of fine-grained sandstone. The Upper Disang Formation is characterized by fine grained flaggy sandstones that alternate with shales and subordinate mudstones occurring higher up. In general, the occurrence and thickness of sandstones-siltstones increases toward the upper part of the sequence. The Lower Disang Formation has yielded Upper Cretaceous foraminifera such as *Bathysiphon* sp., *Globigerinella* sp., *Globigerinoides* sp., *Globorotalia* sp., *Globotruncana* sp. and *Pleurostomella* sp. in the Disang Group of the eastern parts of Manipur State (Mishra, 1983) and Late Eocene Nummulites are reported from the Upper Disang Formation.

The surficial extent of the Disang Group is tectonically limited to the west by the Disang Thrust and to the east by the Naga Ophiolite complexes. The base of the Disang Group is nowhere exposed but the argillaceous bed with limestone inter-bands was earlier considered to represent the Lower section of the formation because of associated older fauna. The Disang Group conformably grades upward into the Barail Group through Disang-Barail Transitional Sequences (DBTS).

### 2.3.4 THE DISANG-BARAIL TRANSITIONAL SEQUENCES (DBTS)

The Disang-Barail Transitional Sequences (DBTS) displays a heterogeneous lithology

and overlies gradationally the monotonous argillaceous sediments of Disang Group and in turn passes into the arenaceous sediments of the Barail Group (Pandey and Srivastava, 1998, Srivastava and Pandey, 2001). It comprises of alternating succession of sand-mud lithology. The sand-silt unit in the succession exhibits numerous alternations of thin, flaggy, fine grained sandstone and silty/sandy shale displaying gradational base and erosional top. The contact between sand and shale is usually found to be erosional (Srivastava *et al.*, 2004).

### 2.3.5 BARAIL GROUP

Mallet in 1876 first studied the rock succession of this Group, however, Evans in 1932 named it as Barail and accorded the status of a 'series' to the similar rock associates exposed in the Barail range. Barail Group is differentiated into Laisong Formation being the oldest followed by Jenam Formation and the youngest Renji Formation. Another set of nomenclature is known for Barail Group in the north-eastern part of the Schuppen Belt viz. Naogaon, Baragolai and Tikak Parbat Formations. Borjan Coalfield marks the transition in the nomenclature. In the Inner Fold Belt, the Barails are undifferentiated. A seismic survey (GSI, 1975) conducted in *Dhansiri* valley shows that Barail Group of rocks (Upper Eocene to Oligocene) continues with a reduced thickness in the sub thrust block of the Naga Hills.

The three formations of the Barail Group are briefly discussed below:

1. Laisong Formation: The Laisong Formation is the lowest litho unit of the Barail Group in the Schuppen Belt. It consists largely of hard, compact well bedded sandstones alternating with minor grey and sandy shales and siltstones, occasional carbonaceous shales and thin streaks of coal are also found. This unit has yielded foraminifers viz *Nummulites* sp., *Dictyoconoides*, *Assilina* sp. of Middle Eocene affinity from northeast of Anglewa (Acharyya *et.al.*, 1986). *Nummulites chavanensis* and *Biplanispira* sp. of Upper Eocene age is also reported from Heningkunglwa area in Laisong Formation (RangaRao, 1983). On the basis of lithological characters, a 200 m sequence of current bedded sandstones on the upthrust block of the Chongliyimsen Thrust has been recorded along Mokokchung-Mariani road section. This is referred to as Laisong Formation. In Borjan Coal Belt, the sequence of thin bedded sandstones with alternation of shale and streaks of coal has been designated

as Nagaon Formation, and this is usually considered to be homotaxial to Laisong Formation. Rocks of the Nagaon Formation are exposed in the north-eastern parts of Nagaland.

2. Jenam Formation: The Laisong Formation passes up into a much more argillaceous sequence of dark siltstone, shale, thin sandstone bands, carbonaceous bands and a number of coal seams known as the Jenam Formation in the southern part of the Schuppen Belt. Along Dimapur-Kohima Road section the thickness of this formation is about 800 m (RangaRao, 1983). Jenam Formation of Schuppen Belt is equated with Baragolai Formation of Upper Assam. Within the Schuppen Belt, Jenam Beds are argillaceous in the upper part, thus forming a transition into the overlying Renji Formation (Evans, 1932).
3. Renji Formation: The sandstone dominated Renji Formation above the soft Jenam Formation is a great thickness of hard ferruginous usually massive sandstone showing very little variation in the overall lithology in different tectonic blocks, however the thickness of Renji Formation varies widely due to changes in the depositional environment and unconformable overlap of the Surma Group. The best exposure of Renji Formation is seen in the Changki unit where it can be traced continuously from Moilang to north of Tuli, with a thickness of about 400-500 m. Renji is also developed in the cliffs and peaks of Japfü, rising almost to 10,000 ft. above sea level. The upper units of Jenam Formation and the lower units of Renji Formation is correlated with the lower unit of Tikak Parbat Formation. Tikak Parbat contains workable coal reserves.

It is interpreted that Barail sedimentation commenced in Upper Eocene period, based on available palaeontological records (Acharyya, 1982; RangaRao, 1983). There are abundant plant remains in the Barail Group however, due to the absence of diagnostic fossil beds, the period of Oligocene sedimentation is yet to be precisely confirmed.

#### 2.3.6 JOPI/ PHOKPHUR FORMATION:

Jopi Formation resting unconformably over the Naga Ophiolite suite of rocks is represented by a clastic shallow marine sedimentary cover primarily derived from the ophiolite comprising of repeated molassic sediment sequence of polymictic conglomerate-grit-pebbly and



cobble-like sandstone-greywacke-shale/polymictic tuff breccia. Several cyclic sequences of conglomerate-grit-sandstone-shale are observed, the individual cycles varying in thickness from less than a meter to over 10 m, the overall thickness of the formation being more than 600 m (Agarwal, 1985). The basal conglomerate unit contains angular to sub rounded boulders, cobbles and pebbles derived from the underlying ophiolite suite and embedded in reworked tuffaceous/siliceous cement. The succession grades upward into grit, lithic greywacke, siltstone, sandstone and shale. The sandstone gradually becomes arkosic towards the top. Near Phokphur, the Jopi Formation is referred to as Phokphur Formation. The Plant fossils *Anthocephalus* sp., *Litchi* sp., *Syzygium* sp., indicate a Late Eocene-Oligocene age and a homotaxial relationship with the Barail Group (Chattopadhyay *et. al.*, 1983).

### 2.3.7 SURMA GROUP:

In the Belt of Schuppen the Surma Group rests unconformably on the Barail Group with a characteristic basal conglomerate. These rocks are exposed in the form of a number of long, narrow strips running along almost the entire length on the western margin of Nagaland and gradually thinning out towards the north. Alternations of grey laminated shales, sandy shales, sandstones and thin conglomerates represents the Surma Group of rocks. The overall thickness of this group varies from 300-1250 m. The presence of *Ammonia beccarii*, in the Zubza River section, indicate Miocene or younger age (Ranga Rao, 1983).

Surma Group has been divided into Bhuban Formation and the Bokabil Formation. The Bhuban Formation is further subdivided into the Middle and the Upper Bhuban. The Middle and the Upper units of Bhuban as well as the Bokabil Formation are well exposed in Naga Hills, however, the Lower Bhubans are not represented in Naga Hills. The Bhuban as a whole consists of alternations of sandstones, shaly sandstones, the Middle Bhuban being more argillaceous. Bokabil is usually made up of sandy shales, alternations consisting of laminae of clay-shale and ferruginous sand, massive or false bedded sandstone. The rocks of this group are also reported to be in the core of the Kohima Synclinorium (DGM, 1978).

### 2.3.8 TIPAM GROUP:

The Tipam Group exposed along the western fringe of Nagaland in the Schuppen Belt

occurring as long, narrow strips due to strike faulting, is made up of two Formations, i.e. Tipam Sandstone Formation and the younger Girujan Clay. In Naga Hills the Tipam sandstones gradationally overlies the Surma Group, thereby suggesting that the Tipam-Surma contact is a facies boundary that may be time transgressive (GSI, 1989). Tipam sandstones are massive, highly friable sandstones containing subordinate clay and shale. These rocks are generally coarse grained, occasionally gritty and ferruginous and commonly green in colour due to the presence of chlorite, but are found to be weathered to different shades of brown. These rocks are characterized by multi storied, channeled false-bedded sandstones, that are massive, friable due to poor compaction and cementation. The Girujan Clay Formation occurs as a very distinctive type of rock in which mottled clays predominate with a few silt and sandstone beds. These sediments are of Mio-Pliocene in age.

#### 2.3.9 NAMSANG BED:

The Namsang Formation belonging to the Dupi Tila Group overlies the Girujan Clay with an erosional unconformity. Namsang beds are well exposed in the northern part of the Schuppen Belt and are represented by sandstone, lignite pebbles, conglomerate, grit, mottled clay and lenticular seams of lignite. Pliocene age is assigned to this formation.

#### 2.3.10 DIHING GROUP:

The Dihing Group is represented by the Dihing Formation. This Formation is well developed in Nagaland along the western margin of the Belt of Schuppen. These consist mainly of thick pebbles beds, with clays and sands resting unconformably on the Tipam Group and Namsang Formation.

#### 2.3.11 ALLUVIUM:

Alluvium is represented by the Newer and the Older Alluvium and are designated as Quaternary deposits. The Older Alluvium (high level terraces) occupying the northeastern tract of the Naga-Patkai ranges is composed mainly of boulders and cobbles with considerable amount of clay, silt and sand. The Newer Alluvium covering the Western border of Nagaland occurs as recent alluvial deposits of rivers and streams composed of dark grey clay, silt and sand deposits.

## 2.4. LITHOLOGIC UNITS, THEIR DISTRIBUTION AND FIELD RELATIONSHIPS

The Palaeogene sediments of the study area comprise of both shale and sand units. Lower horizons are dominated by argillaceous sediments with increasing sand contents up in the sequence whereas at upper stratigraphic level sediments are dominated by arenaceous compositions. However, at places they show a mixed lithology of sand - silt-shale (**Fig. 4**).

Geological Survey of India (1988) while working with the sediments of the area have used the terms like Disang (argillaceous units) and Barail (arenaceous unit) Groups; though at places it becomes difficult to differentiate between Upper Disang sediments and Barail sediments as at many places in the study area lithology comprises of alternating sandstone and siltstone-shale succession similar to Disang-Barail Transition, described by Srivastava *et al.* (2004) in the north-west of Kohima town. Precise marking of Disang-Barail contact within the Inner Fold Belt is an intriguing problem; as there is no distinguishable boundary between Upper Disang Formation and the lower Barail sediments. According to Rangarao (1986), thinly bedded sandstones and shale could be correlated with Laisong Formation (lower Barails), though similar characteristics can be observed in Upper Disang Formation also. Many workers (Mathur and Evans, 1964; Pandey and Srivastava, 1998; Nandi, 2000; Sema, 2003; Srivastava *et al.*, 2004; Srivastava and Pandey, 2005; Kumar and Naik, 2006; Acharyya, 2007; Sema and Pandey, 2016; Mishra, 2016; Khalo and Pandey, 2018) while working with the Palaeogene sediments in other parts of the Inner Fold Belt have attributed this to an un-interrupted sedimentation during Eocene-Oligocene period, with many phases of sea level fluctuations; which had resulted in the deposition of numerous beds of both shale and sand.

In the present study, an attempt has been made to correlate this un-interrupted Palaeogene successions with lithological variations through time and changing tectonic regimes.

At the lower horizons the Palaeogene rocks of the study area are made up of well bedded, abundant dark grey splintery shales interbedded with very fine grained, flaggy sandstones (**Plate 1a**) while at higher stratigraphic levels these sequences are represented by multistoried very fine to medium sandstone with minor intercalations of siltstones and shales (**Plate 1b**). They occur as thick bedded, massive sandstones not varying much in their lithological characters. Varied

tectonic signatures like small scale faults, anticlinal structures like folds, exfoliation joints and shear zones are also prominent in the area (**Plate 2b, 2a, 2c, 2d**). Box type of weathering in shales and intensely bioturbated surfaces are common occurrences in the study area (**Plate 3d & 3e**). The sandstones are also traversed by quartz veins (**Plate 3b & 3c**). Planar laminations, asymmetrical, symmetrical/wave ripples, interference and bifurcating ripples, cross and hummocky cross stratifications are the depositional sedimentary structures encountered in the study area.

Age	Group	Belt of Schuppen		Inner Fold Belt		Ophiolite Belt
Recent	Alluvium	Older alluvium Newer alluvium		Older alluvium (High level terraces) Newer alluvium		Older alluvium (High level terraces) Newer alluvium
Pleistocene to Recent	Dihing Group	Dihing Formation				
~~~~~Unconformity~~~~~						
Plio-Pleistocene	Dupitila Group (Moran Grp.)	Namsang Formation				
~~~~~Unconformity~~~~~						
Mio-Pliocene	Tipam Group	Girujan Clay				
		Tipam Sandstone Formation				
	Surma Group	Bokabil Formation				
		Bhuban Formation	Upper Middle	Bhuban Formation	Middle Lower?	
~~~~~Unconformity~~~~~						
Oligocene to Upper Eocene	Barail Group	<b>NE Schuppen</b> Tikak Parbat Baragolia Naogaon	<b>SW Schuppen</b> Renji Jenam Laisong	Barail Group (Undifferentiated)		Jopi Formation (=Phokpur Formation?) (= Lower Barail ?)
-----Gradational Contact-----Disang-Barail Transitional Sequence-----						~~Unconformity~~
Upper Cretaceous to Eocene	Jaintai Group (Eocene)			Disang Group	Upper Lower	Lower Disang _Tectonic contact_ Ophiolite Complex __Tectonic contact__
~~~~~Unconformity~~~~~						
Triassic ?						Nimi Formation __Tectonic contact__
Post Mesozoic ?	Mikir Hill Massif (Pre-Cambrian ?)					Naga Metamorphics (Proterozoic ?)

**Table 1:** Stratigraphic Succession of Nagaland (Modified by DGM, Nagaland, 2008, after Ghose *et al.*, 1986 and Srivastava *et al.*, 2004)

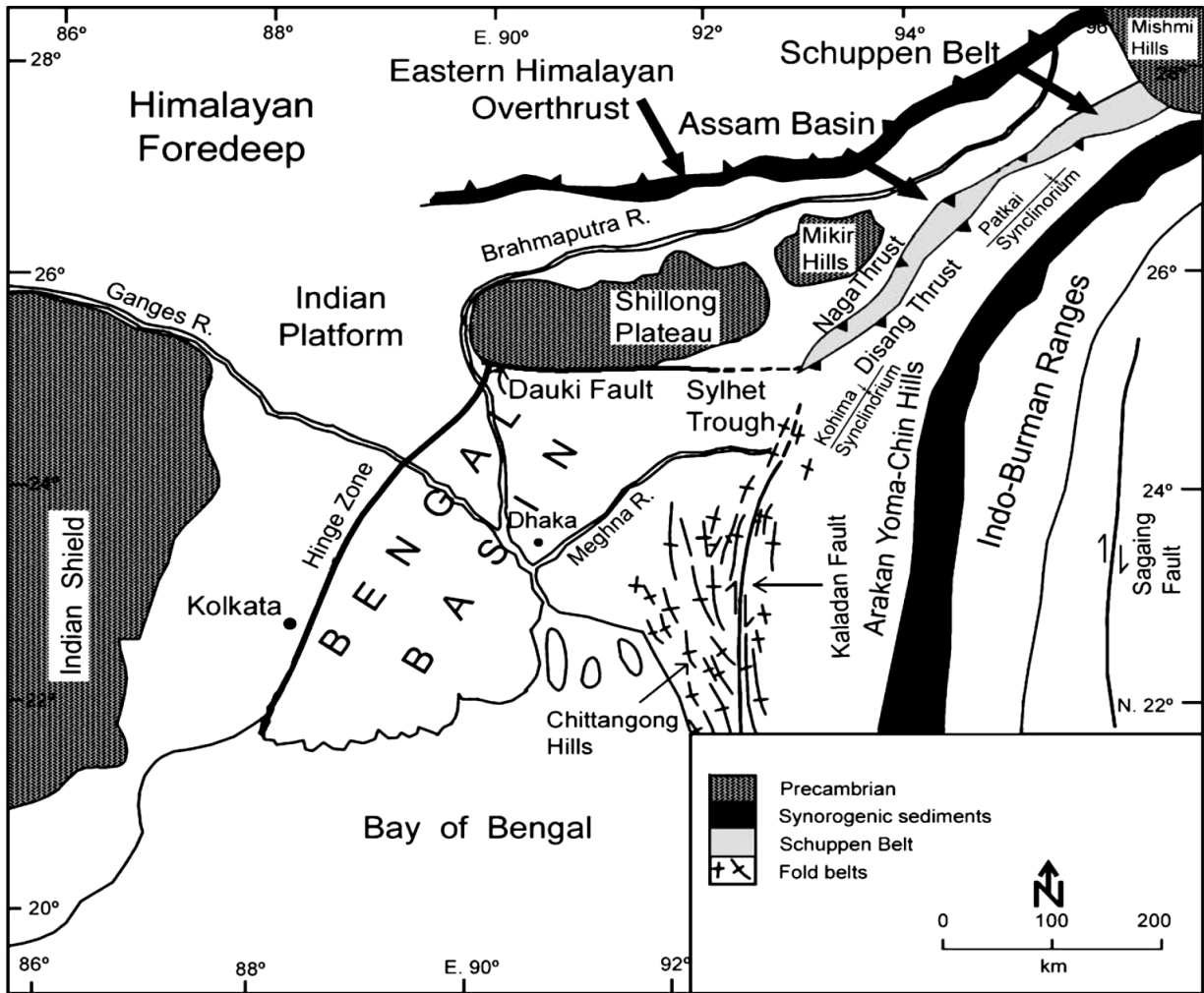


**Fig. 2:** Tectonic features of North-east India (after Uddin *et al.*, 2007)

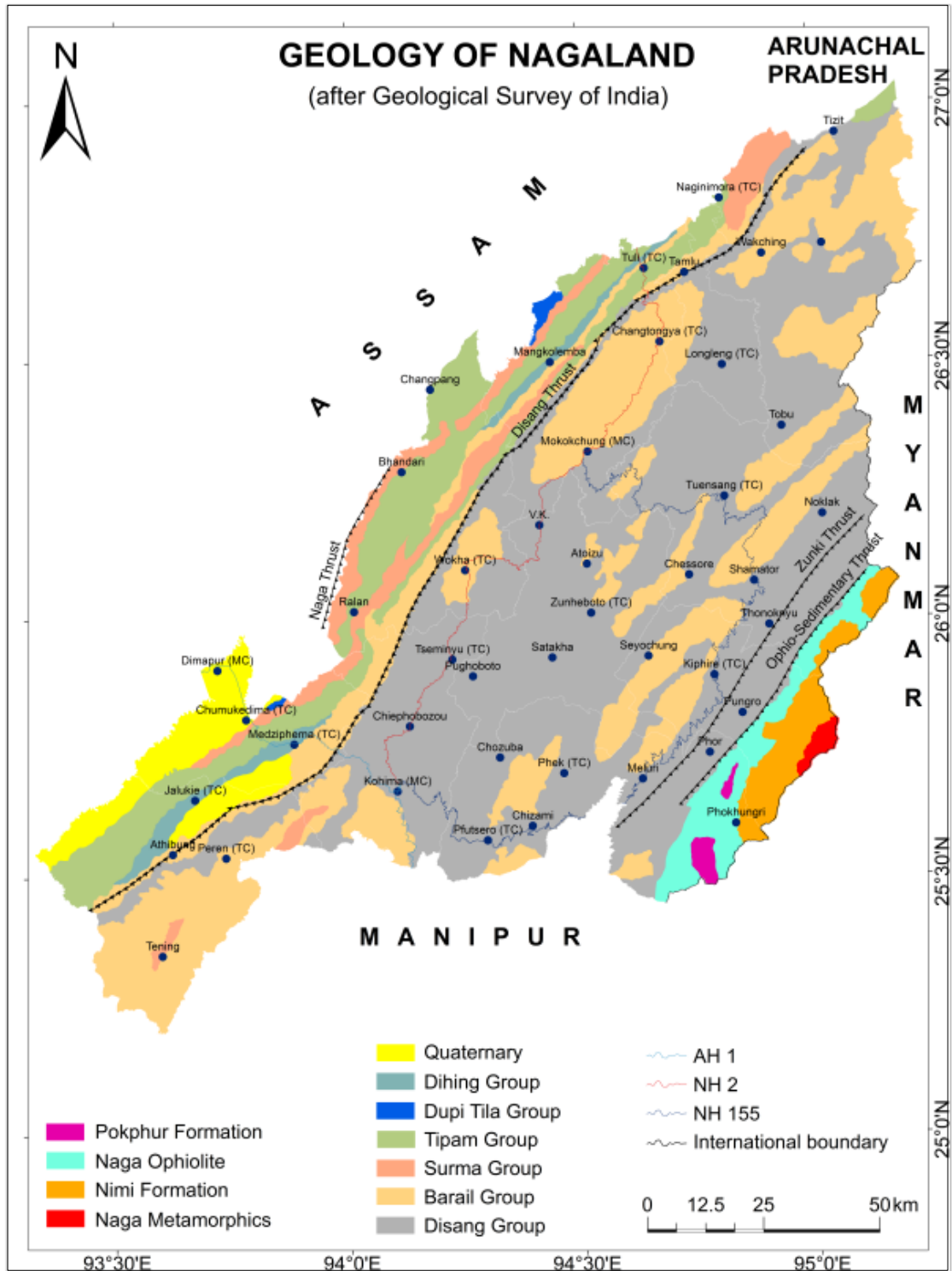


**Fig. 3:** Geological map of Nagaland (After GSI, 2011)

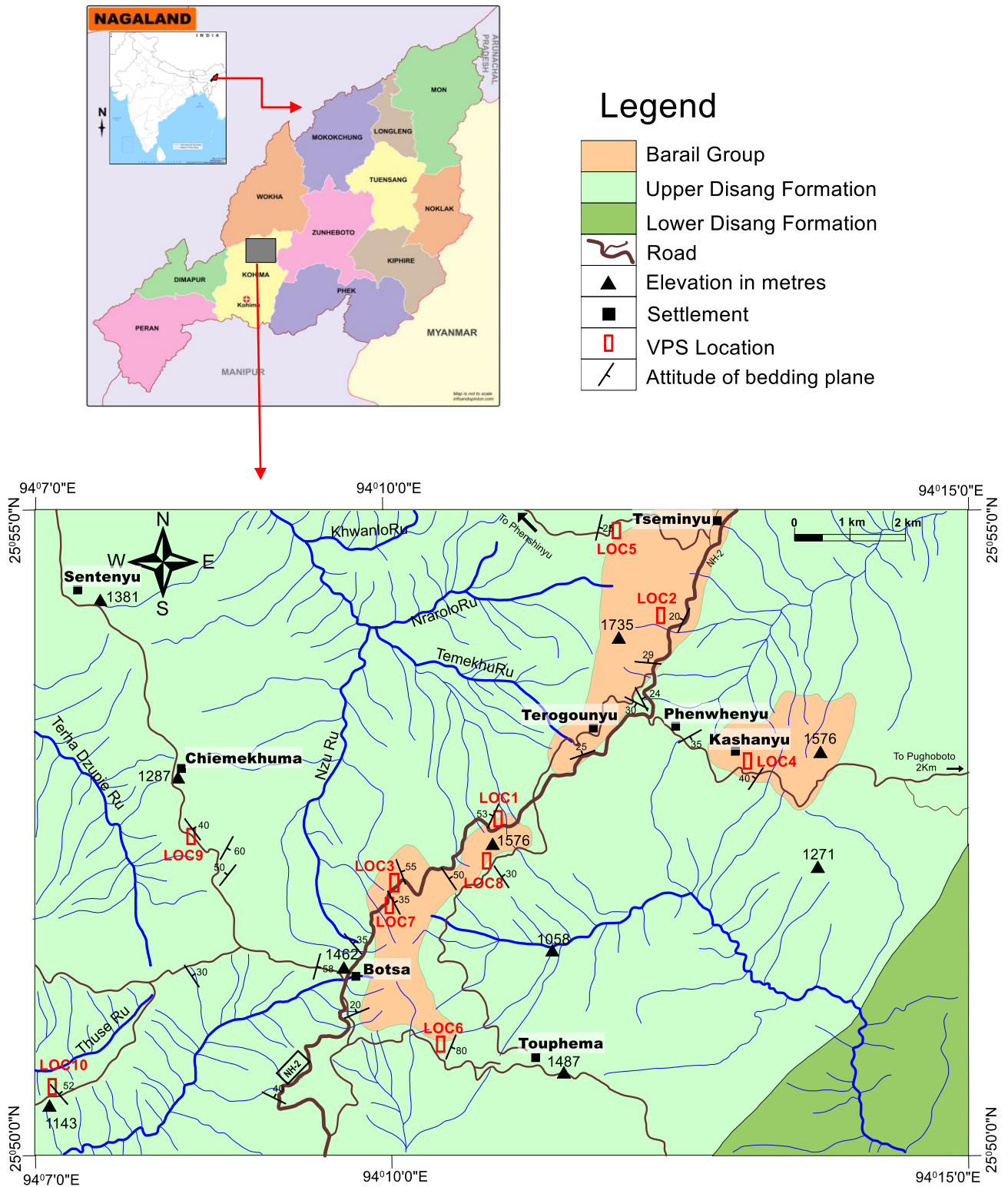


Fig. 4: Geological map of the study area (After GSI, 1988)





**Plate 1:** Field photographs showing a) Exposure of shales c) Multistoried sandstone beds



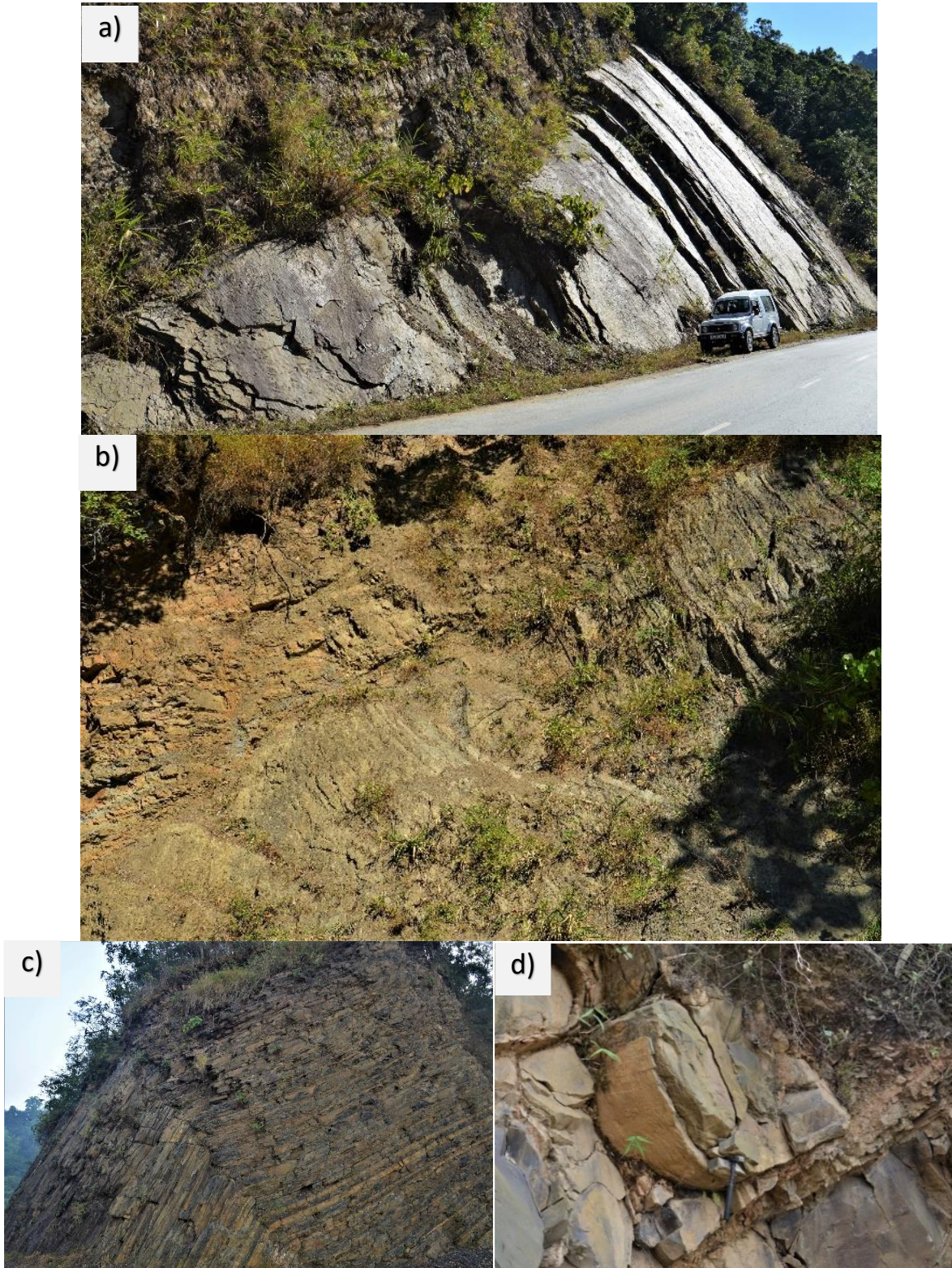


**Plate 2:** Field photographs showing **a)** Limb of a fold **b)** Fault **c)** Symmetrical fold  
**d)** Exfoliation in sandstone



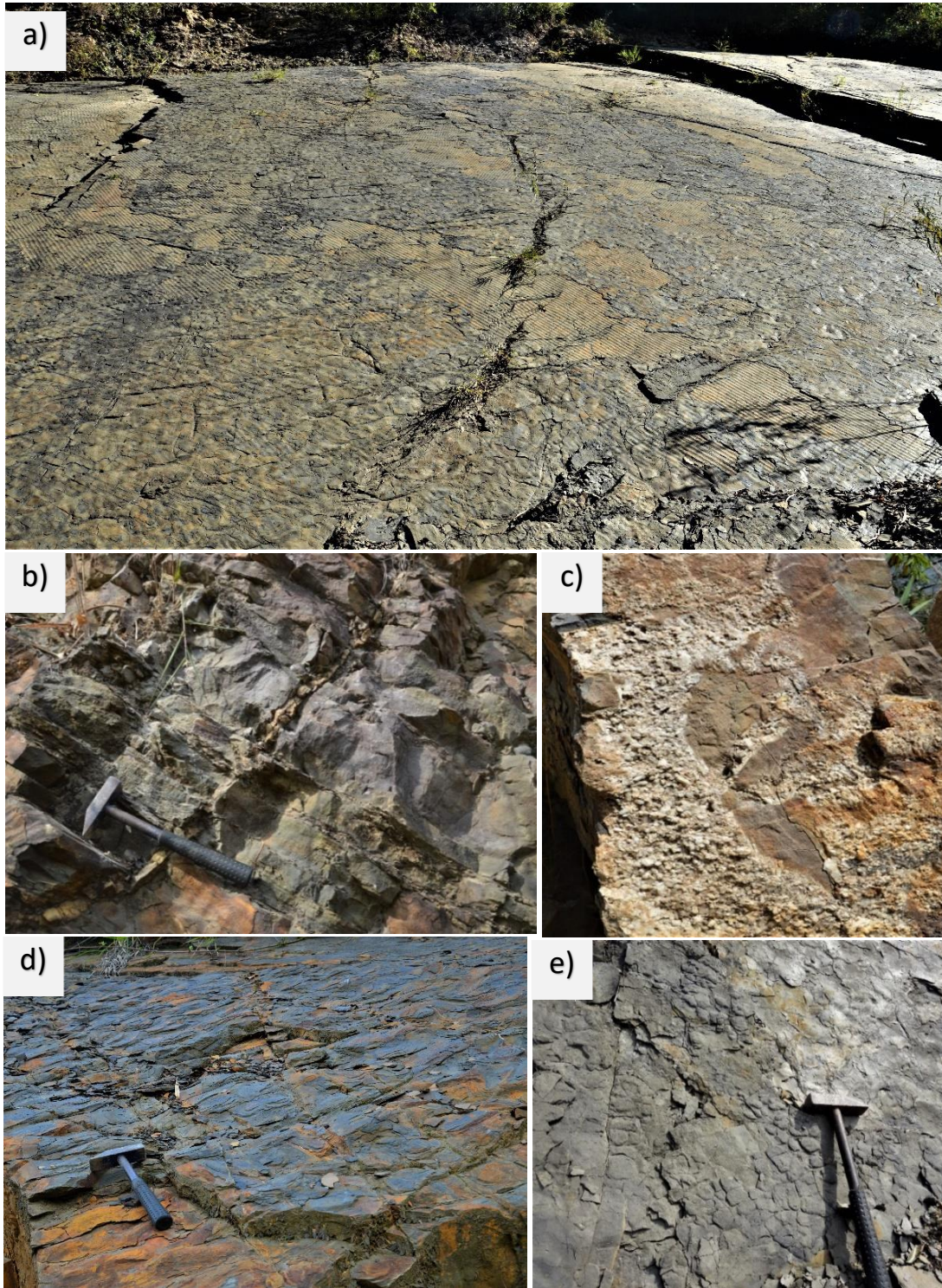


**Plate 3:** Field photographs showing a) Intensely bioturbated surface b) & c) Quartz vein d) & e) Box-work type of weathering in shales

## **CHAPTER 3**

# **LITHOLOGIC DISTRIBUTION, VERTICAL PROFILE SECTIONS AND LITHOFACIES**

### **3.1 GENERAL**

‘Sedimentary facies’ is a distinctive rock unit with specified characteristics that reflect the condition under which it was formed (Reading and Levell, 1996). Description of facies involves documenting lithology, texture, colour, geometry, contained sedimentary structures, paleocurrent patterns and fossil content of a sedimentary rock unit. Facies analysis aids in determination of the process of formation. A facies, thus is the outcome of one or more of the several processes operating in a depositional environment. Recording the details of the stratigraphic successions, both in time and space, and their interpretation help in interpreting the palaeoenvironment. Walther (1894), recognized this and suggested that changes of lithofacies in space and time are sensitive indicators of depositional environment. Facies association, which is a group of facies occurring together in a sedimentary succession, help in ascertaining the combination of processes that were prevailing during the deposition. Nichols (2009) suggested that the facies associations and environment of deposition can be linked as the associations of various processes; provide information on the depositional environment. Studies on the modern sedimentary environments have enhanced the utility of facies analysis in reconstruction of the ancient sedimentary environment (Reineck and Singh, 1980). Such studies have also been considered by Visher (1965), LeBlanc (1972), Selley (1976) and Reading (1978).

### **3.2 PARAMETERS OF SEDIMENTARY FACIES**

A ‘facies’ is defined by a set of parameters including bed geometry, lithology and grain-size, sedimentary structures including biogenic, paleo-current patterns, and fossil contents (Selley, 1970; 1976). These parameters are indicators of the depositional environment.

#### **3.2.1 GEOMETRY**

In the study area, beds with sharp contacts are observed and the exposures of various litho-

units in vertical sections at many locations form the basis for description of lithofacies. They are showing lateral extension and exhibiting a shoestring bedding geometry.

### 3.2.2 LITHOLOGY AND GRAIN-SIZE

The nature of source terrain, mechanism of transportation and the depositional environment can be interpreted by studying the mineralogy and textures of siliciclastics sedimentary rocks. Grain size, an important attribute of siliciclastics, has been utilized by many as a tool for environmental analysis (Wentworth, 1922; Krumbein and Pettijohn, 1938; Sahu, 1964; Visher, 1969; Visher, 1970; Tucker and Vacher, 1980; Sahu, 1983). However, its application in environmental interpretation has been questioned by many workers (Pettijohn, 1975; Selley, 1976; Friedman and Sanders, 1978; Walton, *et al.*, 1980; Reineck and Singh, 1980). Grain size analysis for environmental applications also suffer from limitations such as post depositional changes (Ghosh and Chatterjee, 1994).

In the study area, the grain size variations within the Palaeogene sediments range from clay to silt size and very fine to medium sand size fractions. The grain size in litho-columns exhibits coarsening as well as fining upward trends.

### 3.3.3 SEDIMENTARY STRUCTURES

Allen (1982), and Collinson and Thompson (1994) have described sedimentary structures as important features of sedimentary rocks since they provide information on the hydraulic conditions. They help not only in understanding the processes that produce them but also the depositional environment in which they are formed. Certain sedimentary structures can also help to deduce the way-up strata especially in areas of intensely folded rocks.

In the study area, varied primary and post depositional features as well as biogenic structures were observed. Primary sedimentary structures recorded include planar laminations, cross-stratification, hummocky cross stratification, channels, asymmetrical and symmetrical ripples, interference and bifurcating ripples and bioturbated mud layers. The presence of these structures helps in understanding the depositional processes involved during sedimentation of these sediments.

### 3.2.4 PALAEOCURRENTS

Palaeocurrent is an important attribute in lithofacies interpretation and the measurement of palaeocurrents provide information on the palaeogeography, palaeoslope, current and wind directions. The direction of flow at the time of sedimentation also referred to as the palaeoflow is another basic requirement in the determination of palaeoenvironmental studies from primary sedimentary structures and various scalar features of the rock. Basic information on the palaeocurrent for specific and general environments and their usefulness in reconstructing the environment is provided by Allen (1966, 1967) and Selley (1968).

In the present study, an attempt has been made to deduce the palaeocurrent directions from suitable sedimentary structures recording the direction of movement of the current as well as the trend of the movement of the current.

### 3.2.5 BIOGENIC STRUCTURES/ FOSSILS

Fossils are important element of sedimentary rocks and it provides great use in interpreting the depositional environment as they reflect the environment in which organism had lived. However, all the sedimentary strata don't contain body fossils; in such cases biogenic sedimentary structures play a very important role. Biogenic sedimentary structures are preserved behavioral activities of organism and their presence play a significant role in environmental interpretations specially where body fossils are sparse or absent (Frey, 1975). They are important in providing significant information on the rate of sedimentation, hydrodynamic conditions, oxygenation level, salinity, availability of food, and environment induced stress. Many workers (Howard, 1972; Ekdale *et al*, 1984; Savrda and Bottjer, 1986; and Knaust, 2017) have signified their application as paleoenvironmental indicators.

In the study area, many groups of trace fossils have been documented. Sediments of the area also show various degree of bioturbation. Intensely bioturbated mud is found to be underlain by sandstones.

## 3.3 DESCRIPTION OF SEDIMENTARY STRUCTURES

In the study area, a number of primary sedimentary structures, varying in scale and



geometry, were documented, identified and grouped into four categories; namely depositional, erosional, post-depositional and biogenic (Tucker, 1993).

### 3.3.1 DEPOSITIONAL SEDIMENTARY STRUCTURES

Depositional sedimentary structures are formed during the time of deposition and are generally found on the upper surface of the bed and also within them. The sedimentary structures observed in the area includes bedding, planar lamination, cross-stratification, hummocky cross-stratification and ripple marks.

#### 3.3.1 (A) Bedding

Beds are tabular or lenticular layers of sedimentary rocks that are produced by changes in the pattern of sedimentation characterized by change in the grain size, colour and composition. The measurement of the thickness of a bed is a significant parameter. The Palaeogene sediments of the area display variations in bed thickness, ranging from thinly bedded (few cm) to thickly bedded. Plane beds are generally formed under variety of conditions. During the course of measurements variations within bed thickness has been noticed. upward increase as well as decrease in bed thickness was observed (**Plate 4a**).

#### 3.3.1 (B) Planar Lamination

Planar laminations are internal structures that are parallel to the bedding surface. The sedimentation units are less than 1 cm. in thickness occurring in sandstones as well as mud dominated layers. Laminae can form by a number of mechanisms including alternation of grain size caused by variations in the competency of current. The recorded structures are few millimeters in thickness displaying periodic patterns (**Plate 4b**).

#### 3.3.1 (C) Cross-Stratification

Cross-stratification are internal structures where the stratification dips at an angle to the principal bedding direction. Cross-stratification forms either as a single set or several sets termed as cosets within one bed. Migrating sand waves can also produce cross stratification. In the study area, the occurrence of cross-stratification may be considered as an uncommon feature. Nonetheless, their preservation forms the basis for interpreting the changing energy conditions

through time (**Plate 4c & 4d**).

### 3.3.1 (D) Hummocky Cross-Stratification

Hummocky cross-stratification is a type of cross-stratification characterized by gently undulating low angle sets of cross laminations with convex upward hummock and concave downward swales. In the study area, micro hummocky cross-stratification is recorded reflecting it to be the result of storm generation (**Plate 4e**).

### 3.3.1 (E) Ripple Marks

Ripple marks are among the most common sedimentary structures preserved on the bedding surfaces and common in sand size sediments but can also occur in fine and coarser sediments. Ripple marks provide useful information about the palaeoflow conditions and palaeocurrent direction. Their migration under conditions of net sedimentation, give rise to various types of cross-stratification. In the study area, wave formed ripples or symmetrical ripples occur in sandstones as well as mudstones (**Plate 5a, 5b, 5e & 5f**). the crest of wave formed ripples is generally straight and the bifurcation of the crests is common (**Plate 5a, 5e & 5f**). Interference ripples are also recorded on sandstone beds indicating the existence of two successive current directions (**Plate 5c & 5d**). Small crested asymmetrical ripples were also recorded in the study area (**Plate 6a, 6b & 8c**).

## 3.3.2 EROSIONAL SEDIMENTARY STRUCTURES

### 3.3.2 (A) Channels

A turbulent flow over a deposited sediment results in partial removal of sediments commonly known as channels. They are recognized by their cross-cutting relationship with underlying sediments and show a concave-up profile (**Plate 6c**). Channeled sediments are generally coarser than the sediments below or adjacent.

## 3.3.3 POST DEPOSITIONAL SEDIMENTARY STRUCTURES

Post depositional sedimentary structures are sediment deformation occurring at the time of deposition or shortly thereafter through mass movement of sediments and through internal reorganization by dewatering and loading. In the study area, structures documented include load



casts (**Plate 6e & 6f**) and intraclasts (**Plate 6d**). Load casts occurring are irregular protuberances on the soles on sandstone beds that overlie shales.

### 3.3.4 BIOGENIC SEDIMENTARY STRUCTURES/ TRACE FOSSILS

These are structures preserved in sediments due to the activities of organisms. Such organically produced markings are called trace fossils, also referred to as ichnofossils. They are resulted from burrowing, boring, feeding, resting and locomotion activities of organisms. The disruption of sediments due to the activity of organisms commonly referred to as bioturbation (**Plate 7b & 7e**) is a common occurrence in the study area and the bioturbation index grading from 1 to 4 (Tucker, 1989). The trace fossils identified are observed on the top of the bedding surface. Ethologically, they are either domichnia or fodinichnia and belong to *Skolithos* and *Cruziana* ichnofacies, however, a few of them also belong to *Nereites* ichnofacies.

In the present study 12 ichnogenera comprising of 14 ichnospecies were identified. The descriptions of the identified trace fossils in the study area are as follows:

***Chondrites intricatus* (Brongniart, 1828):** These are endichnial, full relief traces showing plant-like dendritic pattern. These are smooth walled burrow systems penetrating downward and are generally straight. Width of the tunnel is about 0.2 cm which remains constant throughout. Angle of branching is less than 45° with second- and third-order branching. This has been documented from the mudstone and very fine grain sandstone beds (**Plate 9a & 9c**).

***Cruziana aegyptica* (Sielacher, 1990):** Small convex bilobate trials preserved as positive hyporelief, formed by two parallel to sub-parallel asymmetric ridges that is separated by a median line. Trial varies from straight to curved meandering extending upto 11 cms long, 0.8 cms wide and 0.2 cms high. Striae within the lobes are rarely present, mostly smooth (**Plate 11e**).

***Diplocraterion* isp. (Torell, 1870):** *Diplocraterion*, preserved in full relief, is characterized by vertical U-shaped protrusive burrows with spreiten. The specimens on the bedding planes are dumb-bell shaped with two vertical openings joined by a lamina of reworked material. Entire length of vertical tubes of the specimens is not visible, and only top bedding plane view is present. Burrow fills are similar in composition to host rock. Tubes are 0.5cm in diameter and the distance between the tubes are 1.5 – 2 cm. This has been recorded from very fine grain sandstone beds

(Plate 9d).

***Lockeia siliquaria* (James, 1879):** Hypichnial preservation of small almond shaped protuberance, aligned parallel to sub-parallel to each other, with tapering at one end and obtuse at other. Surface is smooth; some specimens show corrugated lateral sides. Burrow fill is identical to the host rock. Most burrows occur in isolation or in groups of three or more. Observed specimens show a maximum length of 7-10mm and width is 4-5mm. Large specimens display hypichnial ridges. This ichnospecies is recorded from very fine grain sandstone beds (Plate 9d).

***Monocraterion* isp. (Torell, 1870):** *Monocraterion* isp. is vertical burrow with a funnel-shaped opening; the vertical structure is perpendicular to the bedding plane and ranges from 1-4 cm in diameter. They are unbranched with a central vertical tube. This is documented from very fine grain sandstone (Plate 9f).

***Nereites* isp. (Weller, 1899):** Unbranched, irregularly winding/meandering trail of about 5 - 15 cm length and upto 5 mm wide, composed of a central zone having a meniscate structure, a lobate lower part surrounded by a bounding zone and a smooth upper part where laminations are poorly visible in the lobes. These are found to be associated with mudstone (Plate 11a & 11b).

***Palaeophycus tubularis* (Hall, 1847):** *Palaeophycus tubularis* occur as straight and unbranched burrows, cylindrical in cross-section, oriented horizontal to inclined in burrows with thin burrow lining. Burrow wall unornamented with sediment fill identical to host rock. The diameter of the burrow ranges between 1-1.2cm and the length ranges between 3-5 cm. This ichnospecies is found to be associated with siltstone (Plate 9c).

***Planolites beverleyensis* (Billing, 1862):** The burrows are straight, unbranched, cylindrical in cross-section, unlined, smooth walled, and parallel to the bedding plane. Length of the burrow varies between 6-8 cm and diameter ranges between 4-6mm. this ichnospecies are occurring in shales and very fine grain sandstones (Plates 8b, 9d, 9e & 11d).

***Rusophycus aegypticus* (Sielacher, 1990):** Heart shaped bilobate, segmented into two lobes that are joined by a median line, consisting of double ridges in the form of a delicate bioglyph of ridges. It is approximately 1.6 cms long and 0.8 cms wide. The anterior end is semi-circular while the posterior end tapers down. Stiae within the lobes are rarely present, mostly smooth (Plate

**11e).**

***Scolicia plana* (Książkiewicz, 1970):** Preserved as composite winding epirelief form, with meandering to coiling bilobated trail. The length of the trail is 10 cm to 50 cm and width is 2cm to 6 cm wide. Locally discontinuous but parallel sediment strings on the lower side. Trails are smooth convexed dissected by a narrow central furrow. According to Uchman (1998), *Scolicia* with flat median ridge divided by shallow furrow or crest is identified as *Scolicia plana*. This ichnospecies is recorded from very fine grain sandstone (**Plate 10f & 11c**).

***Scolicia prisca* (Quatrefages, 1849):** Endichnical, meandering burrow trace occurring as ribbon, parallel to the bedding plane. The burrow morphology consists of central furrow flanked by two ridges. Trails extend from 70 cm up to 185 cm, width of the trail is 2.9 cm. The burrow material is coarser than the surrounding rock. This ichnospecies is recorded from mudstone and very fine grain sandstone (**Plate 10a, 10b, 10c & 10d**).

***Skolithos verticalis* (Hall, 1843):** These are endichnial cylindrical to sub-cylindrical, unbranched burrows with smooth walls. Burrows are straight to slightly curved and oriented perpendicular to the bedding plane. Burrow diameter ranges from 5–8mm. Burrow fills are similar to the host rock. On the bedding surface they appear as circular marking. This is documented from siltstone facies (**Plate 8g, 9c, 9d & 9f**).

***Thalassinoides suevicus* (Reith, 1932):** These are unornamented, smooth walled, three-dimensional burrows. The burrow systems show networks of Y-shaped branching with occasional enlargements at bifurcation points. The vertical shafts of the burrows are straight to curved, while horizontal tunnels bifurcate at angles between 45°- 140°. Width of the burrows reach up to 3cm while length ranges from 40- 80 cm. Burrow fill is similar to the host rock. They are found to be associated with fine grain sandstones as well as mudstones (**Plate 8d & 10f**).

***Thalassinoides horizontalis* (Myrow, 1995):** *Thalassinoides horizontalis* is a smooth, unlined, three-dimensional horizontal burrow system. The burrow system is dominated mainly by horizontal tunnels, that are straight to slightly curved with a constant diameter. Length of the tunnel is 2.5 - 4.5 cm and diameter is 0.3 cm. The tunnels bifurcate at an angle of 80°-120°. They are recorded from very fine grain sandstones (**Plate 8e, 8f & 10e**).

### 3.4 FACIES SCHEME

To have a better sense of understanding of the lithologic variability in space and time, it is of utmost importance for us to generalize, simplify and also to categorize the field observations. As lithofacies analysis helps in understanding the depositional environments in which the sediments were deposited. Following that, a lithofacies scheme, based on the various parameters as suggested by Shelley (2000) such as lithology including grain size, primary sedimentary structures, bed geometry, fossils /trace fossils and palaeocurrent and also on the observations made in the field on ten (10) vertical profile sections, was developed. In the study area outcrops were systematically measured, and trace fossil horizons and sedimentary structures were recorded to describe the lithologic variations within the Palaeogene sediments. Altogether six lithofacies were identified. The lithofacies together with their respective codes and their probable environment is given in **Table 2**. Facies codes are taken from Miall (1990).

### 3.5 DESCRIPTION OF LITHOFACIES IN THE STUDY AREA

1. *Very fine to medium massive sandstone facies (Sm)*: This facies is characterized by very fine to medium grained sandstone. The thickness of the sandstone beds ranges from 1 meter up to 5 meters thick (**Plate 7a**). This facies has been recorded at higher stratigraphic levels only.
2. *Very fine to medium plane laminated sandstone facies (Fl)*: Very fine to medium grain sandstones with plane laminations showing color variations characterizes this facies (**Plate 7d & 7f**) and occasionally showing low angled cross laminations (**Plate 4c & 4d**). The thickness of the beds ranges from a few cm to 1 meter. The trace fossils identified from this facies are mostly horizontal in disposition. The recorded traces include *Thalassinoides horizontalis* (**Plate 8e, 8f & 10e**), *Planolites beverleyensis* (**Plate 8b**) and *Skolithos verticalis* (**Plate 8g**). Bioturbation activities are common features in this facies. This facies has been recorded from lower stratigraphic levels.
3. *Coarse silt to very fine sandstone facies (Fsm)*: This facies is characterized by coarse silt to very fine grained sandstones (**Plate 7c & 8a**). The most important sedimentary feature recorded from this facies is hummocky cross stratification (**Plate 4e**). Its thickness varies

between 0.10 m to 0.35 m thick. *Chondrites intricatus*, *Palaeophycus tubularis*, *Skolithos verticalis* and *Thalassinoides horizontalis* are the trace fossils recorded from this facies. Recorded from lower stratigraphic levels only.

4. ***Rippled sandstone facies* ( $S_r$ ):** The lithology is represented by very fine to medium grained sandstones in this facies (**Plate 6a, 6b & 8c**). Asymmetrical ripple marks or current ripples are recorded from this facies. The thickness of the bed varies from 0.5m to a meter. Strong bioturbation activities are prominent in this facies. This facies has been recorded at higher stratigraphic levels.
  
5. ***Wave rippled siltstone facies* ( $S_{r_w}$ ):** This facies is represented by very fine to fine grained sandstones. Symmetrical ripple marks with strong bioturbation is recorded from this facies (**Plate 5a, 5b, 5e & 5f**). The presence of carbonized matter is also identified (**Plate 9b**). Thickness varies from a few cms to 2 meters. Symmetrical ripple marks with occasional bifurcation and interference ripples with mud drapes are the characteristic structures of this facies (**Plate 5e, 5f, 5c & 5d**). This facies is represented by *Chondrites intricatus*, *Cruziana aegyptica*, *Diplocraterion* isp., *Lockeia siliquaria*, *Monocraterion* isp., *Rusophycus aegypticus*, *Planolites beverleyensis*, *Scolicia plana*, *Scolicia prisca*, *Skolithos verticalis*, *Thalassinoides horizontalis* and *Thalassinoides suevicus*. This facies has been recorded at higher stratigraphic levels.
  
6. ***Mudstone facies* ( $F_m$ ):** This facies is represented by mudstones as well as shales with plane laminations (**Plate 7b, 7c, 7f & 8a**). Bioturbation is intense in this facies (**Plate 7b**). The facies shows degree of bioturbation ranging from BI-1 to 3, suggesting an increase bioturbation as compared to siltstone-sandstone facies. Trace fossils are dominated by horizontally oriented traces of *Chondrites intricatus*, *Nereites* isp. *Planolites beverleyensis*, *Scolicia plana* and *Thalassinoides suevicus*. Trace fossils recorded from this facies are all horizontal in disposition. The ichnofossil assemblage of this facies represents a mixed *Cruziana-Nereites* ichnofacies. This facies has been recorded from lower horizons only.

### 3.6 DESCRIPTION OF VERTICAL PROFILE SECTIONS (VPS)

In the study area, a total of 10 vertical profile sections were measured and meticulously studied

at different locations to establish the time and spatial distribution relationships of various lithofacies (**Fig. 6 to 15**). The sections of all thus studied are described briefly in the following subsections. The reference symbols used in constructing the vertical profile sections are shown in **Fig. 5**.

3.6.1 VPS 1 ALONG NH-2 7 KM FROM BOTSA (25° 52' 43.89" N, 94° 11' 04.32" E)

This VPS was measured along NH-2, 7 km from Botsa. It is characterized by the presence of *Sm* and *Fl* facies displaying an overall coarsening upward trend. The total thickness measured, corresponds to around 5 m (**Fig. 6**).

3.6.2 VPS 2 AROUND 2.5 KM FROM TEROGUNYU TOWARDS TSEMINYU (25° 54' 11.26" N, 94° 12' 24.35" E)

This vertical profile section was measured around 2.5 km from Terogunyu towards Tseminyu with a total thickness of 4.8 m. This section is characterized by *Sm*, *Fl*, *Fsm* and *Fm* facies. An overall coarsening upward trend exhibits this facies succession (**Fig. 7**).

3.6.3 VPS 3 AROUND 3 KM FROM BOTSA TOWARDS NORTH (25° 52' 10.33" N, 94° 10' 09.36" E)

Around 3 km from Botsa a 5 m thick vertical profile section was measured represented by *Fsm*, *Sr*, *Sr<sub>w</sub>* and *Fm* facies. This section displays a fining upward trend (**Fig. 9**).

3.6.4 VPS 4 NORTH-EAST OF NH-2 TOWARDS PUGHOBOTO (25° 52' 0.736" N, 94° 13' 0.425" E)

Towards Pughoboto, this road section measuring 6.9 m thick is characterized by *Sm*, *Fl* and *Fm* facies. The section displays a coarsening upward trend (**Fig. 8**).

3.6.5 VPS 5 TOWARDS PHENSHENYU FROM TSEMINYU (25° 54' 9.23" N, 94° 03' 0.66" E)

From Tseminyu towards Phenshenyu this vertical profile section was measured in a 7.8 m section. *Sm*, *Fl* and *Fsm* facies corresponds to this section. In this vertical profile section coarsening

upward trend was recorded (**Fig. 10**).

3.6.6 VPS 6 ON THE WAY TO TOUPHEMA FROM BOTSA (25° 50' 51" N, 94° 10' 1" E)

This vertical profile section was measured on the road section to Touphema from Botsa. *Sm*, and *Fl* facies comprises of this 6.35 m section displaying a fining upward trend (**Fig. 11**).

3.6.7 VPS 7 AROUND 2 KM FROM BOTSA TOWARDS NORTH (25° 52' 7" N, 94° 09' 57" E)

This 51 m section has been measured around 2 km from Botsa. This section is represented by *Sm*, *Fl*, *Fsm* and *Fm*. It displays an overall fining upward trend (**Fig. 13**).

3.6.8 VPS 8 3 KM FROM TEROGUNYU JUNCTION TOWARDS EAST (25° 52' 17.62" N, 94° 11' 6.65" E)

This Vertical profile section was measured 3 km from Terogunyu junction towards east direction. The lithofacies *Ss*, *Fl*, *HCS*, *Sn* and *Fm* are well represented here. The total thickness measured is 18.7 m displaying a fining upward trend. (**Fig. 12**)

3.8.9 VPS 9 TOWARDS SEDENYU FROM BOTSA (25° 52' 22.23" N, 94° 08' 20.4" E)

This section measuring 18.1 m in thickness is towards Sedenyu. *Fl*, *Fsm* and *Fm* facies represents this section. This succession exhibits a fining upward sequence (**Fig. 14**).

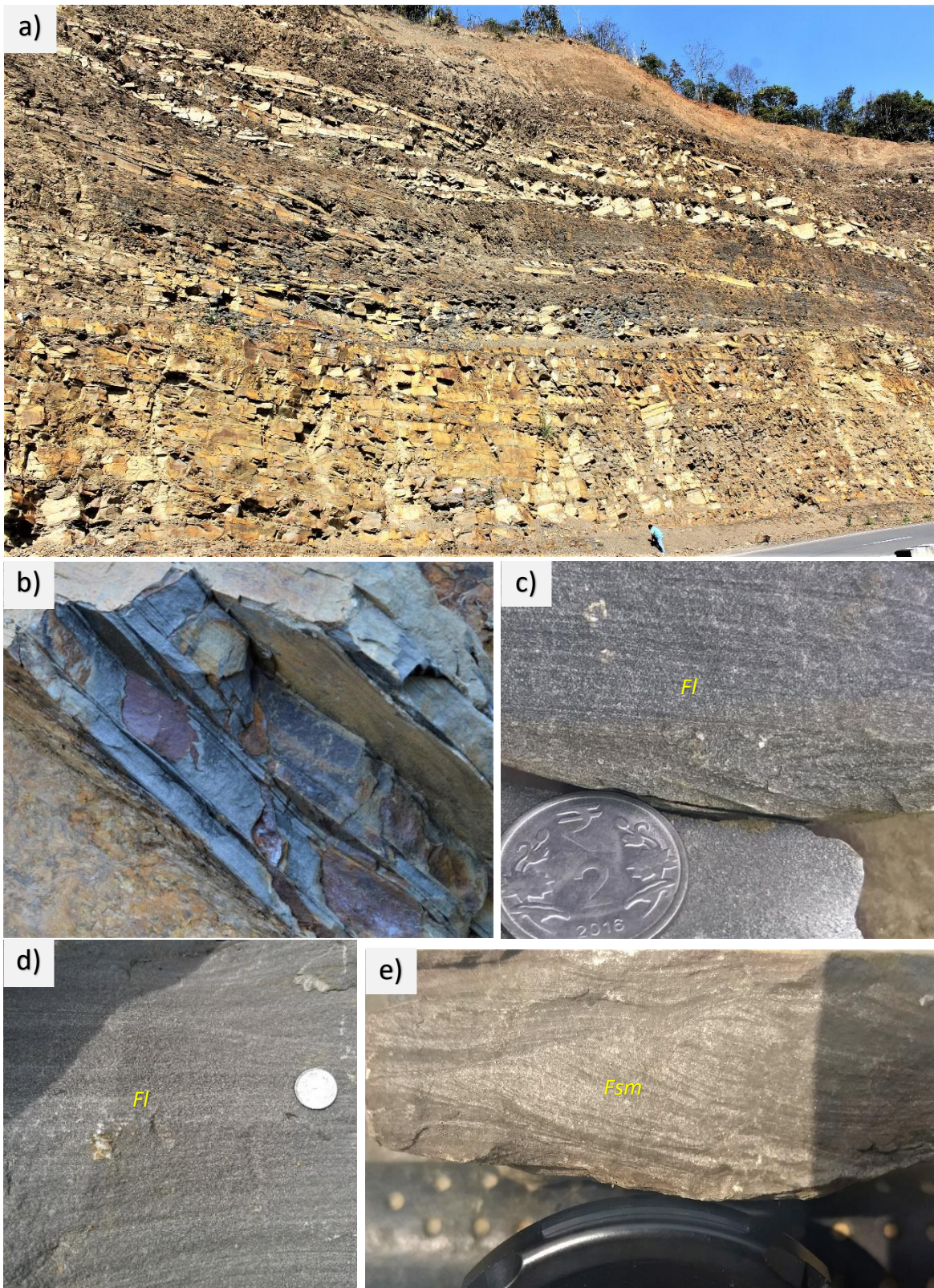
3.8.10 VPS 10 TOWARDS TEICHUMA FROM BOTSA (25° 50' 40.41" N, 94° 07' 22.5" E)

This 5.6 m thick section is towards Teichuma from Botsa. This section is characterized by *Sm*, *Sr*, *Sr<sub>w</sub>* and *Fm* facies exhibiting a fining upward trend (**Fig 15**).

<b>Facies code</b>	<b>Lithofacies</b>	<b>Sedimentary structures</b>	<b>Interpretation</b>
<i>Sm</i>	Very fine to medium massive sandstones	Thickly bedded massive sandstones	Upper shoreface, high energy
<i>Fl</i>	Very fine to medium plane laminated sandstones	Plane laminations, occasional low angled cross laminations, Horizontal bedding showing colour variations, horizontal and vertical trace fossils, bioturbation	Lower shoreface, low energy
<i>Fsm</i>	Coarse silt to very fine sandstones	Hummocky cross stratification, bioturbation, horizontal and vertical trace fossils	Storm deposits, below normal wave base, lower shoreface
<i>Sr</i>	very fine to medium grained sandstones	Asymmetrical ripple marks or current ripples, intense bioturbation	Tidal channels, upper shoreface
<i>Sr<sub>w</sub></i>	Very fine to fine grained sandstones	Symmetrical ripple marks, interference ripples, bioturbation, vertical and horizontal trace fossils/ traces dominant	Upper shoreface, wave action
<i>Fm</i>	Mudstones and shales	Bioturbation, plane laminations, tabular silt beds, horizontal trace fossils	Offshore-transition

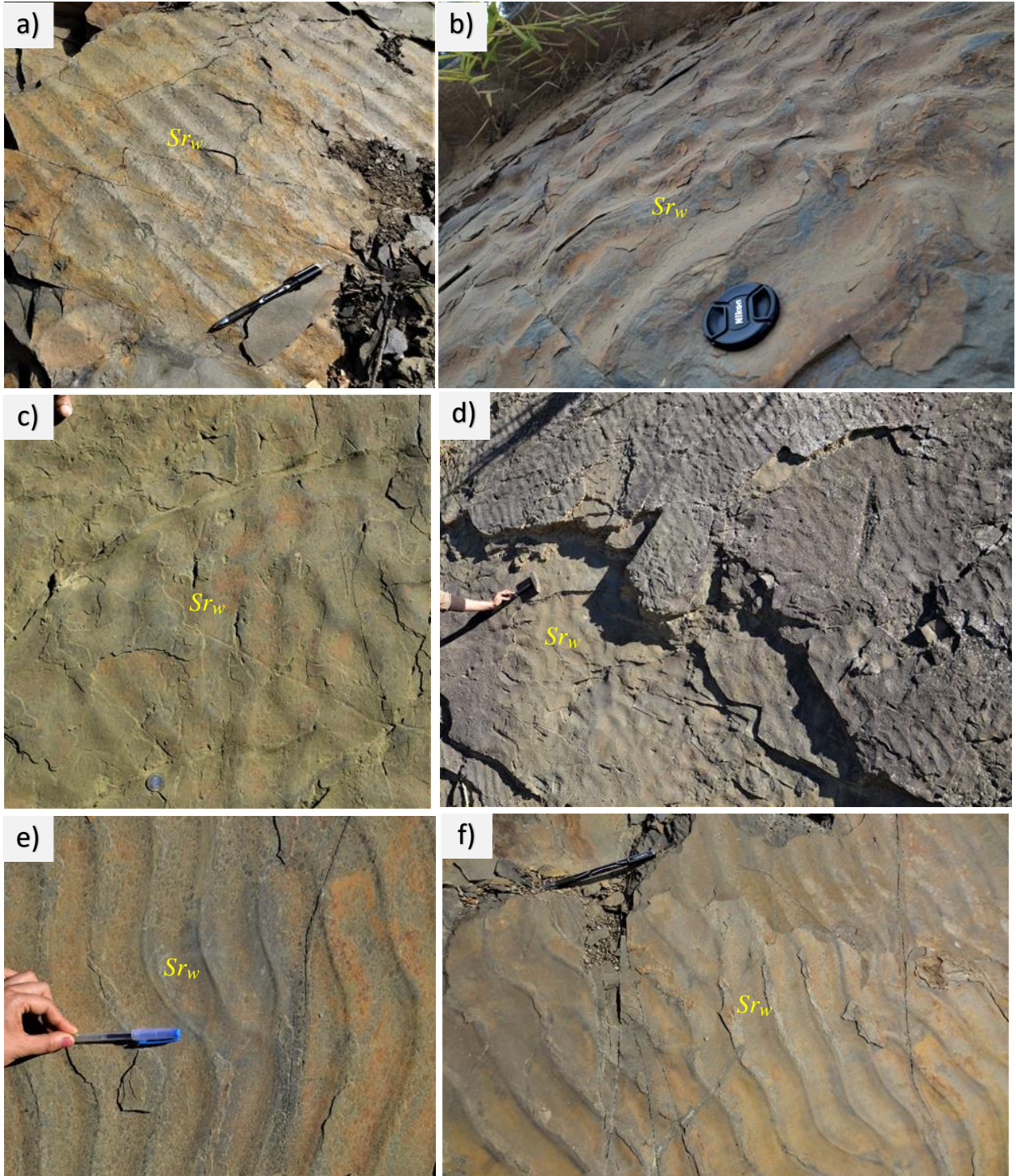
**Table 2:** Lithofacies scheme for the Palaeogene sediments of the study





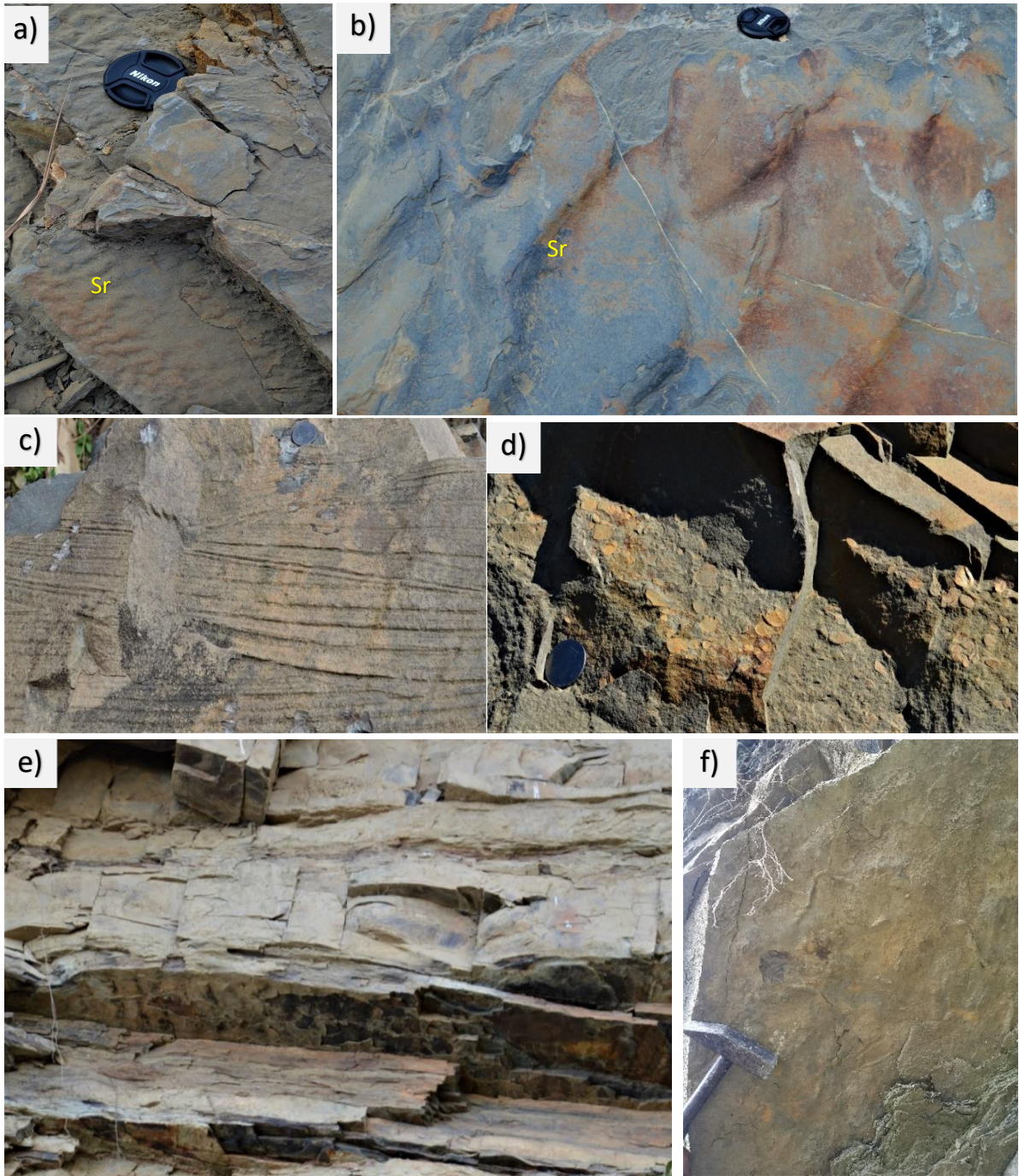
**Plate 4:** Field photographs showing **a)** Lateral extension of beds with varying thickness **b)** Planar lamination **c) & d)** Low angle cross-stratification (*Fl*) **e)** Hummocky cross-stratification (*Fsm*)





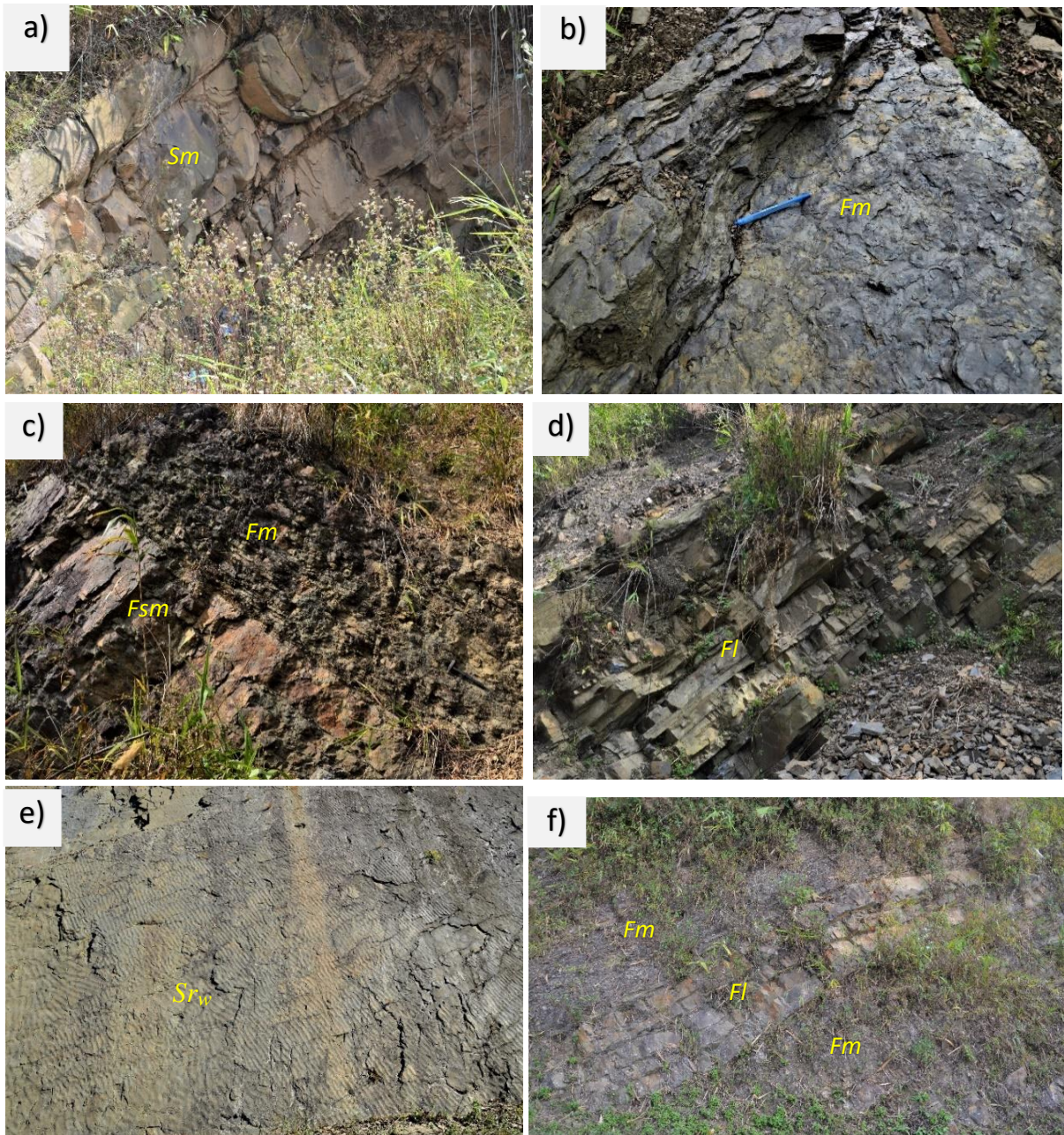
**Plate 5:** Field photographs showing **a)** Symmetrical/ Wave ripples with ripples bifurcating ( $Sr_w$ ) **b)** Symmetrical/ Wave ripples with high crest **c) & d)** Interference ripples **e) & f)** Bifurcating ripples in Symmetrical/ Wave ripples





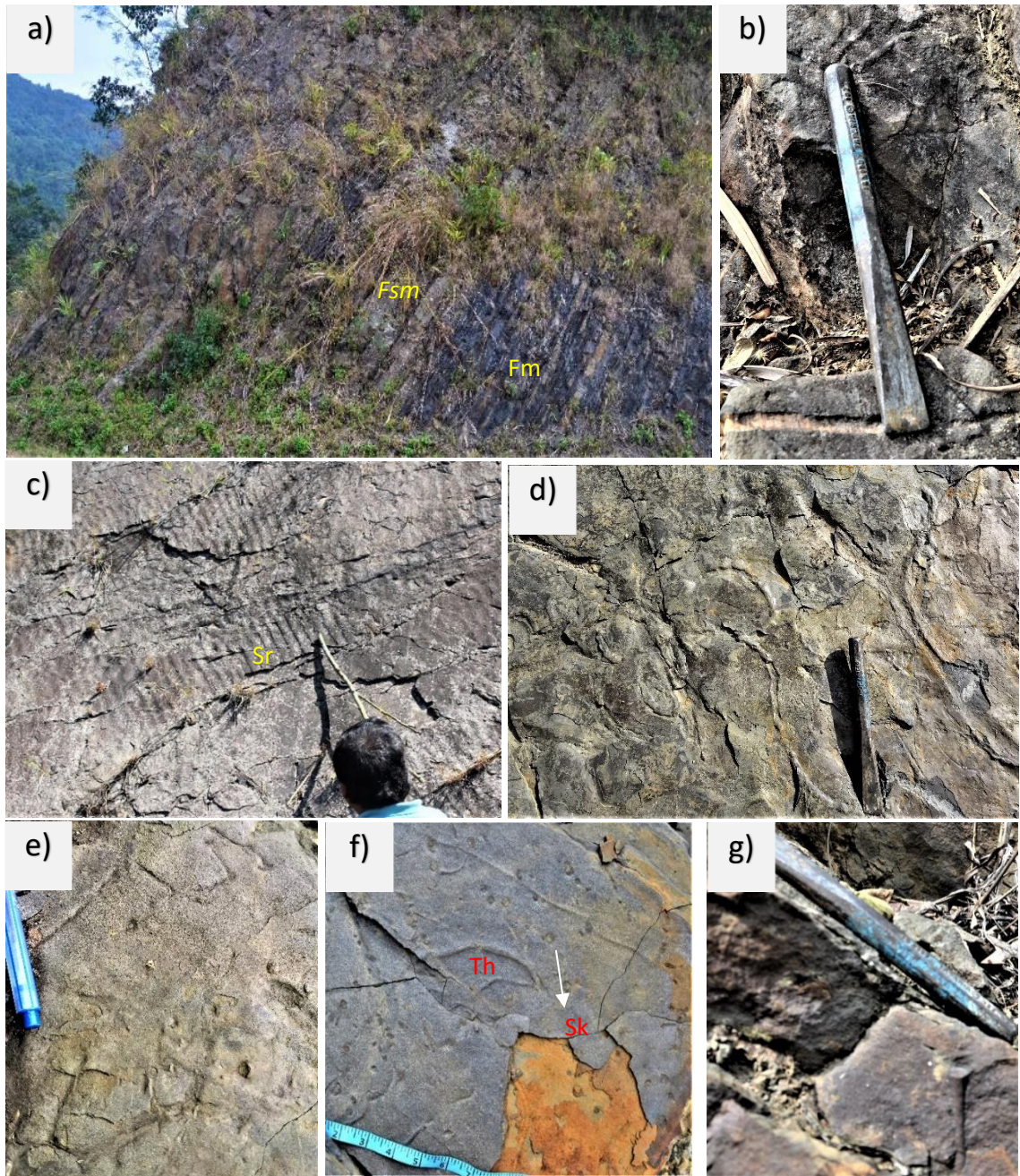
**Plate 6:** Field photographs showing a) & b) Assymetrical/Current ripples c) Channels  
d) Intraclasts e) & f) Load cast





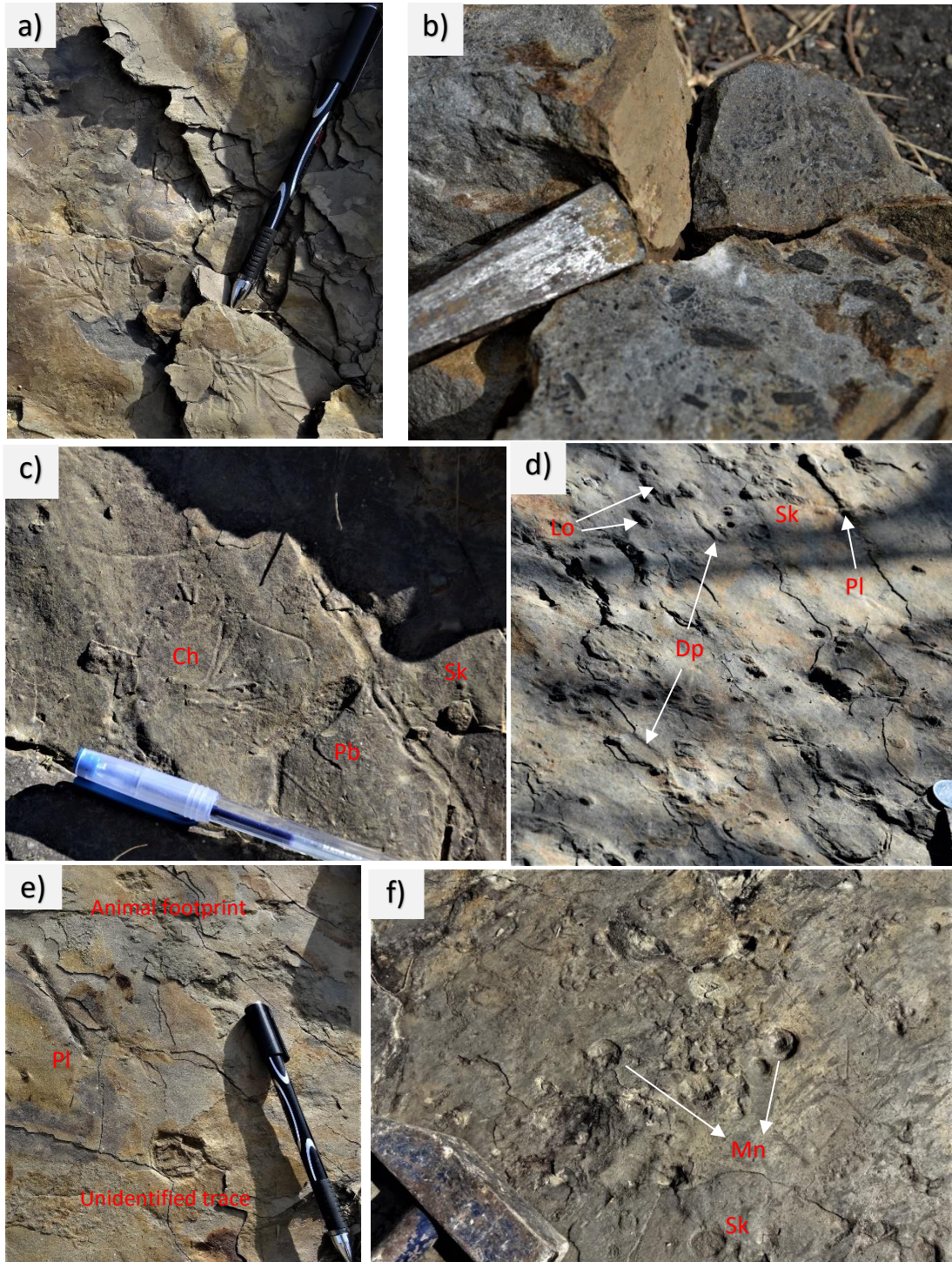
**Plate 7:** Field photographs showing **a)** Massive sandstone bed (*Sm*) **b)** Mudstone facies showing intense bioturbation (*Fm*) **c)** Fining upward sequence (*Fsm* & *Fm*) **d)** Plane laminated sandstone facies (*Fl*) **e)** Bioturbated ripple bedded sandstone facies (*Sr<sub>w</sub>*) **f)** Alternate coarsening and fining upward sequence (*Fm* & *Fl*)





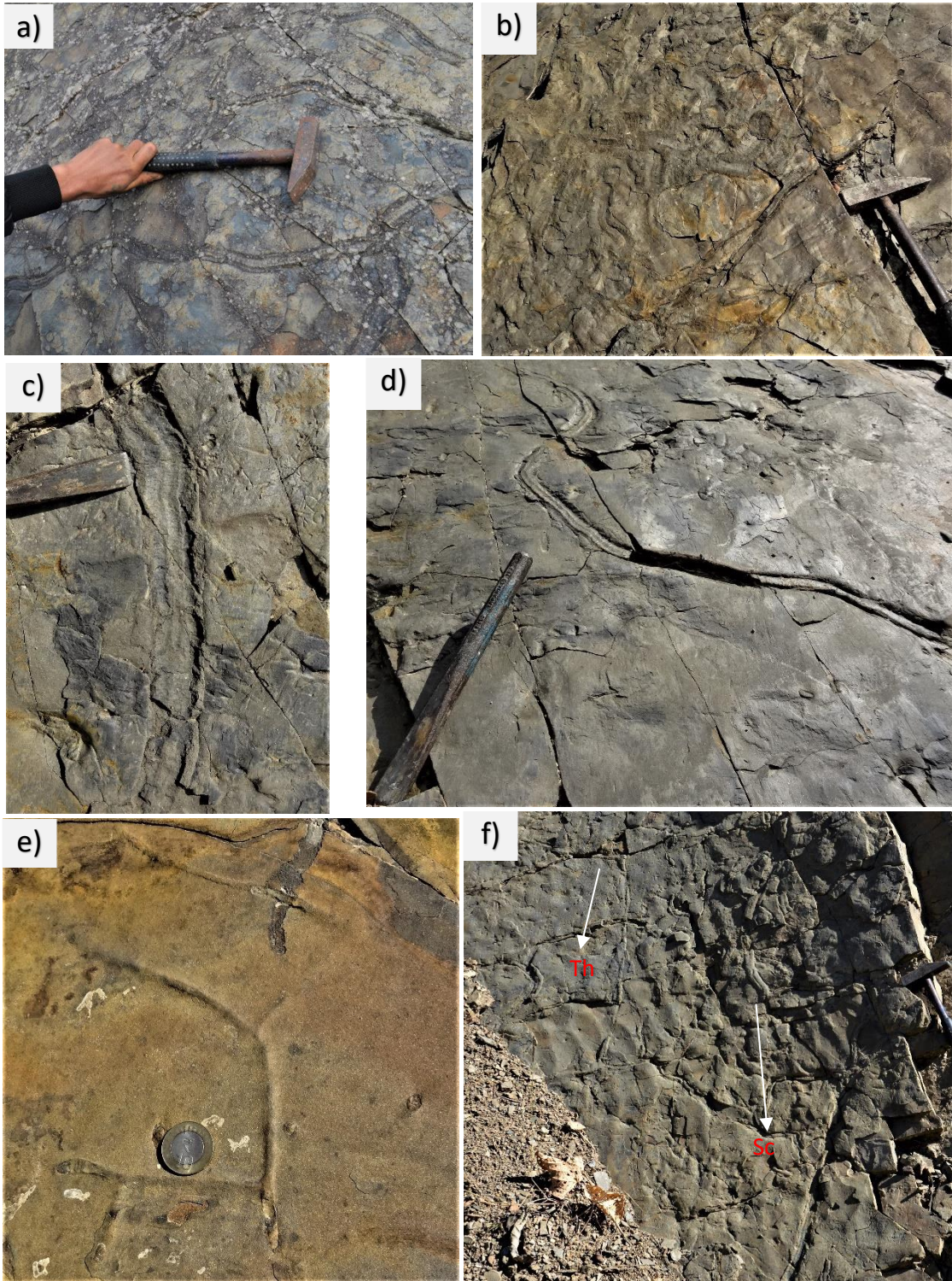
**Plate 8:** Field photographs showing **a)** Coarsening upward sequence **b)** *Planolites beverleyensis* **c)** Low crested asymmetrical ripple mark **d)** *Thalassinoides suevicus* **e)** & **f)** *Thalassinoides horizontalis* (Th), *Skolithos verticalis* (Sk) **g)** *Skolithos verticalis*





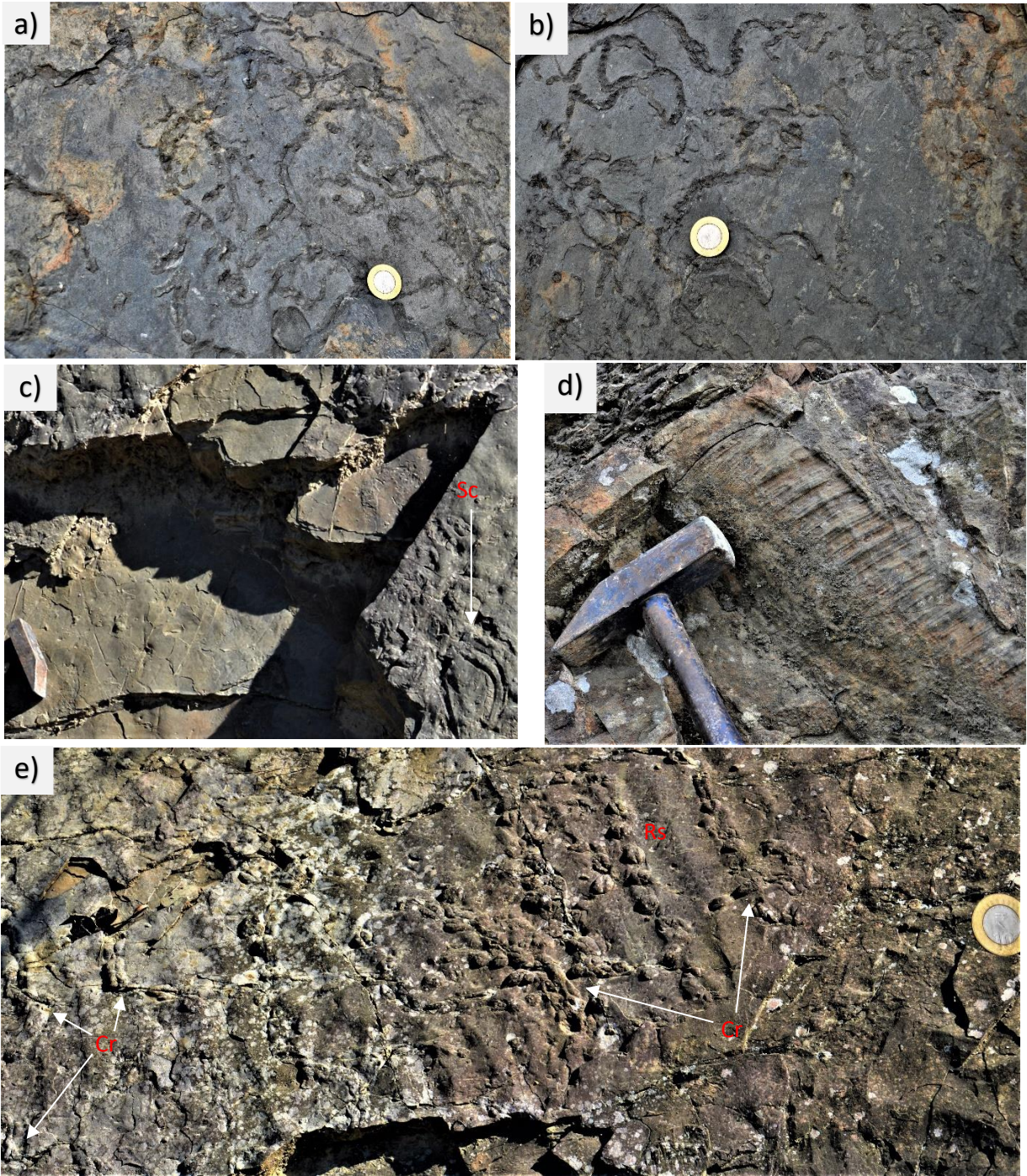
**Plate 9:** Field photographs showing a) *Chondrites intricatus* with endichnial traces b) Carbonised plant material c) *Palaeophycus tubularis* (Pb), *Chondrites intricatus* (Ch), *Skolithos verticalis* (Sk) d) *Diplocraterion* isp (Dp) dumb bell shaped trace, *Hypichnia* preserved *Lockeia siliquaria* (Lo), *Skolithos verticalis* (Sk) and *Planolites beverleyensis* (Pl) e) *Planolites beverleyensis* (Pl) f) *Skolithos verticalis* (Sk), Epichnial *Monocraterion* isp (Mn)





**Plate 10:** Field photographs showing **a) & d)** Trails of *Scolicia prisca* **b) & c)** *Scolicia prisca* showing coarser material than the host rock **e)** *Thalassinoides horizontalis* **f)** *Thalassinoides suevicus* (Th) and *Scolicia plana* (Sc)











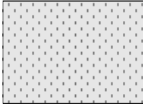
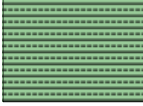
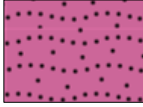
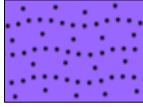
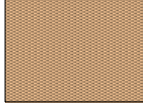
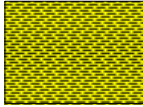





**Plate 11:** Field photographs showing **a) & b)** *Nereites* isp. **c)** *Scolicia plana* (Sc) **d)** *Planolites beverleyensis* (Pl) **e)** *Rusophycus aegypticus* (Rs), *Cruziana aegyptica* (Cr)




## Facies type

	Very fine to medium massive sandstone facies ( <i>Sm</i> )
	Very fine to medium plane laminated sandstone facies ( <i>Fl</i> )
	Ripple sandstone facies ( <i>Sr</i> )
	Wave rippled siltstone facies ( <i>Sr<sub>w</sub></i> )
	Coarse silt to very fine sandstone facies ( <i>Fsm</i> )
	Mudstone Facies ( <i>Fm</i> )

## Symbols used in VPS

	Planar lamination
	Cross bedding
	Symmetrical ripple marks
	Assymmetrical ripple marks
	Interference ripples
	Hummocky cross stratification
	Channels
	Load cast
	Carbonised matter
	Bioturbation
	Weathered material

## TRACE FOSSILS

	<i>Chondrite intricatus</i>
	<i>Cruziana aegyptica</i>
	<i>Diplocaterion isp.</i>
	<i>Lockeia siliquaria</i>
	<i>Monocraterion isp.</i>
	<i>Nereites isp.</i>
	<i>Palaeophycus tubularis</i>
	<i>Planolites beverleyensis</i>
	<i>Rusophycus aegypticus</i>
	<i>Scolicia</i>
	<i>Skolithos verticalis</i>
	<i>Thalassinoides</i>

**Fig 5:** Reference table for symbols used in vertical profile sections

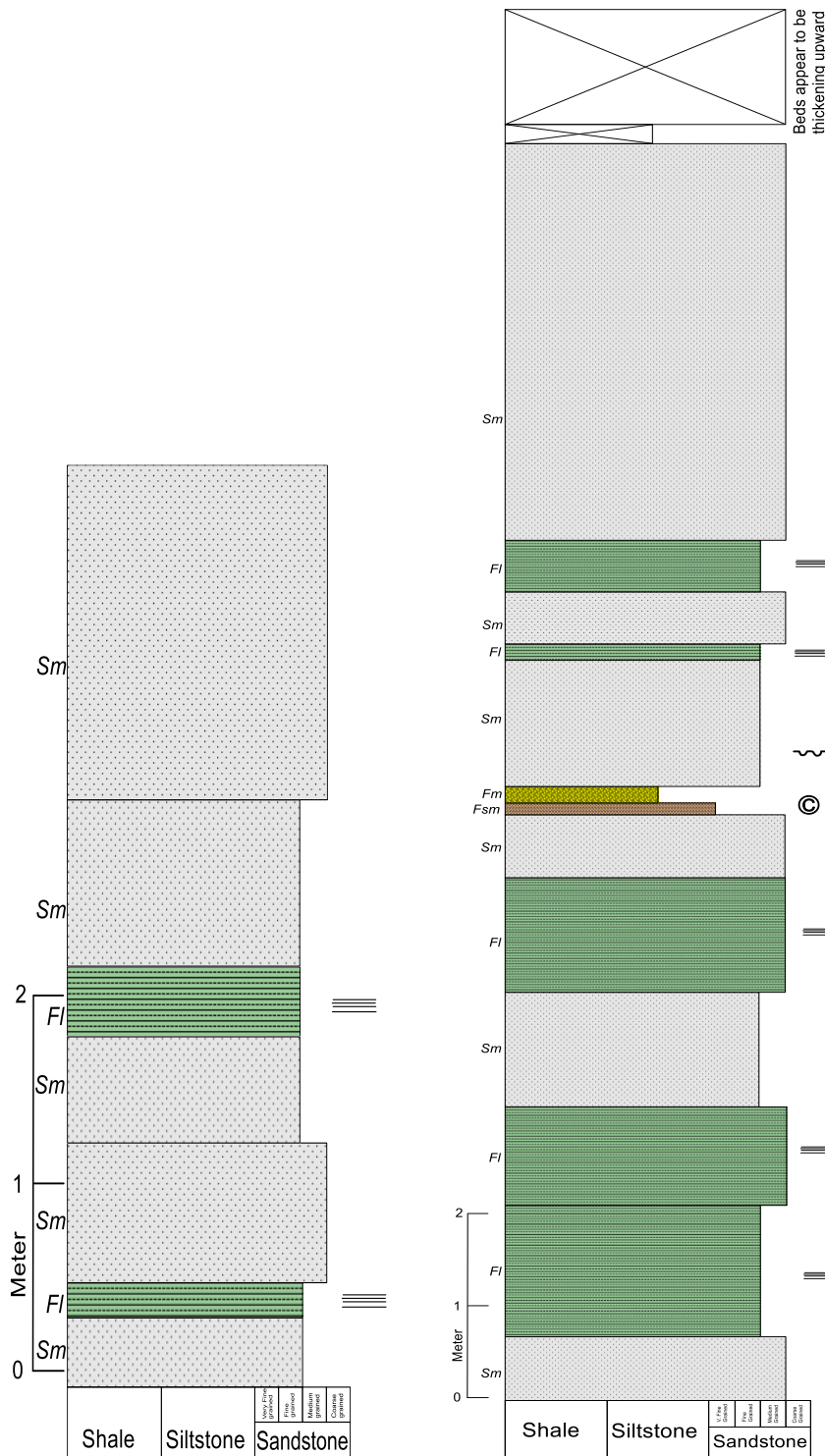


**Fig 6:** VPS 1 along NH-2, 7 km from Botsa (25° 52' 43.89" N, 94° 11' 04.32" E)

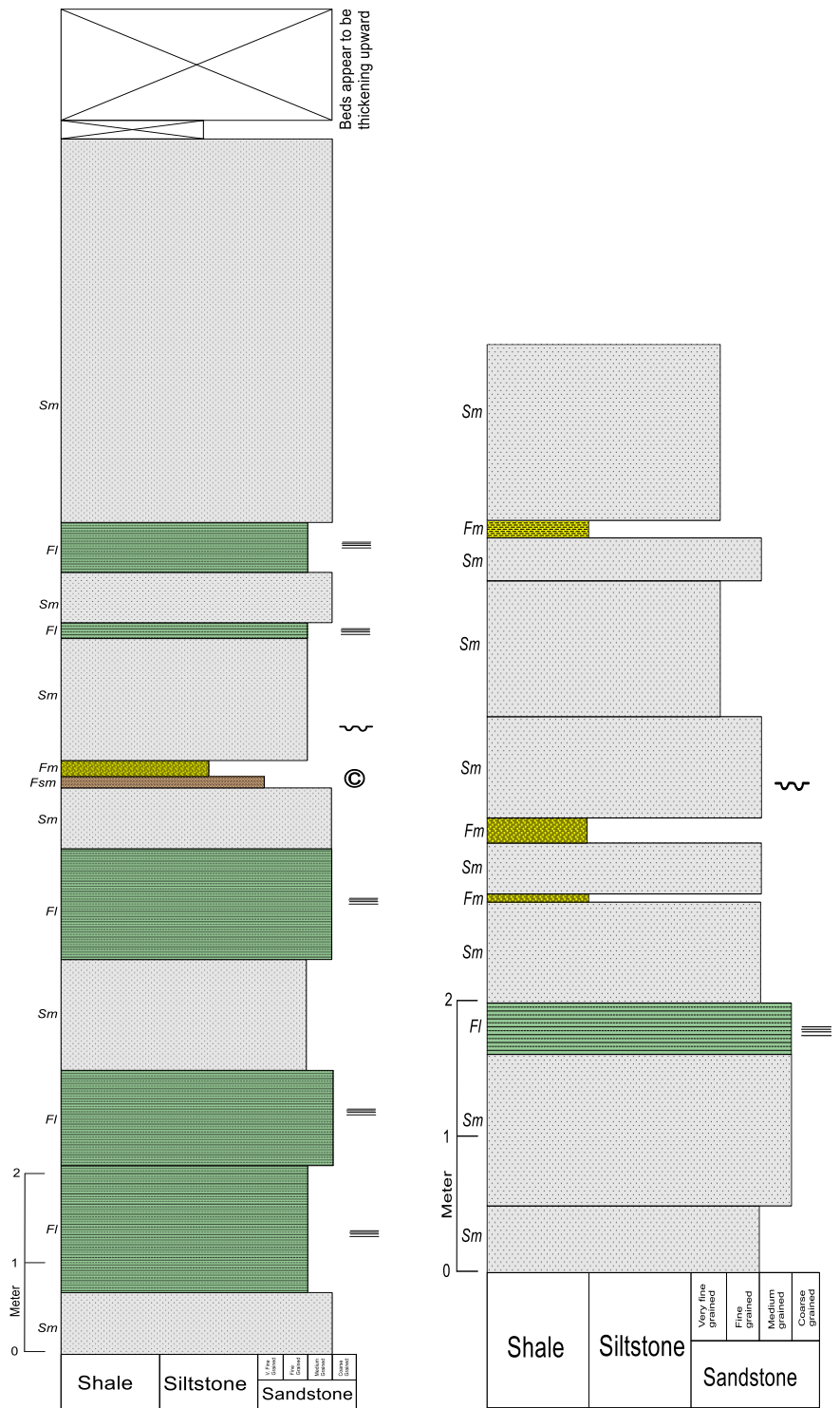


**Fig 7:** VPS 2 around 2.5 km from Terogunyuu towards Tseminyu (25° 54' 11.26" N, 94° 12' 24.35" E)

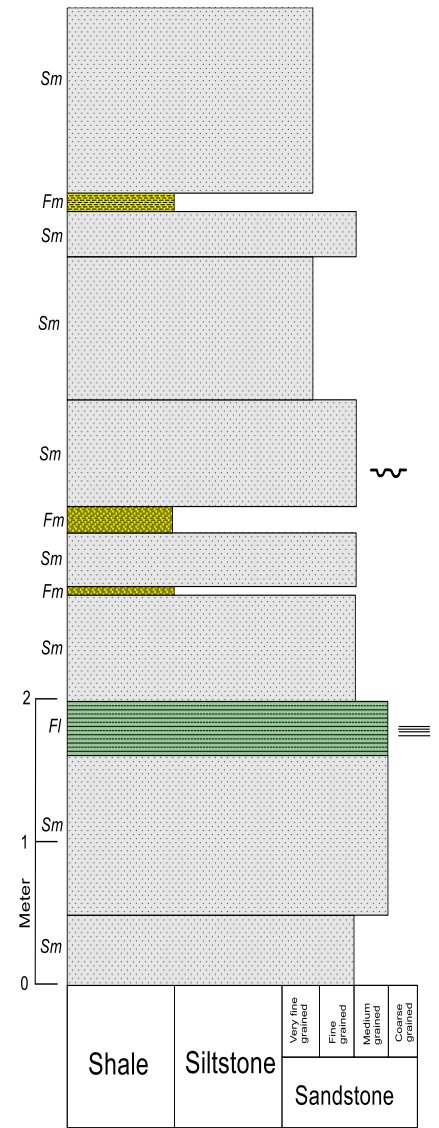


**Fig 8:** VPS 4 North-East of NH-2 towards Pughoboto (25° 52' 0.736" N, 94° 13' 0.425" E)

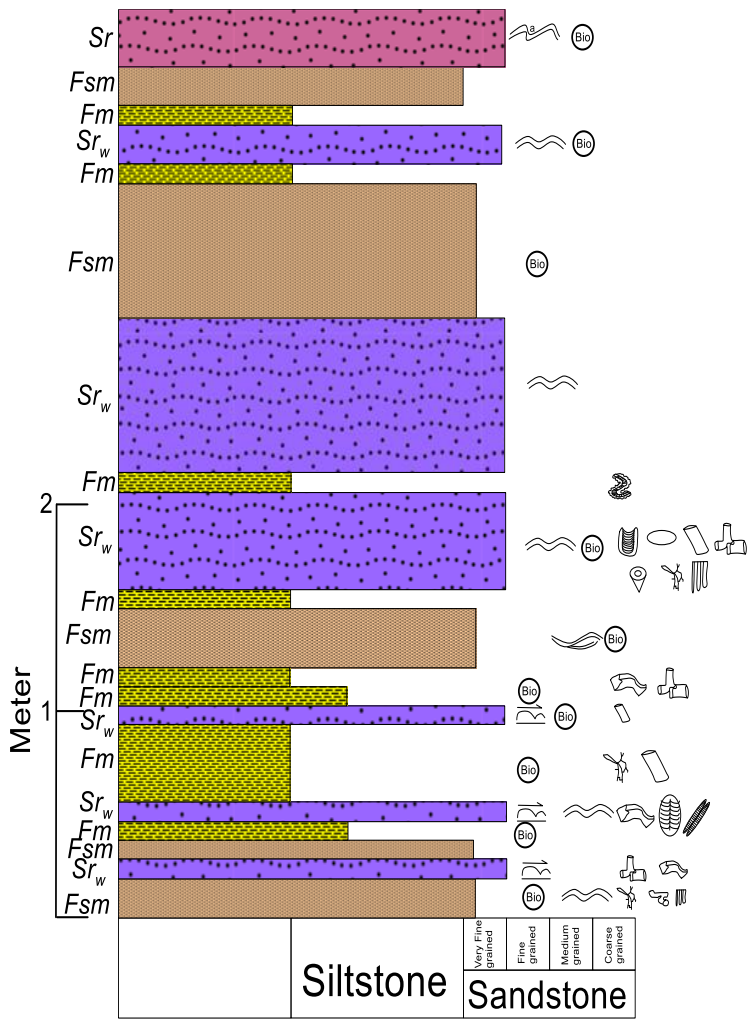


**Fig 9:** VPS 3 around 3 km from Botsa towards north (25° 52' 10.33" N, 94° 10' 09.36" E)

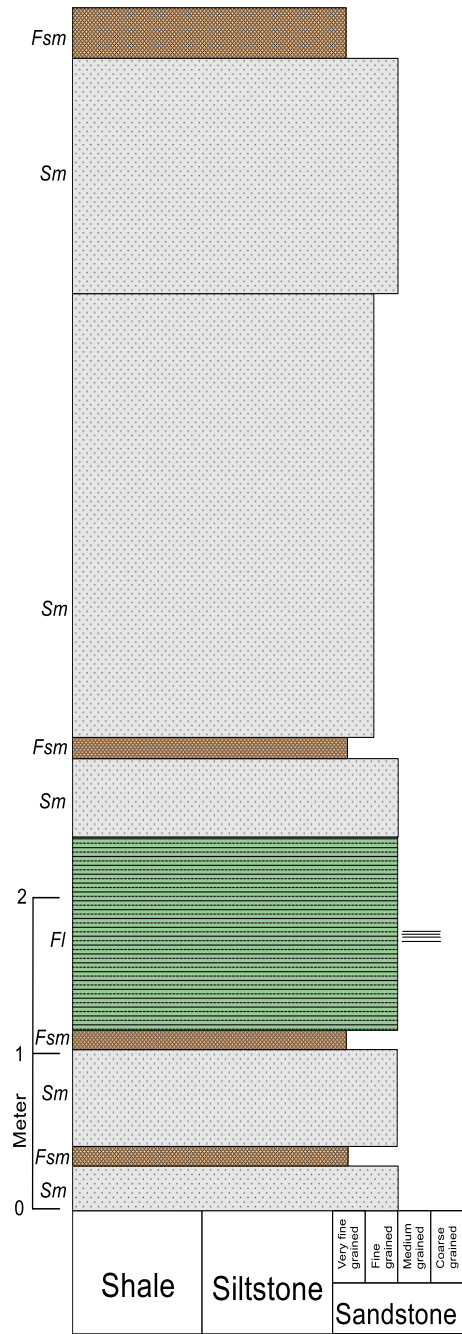


**Fig 10:** VPS 5 towards Phenshenyu from Tseminyu (25° 54' 9.23" N, 94° 03' 0.66" E)

[LITHOLOGIC DISTRIBUTION, VERTICAL PROFILE SECTIONS AND LITHOFACIES]

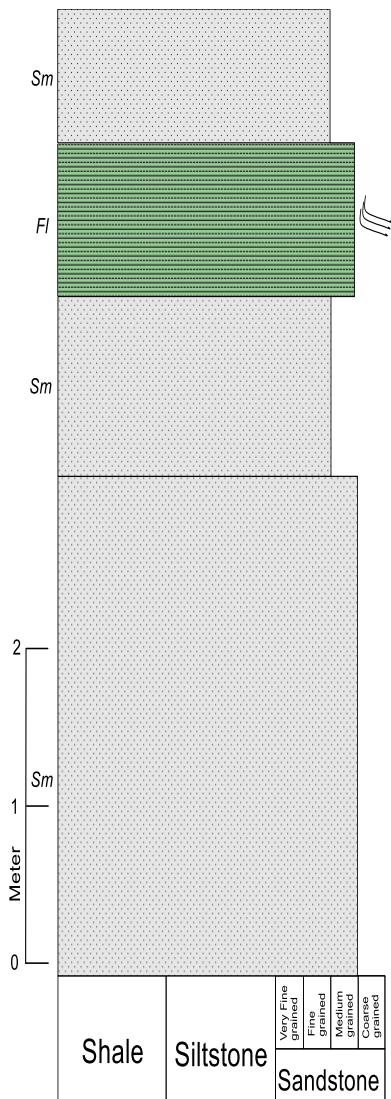


**Fig 11:** VPS 6 From Botsa on the way to Touphema (25° 50' 51" N, 94° 10' 1" E)

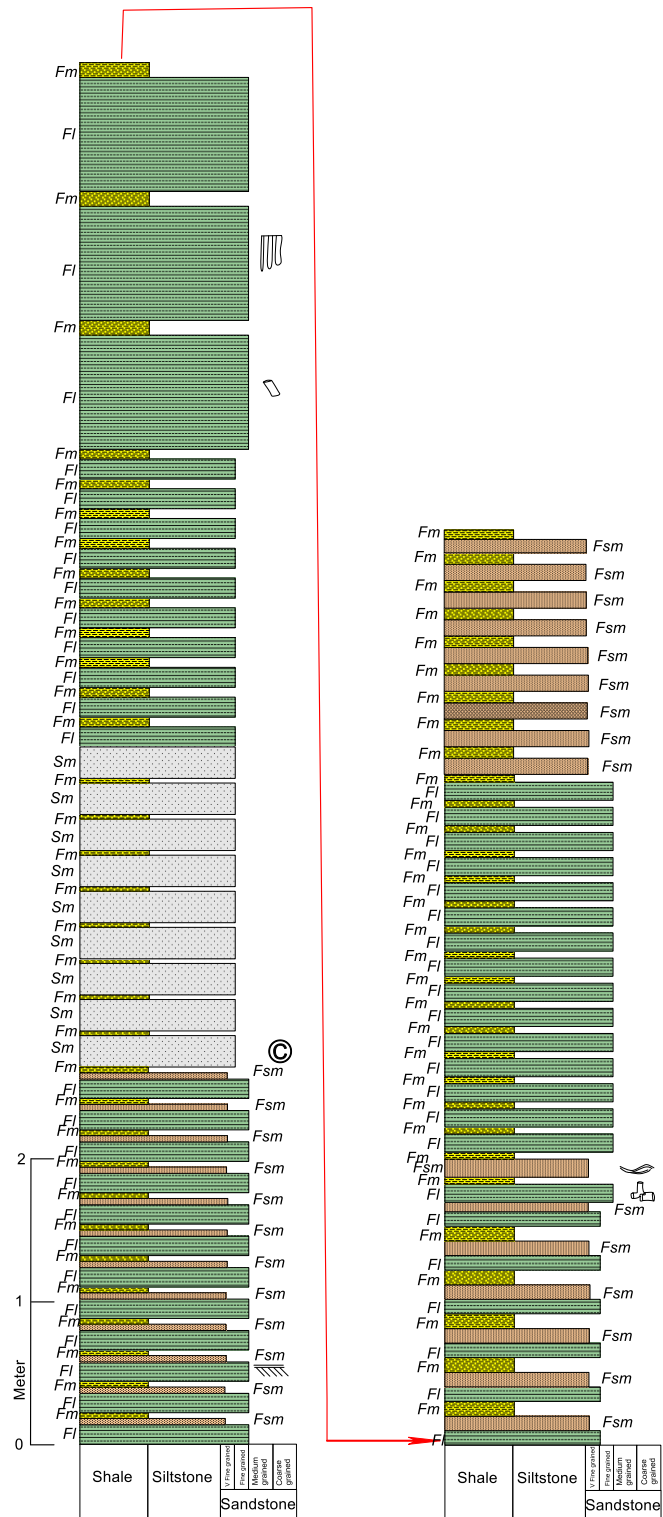


**Fig 12:** VPS 8 3 km from Terogunyu junction towards east direction (25° 52' 17.62" N, 94° 11' 6.65" E)

[LITHOLOGIC DISTRIBUTION, VERTICAL PROFILE SECTIONS AND LITHOFACIES]

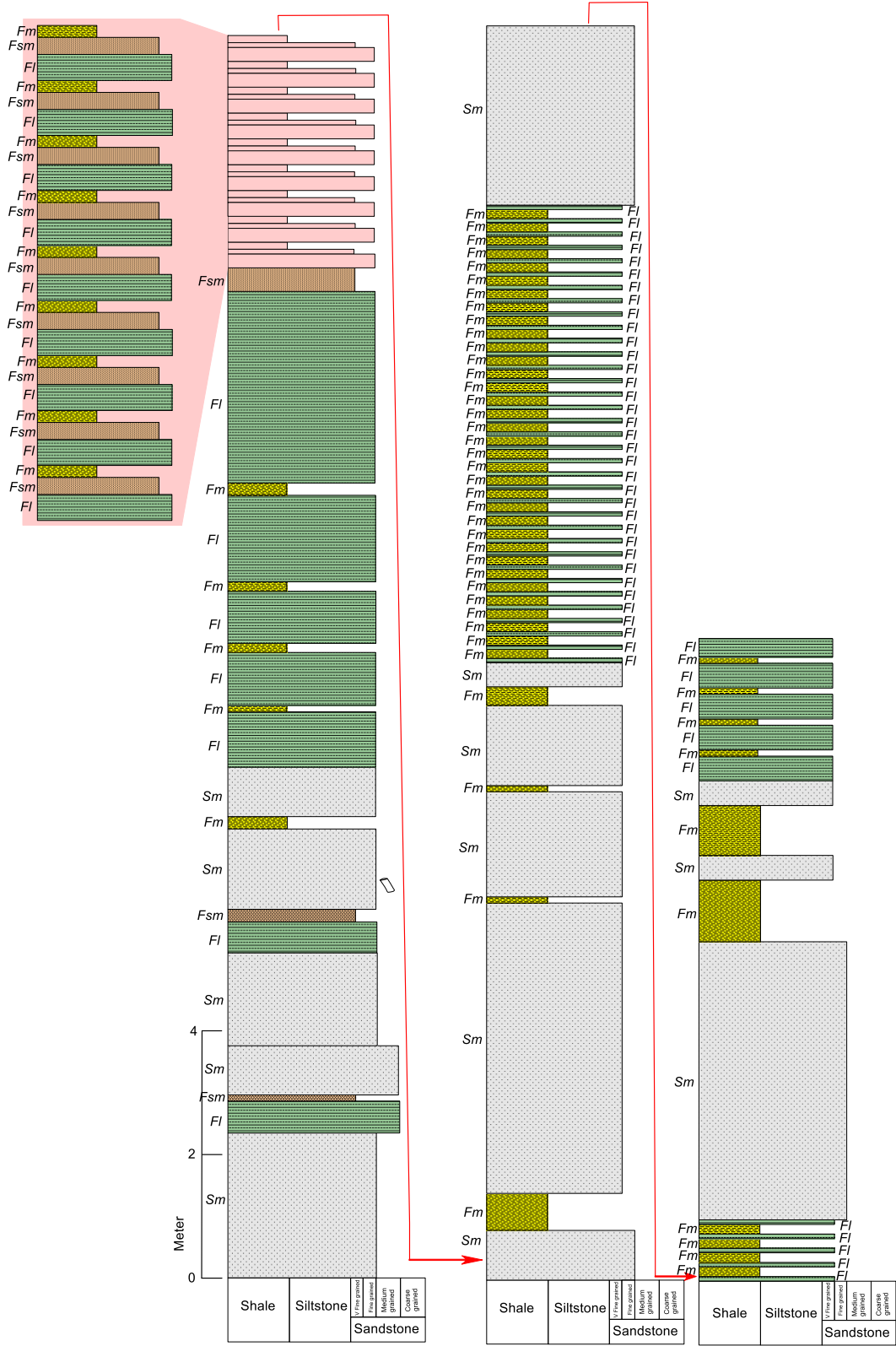
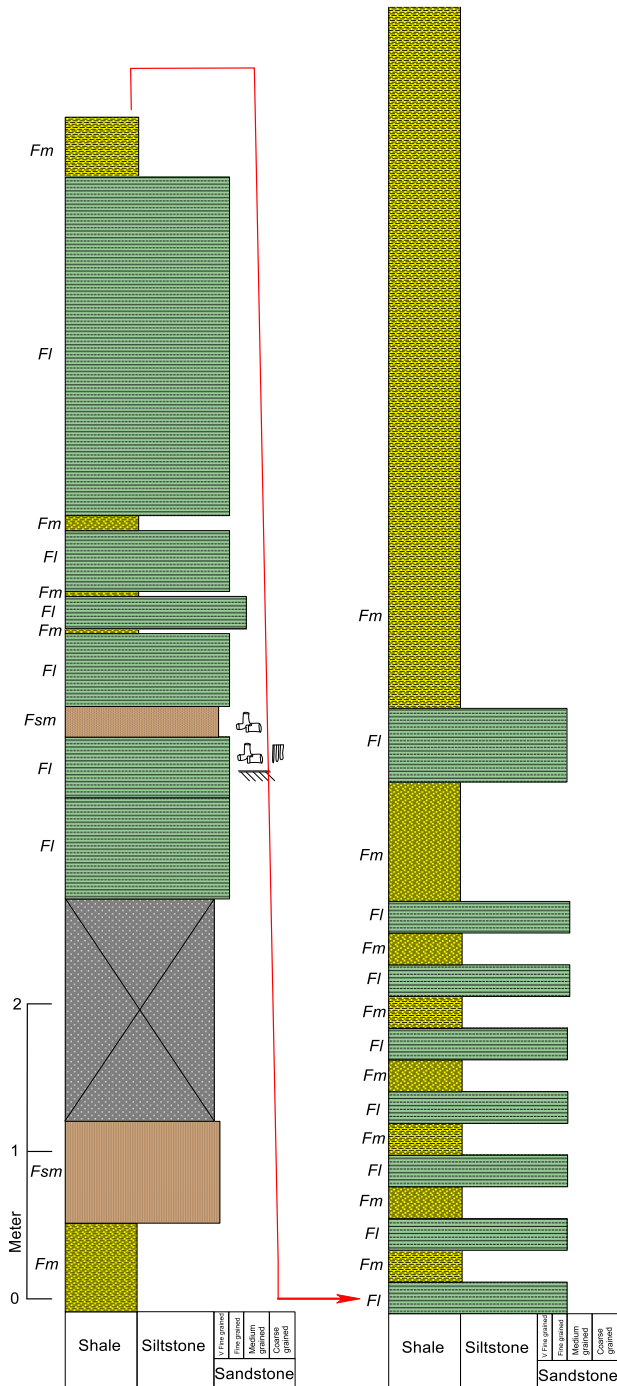
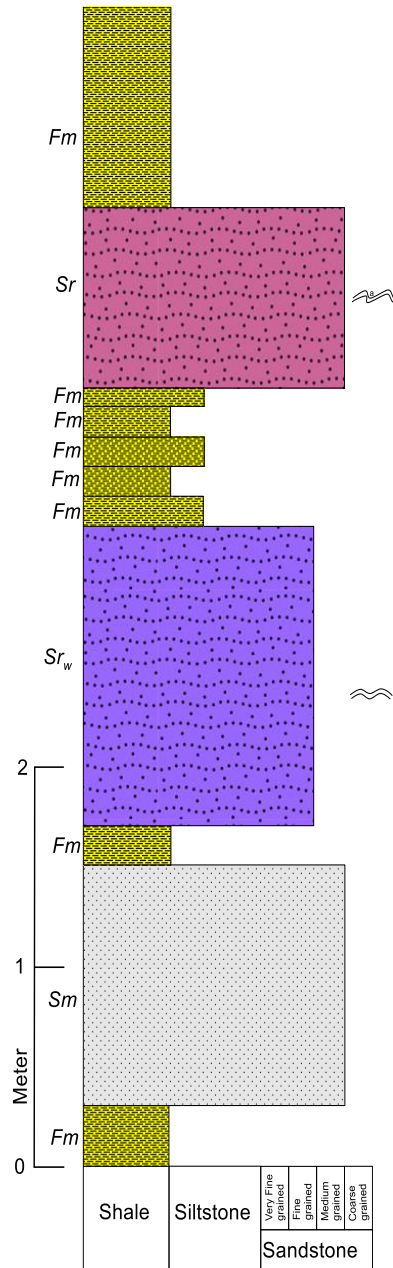


Fig 13: VPS 7 Towards north around 2 km from Botsa (25° 52' 7" N, 94° 09' 57" E)





**Fig 14:** VPS 9 towards Sedenyu from Botsa (25° 52' 22.23" N, 94° 08' 20.4" E)



**Fig 15:** VPS 10 From Botsa towards Teichuma (25° 50' 40.41" N, 94° 07' 22.5" E)

## CHAPTER 4

### GRAIN SIZE ANALYSIS

#### 4.1 GENERAL

Sedimentary texture encompasses the grain size and its distribution, morphology and surface features of grains and the fabric of the sediment. Texture is an important aspect of siliclastic sedimentary rocks and can be a valuable tool for environmental analysis. Griffiths (1967) derived an equation to illustrate the relationship between textural properties of clastic sedimentary rocks and the processes operative during sedimentation. The equation is expressed as:-

$$P=f(m, s, sh, o, p)$$

where,

P, an index characterizing the rocks, is a function (*f*) of the proportions and types of mineral species (*m*), their sizes (*s*), shapes (*sh*); orientation (*o*) and packing (*p*).

Therefore, studying the characteristic aspects of clastic sediments will not only enhance our understanding of the mechanism of transport and depositional environments but also throw light on the history of the provenance.

This chapter is an attempt to interpret the grain size data in terms of processes responsible for the development of Palaeogene sediments in the study area.

#### 4.2 GRAIN SIZE ANALYSIS

Grain size is an important aspect of clastic sediments having a fundamental relationship with the physical forces of transportation and deposition of sediments. The energy conditions of the depositional environment as well as the depositing medium are factors that determine the grain size of clastic sediments, the application of which helps in interpreting the environment. Generally, coarser sediments indicate higher energy conditions whereas finer sediments specify low energy conditions. The size of the grains also decreases in the direction of transport. Many workers like Wentworth (1922), Krumbein and Pettijohn (1938), Folk (1966), Friedman (1967), Visher (1969)

Sengupta (1982) and McLennan *et al.* (1993) have studied the statistical attributes of grain size in deciphering the environment, however, Pettijohn *et al.* (1973) have opined that the relationship between grain size distribution to their environment of deposition is limited because results are inconsistent. According to Reineck and Singh (1980), grain size distribution is a function of hydrodynamics and similar hydrodynamics may operate in various environments thereby resulting in similar grain size distributions. The effectiveness of several techniques available for classifying and discriminating the sedimentary environment through grain size attributes is, therefore, still debated.

However, considering the above, an attempt has been made to reconstruct the depositional environment of the Palaeogene sediments of the study area employing the techniques.

#### 4.2.1 METHOD OF STUDY

Depending upon the sizes of the particles and their state of consolidation several methods for measuring the grain size of siliciclastics are available. The thin section technique of grain size analysis has been employed for the present study since the rocks are lithified and compact. Several workers including Friedman (1962), Stauffer (1966), Conner and Frem (1966), Smith (1966) and Textoris (1971) have justified this technique of particle size measurement which has been in practice since the mid-20<sup>th</sup> century.

Grain size measurement of 42 representative sandstone samples from different lithofacies was carried out with the help of Leica microscope DM 2700 P (TL/RL) at the Department of Geology, Nagaland University, Kohima Campus, Meriema. In each of the thin section more than 250 grains were measured. The grain size values thus obtained were grouped into half phi ( $\phi$ ) intervals and were used in plotting cumulative curves on arithmetic probability paper.

#### 4.2.2 GRAIN SIZE DISTRIBUTION AND STATISTICAL PARAMETERS

The cumulative curves plotted using measurement data of various samples have been shown in **Figs. 16 to 21** and the statistical parameters namely, Graphic mean ( $M_z$ ), Inclusive Graphic Standard Deviation ( $\sigma_I$ ), Simple Sorting Measures ( $SO_S$ ), Simple Skewness Measures ( $\sigma_S$ ), Inclusive Graphic Skewness ( $SK_I$ ) and Graphic Kurtosis ( $K_G$ ) were obtained from the data of the



drawn cumulative curves. The data on grain size distribution and descriptive statistical measures have been presented in **Table 3**.

To understand the transport mechanism and probable depositional environments method suggested by Visher (1969) was followed. Using the obtained data, analysis and comparative studies of different cumulative curves were also performed. Analysis of cumulative curves suggests a shallow marine to near shore complex with fluctuating energy regime at the time of deposition of these sediments.

The statistical measures of grain size distributions were calculated using formulae proposed by Folk and Ward (1957) and later modified by Friedman and Sanders (1978). Phi-values ( $\phi$ ) for different percentiles were read from the cumulative curves. Median denotes the mid-point of the grain size population(s) (i.e., half the percentiles are finer and half coarser than  $\phi_{50}$ ). Median corresponds to the 50<sup>th</sup> percentile diameter on the cumulative curve. The mode is the most frequently occurring particle size in a population and corresponds to maximum frequency and can be read directly from size frequency distribution. Other statistical parameters are determined using the following formulae:

- i. Graphic mean ( $M_z$ ):

$$M_z = \frac{\phi_{16} + \phi_{50} + \phi_{84}}{3}$$

- ii. Inclusive Graphic Standard Deviation ( $\sigma_I$ ):

$$\sigma_I = \frac{\phi_{84} - \phi_{16}}{4} + \frac{\phi_{95} - \phi_5}{6.6}$$

Verbal Classification:

$\sigma_I$ under $\phi_{0.35}$	very well sorted
0.35 to $\phi_{0.50}$	well sorted
0.50 to $\phi_{0.71}$	moderately well sorted
0.71 to $\phi_{1.00}$	moderately sorted
2.00 to $\phi_{4.00}$	very poorly sorted
Over $\phi_{4.00}$	extremely poorly sorted

- iii. Simple Sorting Measures ( $SO_S$ ):

$$SO_S = \phi_{95} - \phi_5$$

- iv. Simple Skewness Measures ( $\sigma_s$ ):

$$(\sigma_s) = (\phi_{95} + \phi_5) - 2\phi_{50}$$

- v. Inclusive Graphic Skewness ( $SK_I$ ):

$$SK_I = \frac{(\phi_{84} + \phi_{16}) - 2\phi_{50}}{2(\phi_{84} - \phi_{16})} + \frac{(\phi_{95} + \phi_5) - 2\phi_{50}}{2(\phi_{95} - \phi_5)}$$

Verbal Classification:

$SK_I$ from +1.00 to +0.30	strongly define- skewed
+0.30 to +0.10	define- skewed
+0.10 to -0.10	near symmetrical
$SK_I = 0.00$	symmetrical
$SK_I$ -0.10 to -0.30	coarse- skewed
-0.30 to -1.00	strongly coarse skewed

- vi. Graphic Kurtosis ( $K_G$ ):

$$K_G = \frac{\phi_{95} - \phi_5}{2.44(\phi_{75} - \phi_{25})}$$

Verbal Classification:

$K_G$ under 0.67	very platykurtic
0.67 to 0.90	platykurtic
0.90 to 1.11	mesokurtic
1.12 to 1.50	leptokurtic
1.51 to 3.00	very Leptokurtic
Over 3.00	extremely Leptokurtic

The normal Phi-curve has a Kurtosis of 1.00.

#### 4.2.2 (A) Mean Grain Size ( $M_z$ ):

In present study, graphic measures are preferred as these are simpler to calculate and generally independent of inaccuracies introduced in truncating and grouping of data (Jacquet and Varnet, 1976; Swan *et al.*, 1978). Mean grain size is the average grain size of sediments and thus relates to hydraulic conditions of the depositional environment. In the study area, in general, it shows a decreasing trend towards southeast.  $M_z$  values of the studied sediments range between 2-4 $\phi$ .

#### 4.2.2 (B) Standard Deviation ( $\sigma_I$ ):

The mathematical expression of sorting is standard deviation which reflects the measure of the range of grain sizes and the magnitude of the spread or the scatter of these sizes around the mean size. Standard deviation specifies the sorting or current and wave condition of the depositional environment. The values of standard deviation ( $\sigma_I$ ) or the overall sorting of the grains in present study suggest moderately to moderately well sorted nature of the grains.

#### 4.2.2 (C) Skewness ( $SK_I$ ):

Skewness is an additional measure of grain size sorting reflecting sorting in the tails of the distribution measuring the deviation of mean from the median of the grain size distributions. It also provides a clue about the symmetry of the frequency curves. On an average, the size distributions are mostly defined skewed to nearly symmetrical.

#### 4.2.2 (D) Kurtosis ( $K_G$ ):

It measures the degree of peakedness of frequency curves with respect to normal probability curve ( $K_G = 1.00$ , Mesokurtic). Sharped peaked curves are said to be leptokurtic; flat peaked curves are platykurtic. Sharp peaked curves indicate a better sorting in the central portion of the grain size distribution than in the tails and flat peaked curves indicate the opposite. In the study area, the value of kurtosis indicates predominance of leptokurtic to mesokurtic distribution.

#### 4.2.3 BIVARIATE STATISTICAL AND TEXTURAL PARAMETERS

Bivariate plots employing various statistical parameters and their interrelationship have proved to be the suitable means of determining various environment of deposition i.e., River, Dune, Beach, Shallow marine, etc. Bivariate plots used in the present study include Graphic Skewness versus Graphic Standard deviation, Graphic Mean versus Graphic Skewness, Graphic Standard Deviation versus Graphic Kurtosis. The values used in this exercise correspond to the sieve equivalents.

##### 4.2.3 (A) Graphic Skewness ( $SK_I$ ) Vs Graphic Standard Deviation ( $\sigma_I$ ):

Using Standard Deviation (sorting) and Graphic Skewness, Friedman (1961) proposed a discriminatory plot for distinguishing between beach and river sands. Data points in the above plot suggest the influence of both river as well as beach environments for the studied sediments (**Fig. 22**). Same results were also obtained by using Moiola and Weiser (1968) plot (**Fig. 23**).

##### 4.2.3 (B) Graphic Mean ( $M_z$ ) Vs Graphic Skewness ( $SK_I$ ):

For distinguishing river, wave and slack water processes, plots suggested by Stewart, (1958), Friedman (1961), Moiola and Weiser, (1968) and have been utilized. The values for the mean size ( $M_z$ ) and median ( $\phi_{50}$ ) in the present study were found nearly identical in most of the samples. The points on the plot indicate that the deposition of the Palaeogene sediments was influenced mainly by wave processes. (**Fig. 24**)

##### 4.2.3 (C) Graphic Standard Deviation ( $\sigma_I$ ) Vs Graphic Kurtosis ( $K_G$ ):

The plot of Inclusive Graphic Standard Deviation ( $\sigma_I$ ) versus Inclusive Graphic Kurtosis ( $K_G$ ) does not provide any environmental interpretation, however, this has been found appropriate to understand the degree of sorting. The overall sorting of the grains denotes moderately sorted to moderately well sorted (**Fig. 25**).

##### 4.2.3 (D) C-M Diagram:

Folk and Ward, (1957); Mason and Folk, (1958); Harris, (1958), Friedman, (1961, 1962, 1967), Sahu, (1964), Chappell (1967) attempted several statistical parameters to differentiate

depositional environments, however, such attempts seem to achieve limited success in interpreting the environments owing to various reasons. Passega (1957, 1964) suggested the C-M diagram to reflect the processes of sediment deposition. C is the 1 percentile diameter in microns, an approximate value of maximum grain size and M is the median or the 50<sup>th</sup> percentile particle diameter in microns. The points obtained from the C-M plot depends on the mode of deposition of sediments. C-M patterns for the Palaeogene sediments were thus obtained (**Fig. 26**) and compared with their basic C-M patterns (Passega 1957, 1964, 1977) and Passega and Benarjee (1969). The pattern of the Palaeogene sediments from the C-M plot corresponds to Class V and VII suggestive of the sediments being transported by both uniform and graded suspension and with some sediments transported by saltation. The average values for CU (Maximum grain size transported as uniform suspension) and CS (Maximum grain size transported as graded suspension) for the Palaeogene sediments correspond to 220 and 430 microns, respectively. The palaeobathymetric estimation using Passega's (1964) Cs-C depth diagram indicates that the Palaeogene sediments have been deposited under a shallow marine environment. A depth range of very shallow to 70-80 meters has been estimated for these sediments.

#### 4.2.3 (E) Cumulative Curve Analysis:

Tanner (1964), Visher, (1969), and Lambiase, (1982) have recognized that the shape of the cumulative curve is a function of relative proportion of various log normal distributions of grain size sub- populations. Correlation of log normal distributions to specific sediment transport mechanism i.e., the coarsest sub-population representing the bed load or surface creep mechanism of transportation and the finest represents the suspension, the intermediate size being the saltation sub-population have been deduced by many workers (Visher, 1970; Moss, 1972; Middleton, 1976; Sagoe and Visher, 1977). However, Tanner, 1964; Middleton, 1976; James and Oaks, 1977 and Walton *et al.*, 1980 have cautioned the interpretation of cumulative curves with respect to minimum number of grain measure, loss of finer grain size due to diagenetic changes and sampling error.

In the present study, cumulative curves for 42 samples have been plotted to understand the depositional history of the Palaeogene sediments (**Figs. 16 to 21**). Sediments in the study area

appear to have been transported under uniform suspension mechanism with little influence of graded suspension and saltation.

#### 4.2.3 (F) Linear Discriminant Functions:

Linear discriminant function of Sahu (1964) and Sevon (1966), in which all the statistical parameters used in the analysis have been combined to a linear equation have been attempted in the present study. Nonetheless, the effectiveness of discriminant functions to decipher various depositional environments has been questioned by Tucker and Vacher (1980).

In the present study, the four empirically established discriminant functions of Sahu (1964) to differentiate sediments from eolian, beach, shallow agitated marine, fluvial (deltaic) and turbidite environments are as follows:

- i)  $Y_1$ : Differentiates eolian from beach environment.

It is expressed as,

$$Y_1 = -3.5688 M_Z + 3.7016 \sigma_I^2 - 2.0766 SK_I + 3.1135 K_G$$

If,

$Y_1 < -2.7411$ , it indicates eolian deposition

$Y_1 > -2.7411$ , it indicates beach deposition

- ii)  $Y_2$ : Differentiates beach from shallow agitated marine environment.

It is expressed as,

$$Y_2 = 15.6534 M_Z + 67.7091 \sigma_I^2 - 18.1071 SK_I + 18.5043 K_G$$

If,

$Y_2 < 65.3650$ , it indicates beach deposition

$Y_2 > 65.3650$ , it indicates shallow agitated marine processes

- iii)  $Y_3$ : Differentiates shallow agitated marine processes from fluvial (deltaic) deposition.

It is expressed as,

$$Y_3 = 0.2852 M_Z + 8.7604 \sigma_I^2 - 4.8932 SK_I + 0.04821 K_G$$

If,

$Y_3 < -7.4190$ , it indicates fluvial (deltaic) deposition

$Y_3 > -7.4190$ , it indicates shallow agitated marine deposition

- iv)  $Y_4$ : Differentiates fluvial (deltaic) environment from turbidity current deposition.

It is expressed as,

$$Y_4 = 0.7215 M_Z + 0.4030 \sigma_I^2 - 6.7322 SK_I + 5.2927 K_G$$

If,

$Y_4 < 9.8433$ , it indicates turbidity current deposition

$Y_4 > 9.8433$ , it indicates fluvial (deltaic) deposition

In the above discriminant functions,  $M_Z$ ,  $\sigma_I^2$ ,  $SK_I$  and  $K_G$  represent Graphic Mean, the variance, Graphic Skewness and Graphic Kurtosis, respectively. Results obtained through these four discriminant functions have been presented in **Table 4**.

Based on the discriminant functions used, the Palaeogene sediments have been found to be associated dominantly with shallow agitated marine processes with minor elements of eolian and turbidity current deposition.

Sahu (1964) has suggested a discriminatory plot for discrimination among the various environments. In the given plot all the possible environments are represented making it more useful for interpretation of the depositional environments. For the purpose standard deviation of all the samples have been plotted against deviation in kurtosis and mean size (**Fig. 28**). This helps in further discrimination among the environments. Analysis of this plot suggests an overall shallow marine environment associated with fluctuation in the sea levels as well as energy conditions during the deposition of the studied sediments.

#### 4.2.3 (G) Multigroup Discriminant Function Analysis:

The linear discriminant function of Sahu (1964) could not yield optimal result for Palaeogene sediments because of the fact that this hypothesis is restricted to two groups only;

whereas samples may not belong to any of the two environments, i.e., eolian-beach, beach-shallow agitated marine, shallow agitated marine fluvial (deltaic) and fluvial (deltaic) turbidite. Therefore, the application of multigroup discrimination after Sahu (1983) was tested, as the method ensures:

- i) the alternative hypothesis may belong to anyone of the several groups;
- ii) ratio of among-group to within group quadratic forms is to be maximized;
- iii) only significant number of coordinates are to be retained for the discrimination space; and
- iv) a simple euclidean distance for purposes of classification in the discrimination space.

In the present investigation, Sahu's (1983) empirically retained discriminating Eigen's vectors  $V_1$  and  $V_2$  have been used. These discriminant functions may be expressed as:

$$V_1 = 0.48048 M_Z + 0.62301 \sigma_I^2 + 0.40602 SK_I + 0.44413 K_G$$

$$V_2 = 0.24523 M_Z + 0.45905 \sigma_I^2 + 0.15715 SK_I + 0.83931 K_G$$

where,

$M_Z$ ,  $\sigma_I^2$ ,  $SK_I$  and  $K_G$  represents the mean size, the size variance, graphic skewness and graphic kurtosis, respectively.

Values of  $V_1$  and  $V_2$  for different samples of the Palaeogene sediments in and around Botsa are listed in **Table 5**. The diagram of  $V_1$  and  $V_2$  with  $V_1 \wedge V_2 = 74.4^\circ$ , after Sahu (1983) was used suitably for the distinction of depositional environment of the Palaeogene sediments under study. The plot (**Fig. 27**) specifies a shallow marine environment for the deposition of the Palaeogene sediments.

#### 4.2.4 DISCUSSION AND GEOLOGICAL INTERPRETATION

Bivariate and multivariate analysis of the studied sediments suggests varied sedimentary environments. This could be attributed to the fact that they not only represent limited environments but also do not consider the effect of variations in grain size, sedimentation processes, climate, tectonic and wave energy fluctuations within the depositional environments. Furthermore, it may



also be noted that the boundaries among different environments in these bivariate plots are purely subjective. However, various discriminatory methods suggested by Sahu (1964) including the multigroup discrimination and plot of  $V_1$  and  $V_2$  (Sahu, 1983), the C-M patterns and shapes of cumulative grain size distribution curves are still valid for discriminating broad aspects of depositional environment.

Statistical and textural parameters of these sediments suggest that they may have been deposited in the upper shoreface-shallow marine agitated environment. Skewness being  $<1$  too supports the above view (Reineck and Singh, 1980). Variations in textural parameters can be attributed to fluctuating energy regime during the deposition (Duane, 1964; Casshyap and Khan, 1982; Mahendar and Banerji, 1989; Chaudhary, 1993; Lakhar and Hazarika, 2000). According to Ghosh and Chatarjee, (1994) stratigraphic changes and the variability of size parameters perhaps indicate changes in environmental energy conditions, such as water depth and wave intensity. Grain size variation, both laterally and vertically, also indicates a fluctuating energy regime within a shallow marine depositional set up (Srivastava and Pandey, 2008).

### **4.3 TEXTURAL MATURITY**

According to Folk (1951, 1974) textural maturity of sandstones can be determined on the basis of matrix, sorting and rounding of the framework grains. The matrix content of the studied sediments varies from 1.96 to 12.02 percent, suggesting an immature to matured nature for the sediments. Presence of moderately sorted to moderately well sorted grains denote sub matured to matured character. This is further corroborated by the association of sub- rounded grains with both matrix- poor and matrix-rich sediments.

Diagenetic processes, biogenic activities and/or mixing of two grain populations (Pettijohn *et al.*, 1972) could be responsible for this textural inversion within upper shore face environment.

### **4.4 PALAEOCURRENT ANALYSIS**

On the basis of the systematic measurement of both the directional structures as well as the scalar quantities, the dispersal patterns and depositional environments of siliciclastic rocks are interpreted (Potter and Pettijohn, 1977). In the study area, only a few directional structures like

asymmetrical ripple marks and cross beddings are observed and measured for the palaeocurrent analysis. Systematic recordings of scalars like grain size variations and proportions of sand and mud have been worked upon to understand the dispersal patterns in the study area.

Average grain-size variations indicate that the power of transporting medium was decreasing gradually from NE towards SW. In the central part of the basin grain size variation, that has been observed suggest that competency of the transport medium was decreasing from NNE to SSW and in the south of the basin it was inferred as NW to SE. This is further corroborated by the decreasing sand-mud ratio in the direction inferred from variation in average grain size. The palaeocurrent directions measured directly at outcrop especially from asymmetrical ripples (N120°), are also in conformity with the direction obtained through scalars. Following above observations in can be suggested that the basin was undulatory in nature and sediments supply was made from different directions. This can be attributed to the changing drainage system in the source area owing to the changing plate interactions.

<b>Sample No.</b>	<b><math>M_z</math></b>	<b><math>\sigma_I</math></b>	<b><math>SO_s</math></b>	<b><math>\sigma_s</math></b>	<b><math>SK_I</math></b>	<b><math>K_G</math></b>
L1A1	2.56	0.52 (Moderately well sorted)	1.7	0.22 (Nearly symmetrical)	0.09	1.04 (Mesokurtic)
L1A3	2.93	0.56 (Moderately well sorted)	1.93	-0.07 (Symmetrical)	0	1.24 (Leptokurtic)
L1A4	3.1	0.54 (Moderately well sorted)	1.98	0.46 (Define skewed)	0.15	1.36 (Leptokurtic)
L1A6	2.92	0.51 (Moderately well sorted)	1.77	0.45 (Define skewed)	0.17	1.17 (Leptokurtic)
L1A7	2.87	0.54 (Moderately well sorted)	1.84	0.16 (Define skewed)	0.11	1.13 (Leptokurtic)
L2A8	2.75	0.5 (Moderately well sorted)	1.74	0.06 (Nearly symmetrical)	0.07	1.15 (Leptokurtic)
L2A9	2.8	0.52 (Moderately well sorted)	1.72	0.08 (Nearly symmetrical)	-0.01	1.04 (Mesokurtic)
L2A10	3.31	0.66 (Moderately well sorted)	2.16	0.34 (Define skewed)	0.14	0.97 (Mesokurtic)
L2A13	3.2	0.72 (Moderately sorted)	2.47	0.17 (Nearly symmetrical)	0.03	1.06 (Mesokurtic)
L2A15	2.92	0.64 (Moderately well sorted)	2.1	0.3 (Define skewed)	0.1	0.97 (Mesokurtic)
L2A16	2.76	0.7 (Moderately well sorted)	2.28	0.56 (Define skewed)	0.2	0.96 (Mesokurtic)

L3A17	3.6	0.58 (Moderately well sorted)	1.9	0.34 (Define skewed)	0.12	1.02 (Mesokurtic)
L3A18	3.5	0.56 (Moderately well sorted)	1.88	0.16 (Nearly symmetrical)	0.07	1.06 (Mesokurtic)
L3A19	3.58	0.55 (Moderately well sorted)	1.85	0.15 (Nearly symmetrical)	0.05	1.07 (Mesokurtic)
L3A21	3.59	0.55 (Moderately well sorted)	1.83	0.29 (Define skewed)	0.17	1.07 (Mesokurtic)
L4A22	2.87	0.71 (Well sorted)	2.29	0.61 (Define skewed)	0.18	0.94 (Mesokurtic)
L4A23	2.95	0.65 (Moderately well sorted)	2.05	0.51 (Define skewed)	0.23	0.88 (Platykurtic)
L4A24	3.05	0.63 (Moderately well sorted)	2.03	0.23 (Nearly symmetrical)	0.09	0.96 (Mesokurtic)
L4A25	3.28	0.55 (Moderately well sorted)	1.86	-0.06 (Nearly symmetrical)	-0.01	0.98 (Mesokurtic)
L4A26	3.3	0.62 (Moderately well sorted)	2.2	0.5 (Define skewed)	0.18	1.2 (Leptokurtic)
L4A27	3.15	0.54 (Moderately well sorted)	1.75	0.25 (Define skewed)	0.17	0.96 (Mesokurtic)
L5A28	3.51	0.55 (Moderately well sorted)	2	0.12 (Nearly symmetrical)	-0.02	1.36 (Leptokurtic)
L5A30	3.41	0.52 (Moderately well sorted)	1.79	-0.01 (Nearly symmetrical)	0.02	1.11 (Leptokurtic)

L5A31	3.49	0.57 (Moderately well sorted)	1.91	-0.01 (Nearly symmetrical)	0.05	1.03 (Mesokurtic)
L5A32	3.71	0.45 (Well sorted)	1.53	0.25 (Nearly symmetrical)	0.09	1.06 (Mesokurtic)
L6A33	3.17	0.67 (Moderately well sorted)	2.35	0.41 (Define skewed)	0.15	1.34 (Leptokurtic)
L6A34	3.37	0.73 (Moderately sorted)	2.38	0.64 (Define skewed)	0.15	0.95 (Mesokurtic)
L6A35	4.22	0.67 (Moderately well sorted)	2.25	0.45 (Define skewed)	0.18	1.18 (Leptokurtic)
L6A36	4.05	0.64 (Moderately well sorted)	2.2	0.52 (Define skewed)	0.16	1.07 (Mesokurtic)
L7A37	3.04	0.71 (Moderately sorted)	2.36	0.32 (Define skewed)	0.12	0.99 (Mesokurtic)
L7A38	3.11	0.72 (Moderately sorted)	2.35	0.65 (Strongly define skewed)	0.31	1.05 (Mesokurtic)
L7A39	2.67	0.7 (Moderately well sorted)	2.23	0.15 (Nearly symmetrical)	0.09	0.9 (Mesokurtic)
L7A44	3.4	0.61 (Moderately well sorted)	2.01	0.15 (Nearly symmetrical)	0.07	1 (Mesokurtic)
L7A46	3.36	0.7 (Moderately well sorted)	2.48	0.56 (Define skewed)	0.18	1.22 (Leptokurtic)
L8A49	3.1	0.65 (Moderately well sorted)	2.21	0.07 (Nearly symmetrical)	0.03	1.08 (Mesokurtic)

L8A50	3.17	0.63 (Moderately well sorted)	2.14	0.06 (Nearly symmetrical)	0.03	1.02 (Mesokurtic)
L9A52	3.59	0.73 (Moderately sorted)	2.53	0.51 (Define skewed)	0.11	1.13 (Leptokurtic)
L9A54	3.48	0.77 (Moderately sorted)	2.63	0.11 (Nearly symmetrical)	0.02	1.11 (Mesokurtic)
L9A55	3.37	0.68 (Moderately well sorted)	2.18	0.3 (Define skewed)	0.12	0.99 (Mesokurtic)
L9A56	3.36	0.57 (Moderately well sorted)	1.9	0.36 (Define skewed)	0.14	1.14 (Leptokurtic)
L10A57	3.07	0.71 (Well sorted)	2.37	0.47 (Define skewed)	0.17	1 (Mesokurtic)
L10A58	3.17	0.74 (Well sorted)	2.48	0.48 (Define skewed)	0.17	0.99 (Mesokurtic)
L10A59	3.5	0.94 (Moderately sorted)	3.22	0.92 (Define skewed)	0.27	1.2 (Leptokurtic)

**Table 3:** Grain size data and statistical measures of selected samples

Sample No.	$Y_1$		$Y_2$		$Y_3$		$Y_4$	
L1A1	-5.08407	Eolian	75.99608	Shallow	2.70867	Shallow	6.85452	Turbidity
L1A3	-5.43502	Eolian	90.04337	Shallow	3.64267	Shallow	8.80332	Turbidity
L1A4	-6.06102	Eolian	90.7193	Shallow	2.77023	Shallow	8.54240	Turbidity
L1A6	-6.16834	Eolian	81.89089	Shallow	2.33592	Shallow	7.25958	Turbidity
L1A7	-5.87324	Eolian	83.58731	Shallow	2.88928	Shallow	7.42842	Turbidity
L2A8	-5.45364	Eolian	79.98657	Shallow	2.68731	Shallow	7.70022	Turbidity
L2A9	-5.73292	Eolian	81.5636	Shallow	3.26644	Shallow	7.70090	Turbidity
L2A10	-7.47094	Eolian	96.72101	Shallow	4.12175	Shallow	6.75512	Turbidity
L2A13	-6.26324	Eolian	104.2626	Shallow	5.35833	Shallow	7.92601	Turbidity
L2A15	-6.09229	Eolian	89.58004	Shallow	3.97848	Shallow	6.73254	Turbidity
L2A16	-5.46246	Eolian	90.52355	Shallow	4.14739	Shallow	5.92336	Turbidity
L3A17	-8.67588	Eolian	95.83112	Shallow	3.43570	Shallow	7.32365	Turbidity
L3A18	-8.17503	Eolian	94.36753	Shallow	3.45404	Shallow	7.79063	Turbidity
L3A19	-8.42896	Eolian	95.41542	Shallow	3.47796	Shallow	8.03145	Turbidity
L3A21	-8.71384	Eolian	93.3991	Shallow	2.89363	Shallow	7.23080	Turbidity
L4A22	-5.82358	Eolian	93.19218	Shallow	4.39918	Shallow	6.03719	Turbidity
L4A23	-6.70177	Eolian	86.90378	Shallow	3.45959	Shallow	5.40786	Turbidity
L4A24	-6.61361	Eolian	90.7511	Shallow	3.95275	Shallow	6.83562	Turbidity
L4A25	-7.51393	Eolian	90.14044	Shallow	3.68165	Shallow	7.74259	Turbidity
L4A26	-6.99173	Eolian	96.62948	Shallow	3.48573	Shallow	7.67530	Turbidity
L4A27	-7.5264	Eolian	83.7381	Shallow	2.66735	Shallow	6.32675	Turbidity
L5A28	-7.13086	Eolian	100.9534	Shallow	3.81450	Shallow	9.98708	Fluvial
L5A30	-7.75424	Eolian	91.86427	Shallow	3.29699	Shallow	8.30953	Turbidity

L5A31	-8.14939	Eolian	94.78313	Shallow	3.64659	Shallow	7.76384	Turbidity
L5A32	-9.37726	Eolian	89.77013	Shallow	2.44278	Shallow	7.76273	Turbidity
L6A33	-5.79085	Eolian	102.0956	Shallow	4.16724	Shallow	8.55045	Turbidity
L6A34	-7.40794	Eolian	103.6972	Shallow	4.94136	Shallow	6.66444	Turbidity
L6A35	-10.0985	Eolian	115.0278	Shallow	4.31219	Shallow	8.25922	Turbidity
L6A36	-9.93828	Eolian	108.0324	Shallow	4.01199	Shallow	7.67318	Turbidity
L7A37	-6.15	Eolian	97.8649	Shallow	4.74367	Shallow	6.82842	Turbidity
L7A38	-6.55463	Eolian	97.59879	Shallow	3.96209	Shallow	5.92313	Turbidity
L7A39	-5.09966	Eolian	89.99627	Shallow	4.65708	Shallow	6.28140	Turbidity
L7A44	-7.78842	Eolian	95.65292	Shallow	3.93511	Shallow	7.42450	Turbidity
L7A46	-6.7527	Eolian	105.0889	Shallow	4.42890	Shallow	7.86700	Turbidity
L8A49	-6.19907	Eolian	96.57407	Shallow	4.49066	Shallow	7.92106	Turbidity
L8A50	-6.73046	Eolian	94.82619	Shallow	4.28346	Shallow	7.64369	Turbidity
L9A52	-7.54958	Eolian	111.196	Shallow	5.20851	Shallow	8.04515	Turbidity
L9A54	-6.81029	Eolian	114.7962	Shallow	6.14218	Shallow	8.49001	Turbidity
L9A55	-7.48206	Eolian	100.2071	Shallow	4.47247	Shallow	7.04971	Turbidity
L9A56	-7.52985	Eolian	93.15402	Shallow	3.17443	Shallow	7.64634	Turbidity
L10A5 7	-6.32976	Eolian	97.61419	Shallow	4.50804	Shallow	6.56638	Turbidity
L10A5 8	-6.55676	Eolian	101.9398	Shallow	4.91716	Shallow	6.60313	Turbidity
L10A5 9	-6.04455	Eolian	131.9309	Shallow	7.47557	Shallow	7.41488	Turbidity

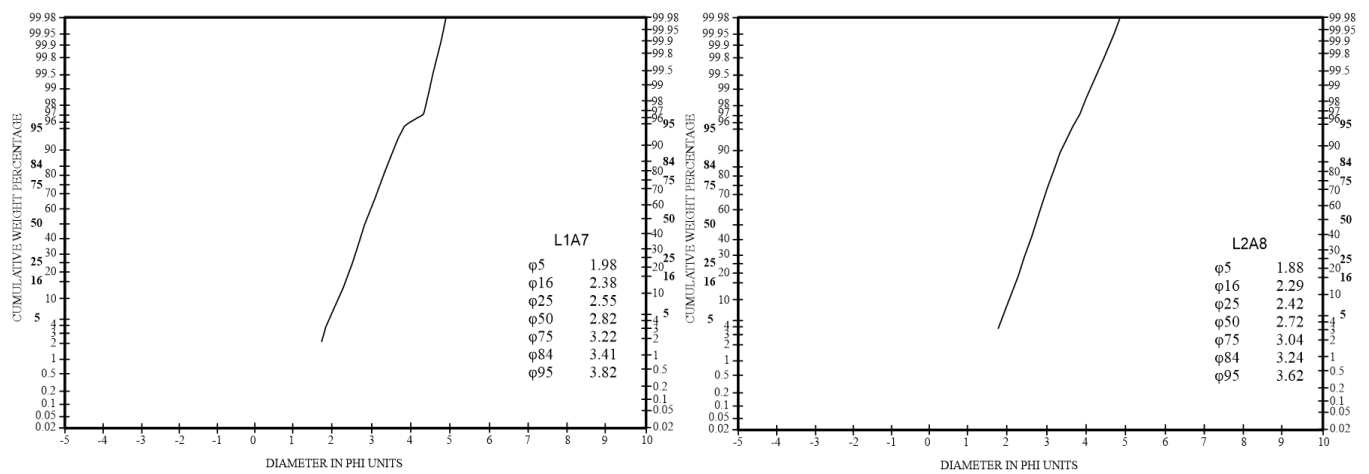
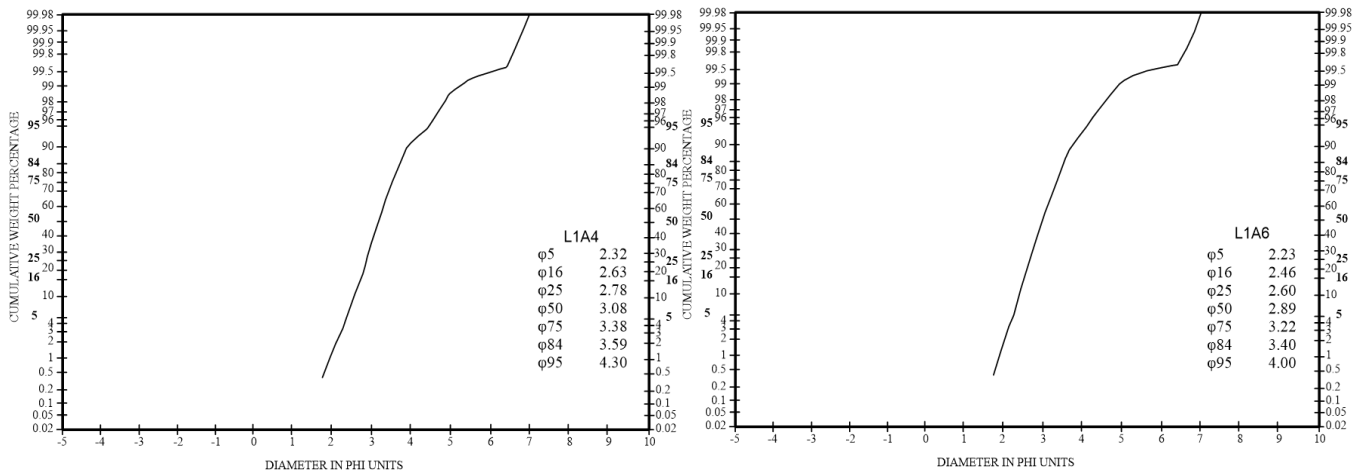
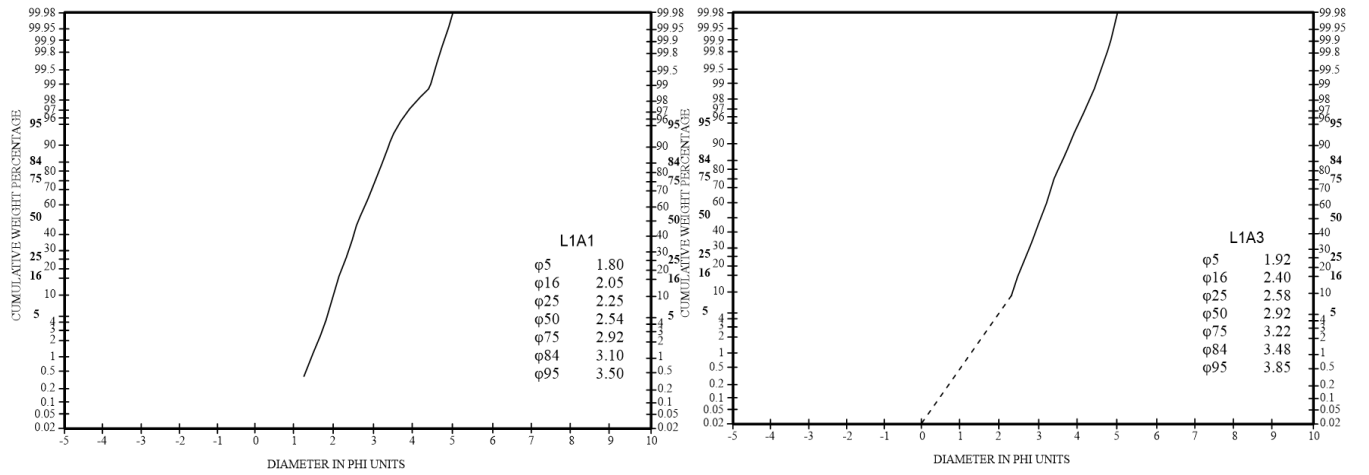
**Table 4:** The four discriminant functions of Palaeogene sediments (after Sahu, 1964)



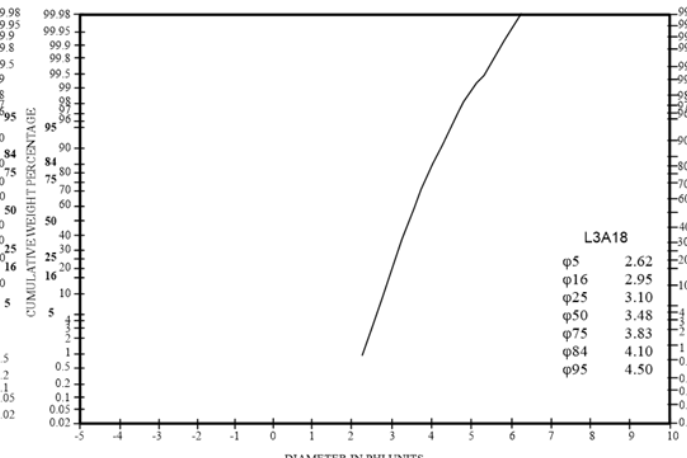
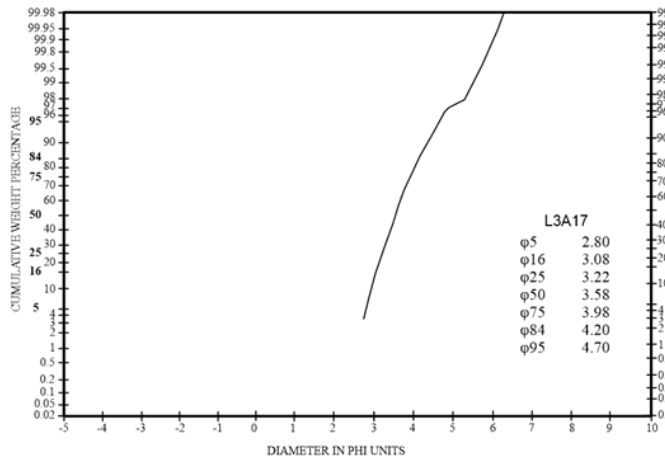
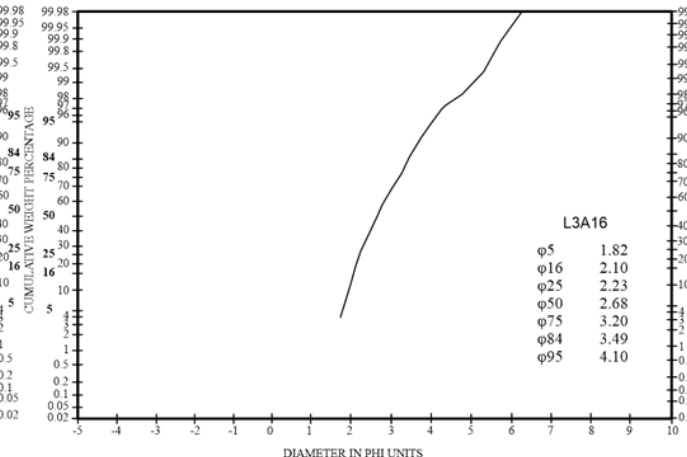
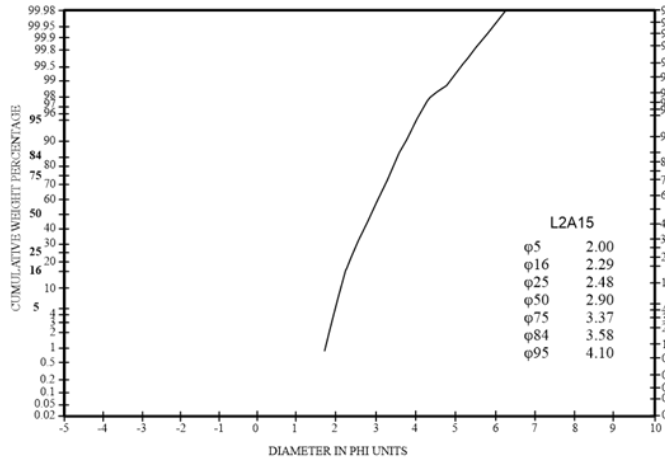
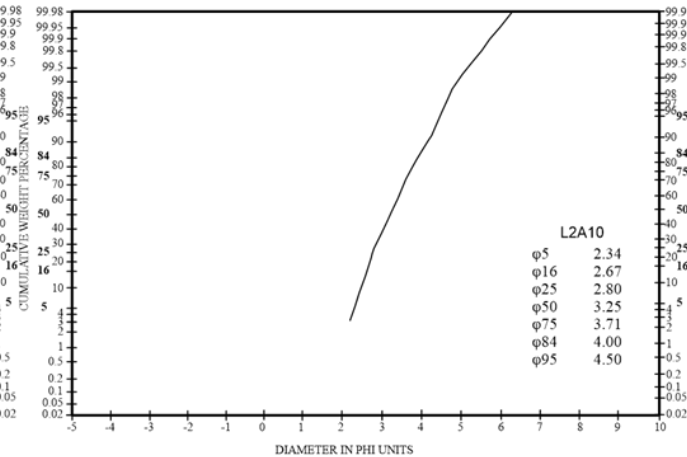
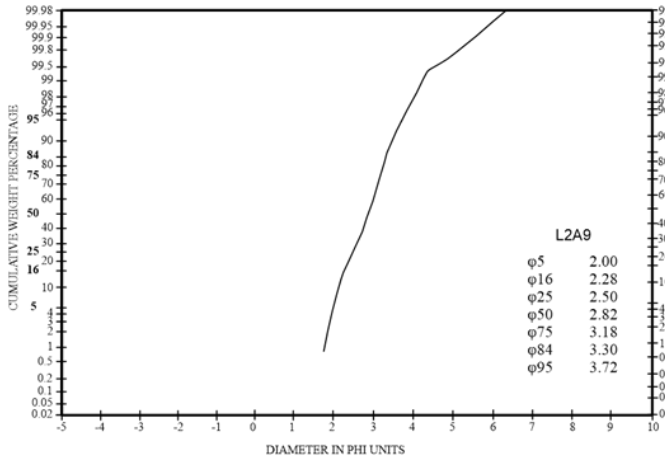
Sample No.	$V_1$	$V_2$	Sample No.	$V_1$	$V_2$
<b>L1A1</b>	1.82384	1.36240	<b>L5A30</b>	2.29176	1.64059
<b>L1A3</b>	2.15390	1.61531	<b>L5A31</b>	2.31644	1.56333
<b>L1A4</b>	2.21427	1.74424	<b>L5A32</b>	2.34297	1.69237
<b>L1A6</b>	2.01565	1.55195	<b>L6A33</b>	2.33702	1.67241
<b>L1A7</b>	2.01785	1.50108	<b>L6A34</b>	2.31224	1.35556
<b>L2A8</b>	1.95940	1.51382	<b>L6A35</b>	2.75828	1.79090
<b>L2A9</b>	1.97976	1.43697	<b>L6A36</b>	2.61138	1.67807
<b>L2A10</b>	2.23573	1.40387	<b>L7A37</b>	2.16568	1.32615
<b>L2A13</b>	2.31910	1.43171	<b>L7A38</b>	2.15773	1.35725
<b>L2A15</b>	2.04839	1.32646	<b>L7A39</b>	1.95133	1.17106
<b>L2A16</b>	1.97656	1.22620	<b>L7A44</b>	2.28116	1.49127
<b>L3A17</b>	2.34359	1.56564	<b>L7A46</b>	2.38844	1.59471
<b>L3A18</b>	2.31941	1.59301	<b>L8A49</b>	2.22019	1.46800
<b>L3A19</b>	2.36349	1.62926	<b>L8A50</b>	2.21122	1.44656
<b>L3A21</b>	2.31957	1.61285	<b>L9A52</b>	2.51413	1.56688
<b>L4A22</b>	2.03743	1.23306	<b>L9A54</b>	2.52631	1.50972
<b>L4A23</b>	1.97808	1.23192	<b>L9A55</b>	2.29826	1.42621
<b>L4A24</b>	2.10256	1.35734	<b>L9A56</b>	2.26629	1.60964
<b>L4A25</b>	2.20374	1.48958	<b>L10A57</b>	2.16424	1.33404
<b>L4A26</b>	2.28494	1.61168	<b>L10A58</b>	2.234947	1.33020
<b>L4A27</b>	2.05252	1.41763	<b>L10A59</b>	2.65550	1.41743
<b>L5A28</b>	2.48708	1.86649			

**Table 5:** Values of  $V_1$  and  $V_2$  for different samples of Palaeogene sediments

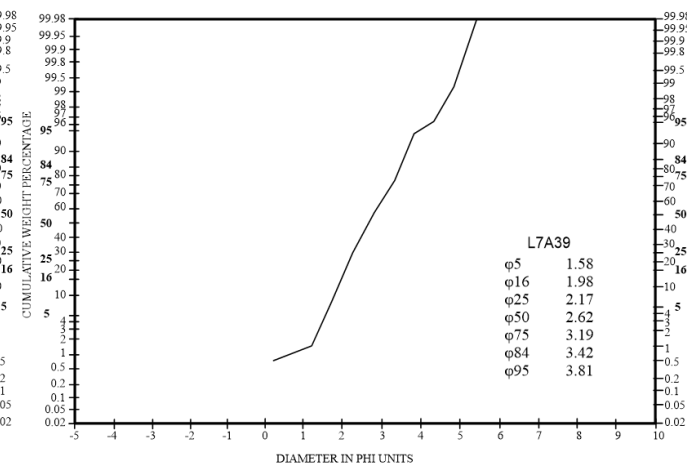
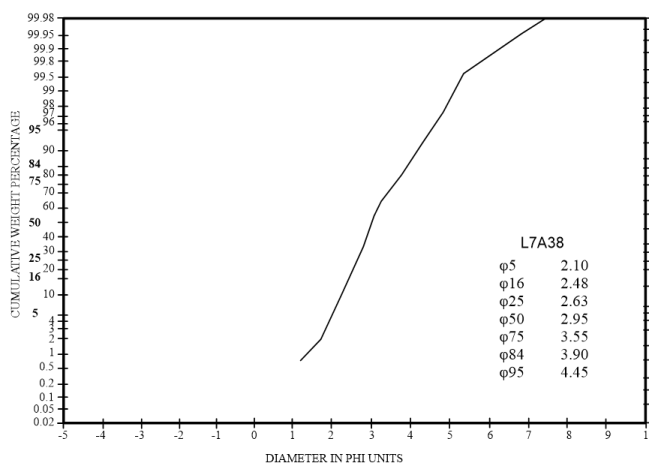
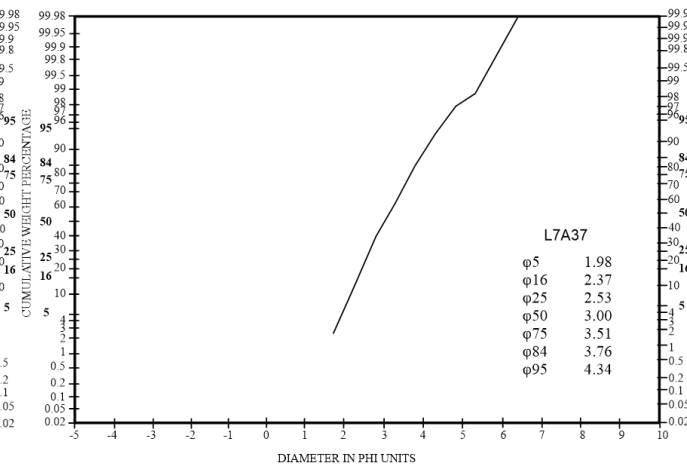
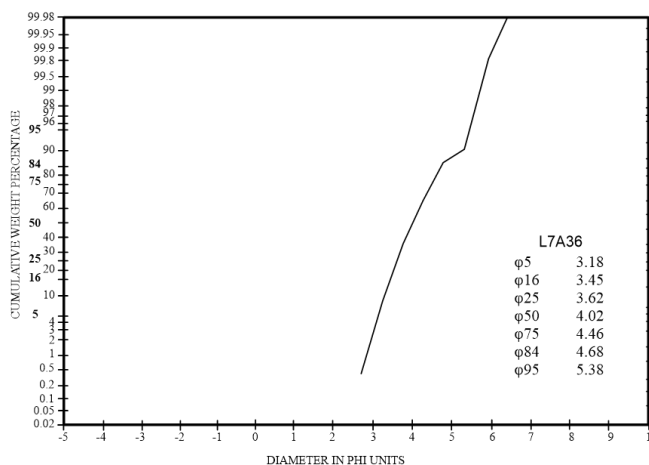
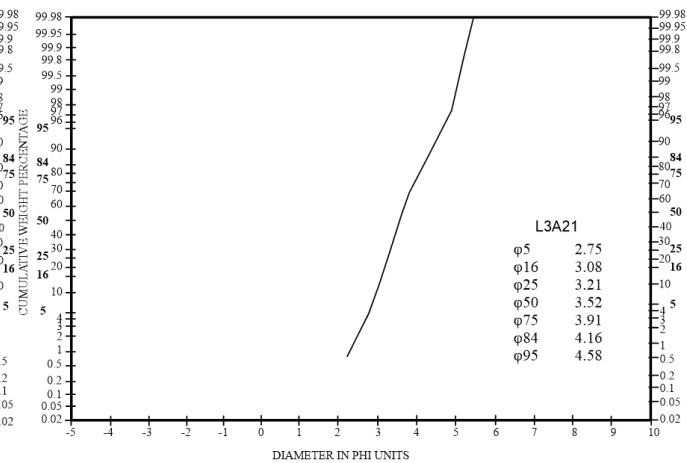
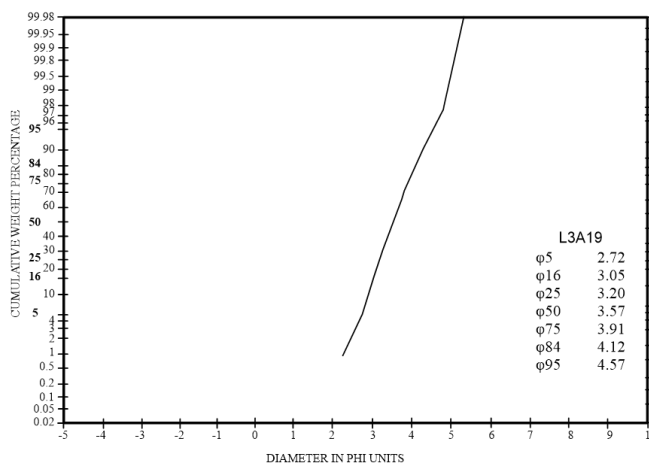
[GRAIN SIZE ANALYSIS]



[GRAIN SIZE ANALYSIS]



[GRAIN SIZE ANALYSIS]



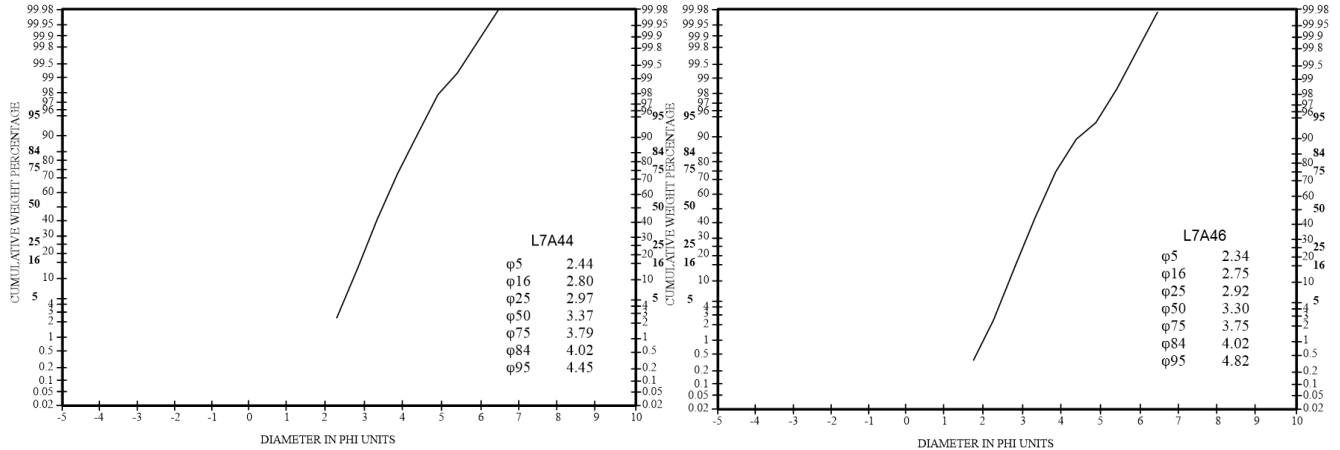
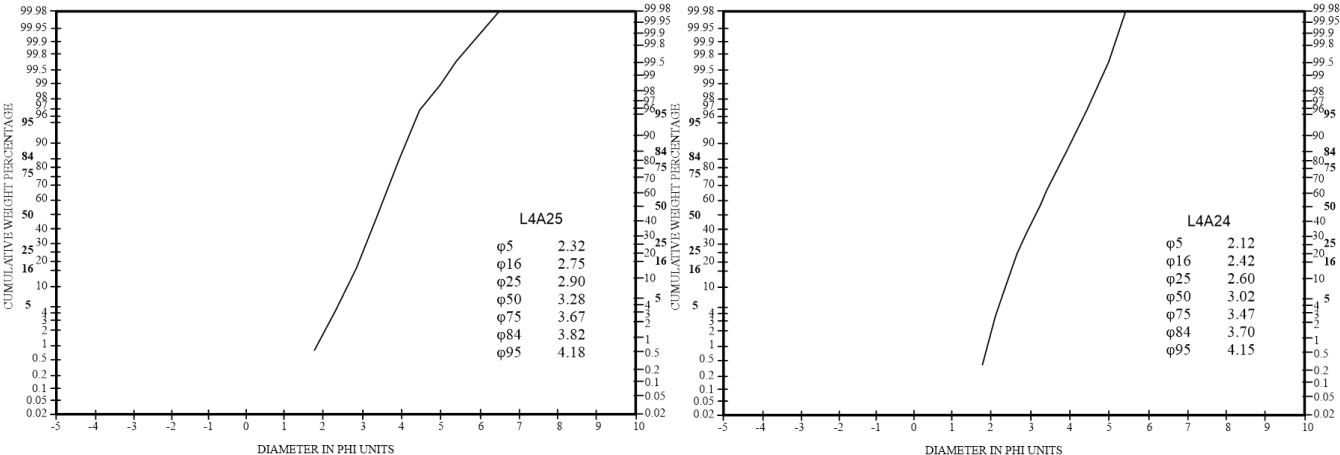
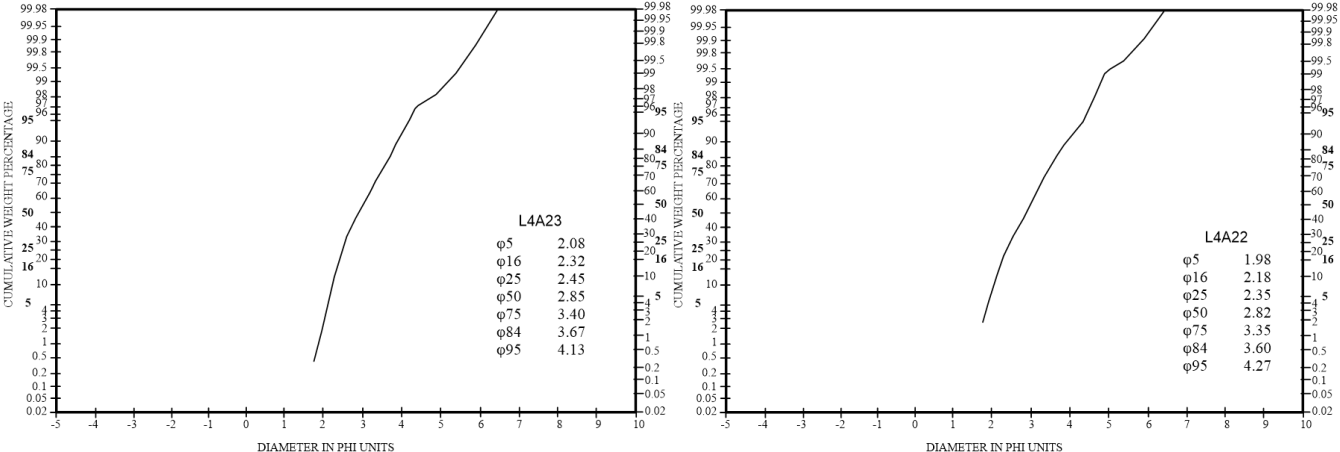
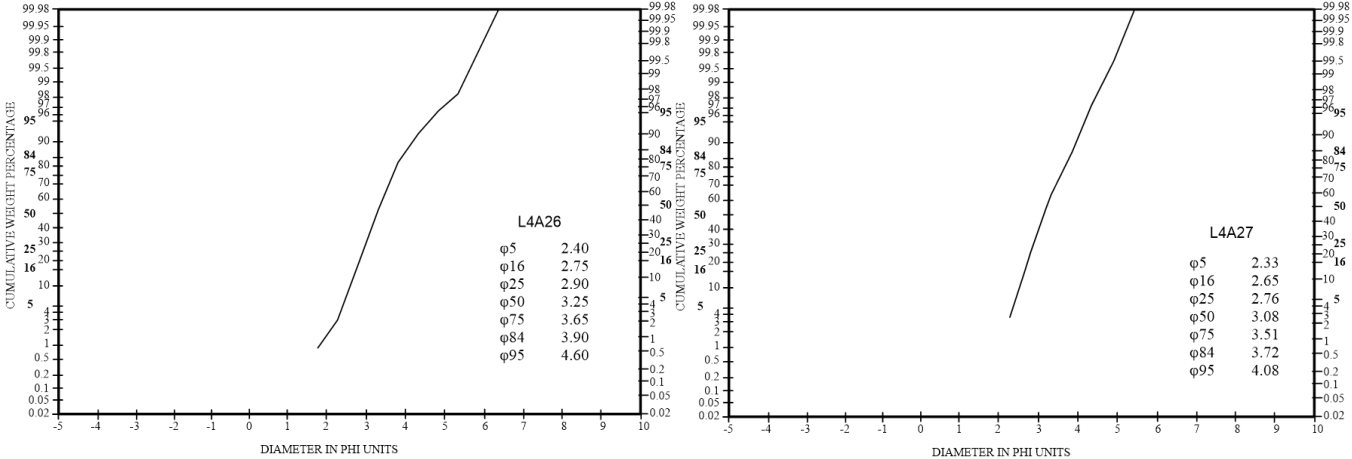
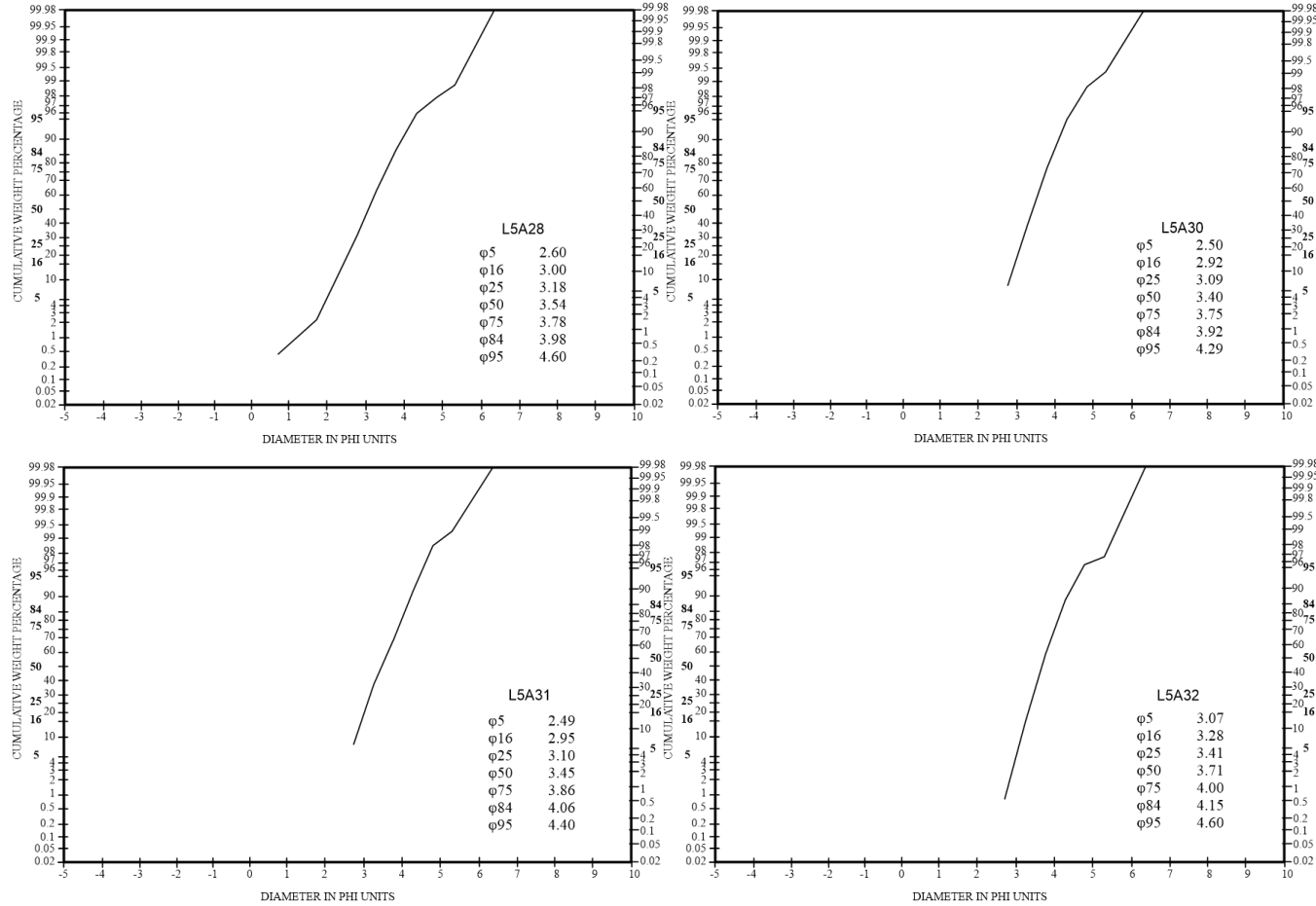


Fig 16: Grain size distribution curves of samples along NH- 2 road section





**Fig.17:** Grain size distribution curves of samples towards Pughoboto (25° 52' 0.736" N, 94°13'.425" E)



**Fig. 18:** Grain size distribution curves of samples towards Phenshenyu from Tseminyu (25° 54' 9.23" N, 94° 03' 0.66" E)

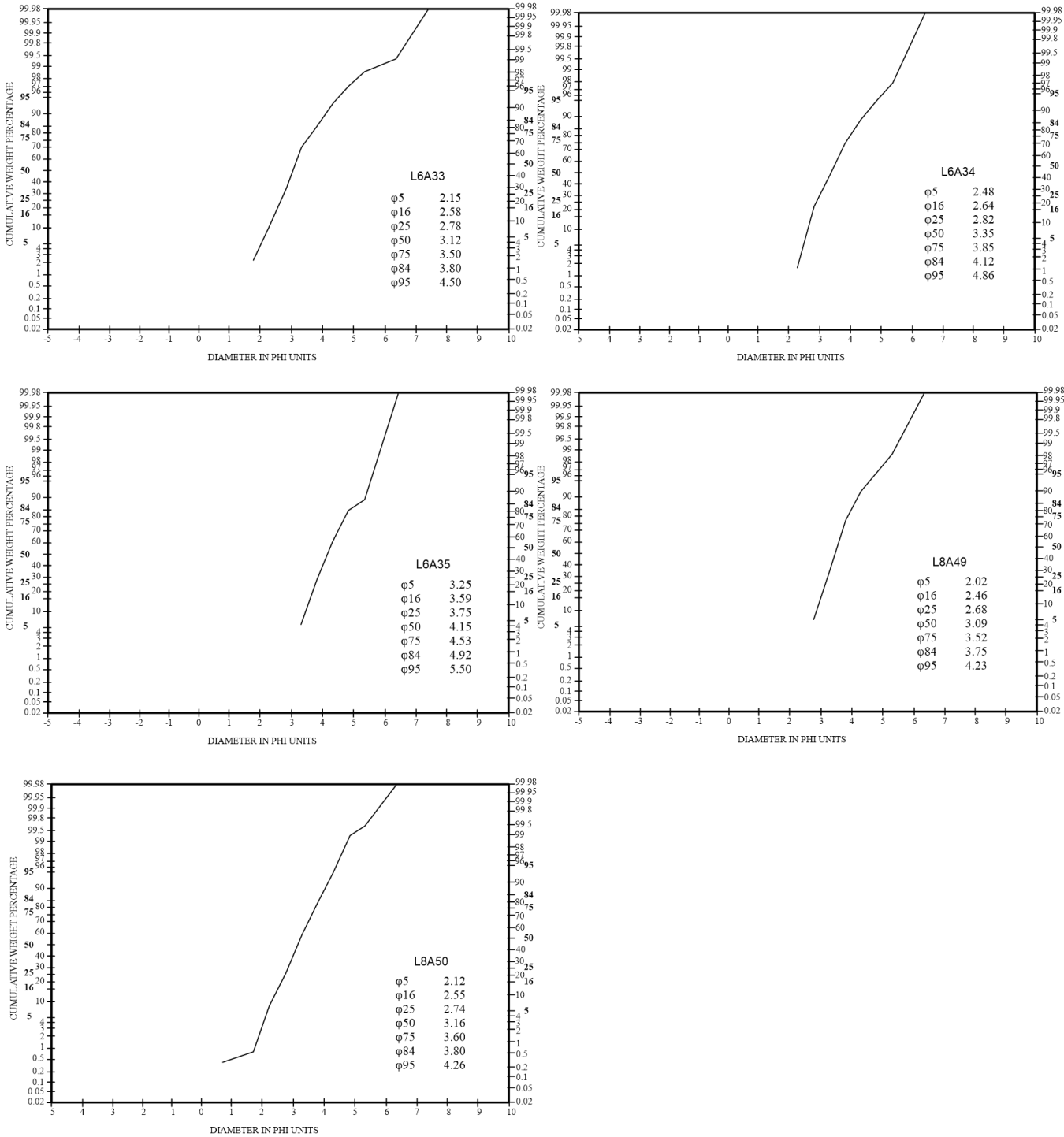


**Fig. 19:** Grain size distribution curves of samples towards Tuophema from Botsa (25° 50' 51" N, 94° 10' 1" E) & (25° 52' 17.62" N, 94° 11' 6.65" E)

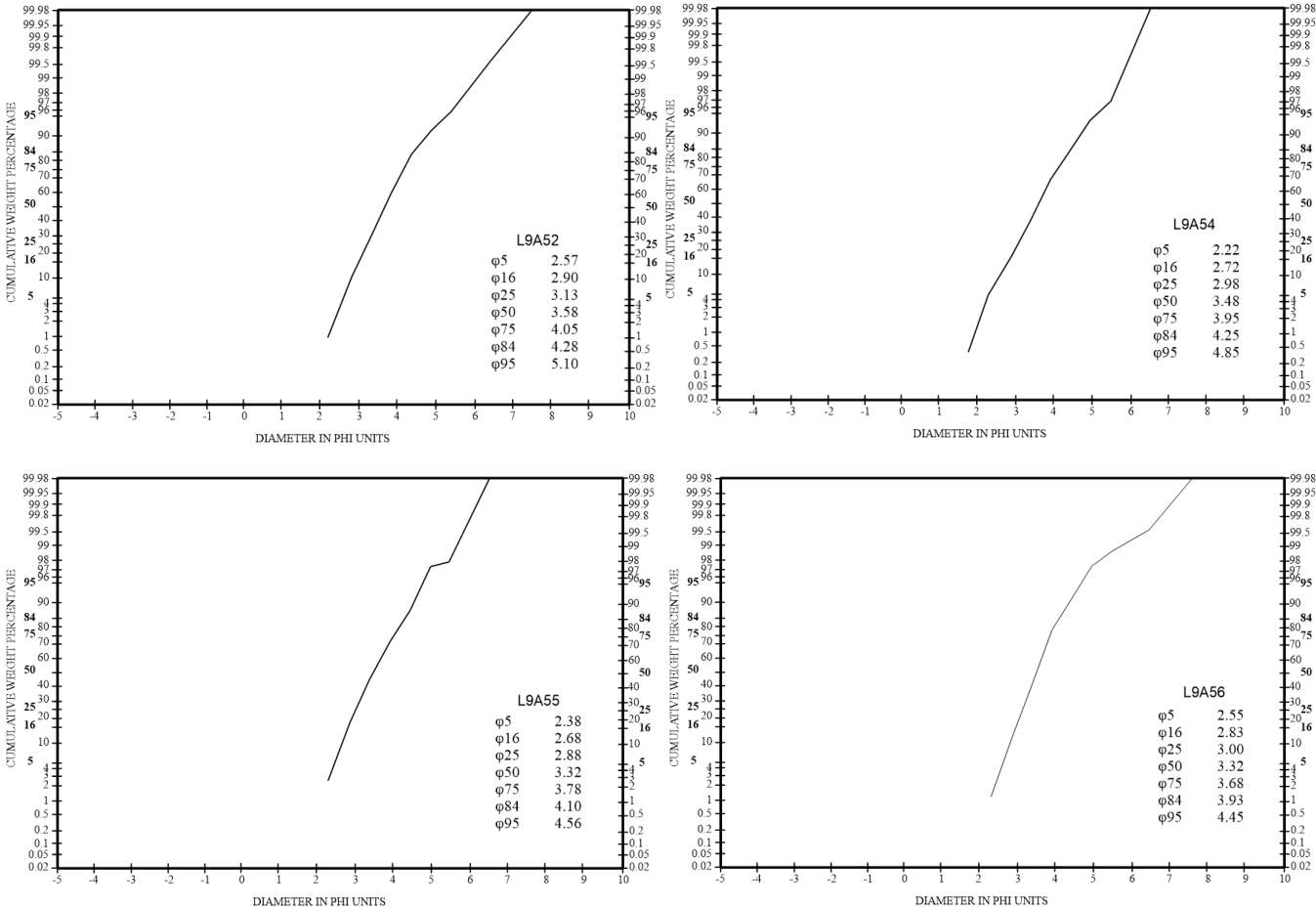


**Fig. 20:** Grain size distribution curves of samples towards Sedenyu from Botsa (25° 52' 22.23" N, 94° 08' 20.4" E)



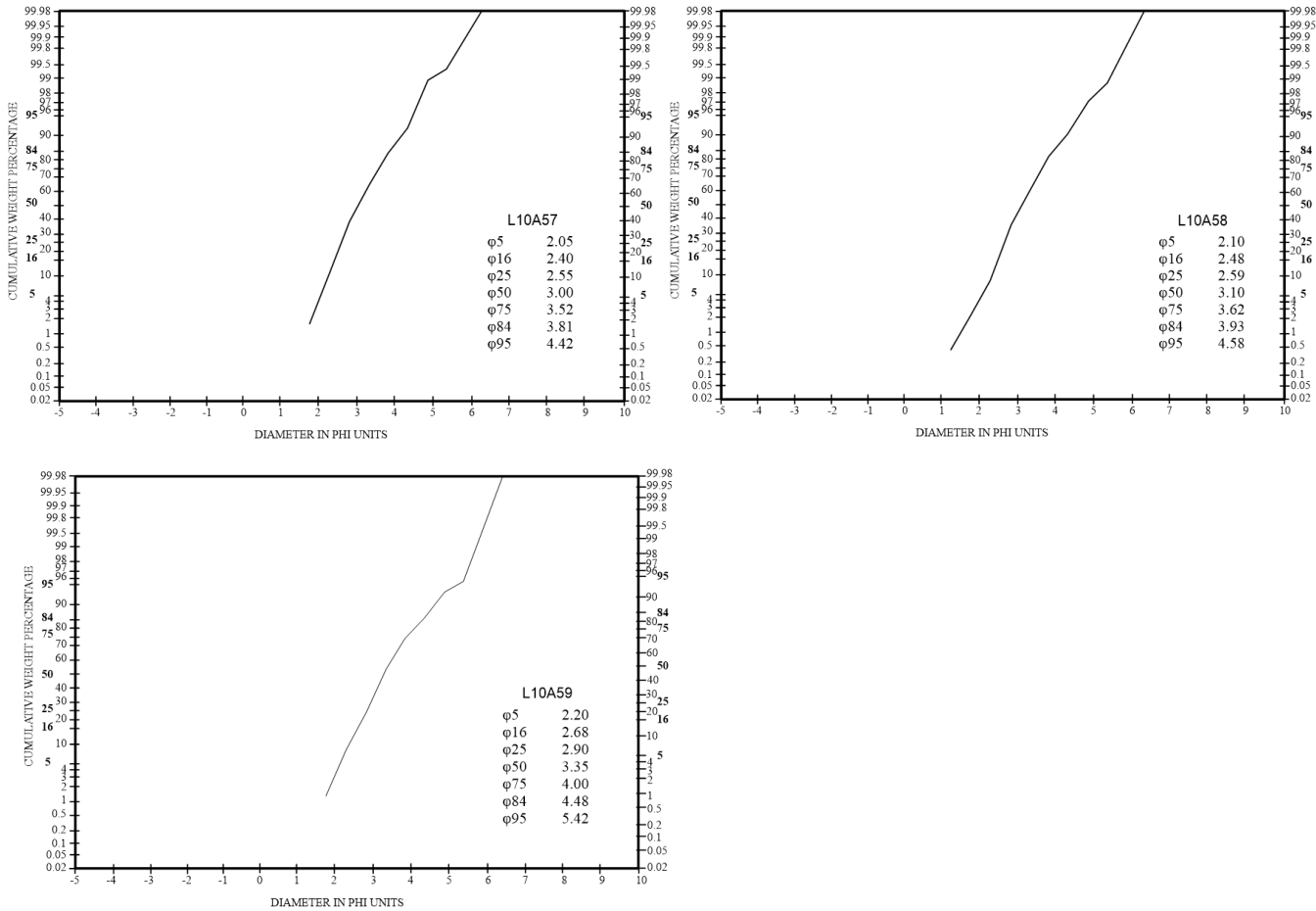


**Fig. 21:** Grain size distribution curves of samples towards Teichuma from Botsa (25° 50' 40.41" N, 94° 07' 22.5" E)

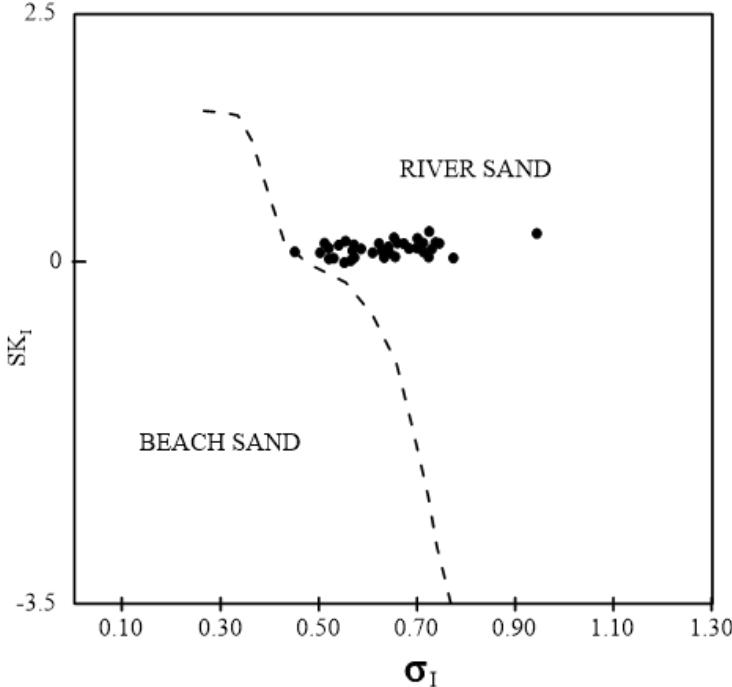


**Fig. 22:** Inclusive Graphic Skewness plotted against Inclusive Standard Deviation (after Friedman, 1961)

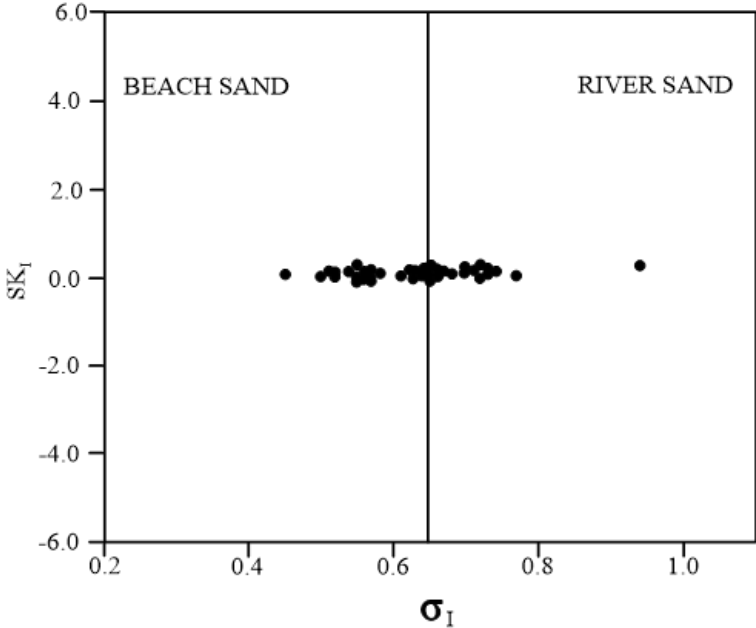


**Fig. 23:** Graphic Skewness plotted against Inclusive Standard Deviation (after Moiola and Weiser, 1968)

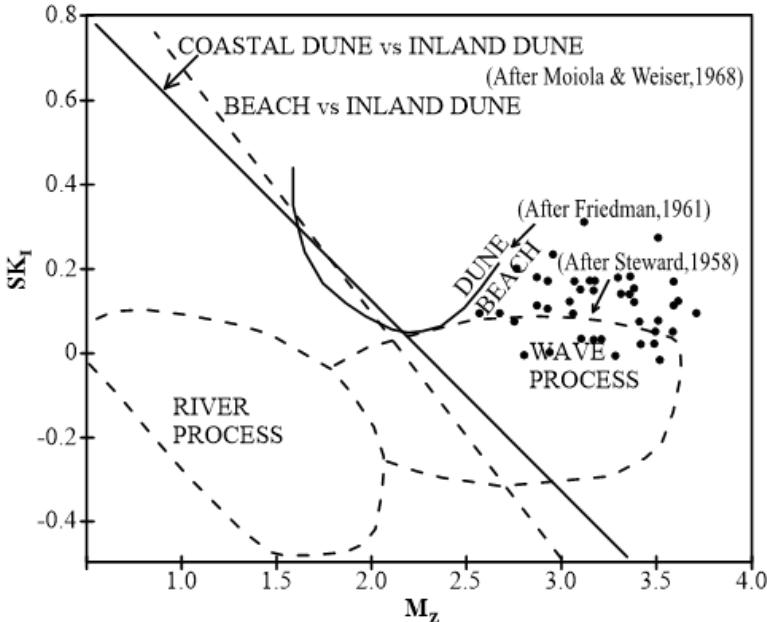


Fig. 24: Plot of Graphic Skewness plotted against Graphical Mean

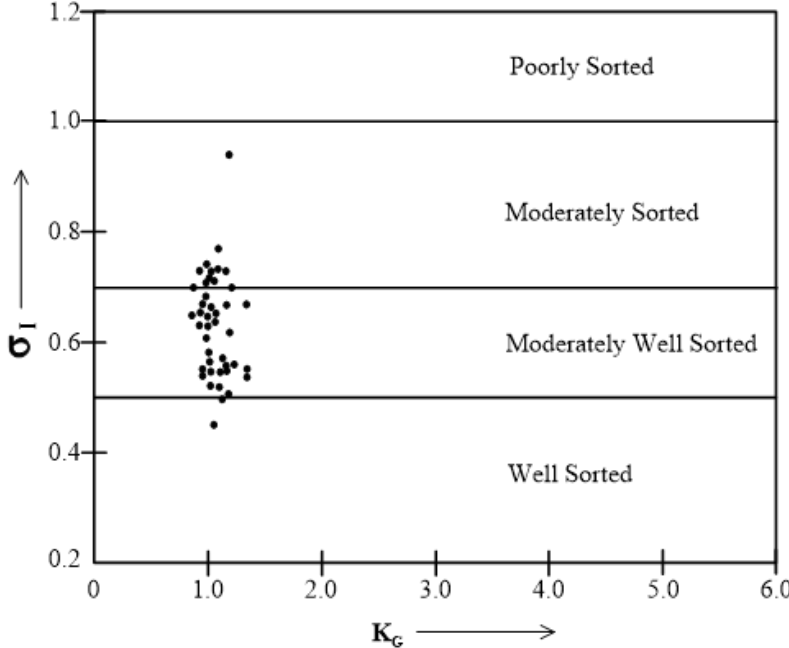


Fig. 25: Plot of Inclusive Graphic Standard Deviation versus Graphic Kurtosis

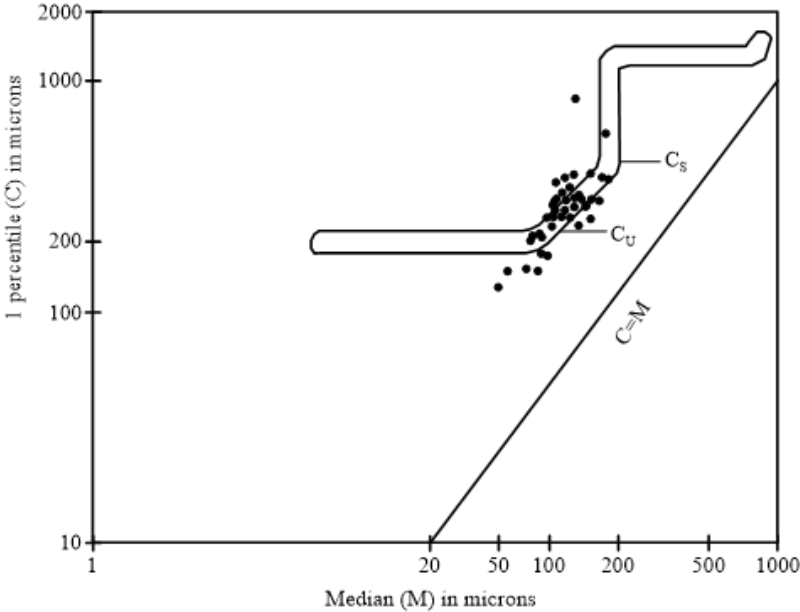


Fig. 26: C-M diagram plot of Palaeogene sediments (after Passega, 1957)

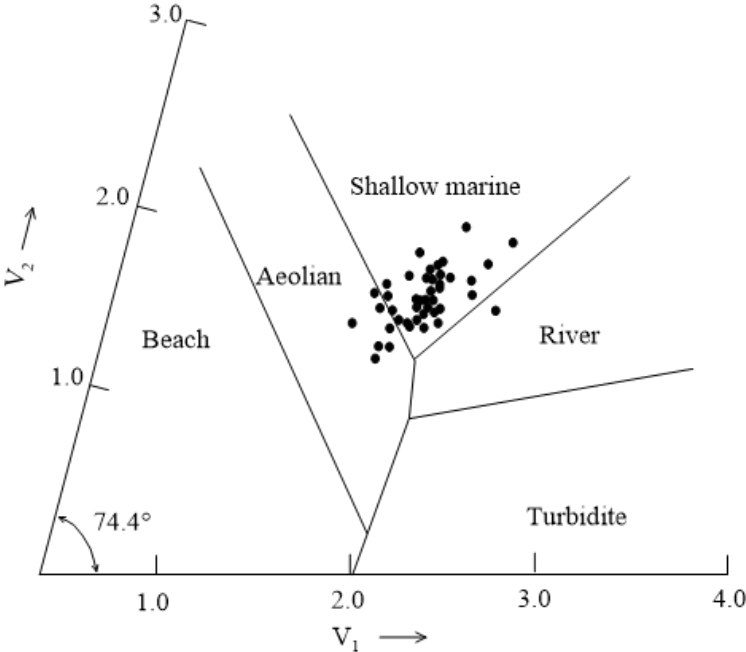
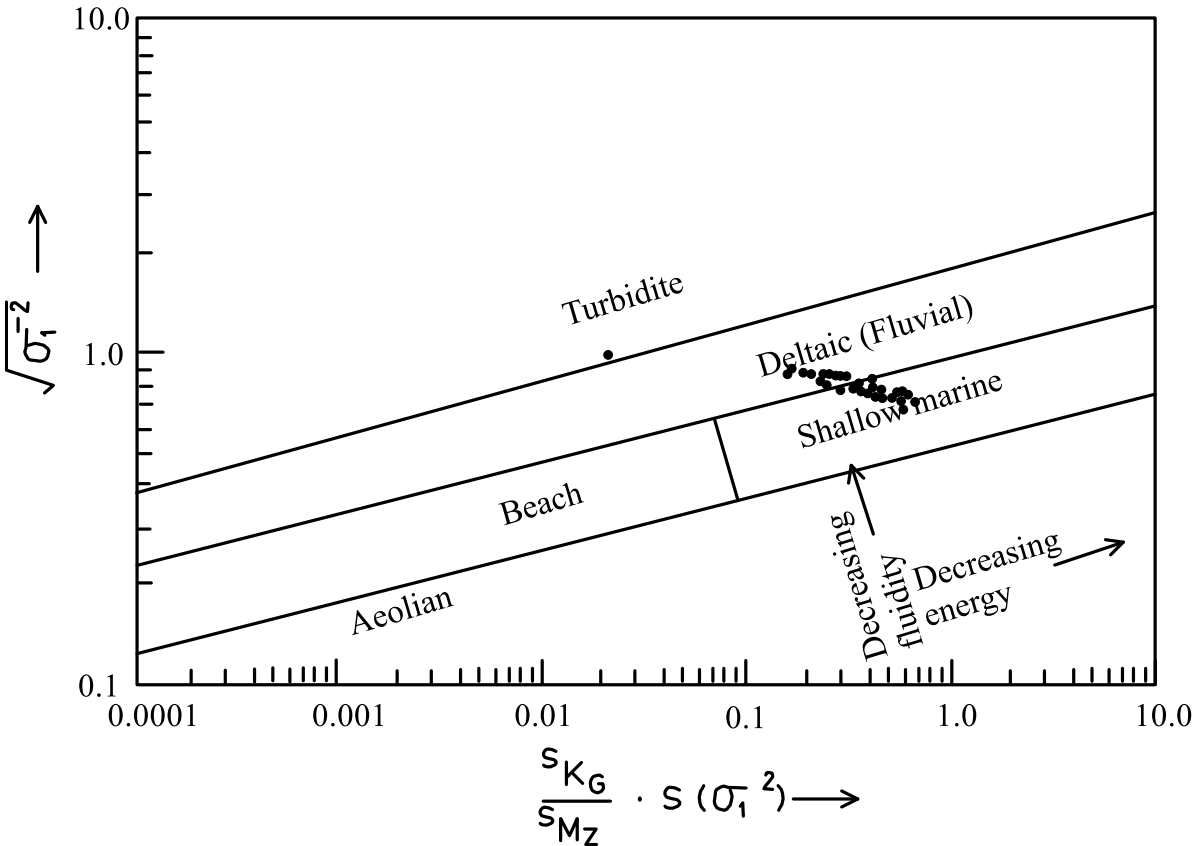


Fig. 27: Plot of V<sub>1</sub> against V<sub>2</sub> of Palaeogene sediments (after Sahu, 1983)



**Fig. 28:** The log-log plot of mean phi deviation versus the ratio of standard deviation of kurtosis to standard deviation of mean size times the standard deviation of variance (after Sahu, 1964)

## CHAPTER 5

### PETROGRAPHY AND MAJOR OXIDE GEOCHEMISTRY

#### 5.1 GENERAL

Petrographic study of clastic rocks is an important aspect of provenance studies as detrital composition of siliclastics rocks provides an insight into the source rock lithology. The mineralogical composition of clastic sediments in conjunction with textures bears a direct relationship with provenance, transportation processes, depositional environment and diagenesis of sediments (Suttner, 1974; Pettijohn, 1975). The detrital composition of clastic rocks has been correlated with the rate of source area uplift and basin subsidence by many workers (Dickinson and Rich, 1972; Dickinson and Suczek, 1979; Dickinson *et al.*, 1983 and Miall, 1990). The occurrence of a particular mineral assemblage has been utilized by many (Uddin and Lundberg, 1998 a and b; Singh *et al.*, 2004; Srivastava *et al.*, 2004; Mishra and Tiwari, 2005; Srivastava and Pandey, 2011; Imchen *et al.*, 2014; Srivastava and Kichu, 2021) in evaluating the tectonic events that control specific petrographic characters of a rock unit in a stratigraphic succession. However, Mack (1984) suggests that when evaluating the provenance on the basis of petrographic composition care must be taken while sampling. Petrographic studies also shed light on the climatic conditions and the relief of the source area (Mack, 1984) besides unveiling the nature of cementation and the effects of pressure solution in changing clastic grains.

For the purpose of the study, 42 thin sections were studied under the microscope and considerable data on the modal composition as well as diagenetic features were generated. Both whole rock and clay fractions were analyzed for their clay and other mineral contents using XRD technique. Further, Scanning Electron Microscopic examination of 5 freshly fractured sandstone sample surfaces have also been carried out, to corroborate the petrographic observations. To complement the data generated on modal composition, 30 samples were also analyzed through XRF for their major oxides composition.

## 5.2 PETROGRAPHY

The steel grey to dark grey Palaeogene sandstones of the study area comprise of very fine to medium sand fractions and are hard and compact in nature. In each of the thin sections, more than 200 grains were counted for assessing the framework composition. A brief description of framework grains has been presented in subsection 5.2.1. The overall detrital composition of the Palaeogene sediments in the study area can be expressed as Q 70.44%, F 0.96%, RF 9.91%, Mi 2.13%, and HM 2.37%, including both opaques and non-opaques; and CT 4.44 %, MX 9.74 % by volume (**Table 6**).

### 5.2.1 FRAMEWORK GRAINS

**Quartz:** Quartz is the most abundant constituent in these sandstones. Genetically, there are three basic types of quartz namely, non-undulatory quartz, undulatory quartz and polycrystalline quartz, which encompasses the total quartz in a clastic rock (Conolly, 1965). Blatt and Christie (1963) have opined that monocrystalline non-undulatory quartz grains (QNU) are generally identified by their complete extinction upon a slight (less than 1°) rotation of the microscopic stage (**Plates 13f, 16d, 16f & 17d**), while the monocrystalline undulatory quartz grains (QU) can be distinguished by their wavy or undulose extinction greater than about 5° *i.e.*, as the grain is rotated the different parts of the grain show extinction at different angles thus exhibiting a pattern of sweeping extinction (**Plates 12c, 13b, 13c, 13d, 13f, 14c, 14f, 15d & 17d**). This is also known as strained quartz and its presence can be an indicator of the provenance (Boggs Jr, 2012). Polycrystalline quartz is made up of aggregates of 2 to 3 units as well as > 3 units (**Plates 13e, 14a, 15e, 15f, 17b & 17e**). The presence of smooth, non-sutured boundaries between separate units distinguishes the polycrystalline quartz from metaquartzite rock fragments (Boggs Jr., 2012).

Quartz is the dominant framework grain in the studied sandstones. It comprises of non-undulatory (90.03%), undulatory (5.33%) and polycrystalline varieties (4.64%) (**Table 7**). The quartz grains occur in varying shapes from angular to sub-angular to sub-rounded (**Plates 12, 13, 14, 15, 16 & 17**) and the presence of inclusions in some of the quartz grains were also observed (**Plates 12a, 12e, 13e, 14c, 15a, 15e**).

**Feldspar:** Feldspar ranges between 0 to 3.97 % with an average of 0.96 % (**Table 6**). The plagioclase feldspar (73.01%) exhibiting the multiple, parallel lamellae characteristic of albite twinning that represents the sodic end member is the most common variety occurring in the Palaeogene sediments (**Plates 12c, 12e, 12f, 13b, 13d, 13e, 14f, 15b, 15e, 16a, 16b, 16c, 16e, 17a, 17b, 17c & 17d**), the occurrence of K feldspar is rare. However, a few K-feldspar grains were observed in the sandstones at the upper stratigraphic horizon (**Plates 14c, 15d, 15e & 15f**). The feldspar grains are mostly euhedral to subhedral and tabular parallel with silica precipitation and altered into matrix at places (**Plates 13b, 13e, 15e, 16c & 17d**).

**Mica:** The Palaeogene sediments commonly contain flakey elongate mica minerals like biotite and muscovite occurring as shreds and flakes that are bent showing kink bending and are also squeezed and warped around quartz grains (**Plate 12a, 12d, 14a, 14b, 17a, 17c, 17d**). The content of mica minerals in the Palaeogene sediments of the study area ranges from 0.82 % to 3.82 % (**Table 6**).

**Rock Fragments:** According to Dickinson, (1970) rock fragments constitute a significant portion of the detrital component next to quartz and are identified by their compositional and textural criteria. Identification of rock fragments is important in sandstone classification and they are also important in characterization of the provenance. Rock fragments in the studied sandstones comprise of igneous, metamorphic and sedimentary fragments. On an average they constitute around 9.91 % of all the detrital fractions and range from 3.13 % to 16.76 % (**Table 6**). Sandstones, siltstones and cherts constitute the sedimentary rock fragments (**Plates 12a, 13b, 13c, 13d, 13f, 14a, 14f, 15a, 15c, 15f & 16f**), whereas schist and phyllites represent the metamorphic rock fragments (**Plates 13b, 13f, 16b & 17f**). Volcanic fragments represent the igneous fractions (**Plates 14d, 14f, 15b, 15f, 16a & 16b**).

## 5.2.2 MATRIX AND CEMENT

Matrix is the fine-grained material in which the large grains are embedded. These fine-grained materials fill the interstitial spaces among the framework grains. Matrix of a maximum size of 0.03 mm appears to be favored by many workers (Boggs, Jr., 2012), however, the upper size limit of material in sandstones considered to be matrix is arbitrary and debatable. The proportion of matrix to framework is an important determinant of sandstone classification. In the



Palaeogene sandstones of the study area, matrix ranges from 5.44 % to 18.54% by volume (**Table 6**). The matrix digested grain boundaries have also been noticed in the studied sediments (**Plates 12a, 14b, 15c, 16e & 17a**).

Cements are authigenic materials that are chemically precipitated in pore spaces within the sediments or rocks. The most common cements are carbonates, silicates especially quartz and clay minerals, sulfates and chlorides. Ferruginous cements are also primarily common. In the present study, total cement ranges from 2.78 % to 6.78 % by volume (**Table 6**). Silica as well as iron cements are observed with yellowish/red coloured iron oxides occurring around the grains or as over-coating (**Plates 12a & 15d**). The presence of calcite occurring as cements are also observed (**Plates 12f, 13a, 16b, 16c, 16d, 17a & 17e**). Plagioclase feldspar embedded in calcite exhibiting porphyritic texture is also observed (**Plate 16b**).

### 5.2.3 CLAY MINERALS

Both clay fractions as well as whole rock samples were analyzed at Gauhati University, Guwahati, Assam using XRD technique for clay and other mineral contents of the 10 Palaeogene sandstones. Machine was set for both oriented as well as glycolated samples (**Table 9**). Analysis records the presence of kaolinite, illite, chlorite and montmorillonite clay minerals. (**Fig. 30**). In addition to these, other minerals recorded, includes clinocllore (chlorite group), cancrnite (feldspathoid) Zeolite group, Coesite (silica polymorphs), and brushite (gypsum Group). In SEM images also illite and kaolinite were seen.

**Illite:** In almost all the samples illite has been recorded. Decomposition of feldspar and degradation of mica produce illite in the sediments in the early stages of weathering under alkaline conditions with  $\text{Ca}^{2+}$  ions. With increasing depth and temperature transformation of kaolinite into illite happens. Formation of illite is also favored by quick mixing of fresh water sediments with marine sediments as marine sediments contain high concentration of K and Mg (Grim, 1968).

**Kaolinite:** The most abundant clay minerals in these sediments are kaolinite which is recorded in almost all the samples analyzed. Kaolinite is a common alteration product of K-feldspar favored by a good drainage system under acidic condition. Under warm humid climate with acidic condition and extensive leaching, formation of kaolinite has also been recorded in soils.

**Montmorillonite:** In all the glycolated samples, montmorillonite, a member of smectite group has been recorded. It is a weathering product of ferromagnesium rocks such as basalts and gabbros and is chemically denoted as hydrated sodium calcium aluminum magnesium silicate. However, montmorillonite can also be formed under various conditions.

**Chlorite:** Chlorite is also a weathering product of ferromagnesium minerals in such rocks as basalts and gabbros. It has magnesium and iron in its structures. Chlorites are present in low as well medium rank metamorphic rocks. They are also found in deeply buried sediments.

#### 5.2.4 HEAVY MINERALS

Clastic sedimentary rocks may often contain a small percentage of grains that have greater density than  $2.85 \text{ g cm}^{-3}$  called heavy minerals. Heavy mineral studies are undertaken to determine sediment provenance since heavy mineral suites provide important information on the mineralogical composition of the source area. Provenance studies in clastic sediments are carried out by separating heavy minerals from the bulk of the grains using heavy liquids, like Bromoform having a specific gravity of  $2.89 \text{ g cm}^{-3}$ . Altogether 35 indurated samples were studied for their heavy mineral contents to determine the source of the sediments and also the mineralogical maturity of the Palaeogene sediments of the study area. Following the method suggested by Folk (1980) heavy minerals was separated and the grains were mounted on glass slides and examined under the microscope for identification of both opaque heavy minerals as well as non- opaque heavy minerals.

In the present study identified heavy minerals include zircon, tourmaline, rutile, kyanite, sillimanite and opaques. According to the type and shape relative abundance of heavy minerals are represented by Pie diagrams (**Fig. 29**). Heavy minerals recorded include anhedral, euhedral to subhedral and recycled zircon with and without inclusions (**Plate 18**); anhedral, euhedral, subhedral and sub rounded to rounded tourmaline (**Plate 19**); euhedral to subhedral and anhedral to sub rounded rutile (**Plate 20, No. 1-21**); anhedral to sub rounded and euhedral to subhedral kyanite (**Plate 20, No. 22-37**) and sillimanite (**Plate 20, No. 38-41**). The opaque grains are shown in (**Plate 21**).

Dominated by the presence of euhedral and subhedral varieties contribution from a crystalline source is suggestive of the heavy mineral assemblages of the Palaeogene sediments of the study area. Nevertheless, the presence of well-rounded to sub rounded grains signifies either long transport or a recycled origin. Heavy minerals as provenance indicator as well as transport history have been utilized by many workers (Uddin and Lundberg, 1998b; Singh *et al.*, 2004; Mishra and Tiwari, 2005; Srivastava and Pandey, 2011; Srivastava and Kebeule, 2018, Srivastava and Kichu, 2021).

As a measure of mineralogical maturity of sandstones, Hubert (1962) proposed a Zircon-Tourmaline-Rutile (ZTR) index. The ZTR index is the percentage of combined zircon, tourmaline and rutile grains among the transparent, non-micaceous, detrital heavy minerals. ZTR index for the Palaeogene sediments of the study area is high suggesting that the sediments are mineralogically highly matured. As a whole, the heavy mineral assemblage of the Palaeogene sediments of the study area suggests a mixed source. Percentage of angular heavy minerals has increased in the sandstones lying at the upper stratigraphic horizons.

### 5.3 NOMENCLATURE, CLASSIFICATION AND MODAL ANALYSIS

McBride (1963), Dott (1964), Okada (1971), Pettijohn *et al.*, (1972), Pettijohn (1975), Folk (1980) and Zuffa (1980) have all introduced a number of schemes and systems for classification of sandstone but there is no single scheme which satisfies all parameters for classification of sandstone. Depending upon the quartz content and matrix percentage a particular classification can be adopted for sandstone classification. In the present study, Folk's (1980) classification scheme has been used for nomenclature and classification of the sandstones of the area.

Folk's (1980) classification scheme shows the three commonest components of sandstones i.e., detrital quartz, feldspar and rock fragments as the end members to form a triangular plot represented as Q, F and R respectively. Following Folk (1980), the Palaeogene sandstones of the study area have been classified into Quartz arenite and sublith-arenite categories (**Fig. 31**).

To understand the probable provenance and tectonic settings of the Palaeogene sediments of the study area, discriminatory diagrams suggested by Dickinson and Suczek (1979) were used. Dickinson and Suczek (1979) plots of polycrystalline quartz-lithic fragment volcanic-lithic

fragment sedimentary (**Fig. 32**) and the monocrystalline quartz- plagioclase-potash feldspar (**Fig. 37**) indicates that the sediments were derived from a collision suture, fold thrust belt in a continental block provenance with increasing maturity. The triangular plots of quartz total-feldspar-lithic fragment (**Fig. 33**) and mono quartz-feldspar-lithic fragment (**Fig. 34**) suggests that the detritus was mainly supplied by recycled orogen provenances.

Following Dickinson *et al.*, (1983) with quartz-feldspar-lithic fragment (**Fig.35**) and mono crystalline quartz-feldspar-lithic fragment (**Fig. 36**) as end members a dominantly recycled orogenic provenance has been interpreted. The ternary plot of total quartz-feldspar-lithic fragment (after Suttner *et al.*, 1981) suggests that the sediments were influenced by metamorphic humid conditions (**Fig. 38**).

Based on the types of quartz i.e., mono crystalline undulatory, non-undulatory, polycrystalline 2-3 and >3 units, the diamond diagrams (after Basu *et al.*, 1975 and Tortosa *et al.*, 1991) indicates middle and upper rank gneisses and plutonic rocks as the source rocks. **Fig. 39 (a) & Fig. 39 (b)**

## 5.4 DIAGENESIS

Diagenesis is the physical and chemical changes occurring in sediments during and after their deposition. Diagenetic changes begin near the surface and continue up to deeper levels before metamorphism sets in (Blatt *et al.*, 1980). Burial time, temperature and subsurface water chemistry generally control the rate and type of diagenesis. Microscope still remains the main instrument for identification of diagenetic modifications and petrographic examination continues to be the mainstay of diagenetic studies, however, this has been greatly supplemented by the use of Scanning Electron Microscopic (SEM) technique which has significantly improved our understanding of diagenetic process and it has also helped in understanding the physico- chemical conditions which sediments have undergone.

### 5.4.1 SCANNING ELECTRON MICROSCOPY (SEM)

The Scanning Electron Microscope (SEM) which uses a focused beam of high-energy electrons, give information about the sample including external morphology, chemical composition, and crystalline structure. Scanning electron microscope generates signals at the

surface of solid specimens and data are collected over a selected area of the surface of the sample. The SEM using Energy dispersive X-ray spectroscopy (EDS) also analyses selected point locations on the sample; which provides qualitatively or semi-quantitatively chemical compositions.

Pitman (1972), Krinsley and Doornkamp (1973), Ingersoll (1974) Marzolf (1976) have all propounded that diagenetic signatures within sediments is co-relatable with increasing depth. For the purpose of identification of diagenetic features and other related diagenetic signatures five freshly broken sandstone samples were examined through SEM at Gauhati University, Guwahati, Assam. **(Plates 22 & 23).**

#### 5.4.2 EFFECTS OF DIAGENESIS

In addition to compaction and cementation, authigenesis, in which new minerals grow from, are common diagenetic features observed in the Palaeogene sediments of the study area **(Plates 12, 13, 14, 15, 16, & 17)**. Silica overgrowth is considered a common feature of early diagenesis. However, presence of matrix does not allow the overgrowth as it acts as barrier against the silica solution (Carozzi, 1960; Heald and Lorese, 1974). Other diagenetic features observed include fracturing, crushing, bending and warping of micaceous minerals around detrital quartz grains **(Plates 12a, 12d & 14a)**. The presence of these features represents deep burial diagenesis.

#### 5.4.3 DIAGENETIC STAGE

Progressive appearance of certain features characterizes these stages during diagenesis. According to Bjorkum and Gjelsvik, (1988) precipitation of iron oxides indicates redoxomorphic stage whereas modified grain to grain contacts, alteration of feldspar, silica over growth and, corrosion of detrital grains characterizes the locomorphic stage (Borak and Friedman, 1981). Authigenic mica represents the phylломorphic stage.

#### 5.4.4 DIAGENETIC ENVIRONMENT

The Palaeogene sediments in the study area have undergone both early and the late diagenesis. Signatures of early diagenesis include precipitation of silica as overgrowth and also the precipitation of calcite and iron cements. These features are indicative of an early diagenesis (Carozzi, 1960; Heald and Lorese, 1974). According to Sengupta, (1994) albitization of feldspars,

fracturing, crushing, bending and warping of micaceous material around detrital quartz suggests late diagenesis; thus, indicating deep burial, under increasing pressure and temperature conditions.

#### 5.4.5 CEMENTS

Cements are authigenic material precipitated within the pore spaces during diagenesis. A number of different materials can form cement, the most common being silica, carbonate and iron-oxides. The availability of these in pore waters, the temperature and the chemistry of the pore waters determines the type of the cement formed in the sediment. Silica cementations occurs under increased acidity and cooler conditions whereas, carbonate minerals may precipitate as cements if the temperature rises and the acidity decreases (Nichols, 2009).

In the study area silica cement is the dominating cementing material. Silica cement is usually seen as overgrowths of silica on the surfaces as well as around the quartz grains. The precipitation of silica out of the pore fluids nucleates itself on the surface of the quartz grains resulting in the growth of the quartz crystals. Silica overgrowths occurring mostly as epitaxial overgrowths have been observed. Neomorphic quartz has also been noticed. Due to silica precipitation the quartz grains are enlarged thereby forming thick rims of silica cement around detrital quartz grains. The presence of the enlarged quartz grains is commonly identified. The alteration of clay minerals releases much silica, which may help explain silica in muddy sandstones. The underlying thick pile of argillaceous sediments experiencing continuous and uninterrupted loading could have supplied silica for cementation of sediments at the upper stratigraphic horizons. Similarly, the supply for silica cementation could be the result of devitrification of volcanic glasses (Surdam and Boles, 1979), diagenetic transformation of silicates including clay minerals (Towe, 1962) and pressure solution effects (Dapples, 1979). Further, the overgrowths might have occurred above 80°C at a depth of 1.5 to 2 km (Surdam *et al.*, 1989; Dutton and Diggs, 1990).

Calcite is the primary carbonate cementing materials in siliclastics sediments, since they are much more soluble than silica. The occurrence of calcites as carbonate cementing material is common in the study area. Precipitation and dissolution of carbonate minerals takes place during diagenesis.

Other common cement in siliclastics sediments are iron oxides. Ferruginous (iron oxide) cement occurring as shapeless void fillers as well as coating on framework grains are observed in the Palaeogene sediments of the study area. The source of ferrous iron could be attributed to the presence of iron bearing accessory minerals of igneous/metamorphic rock fragments and also phyllosilicates. Walker (1974) has suggested that weathering of iron rich minerals is a major source of iron cement. The leaching of iron rich clays is also another source of iron cement. Dissolution out of the source minerals occurs mostly in reducing conditions and once dissolved iron when exposed to oxygen precipitates readily. Presence of ferruginous cement in the sandstone samples suggests an enhanced oxidation of meteoric water.

#### 5.4.6 QUARTZ OVERGROWTH

Silica cement takes the form of optically continuous overgrowths of quartz grains. Where the surfaces of the grains are free from any coating, quartz overgrowth occurs as epitaxial overgrowth on detrital quartz grains. Such overgrowths are less developed where quartz grains are held together by clay matrix (Heald and Lorese, 1974). According to Burley *et al.* (1985) presence of authigenic quartz in the siliclastics of the study area indicates early diagenesis under eogenetic (shallow depth) marine conditions. Small and sharp polyhedral aggregates of neo-quartz crystals are seen developing at the stress points under shallow diagenetic conditions (Blatt *et al.*, 1980).

#### 5.4.7 ALBITIZATION

Albitization of feldspar is a replacement process which involves replacement of calcic plagioclase or K feldspar with sodic plagioclase and generally progresses along the plane of weakness i.e., fracture and cleavage traces, where fluids could penetrate the crystal. In thin sections, albitized feldspar is identified by their indistinct and diffused twinning and also the presence of small blebs. Partial albitization of K feldspar or the presence of chessboard texture (Walker, 1984) is an indication of albitization (**Plate 12e**). Albitization occurs at temperatures of the order of 100-150°C (Boles, 1982; Surdam *et al.*, 1989) and also at temperatures as low as 70-100°C (Morad *et al.*, 1990). Some albitized feldspar has vague, irregular complex twin lamella which does not pass through the entire crystal. Presence of authigenic feldspar in the studied siliclastics has been attributed to increasing pressure and temperature (>100°C) owing to burial and thermal history.

#### 5.4.8 GRAIN CONTACTS

The nature of the grain contacts determines the degree of compaction of the sediments. Sediments subjected to little overburden pressure will be in contact mainly at points known as point contacts. Under high overburden pressures the boundaries between grains become complex sutured contacts (**Plates 12d, 12e, 13b & 13d**). Long or straight contacts occur in grains whereby reduction in porosity changes the packing of the grains thus bringing the edges of the grains together (**Plates 12d, 14b & 17a**). Pressure solution between grains results in concavo-convex contacts (**Plates 12e, 13c, 13e & 13f**). Reactions between matrix and/or cements results in corroded grain boundaries that are later filled by iron oxide cement imparting a floating character of the grains identified as floating grains. All types of grain contacts namely floating, long, concavo-convex and sutured types have been observed in the Palaeogene sediments of the study area. Penetrative contacts (concavo-convex and sutured) are dominant over the other types. On the basis of dominance of concavo-convex and sutured contacts and low proportion of long and floating contacts a deep burial condition of diagenesis has been deduced for the Palaeogene sediments of the study area.

### 5.5 GEOCHEMICAL ANALYSIS

In the present study, major element geochemistry has been used for better understanding of the provenance and the palaeoclimate. Petrographic studies in conjugation with geochemical analysis not only help in identification of provenance but also in tectonic settings (Bhatia, 1983). Several studies have shown that major element geochemistry reflects provenance differences that depend on the tectonic setting (Bhatia and Crook, 1986; Roser and Korsch, 1986; Skilbeck and Cawood, 1994). Geochemical characteristics and framework composition of sandstones, their provenance type and the tectonic environment have provided considerable impetus to the subject (Kakul, 1968; Crook, 1974; Schwab, 1975; Suttner and Dutta, 1986; and McLennan, 1989).

In the present study, 30 Palaeogene siliciclastic samples have been analyzed for their major element composition and data is represented in **Table 8**. The samples were analyzed using an automatic X-ray Fluorescence Spectrometer at Wadia Institute of Himalayan Geology, Dehradun. The plot of  $\log(\text{Fe}_2\text{O}_3/\text{K}_2\text{O})$  versus  $\log(\text{SiO}_2/\text{Al}_2\text{O}_3)$  (**Fig. 40**), after Herron (1988), has been used to determine the types of sandstones according to their chemical composition. The clustering of



data points suggests presence of mainly two types of the sandstones in the area: graywackes and litharenite.

The bivariate plots of  $\text{Fe}_2\text{O}_3$  (Total) + MgO vs  $\text{K}_2\text{O}/\text{Na}_2\text{O}$  (**Fig. 41**),  $\text{Fe}_2\text{O}_3$  (Total) + MgO vs  $\text{Al}_2\text{O}_3/\text{SiO}_2$  (**Fig. 42**) and  $\text{Fe}_2\text{O}_3$  (Total) + MgO vs  $\text{TiO}_2$  (**Fig. 43**; after Bhatia, 1983), are employed for understanding the tectonic settings. A passive margin/and or transitional tectonic setting for the Palaeogene sediments has been indicated. This is further corroborated by the plot of  $\text{K}_2\text{O}/\text{Na}_2\text{O}$  vs  $\text{SiO}_2$  (after Roser and Korsch, 1986) (**Fig. 44**), where the  $\text{SiO}_2$  content and  $\text{K}_2\text{O}/\text{Na}_2\text{O}$  ratios appear to be particularly sensitive indicators of geotectonic setting. Potter, (1978a, 1978b) have established that passive margin settings are the primary sites of major river systems and typically have provenance comprising of recycled sedimentary debris and/or older plutonic metamorphic material, with a relatively small volcanic component.

Ternary plots of  $\text{Fe}_2\text{O}_3$ - MgO- $\text{TiO}_2$  and CaO- $\text{Na}_2\text{O}$ - $\text{K}_2\text{O}$  (**Fig. 46 & 47**), following Condie (1967) and Le Maitre (1976), indicates a granitic/ granodiorite source for the Palaeogene sediments of the study area. The signatures of granitic and granodioritic provenance appears to have been existed along rifted basin, since passive margins comprises of rifted margin along the edges of the continents, remnant ocean basin adjacent to collision orogen, and inactive or extinct convergent margins.

The bivariate plot of  $\text{Al}_2\text{O}_3+\text{K}_2\text{O}+\text{Na}_2\text{O}$  vs  $\text{SiO}_2$ , after Suttner and Dutta (1986) indicates a largely humid climate for the Palaeogene sediments of the study area (**Fig. 45**). Similar interpretation is also drawn from plot of QFL, after Suttner *et al.*, 1981 (**Fig. 38**).

Sample No.	T. Qtz. %	T. Feldspar %	T. Rock Fragment %	Mica %	Heavy Minerals %	Matrix (Vol %)	Cement (Vol %)
L1A1	71.17	0.87	10.92	3.06	1.31	9.42	3.25
L1A3	71.00	0.44	11.09	2.22	3.99	8.47	2.78
L1A4	70.56	0.87	12.63	1.74	1.31	8.91	3.98
L1A6	67.39	0.00	13.22	2.56	2.13	10.78	3.92
L1A7	65.93	0.43	13.88	1.30	5.21	9.38	3.87
L2A8	67.55	0.00	14.87	1.27	1.27	11.17	3.86
L2A9	65.41	0.42	13.33	3.33	0.83	12.19	4.49
L2A10	66.21	0.86	13.33	2.58	3.01	9.86	4.15
L2A13	72.37	0.00	10.28	1.71	1.28	10.13	4.23
L2A15	75.22	0.44	8.75	2.19	0.87	8.86	3.67
L2A16	68.65	0.44	16.39	2.21	0.89	7.89	3.53
L3A17	69.19	2.06	4.94	2.47	3.71	12.53	5.1
L3A18	72.61	1.23	4.10	0.82	3.28	12.73	5.22
L3A19	68.86	1.26	4.62	2.94	6.30	11.94	4.09
L3A20	71.02	1.28	4.25	2.55	5.95	9.92	5.03
L3A21	74.47	1.27	3.39	2.54	2.96	10.53	4.84
L4A22	68.70	2.11	10.12	1.26	2.11	11.39	4.31
L4A23	68.17	1.67	10.46	0.84	2.51	11.17	5.18
L4A24	71.87	0.85	10.21	1.28	0.85	9.18	5.77
L4A26	68.20	1.26	11.72	1.67	0.84	10.98	5.34
L4A27	68.72	0.84	11.80	1.26	1.69	10.7	4.98
L5A28	66.84	0.75	3.36	2.61	1.12	18.54	6.78

L5A30	72.08	0.00	3.13	1.96	1.18	15.44	6.21
L5A31	69.17	0.00	3.56	2.77	3.56	15.62	5.33
L6A33	70.79	0.00	10.92	1.75	3.93	7.77	4.84
L6A34	67.79	1.31	12.25	3.50	2.62	8.64	3.89
L6A35	69.24	0.00	13.85	3.57	2.68	7.61	3.05
L6A36	70.61	0.88	10.97	2.19	3.07	8.91	3.37
L7A37	71.59	1.32	11.42	1.76	1.76	7.92	4.24
L7A38	71.66	1.33	11.50	2.21	1.77	7.1	4.43
L7A39	67.90	1.34	16.53	0.89	2.68	6.35	4.31
L7A44	65.00	2.12	12.75	3.82	1.27	10.78	4.25
L7A46	64.59	2.55	13.60	2.55	1.70	10.03	4.98
L8A49	78.85	1.35	4.96	2.25	2.70	6.35	3.54
L8A50	82.26	1.82	3.18	2.27	1.36	5.44	3.67
L9A52	76.30	0.00	6.17	2.65	3.09	7.68	4.11
L9A54	79.16	0.00	5.28	1.32	2.20	7.81	4.23
L9A55	78.49	0.00	4.80	2.62	1.31	8.03	4.76
L9A56	72.23	0.00	7.83	3.05	3.92	8.02	4.95
L10A57	64.39	3.97	16.76	1.76	1.32	6.96	4.83
L10A58	68.38	1.31	15.24	1.31	0.87	7.92	4.97
L10A59	68.08	1.76	14.05	0.88	3.07	7.88	4.28

**Table 6:** Detrital composition of Palaeogene sediments in the study area

Sample No	Poly Qtz		Mono Qtz		Percentage			Feldspar		Percentage	
	2-3	>3	Und Qtz	Non-Und Qtz	Poly Qtz	Und Qtz	Non-Und Qtz	K	Plag	K	Plag
L1A1	1	1	2	159	1.23	1.23	97.55	0	2	0	100
L1A3	4	1	1	154	3.13	0.63	96.25	0	1	0	100
L1A4	0	0	1	161	0.00	0.62	99.38	0	2	0	100
L1A6	4	2	2	150	3.80	1.27	94.94	0	0	0	0
L1A7	3	1	3	145	2.63	1.97	95.39	0	1	0	100
L2A8	2	0	0	157	1.26	0.00	98.74	0	0	0	0
L2A9	1	0	1	155	0.64	0.64	98.73	0	1	0	100
L2A10	4	5	0	145	5.84	0.00	94.16	0	2	0	100
L2A13	4	1	3	161	2.96	1.78	95.27	0	0	0	0
L2A15	8	4	5	155	6.98	2.91	90.12	0	1	0	100
L2A16	11	3	7	134	9.03	4.52	86.45	0	1	0	100
L3A17	5	1	9	153	3.57	5.36	91.07	0	5	0	100
L3A18	4	3	0	170	3.95	0.00	96.05	0	3	0	100
L3A19	7	4	8	145	6.71	4.88	88.41	0	3	0	100
L3A20	5	0	2	160	2.99	1.20	95.81	0	3	0	100
L3A21	2	1	9	164	1.70	5.11	93.18	0	3	0	100
L4A22	6	1	11	145	4.29	6.75	88.96	0	5	0	100
L4A23	20	8	12	123	17.18	7.36	75.46	0	4	0	100
L4A24	5	1	9	154	3.55	5.33	91.12	0	2	0	100
L4A26	10	3	9	141	7.98	5.52	86.50	0	3	0	100
L4A27	10	4	4	145	8.59	2.45	88.96	0	2	0	100

L5A28	5	0	12	162	2.79	6.70	90.50	0	2	0	100
L5A30	9	0	8	167	4.89	4.35	90.76	0	0	0	0
L5A31	5	3	5	162	4.57	2.86	92.57	0	0	0	0
L6A33	4	0	5	153	2.47	3.09	94.44	0	0	0	0
L6A34	9	1	9	136	6.45	5.81	87.74	0	3	0	100
L6A35	5	0	9	141	3.23	5.81	90.97	0	0	0	0
L6A36	5	1	15	140	3.73	9.32	86.96	0	2	0	100
L7A37	9	1	11	142	6.13	6.75	87.12	0	3	0	100
L7A38	8	2	18	134	6.17	11.11	82.72	0	3	0	100
L7A39	14	7	20	111	13.82	13.16	73.03	1	2	33.33	66.67
L7A44	4	0	17	132	2.61	11.11	86.27	0	5	0	100
L7A46	9	1	18	124	6.58	11.84	81.58	0	6	0	100
L8A49	9	1	20	145	5.71	11.43	82.86	0	3	0	100
L8A50	4	2	14	161	3.31	7.73	88.95	0	4	0	100
L9A52	5	0	16	152	2.89	9.25	87.86	0	0	0	0
L9A54	4	2	20	154	3.33	11.11	85.56	0	0	0	0
L9A55	5	1	14	160	3.33	7.78	88.89	0	0	0	0
L9A56	4	1	10	151	3.01	6.02	90.96	0	0	0	0
L10A57	4	3	9	130	4.79	6.16	89.04	0	9	0	100
L10A58	5	1	11	140	3.82	7.01	89.17	0	3	0	100
L10A59	4	1	9	141	3.23	5.81	90.97	0	4	0	100

**Table 7:** Recalculated percentages of Quartz and Feldspar in Palaeogene sandstones

## [PETROGRAPHY AND MAJOR OXIDE GEOCHEMISTRY]

Sample	SiO <sub>2</sub>	Na <sub>2</sub> O	MgO	Al <sub>2</sub> O <sub>3</sub>	P <sub>2</sub> O <sub>5</sub>	K <sub>2</sub> O	CaO	TiO <sub>2</sub>	MnO	Fe <sub>2</sub> O <sub>3</sub>	Sum%
L1A1	81.05	0.69	0.58	8.66	0.11	1.14	0.33	0.60	0.03	2.91	96.10
L1A3	78.44	0.78	0.77	10.29	0.12	1.30	0.14	0.73	0.02	3.76	96.35
L1A6	79.30	0.92	0.72	10.92	0.12	1.46	0.17	0.76	0.02	3.27	97.66
L1A7	81.33	0.85	0.81	9.83	0.14	1.18	0.28	0.87	0.01	3.54	98.84
L2A8	81.41	0.82	0.56	8.91	0.09	1.24	0.15	0.51	0.02	2.75	96.46
L2A13	85.32	0.72	0.45	7.80	0.08	1.06	0.12	0.55	0.01	2.29	98.4
L2A15	81.72	0.80	0.53	8.82	0.09	1.25	0.29	0.52	0.02	2.40	96.44
L2A16	91.76	0.45	0.14	3.84	0.05	0.50	0.05	0.28	0.01	1.19	98.27
L3A17	74.99	0.89	1.42	10.25	0.12	1.48	1.76	0.65	0.03	3.35	94.94
L3A19	76.35	0.89	1.24	9.26	0.11	1.25	1.38	0.58	0.03	3.62	94.71
L3A20	74.39	0.79	1.40	8.52	0.12	1.08	1.22	0.52	0.09	5.38	93.51
L3A21	72.61	0.89	1.36	11.66	0.10	1.67	1.04	0.68	0.02	4.28	94.31
L4A22	84.98	0.55	0.53	7.32	0.08	0.93	0.10	0.50	0.01	2.47	97.47
L4A24	78.11	0.74	0.73	10.95	0.08	1.53	0.13	0.48	0.01	3.25	96.01
L4A25	78.86	0.77	0.81	9.60	0.10	1.37	0.51	0.60	0.02	3.51	96.15
L4A27	81.38	0.75	0.66	10.21	0.11	1.43	0.15	0.68	0.01	2.81	98.19
L5A28	72.89	0.78	0.95	12.99	0.10	1.41	0.11	0.68	0.04	4.76	94.71
L5A30	73.78	0.80	0.88	11.93	0.12	1.06	0.05	0.80	0.01	5.29	94.72

<b>L5A31</b>	80.24	0.71	0.79	9.02	0.16	0.79	0.11	1.11	0.01	4.76	97.70
<b>L5A32</b>	73.88	0.98	1.06	12.00	0.10	1.31	0.41	0.86	0.02	4.96	95.58
<b>L6A33</b>	84.55	0.32	0.78	6.32	0.07	0.78	0.07	1.02	0.01	2.71	96.63
<b>L6A36</b>	81.78	0.44	0.80	7.73	0.07	1.03	0.09	0.98	0.01	3.05	95.98
<b>L7A37</b>	84.09	0.77	0.63	6.87	0.06	1.07	0.08	0.60	0.01	2.38	96.56
<b>L7A46</b>	81.23	0.92	0.68	7.93	0.07	1.33	0.12	0.56	0.02	2.97	95.83
<b>L8A49</b>	81.72	0.68	1.02	7.15	0.07	1.21	0.77	0.64	0.02	2.85	96.13
<b>L8A50</b>	88.15	0.76	0.59	6.74	0.06	1.06	0.09	0.52	0.01	2.02	100.00
<b>L9A52</b>	71.61	0.67	1.29	11.97	0.09	1.54	0.92	0.83	0.05	5.04	94.01
<b>L9A55</b>	73.88	0.62	1.41	10.87	0.07	1.35	0.99	0.71	0.03	4.39	94.32
<b>L10A57</b>	78.73	1.00	1.22	8.40	0.07	0.93	0.23	0.54	0.02	4.60	95.74
<b>L10A59</b>	78.24	0.96	1.10	9.75	0.09	1.14	0.14	0.72	0.01	3.73	95.88

**Table 8:** Percentage of Major Oxides in Palaeogene sediments of the study area



Oriented Mount				Sample Heated to 550°C			
2 Theta	Relative Intensity	d spacing	Remarks	2 Theta	Relative Intensity	d spacing	Remarks
6.28	1.83	14.06	Montmorillonite or Chlorite	6.39	0.54	14.27	Very flat peak
8.86	7.09	9.97	Illite	7.02	0.77	12.15	"
11.61	5.78	7.61		8.84	5.3	9.99	Montmorillonite
12.55	4.88	7.04	Kaolinite (001) reflection, Chlorite				No peak at around 12.55-degree 2 theta, confirms presence of Kaolinite
17.74	4.08	4.996	Illite	17.22	3.24	5	Illite
18.05	1.02	4.7	Chlorite				
19.91	1.14	4.46		19.75	2.57	4.49	
20.86	17.56	4.25		20.84	16.64	4.26	
25.22	4.23	3.53	Kaolinite (002) reflection	25.43	1.93	3.5	Kaolinite peak almost disappears
27.92	3.72	3.19					
36.55	6.93	2.46					

**Table 9:** Result of the XRD analysis of the sample No. L2A15



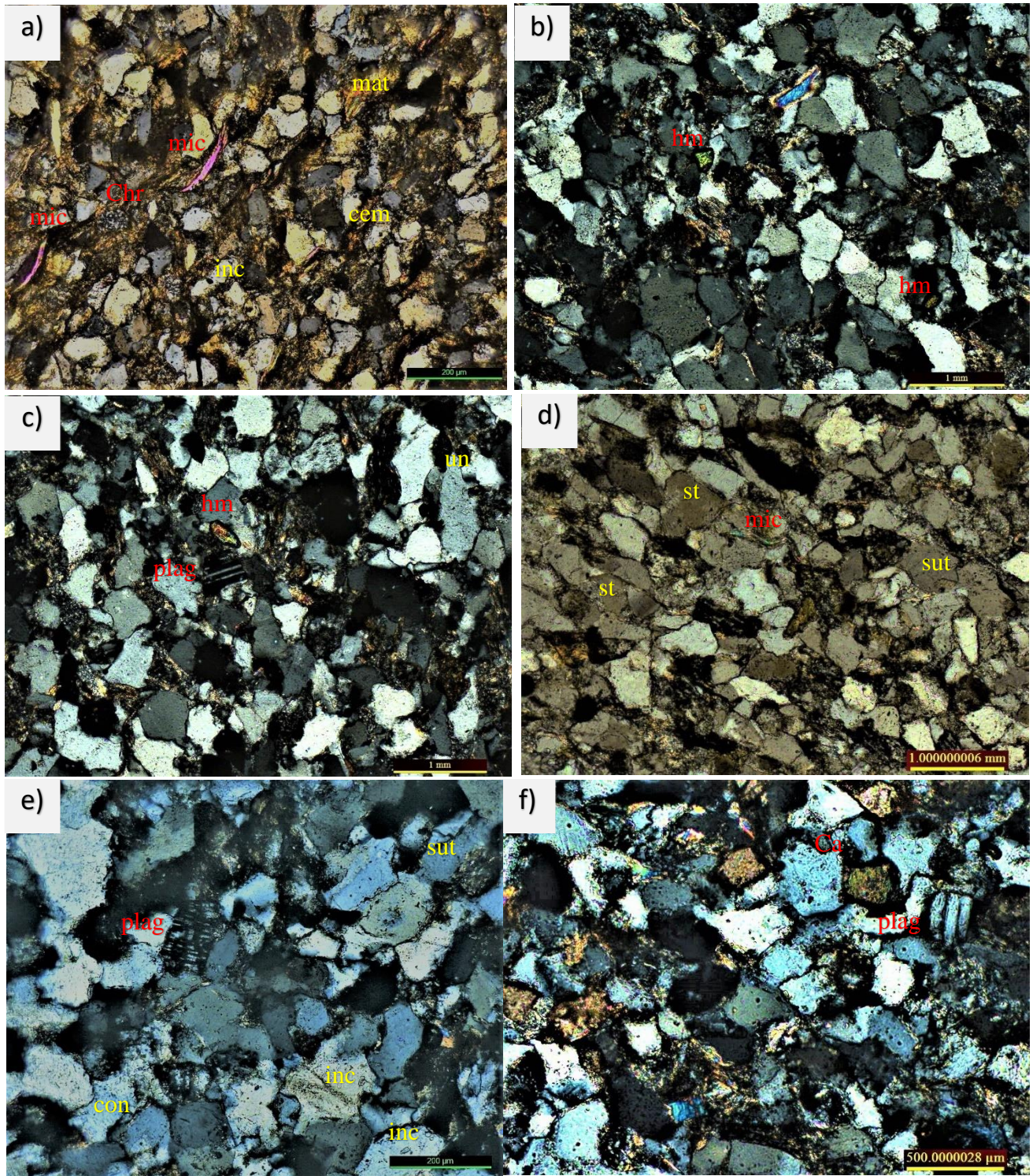


**Plate 12:** Photomicrographs showing a) mica (mic), matrix (mat), Chert (Chr), ferruginous cement (cem), inclusion in quartz (inc); b) undulatory quartz (un), heavy mineral (hm), metamorphic rock fragment (met); c) plagioclase (plag), heavy mineral (hm), undulatory quartz (un); d) straight contact between quartz grains (st), sutured contact (sut), kink bending in mica (mic); e) chessboard plagioclase (plag), inclusion (inc), sutured contact (su), concavo-convex (con); f) calcium carbonate (Ca), plagioclase (plag)



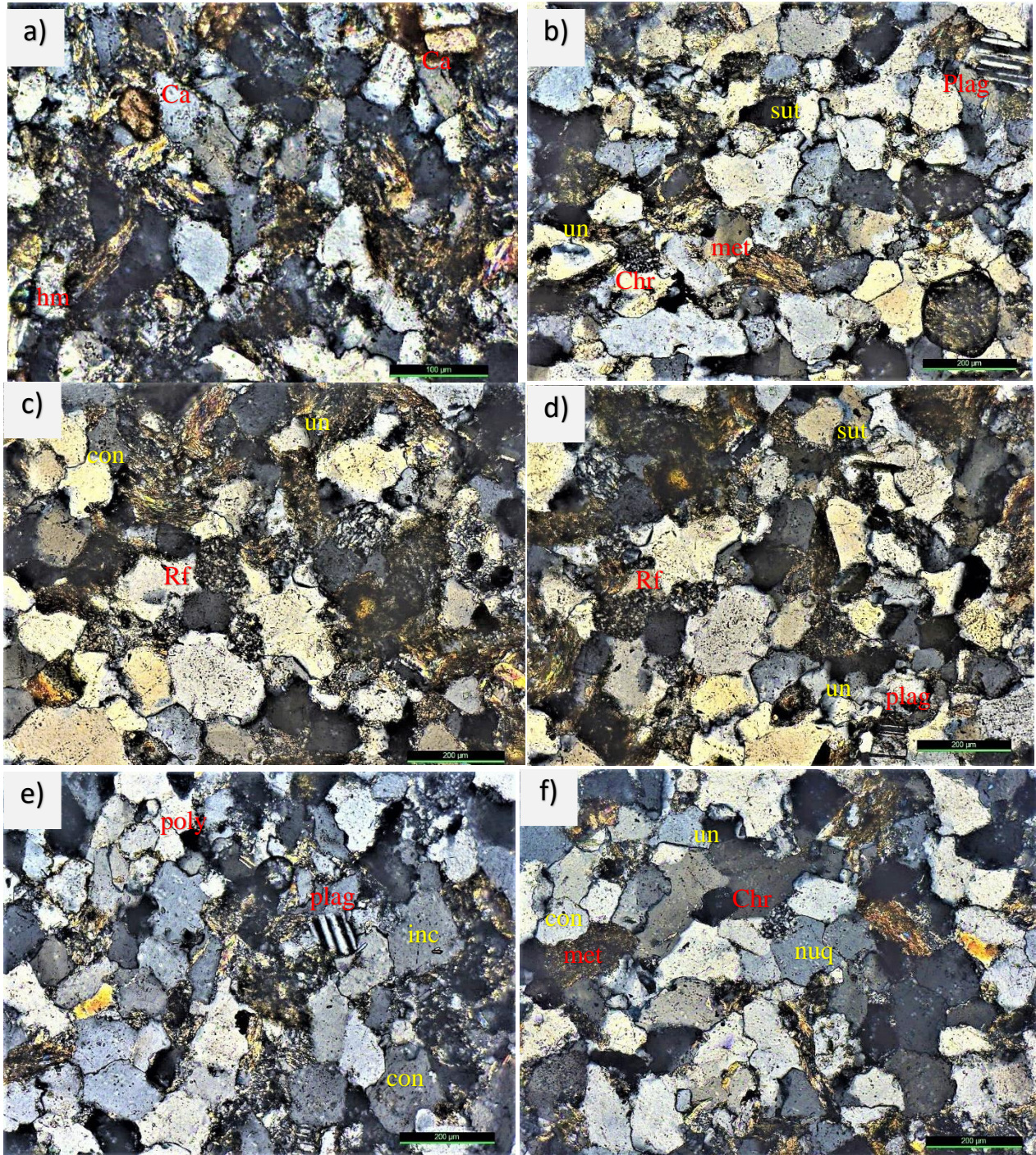


**Plate 13:** Photomicrographs showing a) calcium carbonate (Ca), heavy mineral (hm); b) undulatory quartz (un), schist rock fragment (met), sutured contact (sut), concavo-convex contact (con) Chert (Chr), albitized feldspar (plag); c) concavo-convex contact (con), sedimentary rock fragment (Rf); d) sutured contact (sut), plagioclase (plag); e) plagioclase (plag); inclusion (inc), concavo-convex contact; f) undulatory quartz (un), chert (chr), metamorphic rock fragment (met), non-undulatory quartz (nuq), concavo-convex contact (con)



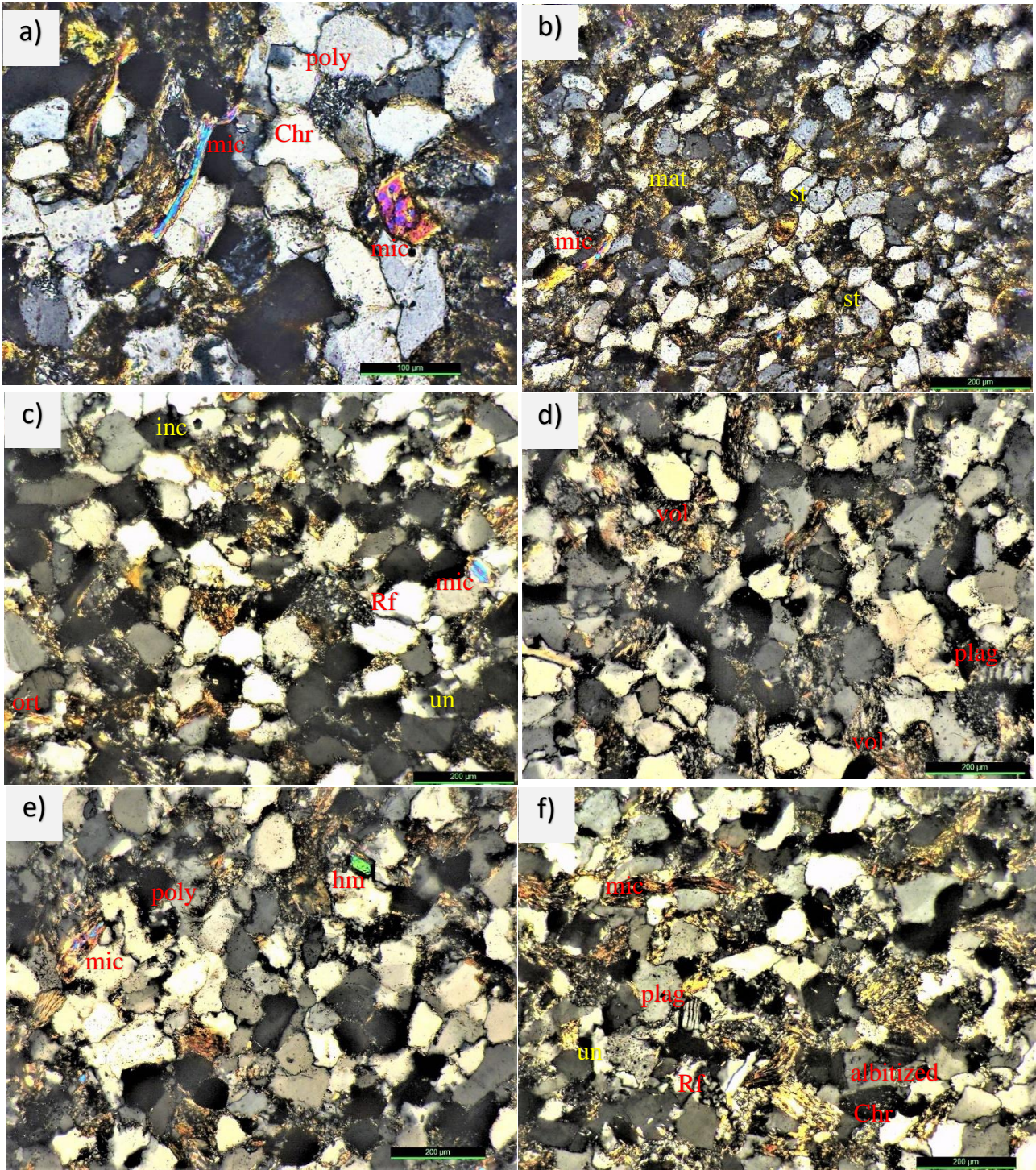


**Plate 14:** Photomicrographs showing a) bending in mica (mic), chert (Chr), polycrystalline quartz (poly); b) matrix (mat) rich rock whereby the contacts between the quartz grains are straight (st), mica (mic); c) sedimentary rock fragment (Rf), mica (mic), undulatory quartz (un), orthoclase (ort), inclusion in quartz (inc); d) devitrified feldspar (plag), volcanics (vol); e) mica (mic), polycrystalline quartz (poly), heavy mineral (hm); f) undulatory quartz (un), chert (chr), plagioclase (plag), sedimentary rock fragment (Rf), mica (mic)



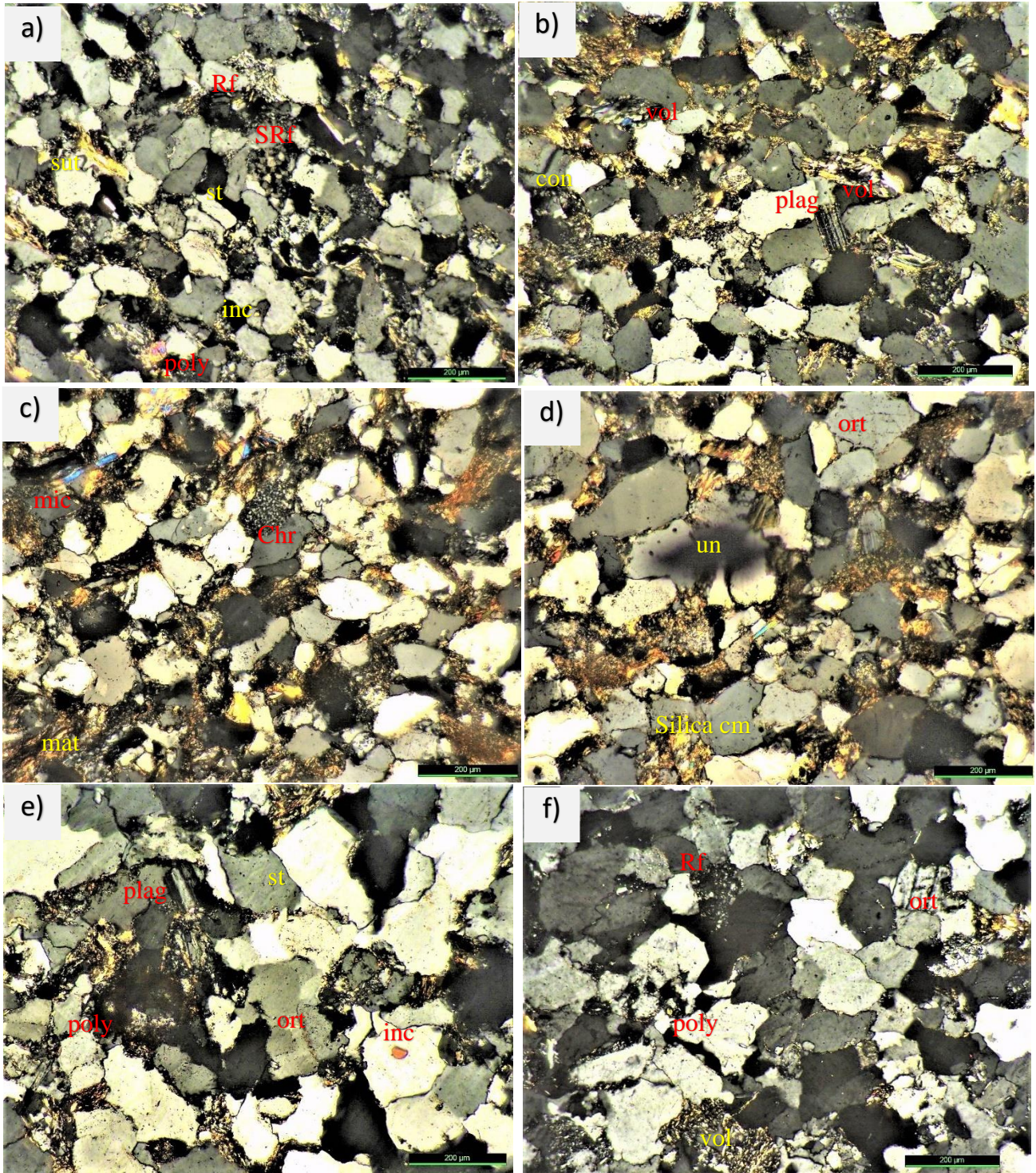


**Plate 15:** Photomicrographs showing a) siltstone rock fragment (SRf), polycrystalline quartz (poly), inclusion in quartz (inc), sedimentary rock fragment (Rf); b) volcanic (vol), concavo-convex contact (con), plagioclase (plag); c) chert (Chr), mica (mic), matrix (mat); d) orthoclase (ort), undulatory quartz (un), silica cementation (silica cm); e) albitized feldspar (plag), polycrystalline quartz (poly), straight contact (st), orthoclase (ort), inclusion in quartz (inc); f) orthoclase (ort), polycrystalline quartz (poly), sedimentary rock fragment (Rf), volcanics (vol)



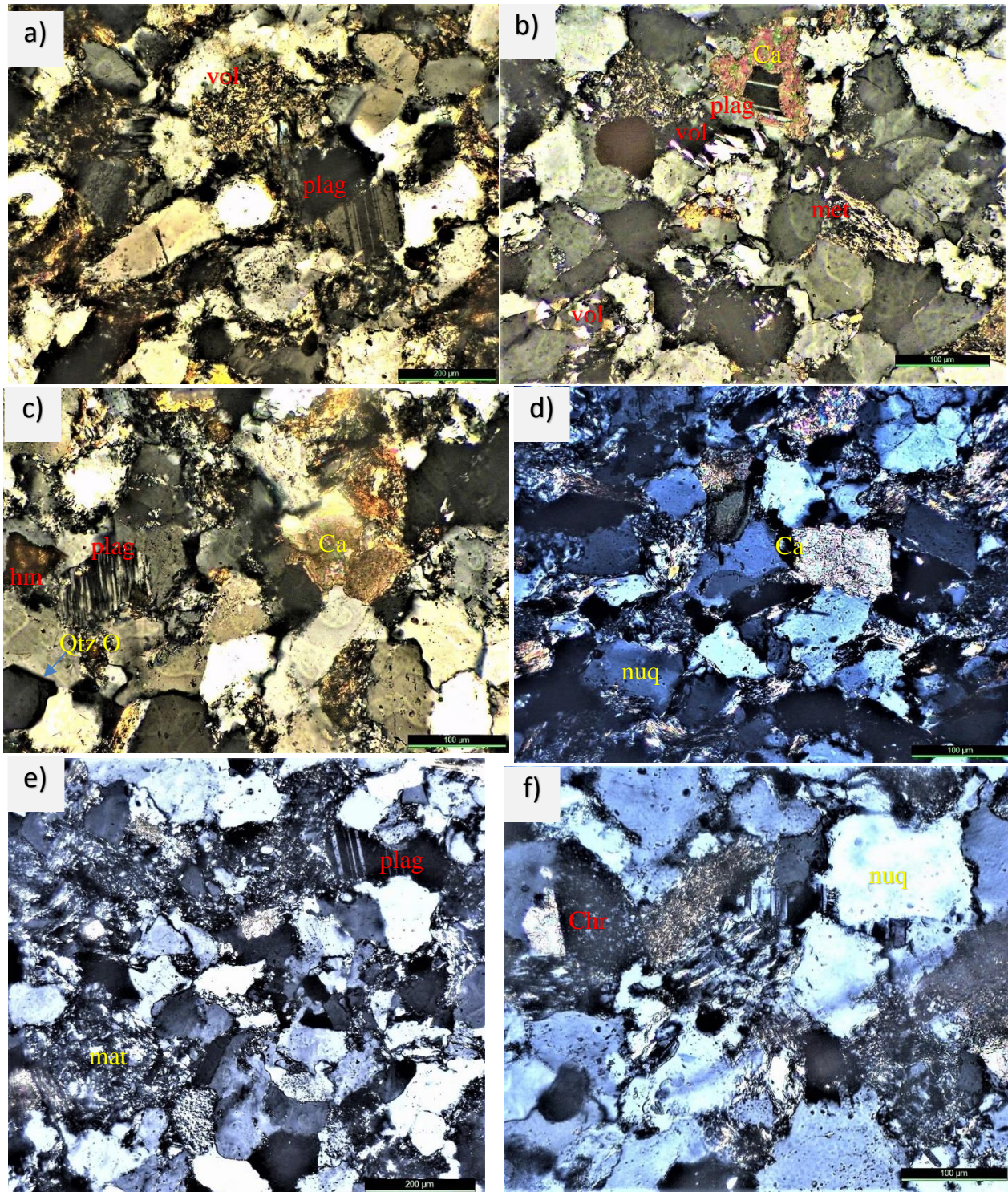


**Plate 16:** Photomicrographs showing a) volcanics (vol), plagioclase (plag); b) metamorphic rock fragment (met), plagioclase (plag) embedded in calcium carbonate (Ca) exhibiting porphyritic texture, volcanic (vol); c) albitized feldspar (plag), heavy mineral (hm), calcium carbonate (Ca), quartz overgrowth (Qtz O); d) calcium carbonate (Ca), non-undulatory quartz (nuq); e) albitized feldspar (plag), matrix (mat); f) chert (Chr), non-undulatory quartz (nuq)



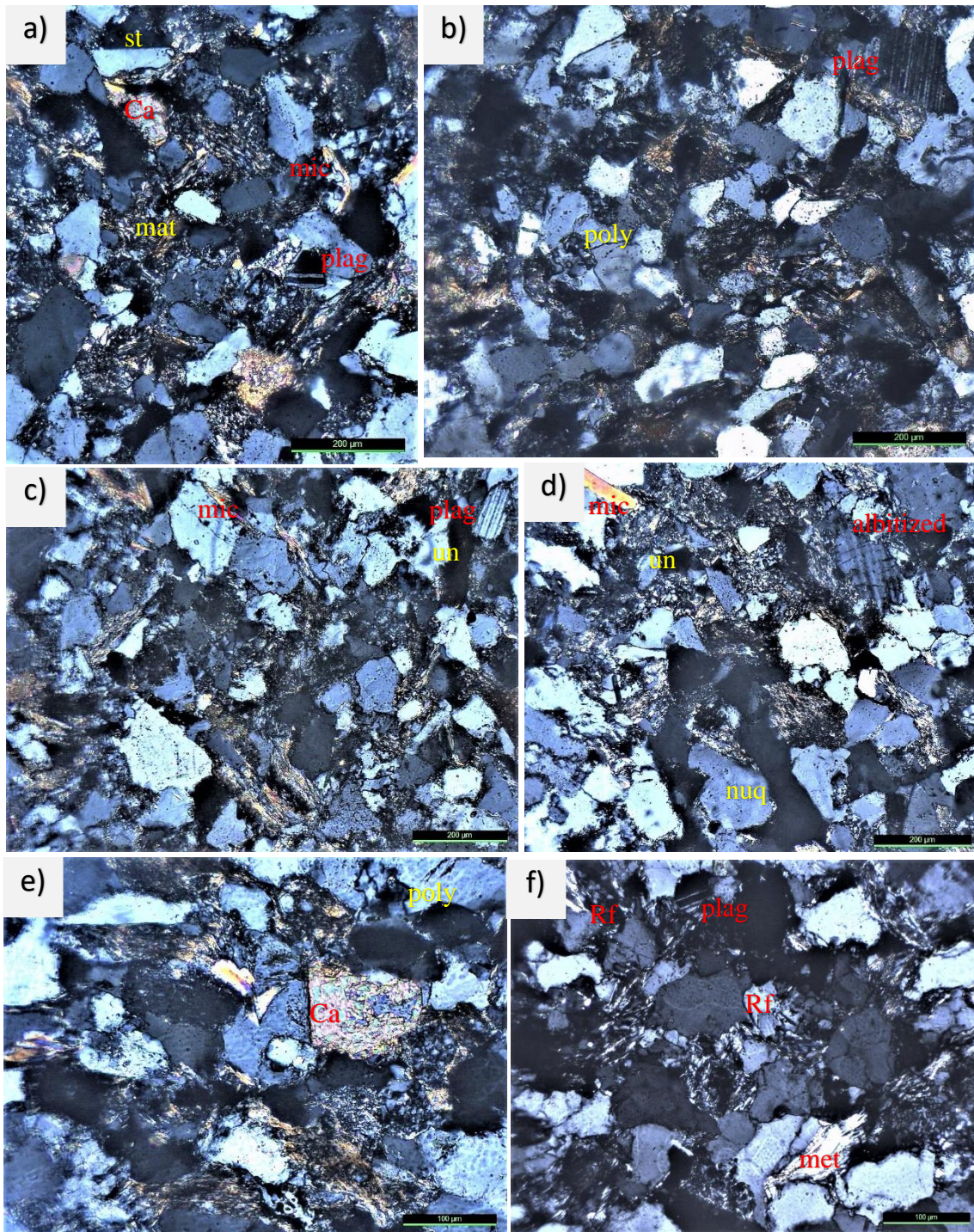


**Plate 17:** Photomicrographs showing a) mica (mic), calcium carbonate (Ca), matrix (mat), plagioclase (plag), straight contact (st); b) polycrystalline quartz (poly), plagioclase (plag); c) plagioclase feldspar (plag), undulatory quartz (un), mica (mic); d) mica (mic); undulatory quartz (un); non undulatory quartz (nuq); albitized feldspar (albitized); e) calcium carbonate (Ca), polycrystalline quartz; f) sedimentary rock fragment (Rf), plagioclase (plag), metamorphic rock fragment (met)





**Plate 18:** Heavy minerals zircon euhedral (1-20); rounded (21-41) with and without inclusions and (42-60) euhedral to subhedral





**Plate 19:** Observed heavy minerals; (1-21) anhedral; (22-45) euhedral to subhedral and (46-53) subrounded to rounded tourmaline with and without inclusions

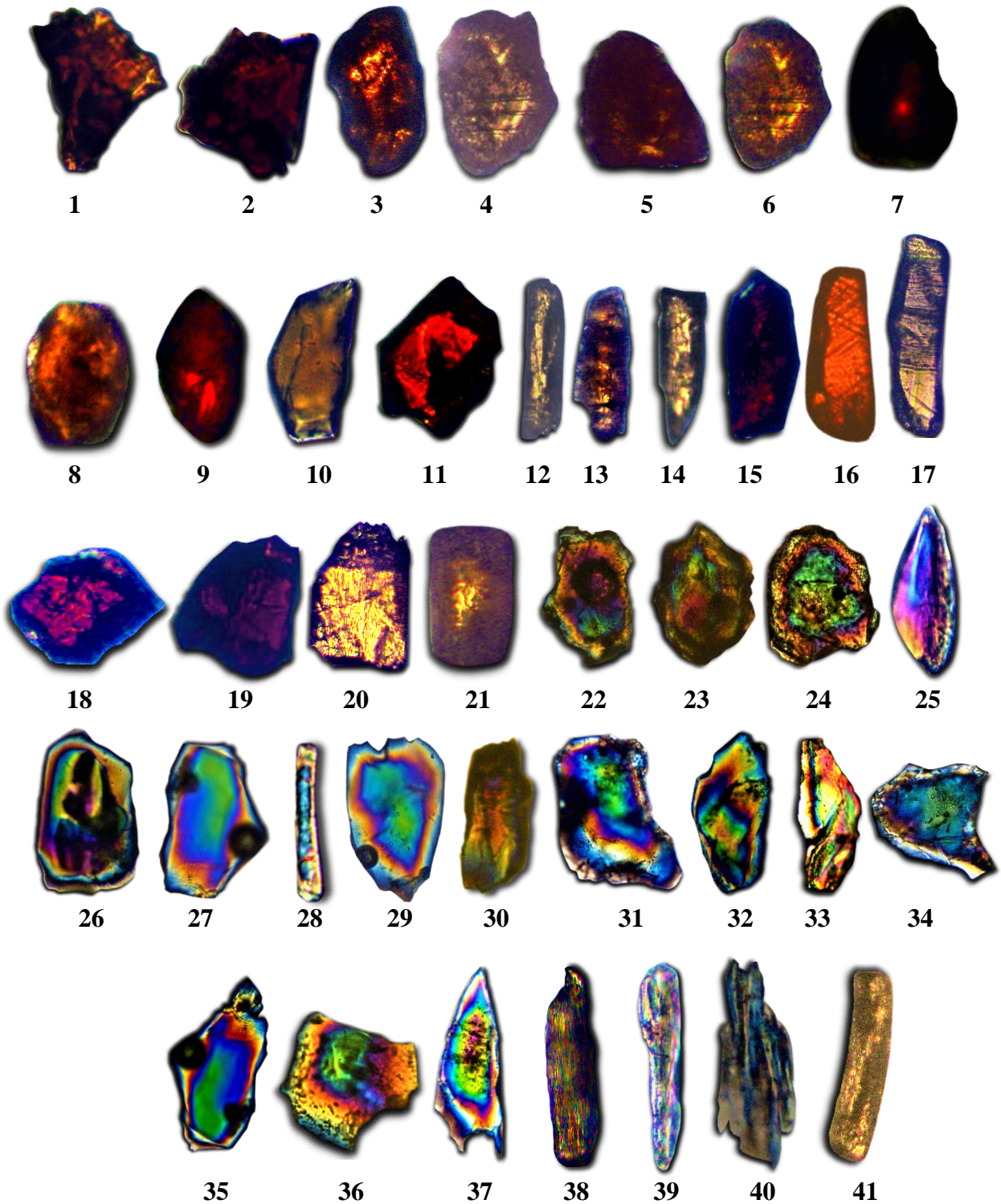


**Plate 20:** Observed heavy minerals; (1-9) anhedral to subrounded rutile, (10-21) euhedral to subhedral rutile, (22-25) anhedral to subrounded kyanite, (26-37) euhedral to subhedral kyanite, and (38-41) sillimanite



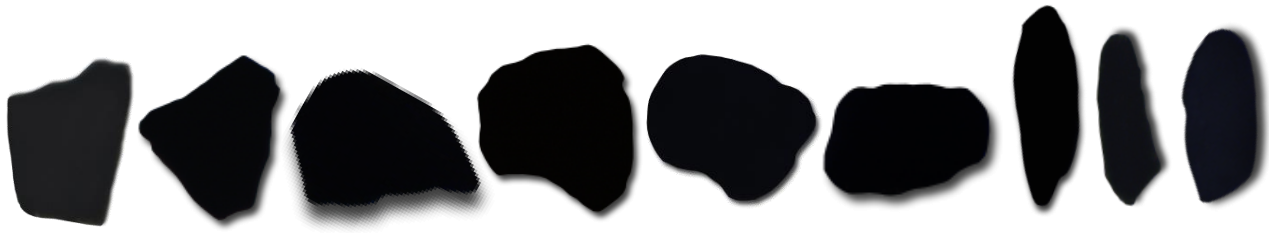


**Plate 21:** Some of the observed opaque minerals

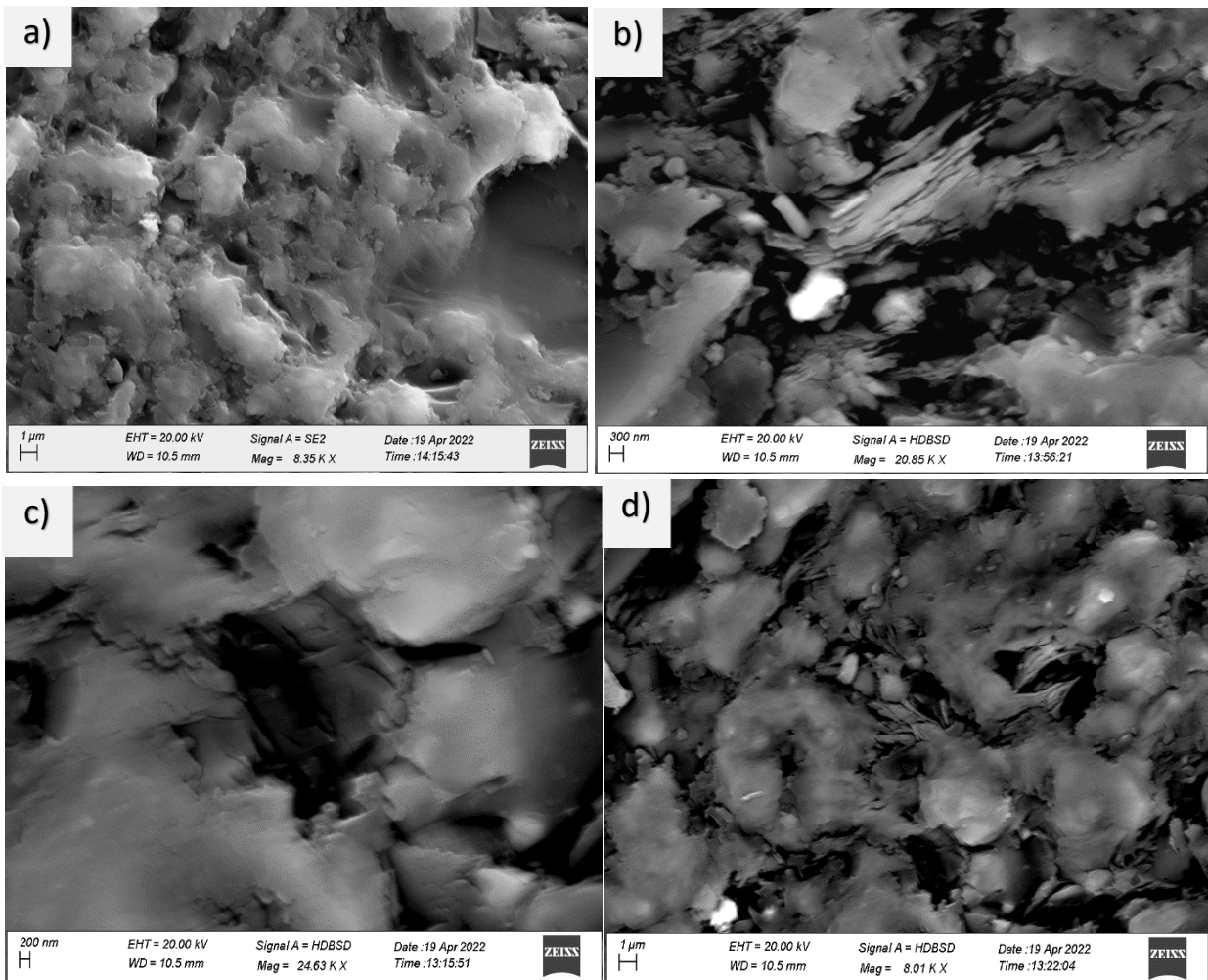


**Plate 22:** a) Illite b) Kaolinite c) Cavity with clay lining d) Illite-Smectite clay

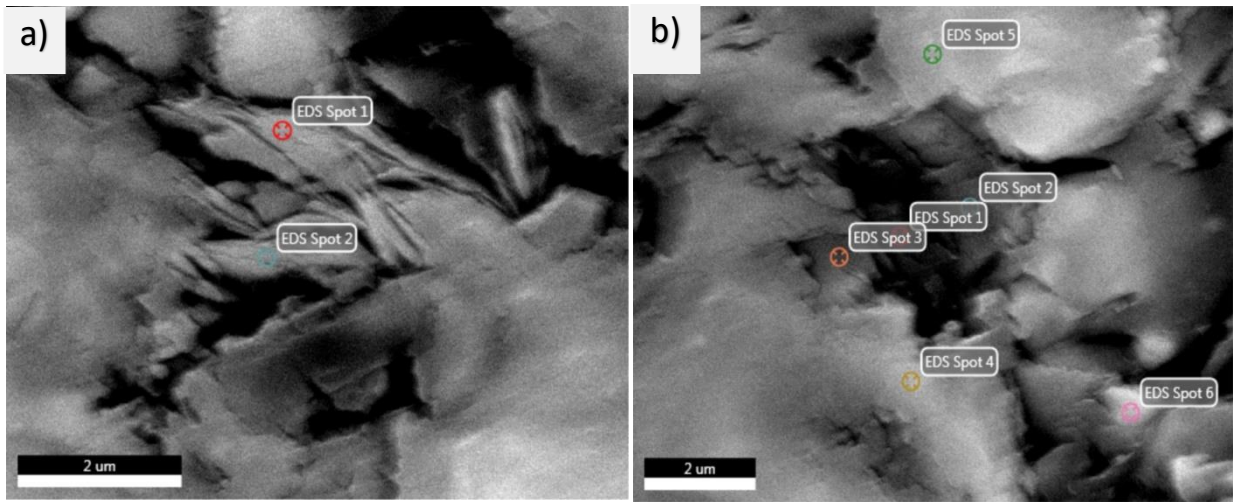


**Plate 23:** a) Brucite b).Brucite within the cavity of feldspar

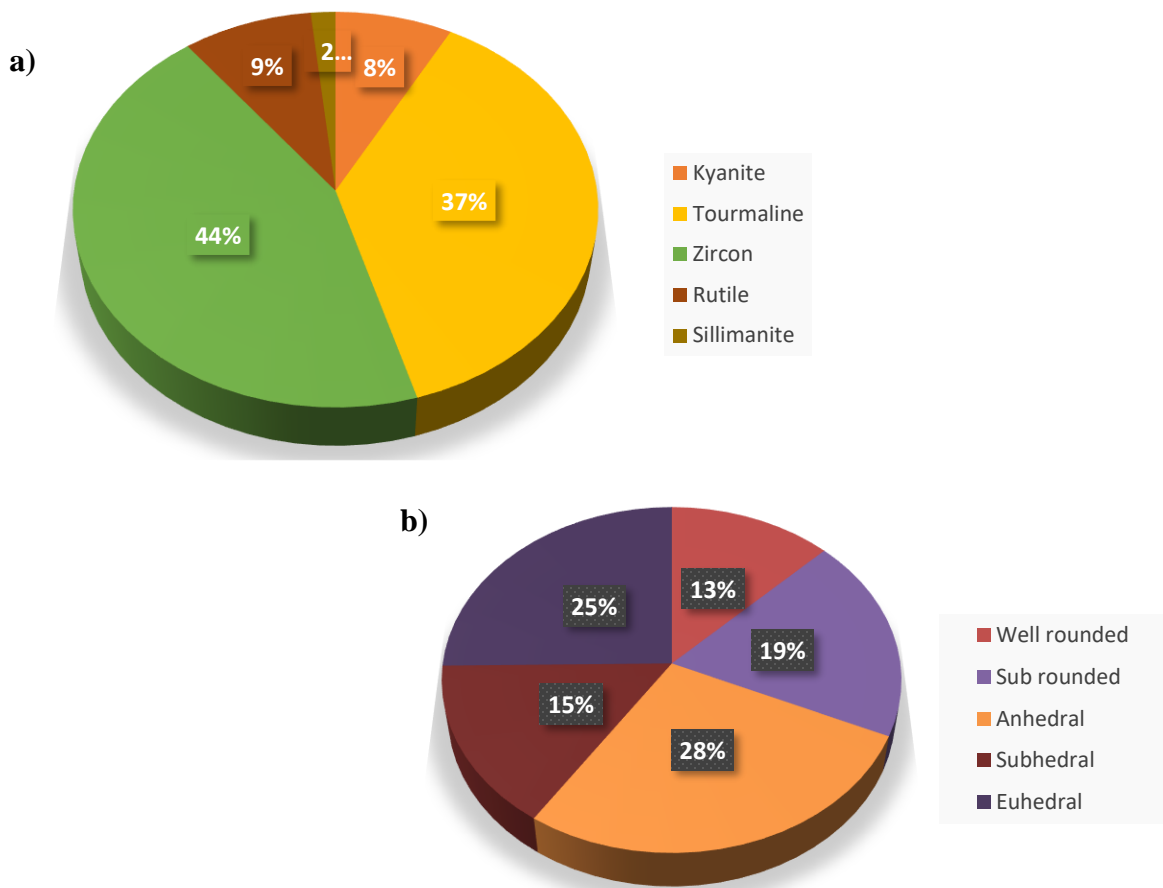


**Fig 29:** Distribution of heavy minerals according to a) variety and b) shape in Palaeogene sediments



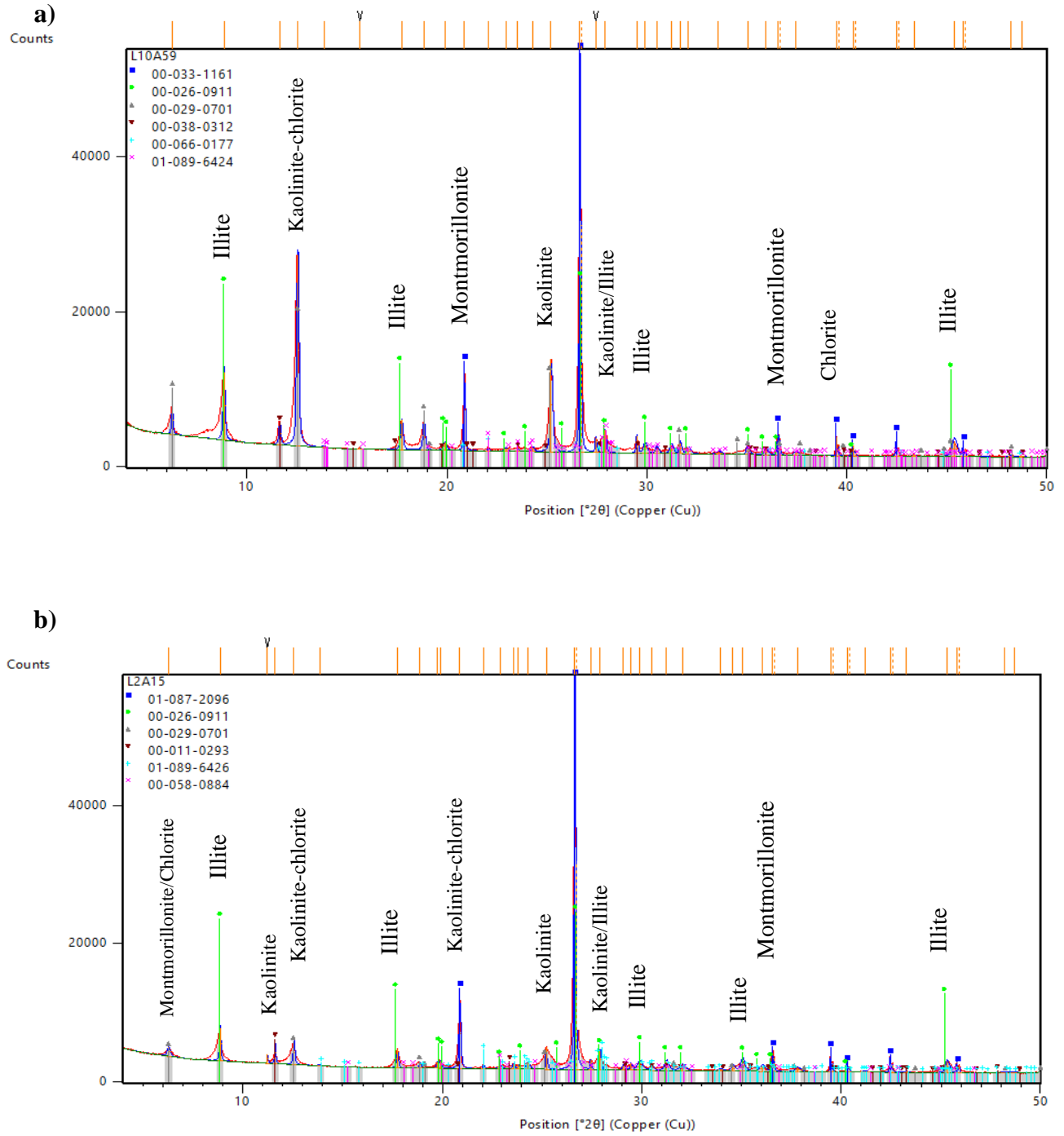


**Fig 30:** XRD curves for samples a) L10A59 and b) L2A15

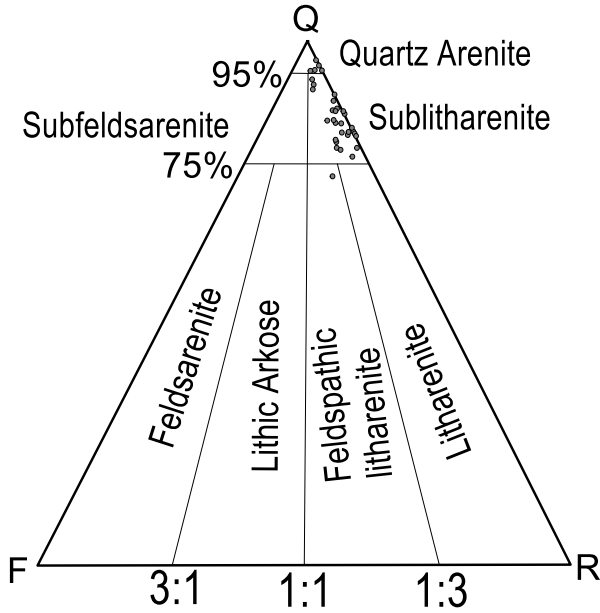


**Fig. 31:** Ternary plot of total quartz, feldspar and rock fragments (after Folk, 1980)

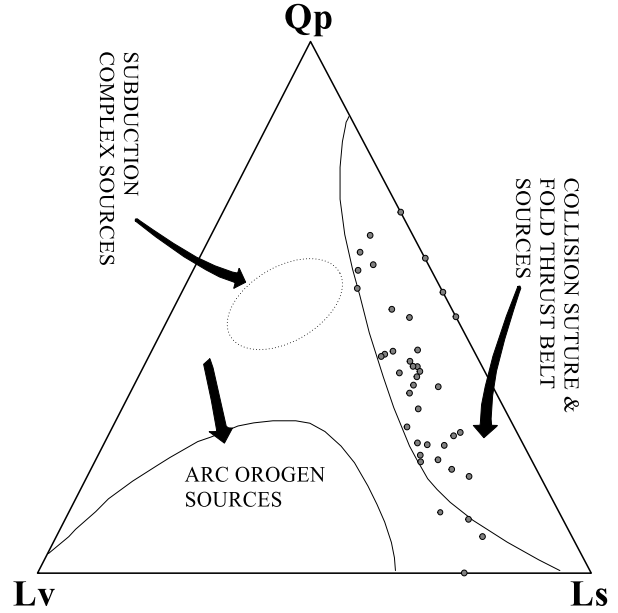


**Fig. 32:** Ternary plot of quartz (poly), lithic (volcanic) and lithic (sedimentary) (after Dickinson & Suczek, 1979)

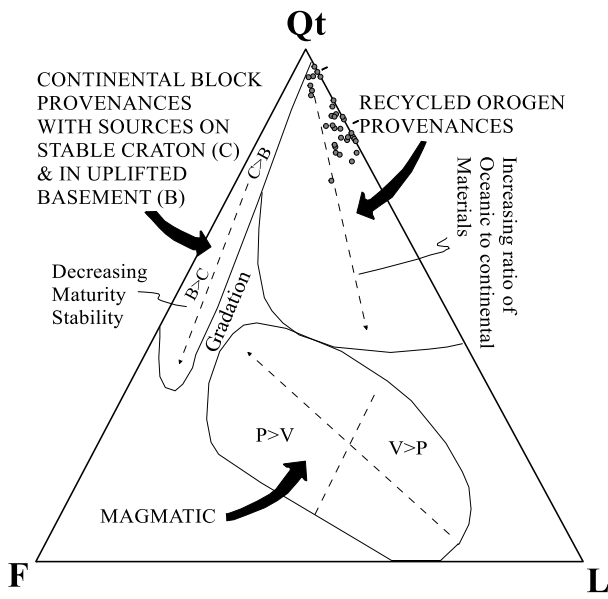


**Fig. 33:** Ternary plot of total quartz, feldspar and lithic fragment (after Dickinson & Suczek, 1979)

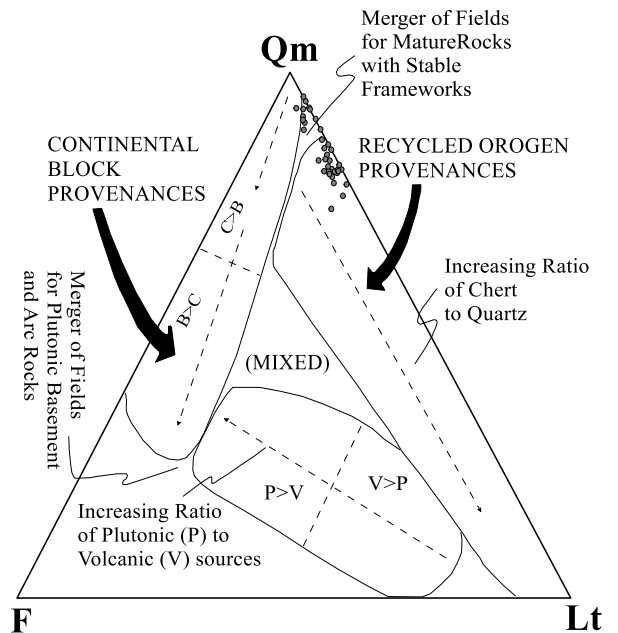


**Fig. 34:** Ternary plot of quartz (mono), feldspar and lithic fragment (after Dickinson & Suczek, 1979)

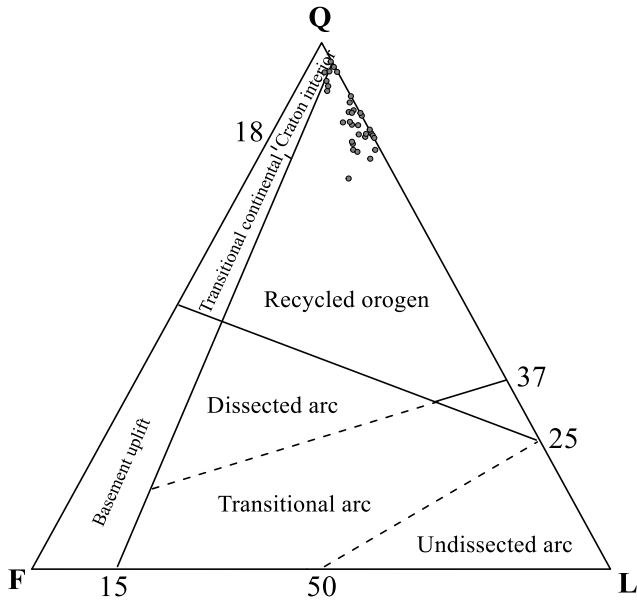


**Fig. 35:** Ternary plot of total quartz, feldspar and lithic fragment (after Dickinson et al., 1983)

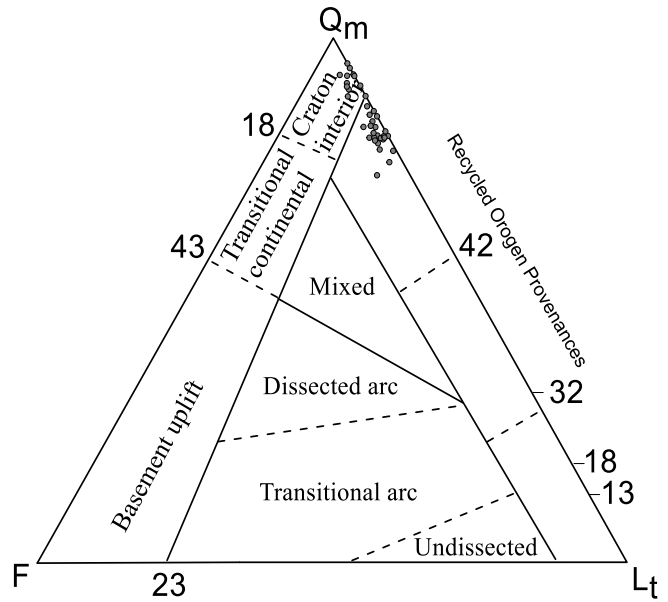


**Fig. 36:** Ternary plot of quartz (mono), feldspar and lithic fragment (after Dickinson et al., 1983)

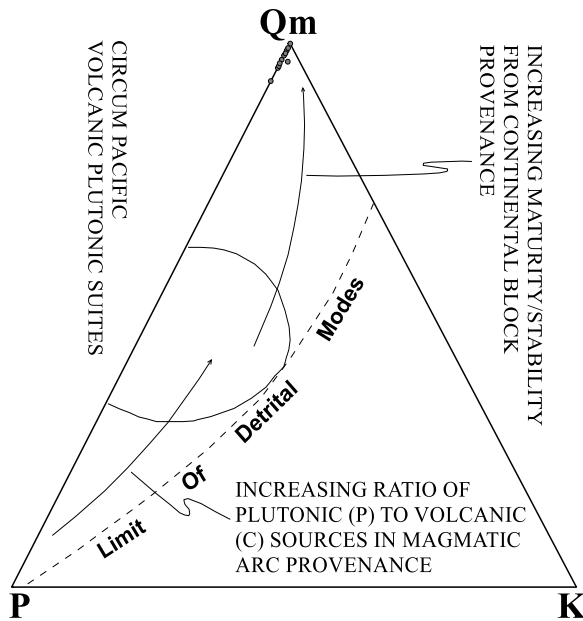


**Fig. 37:** Ternary plot of quartz (mono), feldspar (sodic) and feldspar (potash), (after Dickinson & Suczek, 1979)

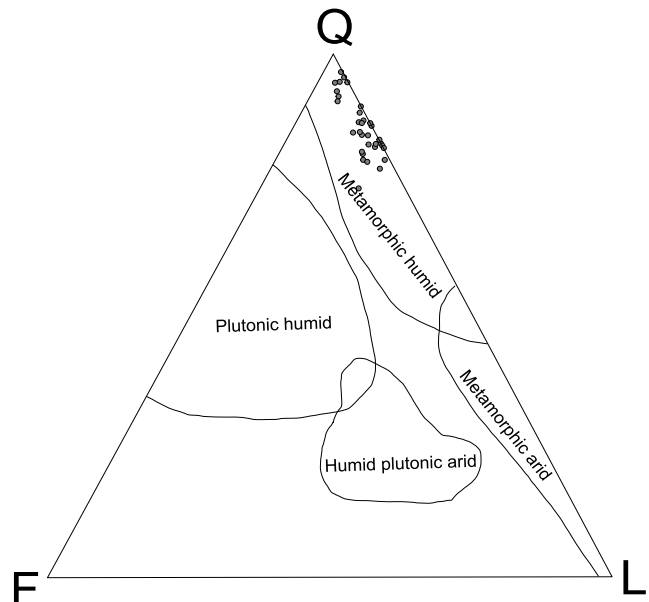


**Fig. 38:** Ternary plot of total quartz, feldspar and lithic fragment (after Suttner et al., 1981)

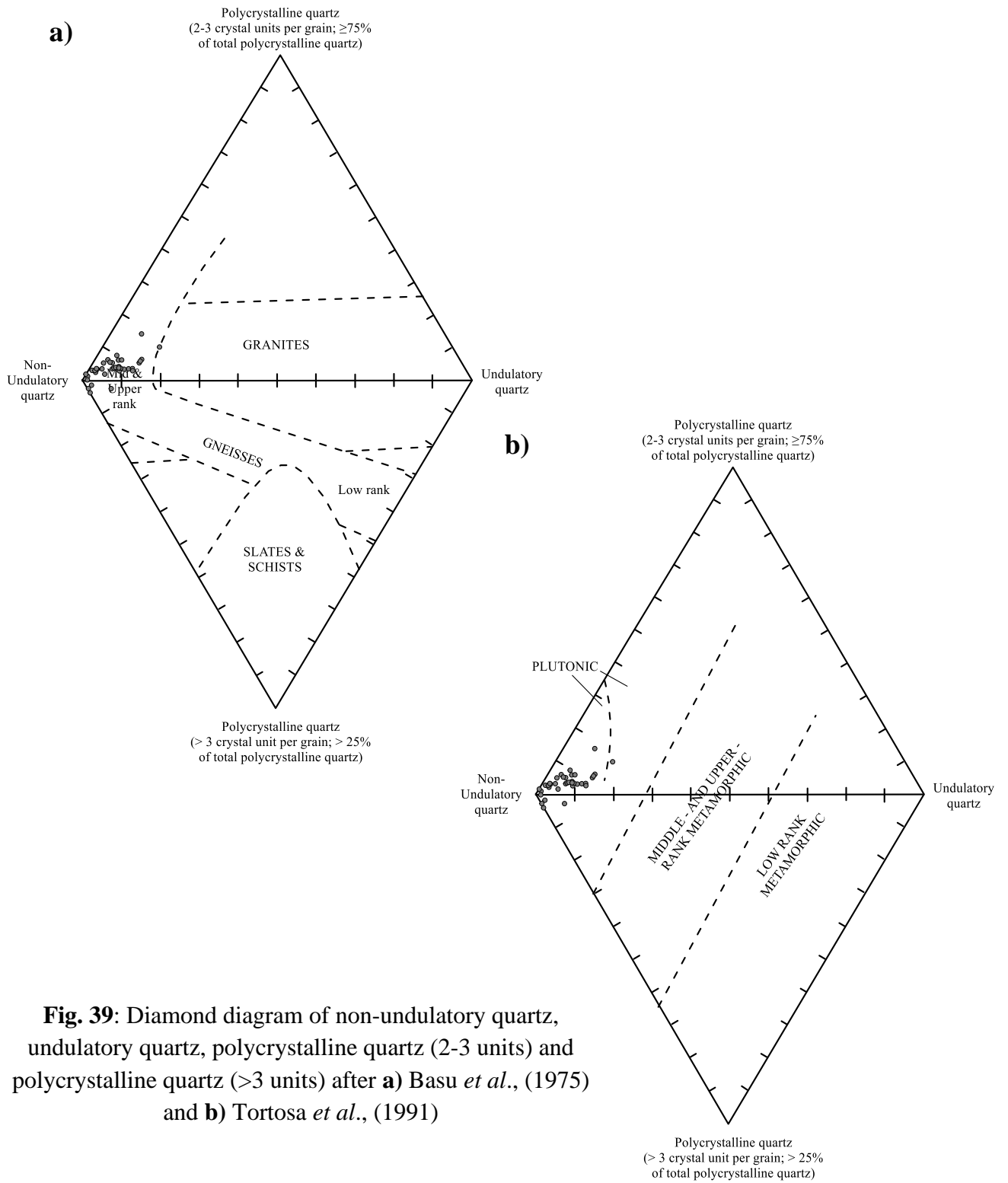


**Fig. 39:** Diamond diagram of non-undulatory quartz, undulatory quartz, polycrystalline quartz (2-3 units) and polycrystalline quartz ( $>3$  units) after **a)** Basu *et al.*, (1975) and **b)** Tortosa *et al.*, (1991)

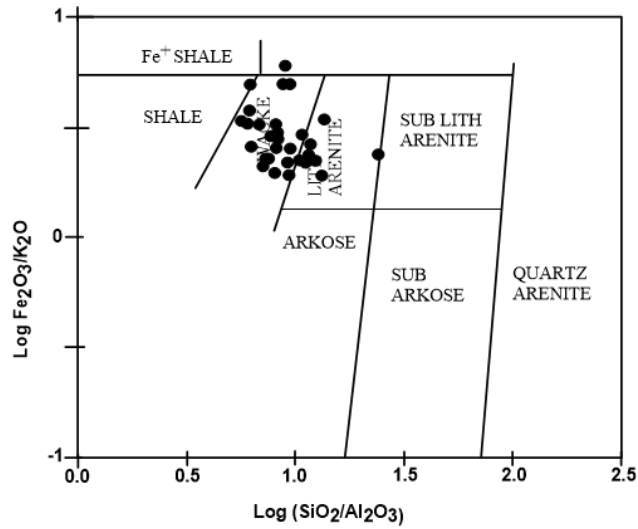


**Fig. 40:** Bivariate Plot of  $\log(\text{Fe}_2\text{O}_3/\text{K}_2\text{O})$  vs  $\log(\text{SiO}_2/\text{Al}_2\text{O}_3)$  (after Herron, 1988)

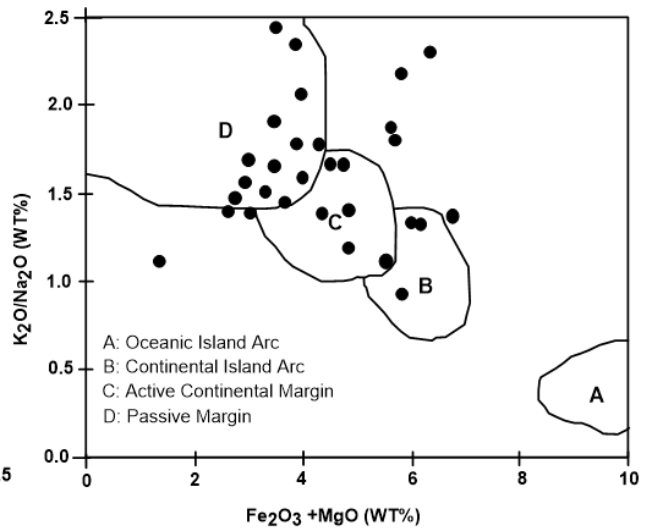


**Fig. 41:** Bivariate Plot of  $(\text{K}_2\text{O}/\text{Na}_2\text{O})$  vs  $(\text{Fe}_2\text{O}_3 + \text{MgO})$  (after Bhatia, 1983)

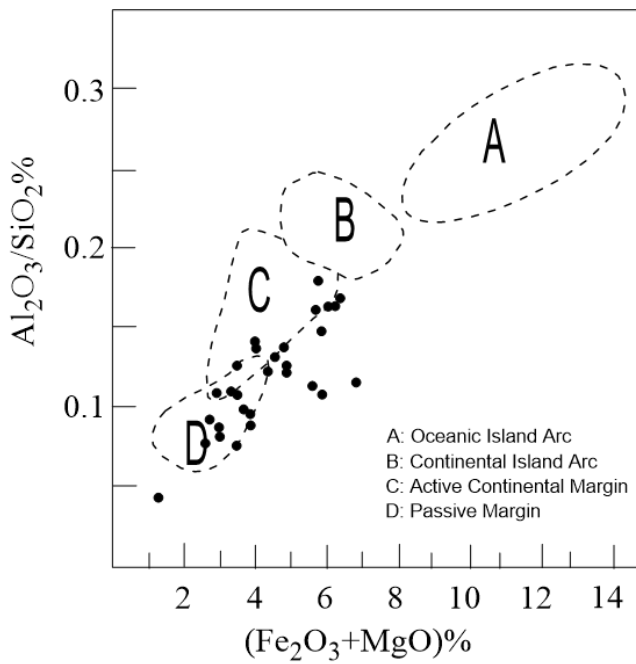


**Fig. 42:** Bivariate Plot of  $(\text{Al}_2\text{O}_3/\text{SiO}_2)$  vs  $(\text{Fe}_2\text{O}_3 + \text{MgO})$  (after Bhatia, 1983)

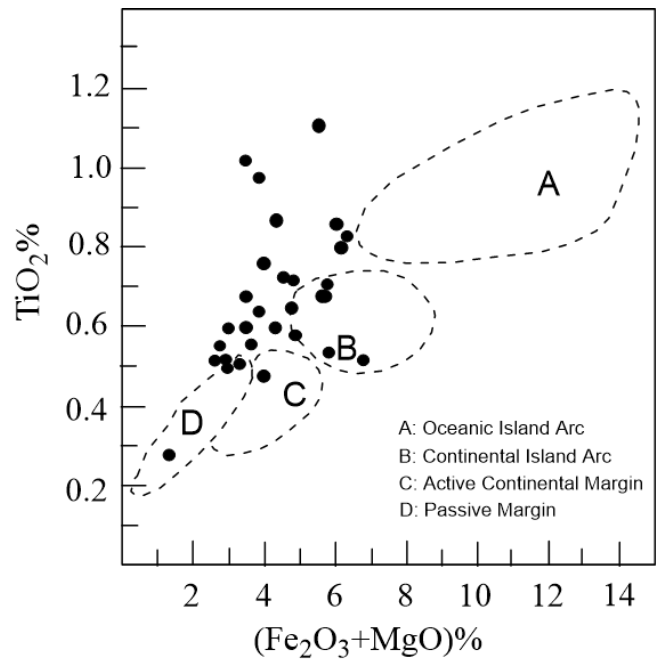


**Fig. 43:** Bivariate Plot of  $(\text{TiO}_2)$  vs  $(\text{Fe}_2\text{O}_3 + \text{MgO})$  (after Bhatia, 1983)



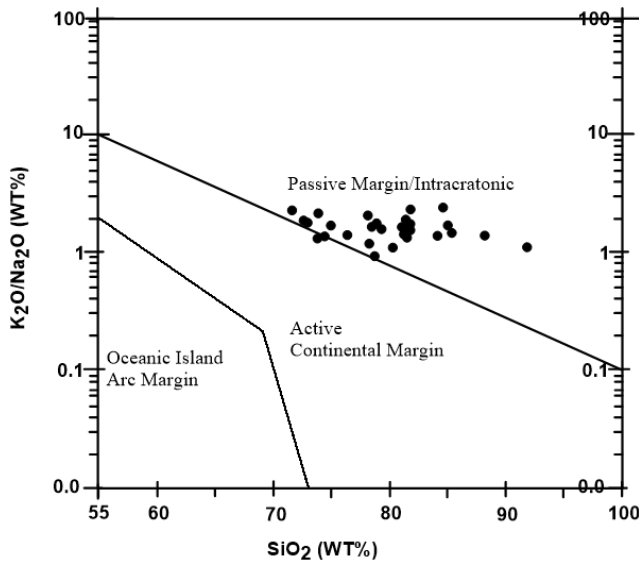


**Fig. 44:** Bivariate Plot of  $(K_2O/Na_2O)$  vs  $(SiO_2)$  (after Roser & Korsch, 1986)

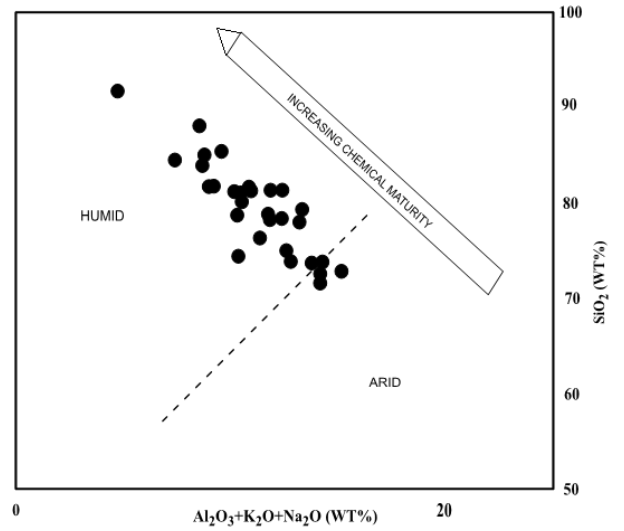


**Fig. 45:** Bivariate Plot of  $(SiO_2)$  vs  $(Al_2O_3+K_2O+Na_2O)$  (after Suttner & Dutta, 1986)

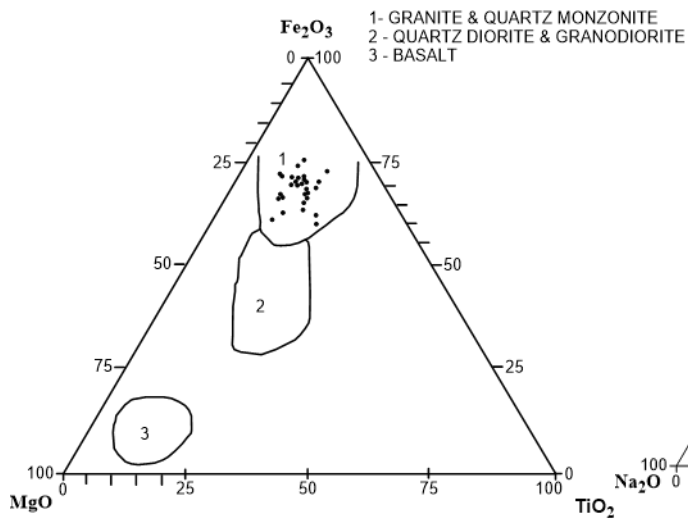


**Fig. 46:** Ternary Plot of  $Fe_2O_3$ - $MgO$ - $TiO_2$  (after Condie, 1967)

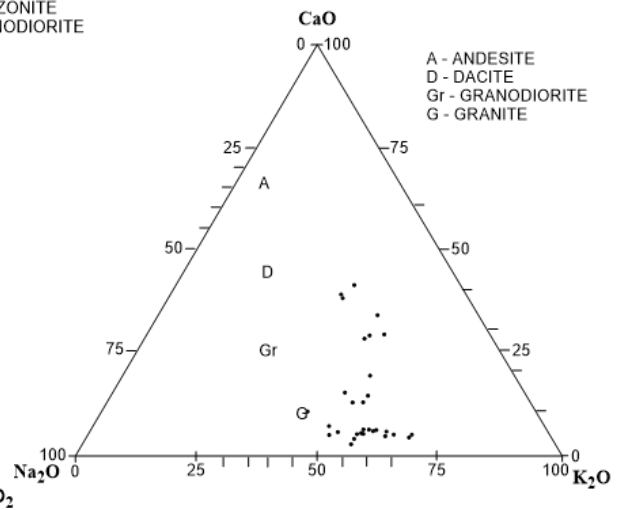


**Fig. 47:** Ternary Plot of  $CaO$ - $Na_2O$ - $K_2O$  (after Le Maitre, 1976)

## **CHAPTER 6**

# **DEPOSITIONAL ENVIRONMENT AND TECTONIC PROVENANCE**

### **6.1 RECONSTRUCTION OF PALAEOENVIRONMENTS**

Study of the of the modern sedimentary processes provides an effective tool in understanding the ancient environments in terms of normal as well as catastrophic processes and their resultant facies mosaic in space and time (Johnson and Stride, 1969; Swift, 1969; Swift *et al.*, 1971; Hubert and Hyde, 1982; Reading, 1986). Normal sedimentary processes, which persist for longer period of time, include climatic changes, pelagic sedimentation, organic growth, diagenetic modifications, tidal and fluvial currents. On the other hand, catastrophic processes such as storm surges, flood, earthquakes, volcanism and tectonic impulses occur instantaneously. According to Goldring (1965), the resultant depositional facies depends upon the preservation potential of the environment. Interpretation of facies sequences of ancient sediments involves the development of the regional framework on the basis of lithology, sedimentary structures, bed geometry and palaeocurrents. This is usually done by reconstructions of paleo-depositional environment and development of a conceptual model.

The present study suggests that the Palaeogene sediments of the study area were deposited in a shallow marine environment with fluctuating energy regime. Study further suggests that the area is dominated by coarsening upward sequences with a few fining upward trends. According to Leeder (1982) such trends can be explained as the progradation of shoreface towards offshore, which were traversed by fining upward tidal-inlet channels. Based on the distribution of identified lithofacies, field relationships, primary sedimentary structures and trace fossils, two major environments have been interpreted. The description of various depositional environments accounted for the generation of different lithofacies in the Palaeogene sediments as given below:

#### **6.1.1 SHOREFACE ENVIRONMENT**

Presence of fine to medium sandstones along with vertical traces at the higher stratigraphic horizons suggest that these sediments were deposited in the upper shoreface environments under high energy conditions. Lithofacies analysis and presence of wave/interference/bifurcating ripples also corroborates the above. According to Renieck and Singh (1980), Reading (1991), Prothero and Schwab (2004) and many more, in the upper shoreface, sandstones develop plane laminations, ripple marks and gently dipping plane

laminations with low concentration of trace fossils dominated by vertical traces. Presence of laterally extensive bedding, moderate compositional maturity, tabular bed geometry and diagnostic assemblage of trace fossils also suggest that these sediments were deposited in the upper shoreface environment. According to Hill *et al.*, (2003) also sediments in the upper shoreface environments are generally dominated by plane lamination and small dimensions cross laminations where oscillatory motions play an important role under storms and fair-weather conditions. He also suggests that hummocky cross-stratification forms in deeper water during storms. In the studied sediments, presence of hummocky cross-stratifications, generally found below the fair-weather wave-base but above the storm wave-base; indicates the storm activities (Dott and Bourgeois, 1982; Harms *et al.*, 1975; Prothero and Schwab, 2004; Singh and Srivastava, 2011). The presence of both feeding and dwelling traces in these sediments, also indicates its deposition in the shoreface-offshore transition zone environments below the normal wave base. Lithofacies analysis, observed sedimentary structures coupled with trace fossil assemblages suggest deposition of these sediments under fluctuating energy conditions.

The lower shoreface is dominated by intensely bioturbated sandy mud. Most of the sedimentary structures are generally obliterated. In this region, horizontal traces dominate as on the lower shoreface-offshore, shelf processes are important as wave effects are very weak. A transition exists between lower shoreface sandstones and offshore mud towards the offshore. This transition is characterized by moderately bioturbated fine sand-mud lithologies. Dominance of horizontal ichno-assemblages associated with fine clastics, also suggests their deposition in the lower shoreface environment under comparatively low-energy conditions.

In the present investigation, the lithofacies  $Sm/Sr/Sr_w$  are considered to represent the upper shoreface, while  $Fl$  and  $Fsm$  characterize the lower shoreface, as evidenced by the following features:

- i. Presence of fine to medium sandstones with plane laminations, ripple marks and gently dipping plane laminations with vertical traces dominated by *Skolithos* ichno-assemblage.
- ii. Presence of asymmetrical ripples with mud drapes and interference ripples in sand lithologies also represent the upper shoreface environment ( $Sr$ ).
- iii. Presence of wave formed ripples in fine to medium sandstones with occasional bifurcations representing upper shoreface environment ( $Sr_w$ ).
- iv. Coarsening and thickening-upward trends with decrease in the shale contents and dominantly vertical trace fossils.

- v. Presence of shale/siltstone with lamination and bioturbation and horizontal traces in *Fl* facies represent the low energy lower shoreface environment.
- vi. Presence of plane laminations well developed horizontal bedding/parallel laminations and horizontal traces.
- vii. Within the overall coarsening upward cycles with occasional preservation of fining upward sequence.
- viii. Laterally extensive sheet/ and or tabular/elongate sand body geometry paralleling the palaeoshore.
- ix. Presence of heterolithic facies along with current and wave formed sedimentary structures is a very significant feature of shoreface deposits with tidal influences.
- x. Presence of micro hummocky cross stratification with mud.

#### 6.1.2 OFFSHORE- TRANSITION ENVIRONMENT

The offshore-transition zone is characterized by alternations of low and high energy conditions and extends from mean storm wave base to mean fair weather wave base. In this region in general sandy and muddy layers are equally represented. Fair weather deposits are represented by fine grained sediments which settle from suspension and the bed is intensely bioturbated. On the other hand, during storms sediments in the shoreface are influenced by meteorologically induced wave and related currents such as oscillatory and shoaling waves which are also supplemented by wind driven currents and probably storm surge ebb currents. Thus, the storm deposits alternate with fair-weather mud-silt. Storm deposits are represented by silt-sand laminae and/or very fine sand beds. Though, intense bioturbation during fair-weather may obliterate bedding and other structures. Deposition of finer sediments and reworking of coarser silt is the characteristic feature of low energy offshore transition environment. Excellent reviews and models for deposits formed in both modern and ancient shallow offshore environments have been provided by Heward (1981); Einsele and Seilacher (1982), and Elliot (1991). Thin im-persistent laminae of well sorted medium to coarse silt stones/ mud stones exhibiting symmetrical ripples are the common features of the offshore transition environment. In the present study, lithofacies *Fm* (mudstone facies) is considered to represent the offshore-transition, owing to the following characteristics:

- i. Finely laminated silt-mud facies comprising plane laminations and burrows.

- ii. Presence of horizontally disposed characteristic ichno-assemblage traces of *Chondrites intricatus*, *Nereites* isp., *Planolites beverleyensis*, *Scolicia prisca*, *Scolicia plana* and *Thalassinoides*.
- iii. Presence of fining and thinning upward sequences in an overall coarsening and thickening upward sequences.

## 6.2 DEPOSITIONAL HISTORY

Textural and mineralogical analysis coupled with lithofacies, and provenance studies of Palaeogene sediments suggest that the deposition of these sediments were mainly controlled by the Eocene-Oligocene tectonic impulses. During early part of the Eocene there had been an open sea sedimentation represented by the thick pile of argillaceous sediments. However, during early -middle Eocene period there occurred a collision of Naga-Chin-Arakan Island arc located towards east within the oceanic domain of India and Myanmar, with the central Myanmar continental block Acharyya (1990 and 2007). He further suggests that owing to the subduction of the Indian plate below the Myanmar plate, drainage in the source region must have been reorganized. This also resulted in the shifting of the depositional site with fluctuations in the sea level. Many workers (Mathur and Evans, 1964; Desikachar, 1974; Acharyya, 1986, & 1990; GSI, 1988; Thong, 1993; Nandi, 2000 & 2017; Acharyya, 2007; Srivastava, 2002; Srivastava *et al*, 2004 & Srivastava and Kichu, 2021) have suggested that during the Eocene-Oligocene period there was continuous sedimentation and deposition kept pace with tectonics of the region. In the northeastern region this tectonic phase has been visualized by Naik (1998) as retrogradation phase leading to the soft collision of northeastern edge of the Indian plate with the Sinian plate. This has resulted in changing the eastern passive margin of India into a collisional belt. Similar opinion has also been expressed by Kumar and Naik (2006) who have suggested that this is a classic example of transformation of a passive margin set up into an active margin setting. The evolution of north-east south-west trending foreland basin has been attributed to this changing plate interaction through time. It seems that the changing plate interaction was responsible for change from dominantly argillaceous facies to a dominantly arenaceous facies through a heterolithic phase.

Processes that have been interpreted from the observed features of the studied sediments point towards a shoreface-offshore transitional environmental regime. In such regions, both tidal (upper shoreface) as well as wave processes play important role. Presence of fining



upward sequence within a dominantly coarsening and thickening sequence reflect the sea level fluctuations in the depositional basin. These fluctuations could be attributed to the changing plate interactions.

On the basis of the distribution of various lithofacies a conceptual depositional model for the Palaeogene sediments has been envisaged (**Fig. 48**). The depositional model illustrates the distribution of various lithofacies for a nearshore-shallow marine environment where sediments were dominated by the wave processes. Presence of westerly wind caused the northwesterly/northerly wave which was accompanied by coast parallel residual currents. Distribution of lithofacies in the study area also points towards a progressive decrease in the energy across the shelf due to decreasing wave intensity with increasing water depth. The transgression and regression is the result of sea level fluctuations owing to changing plate interaction and subsequent uplift.

### 6.3 EVIDENCES FROM ICHNOLOGICAL STUDIES

According to Seilacher (1967), there exist a clear relationship between trace fossils distribution pattern, depth and energy condition as occurrence and distribution of trace fossils are controlled by environmental parameters including oxygen levels, salinity and substrate.

Palaeogene sedimentary succession exposed in and around Botsa records the presence of mainly domichnion, fodinichnia and pascichnia ichnotaxa. Recorded ichnofossils are comprised of *Skolithos*, *Cruziana* and *Nerites* ichnoassemblages. *Skolithos* ichnofacies is represented by *S. verticalis*, *Diplocraterion* isp., *Monocraterion* isp., and *Thalassinoides suevicus* whereas *Cruziana* ichnofacies is represented by *Thalassinoides horizontalis*, *T. suevicus*, *Chondrites intricatus*, *Palaeophycus tubularis*, *Planolites beverleyensis*, *Lockeia siliquaria*, *Scolicia plana* and *S. prisca*. *Nerites* ichnofacies records the presence of *Nerites* isp. and *Scolicia* from the studied sedimentary rocks.

Many workers (Frey, *et al.*, 1990; Walker and James, 1992; MacEachern, *et al.*, 2007; Singh *et al.*, 2008; Patel and Desai, 2009; Khalo and Pandey, 2018; Kichu *et al.*, 2018) have reported *Skolithos* ichno-assemblages from the environments characterized by frequent high energy and high rates of sedimentation. Presence of high-energy environment has been suggested by many (Dam, 1990; Fürsich, 1975) based on the presence of *Diplocraterion*. *Diplocraterion* and *Monocraterion* have also been reported by Schlirf (2003) and Heinberg

and Birkelund (1984) from shallow marine agitated water environments. The dominance of vertical traces (typical members of the *Skolithos* ichnofacies) typifies the foreshore-middle shoreface environments with sandy substrate. According to MacEachern *et al.* (2007), similar conditions may be found in a wide range of high-energy shallow water environments but generally they occur on the shoreface and sheltered foreshore.

*Cruziana* ichnofacies of the studied area is dominated by deposit feeders; characteristic of low-energy environments away from the shoreline. *Cruziana* ichno- assemblage is generally found to be associated with unconsolidated poorly sorted muddy substrate with uniform salinity and moderate energy conditions within a shallow marine setting below fair weather wave base but above a storm wave base (Pemberton, *et al.*, 1992; Sudan *et al.*, 2002; MacEachern *et al.*, 2007; Singh *et al.*, 2008; Khalo and Pandey, 2018; Kichu *et al.*, 2018). Demircan, (2008) suggests that *Planolites* belongs to facies-crossing ichnospecies and it has been reported from a wide range of marine environments from littoral to slope. Tiwari *et al.* (2011) opines that the presence of *Planolites* suggests moderate to low energy shoreface/offshore conditions and unconsolidated substrate. Presence of *Chondrites* and its association with other endobenthos (*Thalassinoides*) suggests well-oxygenated bottom water (Bromley and Ekdale, 1984). According to Uchman and Gaydzicki (2006), *Scolicia* is produced by stenohaline echinoids which indicate a near normal salinity, at least locally. Demircan (2008) has suggested that both *S. plana* and *S. prisca* are exclusively marine and they are found in the lower shoreface/offshore region below the normal wave base. However, variants of *Scolicia* have also been reported from turbidite deposits (Tchoumatchenco and Uchman, 2001; Demircan, 2008). *Lockeia* is common in *Cruziana* ichnofacies, and have been reported from lower shoreface-offshore settings (Schlirf, 2003; Kim, 2008; Paranjape *et al.* 2013). The presence of horizontal biogenic structures (*Thalassinoides*, *Planolites*, & *Palaeophycus*) indicates a reduced energy level similar to lower shoreface–offshore marine settings. However, Pemberton *et al.*, (2001) have suggested that the trace fossils typical of the *Cruziana* ichnofacies are also found close to or below a fair-weather wave base. Palaeogene sedimentary rocks of the studied area also record the presence of *Nereites* ichnofacies which includes *Nereites* isp. and *Scolicia*. However, according to Haentzschel (1975), *Scolicia* represents a wide facies range representing both *Cruziana* and *Nerites* facies.

The vertical distribution of ichnospecies in the studied sediments suggests a marine setting corresponding to shoreface-offshore transition region. A definite trend over time has been noticed on the basis of the distribution of trace fossils in these sediments. The dominance of

*Skolithos* ichnofacies at the higher stratigraphic levels indicates an agitated environment with sandy substrate near the shore line (Frey *et al.*, 1984; Frey *et al.*, 1990). While proposing a shoreface model for trace fossils; Frey *et al.* (1990) and Pemberton and MacEachern (1995) have suggested that the *Skolithos* ichnofacies generally grades seaward into *Cruziana* ichnofacies. Sediments at the lower stratigraphic level are dominated by *Cruziana-Nerites* ichnofacies, suggesting a reduced energy level away from the shore line corresponding to lower shoreface–offshore transition marine settings. The occurrence of various ichnofacies at the same horizon also indicates that the bottom water was well oxygenated, which not only allowed the growth but also sustenance of life.

As suggested by many (Nandi, 2000; Srivastava *et al.*, 2004; Acharyya, 2007; Singh *et al.*, 2008; Tiwari *et al.*, 2011; Srivastava *et al.*, 2017; Khalo and Pandey, 2018; Kichu *et al.*, 2018; Srivastava *et al.*, 2018; Srivastava and Kichu, 2021), NE Indian geology has mainly been controlled by subduction-related processes. The continued subduction of Indian plate below the Myanmar plate resulted in fluctuations in the sea level and energy conditions and also in shifting of the depositional site. Presence of such mixed ichno-assemblage could be attributed to the tectonically controlled sea-level fluctuations. According to Bendella and Mehadji (2014) such patterns in the distributions of trace fossils and sediments are indicative of bathymetric fluctuations and it could be the result of tectonic instability probably.

## 6.4 TECTONO- PROVENANCE

Interpretation of tectonic provenance and basin settings on the basis of detrital constituents, have been attempted by many workers (Dickinson and Suczek, 1979; Ingersoll and Suczek, 1979; Dickinson and Valloni, 1980; Dickinson, 1982; Suczek and Ingersoll, 1985; and Korsch, 1984). Proportion of detrital framework grains has been correlated with the various plate tectonic settings and also the plate interaction. Similar attempts have also been made by later workers (Basu *et al.*, 1975; Uddin and Lundberg, 1998 a & b; Singh *et al.*, 2004; Srivastava *et al.*, 2004; Allen *et al.*, 2008; Srivastava and Pandey, 2011; Srivastava and Kichu, 2021 and many more). Mack (1984) has suggested that while making interpretations based on the sandstone petrography, care must be taken. He also emphasized that processes and conditions under which the sandstones were deposited should also be taken into consideration. He further categorized the sandstones populations into four groups which are not represented on the

triangular provenance diagrams. He considered them as anomalous and exceptions to the relationship between plate tectonic and sandstones compositions.

The different categories of error populations are described below:

- i. Sandstones of transitional tectonic settings.
- ii. Sandstone composition modified by weathering and/or depositional processes.
- iii. Sandstones formed in tectonic settings not shown in the triangular diagrams of above workers.
- iv. Sandstones with detrital carbonate.

Others (Suttner,1974; Davis and Ethridge,1975; Suttner *et al*,1981; McBride 1985) have also suggested that care must be taken while interpreting the lithology and tectonic settings of the source, as the composition of sandstones are affected by more than one factor such as climate and relief, transport related processes, depositional environments/diagenesis and selective destruction of susceptible minerals.

Petrographic composition, heavy mineral suits, and geochemical attributes of studied sediments, suggest a mixed provenance where sedimentation was controlled by changing plate interaction. Based on the ternary plots (Dickenson and Suczek,1979), it may be suggested that the basin received its detritus mainly from a recycled orogen comprising all the three kinds of provenance *viz.* subduction complex province, collision orogenic province and foreland uplift province. Presence of very well-rounded zircon and tourmaline in these sediments supports the above view. Grain size variation in the Palaeogene sequence through time suggests that the subduction related process might have brought the Indian craton lying immediately west close to the depositional site. At the upper stratigraphic horizons, presence of angular grains of tourmaline with inclusions (Srivastava and Kichu, 2021) and zircon suggests supply from a granitic source. They also suggest less transportation and /or nearness of the source. Among the feldspars, it is the plagioclase which dominates over the K-feldspar. K-feldspars have been observed in the sandstones at the higher stratigraphic levels only. Though, plagioclase feldspars are noticed in almost all the samples. Presence of K-feldspar in the sandstones at the higher stratigraphic levels suggests increased supply from a granitic source (acid plutonic) and short transportation which has allowed the preservation of otherwise very susceptible minerals as they can be destroyed by selective destruction. In contrast to that the presence of plagioclase feldspars almost in all the samples analyzed suggest their derivation from multiple sources as plagioclases can be supplied by acid volcanics and also from metamorphic rocks (Pettijohn, *et*

*al.*, 1987, Boggs, Jr. 2012). In addition to that plagioclase feldspar could be of authigenic origin also. Presence of angular, sub-angular/sub-rounded and very well-rounded varieties of zircon, tourmaline and rutile plus sillimanite and kyanite in the examined Palaeogene sandstones points towards a mixed provenance suggesting supply at least from three different sources viz: Indian craton in the west, Naga Metamorphics in the east and also from the sediments formed in the earlier regime. Presence of very well-rounded zircon, rutile and tourmaline in the sandstones at lower horizons suggest their derivation from a sedimentary/recycled source. However, at higher stratigraphic horizons presence of angular zircon and tourmaline suggest a granitic source, thereby indicating nearness of source and less transportation and closure of the basin owing to continued subduction of Indian plate below the Myanmar plate. Srivastava and Pandey (2011) and Srivastava and Kichu (2021), while working with younger Palaeogene sediments (Barail sandstones), have also suggested the same. Clustering of the data points at the quartzose end of  $Q_mPK$  diagram suggest a recycled nature of detritus (**Fig. 37**). Observations documents the presence of mono/polycrystalline quartz, recycled quartz, schist rock fragments, mica, volcanic fragments and euhedral zircons, tourmaline, rutile, sillimanite, and kyanite. Such a mixed detritus suggests that these sediments were deposited during transitional and/or an active phase of tectonic regime (Boggs, Jr, 2012). In the various discriminatory plots based on the major oxide concentration also suggest a transitional /and or active tectonic regime. Further, it may also be envisaged that the deposition of Palaeogene sediments kept pace with changing plate interaction through time. Most of the sandstones belonging to quartz arenite/sublitharenite categories also corroborate the above. Bivariate and triangular plots based on major oxide concentration of these sediments also points towards the same.

Another important observation which has been made in the present work is that there is a clear pattern in the occurrence and the distribution of heavy minerals as well as framework grains. At the lower stratigraphic horizons well rounded grains of zircons along with the well-rounded quartz and plagioclase feldspar are common whereas at the upper horizons it is the angular to sub angular zircon and tourmaline with inclusions and increased content of K-feldspar dominate. Presence of well- preserved and high content of angular grains of heavies also supports a granitic source. Angular/sub rounded rutile grains were observed in almost all the samples analyzed. Such distribution of mineral grains in these sediments suggests at least three sources: recycled/sedimentary, low grade metamorphics and acid plutonic rocks. This also suggests that the Palaeogene sedimentation was mainly controlled by subduction related



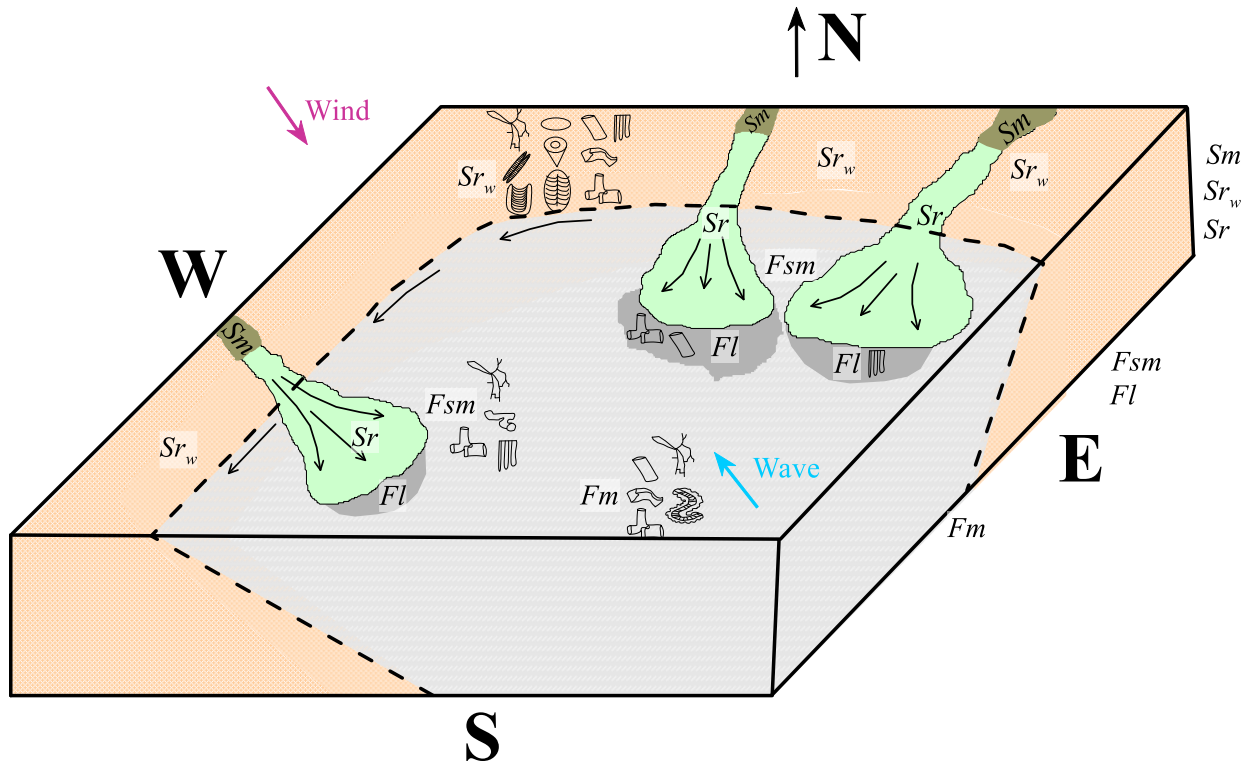
processes. Subduction of Indian plate which started during early Eocene (Acharya, 2007) had created a North-East South-West trending linear depression which was the main depositional site where sediments were mainly supplied by the Karbi Anglong Massif from the west especially during Upper Eocene-Oligocene times. Anti-clock wise movement of Indian plate was responsible for the closure of the basin as well as the upliftment of the sediments formed under earlier tectonic regime. In response to this there would have been reorganization of drainage system in the source area. This process would have reorganized the drainage within the source area and would have started the supply of the sediments from north/northeast directions. The presence of clay mineral montmorillonite and volcanic rock fragments in these sediments suggest their derivations from rising Ophiolites also. However, presence of very well-rounded heavy mineral species suggests a sedimentary source and /or long transportation. Well-rounded heavy mineral grains could have come from the erosion of the sediments deposited under earlier tectonic regime. Heavy minerals from metamorphic source (rutile, sillimanite & kyanite) have the lowest concentration and could have been supplied by a metamorphic source. Similar inferences have also been drawn on the basis of framework grains. Presence of calcite and dolomite in some of the studied sandstones also suggests a shallow marine environment as well as the presence of limestone in the vicinity. Presence of such a varied composition also suggests that the basin had received the sediments from many sources and deposition was controlled mainly by the tectonics of the region.

## **6.5 TRANSPORT MECHANISM AND DISPERSAL**

Transportation and dispersal of the sediments during the deposition of Palaeogene sediments seems to be rather complex owing to the supply from mixed source. The field observations, distribution of litho-units and laboratory investigations suggest that the sediments reached the depositional site mostly through the wave related processes. In addition to that some sediments were also transported by the small tidal inlet channels. Textural analysis of Palaeogene sediments shows a clear basin ward decrease in mean grain size, sand-mud ratio and sediment sorting. Based on the grain size variations and lithofacies distribution, a progressive decrease in energy across the shelf has also been envisaged. Increasing water depth and decreasing wave intensity had resulted in texturally graded shelf setting (Johnson and Baldwin, 1986).

The hydraulic processes controlling the sediment dispersal patterns appear to have been:

- i) net offshore transport of fine sand and silt derived from coastal areas perhaps from tidal inlets through suspension.
- ii) resultant westward current related to easterly winds.
- iii) wave movements towards onshore with increased intensity and decreasing water depth (Curry, 1960).



**FACIES**

- Sm** V fine to medium massive sandstone facies
- Sr<sub>w</sub>** Wave rippled siltstone facies
- Sr** Rippled sandstone facies
- Fsm** Coarse silt to very fine sandstone facies
- Fl** V fine to medium plane laminated sandstone facies
- Fm** Mudstone facies

**ICHNOFOSSILS**

- Chondrite intricatus
- Cruziana aegyptica
- Diplocaterion isp.
- Lockeia siliquaria
- Monocraterion isp.
- Nereites isp.
- Palaeophycus tubularis
- Planolites beverleyensis
- Rusophycus aegypticus
- Scolicia
- Skolithos verticalis
- Thalassinoides

**Fig. 48:** Depositional model for the Palaeogene sediments of the study area

## CHAPTER 7

### SUMMARY AND CONCLUSIONS

The studied Palaeogene (Eocene-Oligocene) sedimentary successions exposed in and around Botsa (25°50'00" N and 25°55'00" N and longitudes 94°08'00" E and 94°15'00" E), present an opportunity to examine their evolution with respect to time. These Palaeogene sedimentary rocks, a part of Kohima Synclinorium within Inner Fold Belt, are represented by shale-silt-mudstone- sandstone litho-units. In the study area, lower stratigraphic horizons are dominated by mainly argillaceous sediments whereas at upper stratigraphic levels, sediments are dominantly arenaceous in composition. However, at places, a mixed lithology of shale-silt-sand similar to Disang Barail Transition reported from NW of Kohima town, have also been observed. Precise marking of Disang-Barail contact in this un-interrupted Palaeogene sedimentation within the Inner Fold Belt is an intriguing problem; as there is no clearly defined boundary between Upper Disang Formation and the lower Barail sediments. Sand size ranging between very fine and medium fractions, showing increasing trends up in the sequence with minor fluctuations, is an important characteristic of this succession. Many dealing with the Palaeogene sediments in other parts of the Inner Fold Belt have attributed this to an un-interrupted sedimentation culminating with Oligocene with many phases of sea level fluctuations; which had resulted in the deposition of numerous beds of both shale and sand.

Sandstones of the study area occur both as thinly and thickly bedded, massive as well as plane laminated; not varying much in their lithological characters. Varied tectonic features like small scale faults, folds, exfoliation joints and shear zones along with depositional sedimentary structures including planar and cross laminations, asymmetrical, symmetrical/wave ripples, interference and bifurcating ripples, hummocky cross stratifications and also biogenetically produced structures have been observed in the field.

Through the present work, for the first time, an attempt has been made to reconstruct the palaeoenvironment applying facies analysis techniques, ichno-assemblages, and also to search for the provenance of the Palaeogene siliciclastics of the study area using petrographic and geochemical attributes.

To accomplish the above objectives, 42 samples representing different stratigraphic horizons were studied for their grain size properties and were analyzed for modal compositions. Additional 30 sandstone samples from different horizons were also analyzed for their major

oxide contents. For identifying the diagenetic changes and surface features in these sandstones, both XRD and SEM studies were performed. More than 30 sandstones samples were also processed for their heavy mineral content. 10 vertical profile sections were constructed and meticulously studied at various locations. Samples were collected both in time and space. Sedimentary and biogenic structures have also been recorded and photographed to supplement the laboratory data.

Based on the field as well as laboratory data following important observations were made:

- i) Progressive increase in the grain size with respect to time.
- ii) Changes in the disposition of the ichnofossils from horizontal to vertical.
- iii) Presence of micro-hummocky cross stratification in the siltstones/very fine sandstones.
- iv) Presence of very well rounded zircon, tourmaline and plagioclase feldspar throughout the successions.
- v) Appearance of angular variety of heavy minerals and K-feldspar at higher stratigraphic levels.

For understanding the changes through time, a lithofacies scheme, based on the facies parameters for simplifying and generalizing the observations made through the study of vertical profile sections, has been developed. Based on the facies parameters (lithology including grain size, bed geometry, sedimentary structures including biogenic and other aspects), total 6 lithofacies have been identified, viz. i) Very fine to medium massive sandstone facies (*Sm*) ii) Very fine to medium plane laminated sandstone facies (*Fl*) iii) Coarse silt to very fine sandstone facies (*Fsm*) iv) Rippled sandstone facies (*Sr*) v) Wave rippled siltstone facies (*Sr<sub>w</sub>*) vi) Mudstone facies (*Fm*). A summary of characteristic attributes of all the lithofacies has been presented in **Table 10**.

The discrimination of depositional environments of various lithofacies has been made using bivariate statistical and textural parameters of grain size distribution. In the Passega's C-M plot, C-M values overall corresponds to Class V and VII suggesting that these sediments were transported by suspension mechanism (both graded and uniform) and with some sediments transported by saltation. The average values for CU and CS for these sediments correspond to 220 and 430 microns, respectively. The palaeobathymetric estimation using Passega's (1964) Cs-C depth diagram indicates that these sediments have been deposited under



a shallow marine environment. A depth range 70/80 meters has been estimated for these sediments. To distinguish the broad aspects of depositional environments, linear discriminant function and log-log plot of  $(\sigma_f^2)$  versus  $(SK_G/SM_z)$ .  $S(\sigma_f^2)$ , after Sahu (1964), and also the multigroup discrimination plot of  $V_1$  and  $V_2$  with  $V_1 \wedge V_2 = 74.4^\circ$ , after Sahu (1983), have been employed. Based on the above plots, it has been inferred that these sediments were deposited in a nearshore-shallow marine environment having a fluctuating energy regime. In the study area, not many directional features have been observed except some channel and some asymmetrical ripples. Based on the average grain size variations within the studied area and also from some directional features encountered, it is suggested that the sediment supply was made from different directions. This also suggests that drainage in the vicinity was continuously being reorganized owing to changing plate interactions.

Litho-facies analysis of the Palaeogene sediments also suggests that they were deposited within a near shore-shallow marine depositional regime with fluctuating sea level and energy. Lithofacies analysis further suggests these sediments were deposited in a shoreface-offshore transition environments ranging from high energy upper shoreface represented by  $Sm$ ,  $Sr$ , and  $Sr_w$  facies through low energy lower shoreface and off-shoreface environments represented by  $Fl$  and  $Fsm$  (lower shoreface) and  $Fm$  facies (Offshore-transition). Presence of hummocky cross stratification also suggests occasional prevalence of high energy conditions owing to storm activities. Grain size variation from clay and silt size fractions to fine to medium sand fractions also suggests a changing energy conditions from low energy lower shoreface to high energy upper shoreface depositional environment. Presence of some fining upward sequences within a general coarsening upward trend, suggests that these sediments were deposited within a prograding shelf with minor fluctuations in sea level as well as energy conditions. Trace fossil dispositions and the nature of the associated sediments also suggest variations in the energy conditions across the shelf. Vertical traces within fine to medium sandstones represent the high energy upper shoreface environment whereas presence of horizontal traces within very fine to fine grained sandstones/ mudstone suggests a low energy lower shoreface environment away from the shore line towards the offshore/offshore-transition. High degree of bioturbation of the very fine-grained sandstones and mudstones also suggest the same.

Based on the distribution of the various lithofacies in the study area, a conceptual model for the deposition of the Palaeogene sedimentary succession has been envisaged. The depositional model depicts a near shore-shallow marine wave dominated shore face

environment. On the basis of lithofacies distributions, and ichno- assemblages a progressive decrease in the energy across the shelf in response to increasing water depth and decreasing of wave intensity has been visualized. Small tidal channels (*Sm*) transporting the material from the upper shoreface region to the lower shoreface and the offshore regions where wave effect is less leading to the development of *Fl* and *Fsm* facies in lower shoreface region. *Fm* is considered to represent the offshore transition. In the upper shoreface region, where wave and tidal processes were dominant, *Sm*, *Sr* and *Sr<sub>w</sub>* lithofacies were developed. Presence of hummocky cross stratification suggest the storm activity.

The average modal composition of different lithofacies may be seen in **Table 7**. On the basis of quartz, feldspar and rock fragments, following Folk (1980) sandstones of the study area are categorized as quartz arenite and sub-litharenite. Geochemically they have been classified as lith-arenite and wacke. Signatures of both early as well as late diagenesis have been observed in these sediments. Based on the petrographic studies, heavy mineral assemblage and major oxides, a mixed provenance has been interpreted. However, an increased contribution from a plutonic source especially at higher stratigraphic levels suggests the nearness of the acid igneous source such as granite most probably from Karbi-Anglong massif lying immediate west of the basin. There is visible change in the heavy mineral assemblages between lower and upper stratigraphic levels. Finer sediments encountered in the early Palaeogene succession are marked by the dominance of rounded variety of zircon and tourmaline and a near absence of K-feldspar whereas comparatively coarser sediments at the higher stratigraphic level are characterized by the presence of more angular variety of heavy minerals specially zircon, tourmaline and rutile along-with the rounded zircons, and appearance of K-feldspar specially orthoclase, suggesting contributions from crystalline sources. This could be attributed to the changing plate interaction and reorganization of the drainage in the source area. Based on the quartz types (undulatory/non undulatory mono-crystalline; 2-3 and > 3 unit polycrystalline) and presence of angular tourmaline, zircon, rutile, kyanite, and sillimanite; contributions from plutonic as well as metamorphic sources have been inferred. This also suggests that these sources were lying close to the basin and continuously supplying the sediments. Based on the matrix content, sorting and roundness these sediments are classified as mature to super mature. Compositionally, the studied sediments are mature to super mature, suggesting moderate to intense chemical weathering in the source region. A humid climate has been envisaged for the weathering and erosion of sediments.

Ternary plots of QFL,  $Q_mFL_t$ ,  $Q_pL_vL_s$  and  $Q_mPK$  (Dickenson and Suczek, 1979) suggest that detritus were largely derived from a recycled orogen. Presence of well-rounded quartz, sedimentary rock fragments, low concentration of feldspar and polycyclic zircon and tourmaline also corroborate the above. In addition to that presence of non-polycyclic grains of tourmaline, zircons and rutile also suggests a crystalline source in the vicinity. However, appearance of K-feldspar (orthoclase) along with euhedral zircons and tourmaline at upper stratigraphic levels suggests that there had also been contributions either from Shillong plateau and/or Karbi Anglong massif (earlier known as Mikir massif) lying immediate west of the basin. This also suggests that during upper Oligocene period, Indian plate owing to continued subduction beneath the Myanmar plate might have been very close to the basin contributing these minerals to the basin. Presence of these minerals in the sediments at higher stratigraphic horizons also points towards a basin of undulatory nature restricting long transport and facilitating the preservation of them. High rate of supply of sediments and/or quick burial could have also been responsible for the preservation of otherwise susceptible minerals such as orthoclase. Presence of very well-rounded zircon, tourmaline and rutile along with presence of sedimentary rock fragments also suggest their derivation from a sedimentary source. In addition, presence of such a mixed detritus suggest that deposition kept pace with changing plate interaction through time and sediments deposited under earlier regime could have also contributed sediments to depositional site. Geochemical analysis (major oxides) of these sediments also supports the above views and is in conformity with the inferences drawn from petrographic study.

The hydraulic processes that controlled the sediment dispersal pattern relate to

- i) onshore directional wave with increased intensity and decreasing water depth.
- ii) net westward current related to easterly winds.
- iii) net offshore transport of silt and silt enriched mud through suspension mechanism.

<b>Facies Code</b>	<b>Lithofacies</b>	<b>Sedimentary structures</b>	<b>Bed Geometry</b>	<b>Modal Composition</b>	<b>Texture</b>	<b>Suggested Environment</b>
<i>Sm</i>	Very fine to medium massive sandstones	Thickly bedded massive sandstones,	Wedge shaped	Quartz 68.6% Feldspar 1.2% Rock f 11.7% Others 18.5%	$M_Z = 3.1$ $\sigma_1 = 0.6$ $SK_I = 0.1$	Upper shoreface, high energy
<i>Sr</i>	Very fine to medium grained sandstones	Assymmetrical ripples or current ripples, bioturbation	Wedge shaped	Quartz 71.2% Feldspar 1.6% Rock f 8.8% Others 18.4%	$M_Z = 3.5$ $\sigma_1 = 0.7$ $SK_I = 0.2$	Tidal channels, upper shoreface
<i>Sr<sub>w</sub></i>	Very fine to fine grained sandstones	Symmetrical ripples, interference ripples, bioturbation, vertical and horizontal trace fossils/ traces dominant	Tabular	Quartz 70.2% Feldspar 1.3% Rock f 7% Others 21.5%	$M_Z = 3.4$ $\sigma_1 = 0.6$ $SK_I = 0.1$	Upper shoreface, wave action
<i>Fsm</i>	Coarse silt to very fine sandstones	Hummocky cross stratification, bioturbation, horizontal and vertical trace fossils	Shoestring	Quartz 69.2% Feldspar 2.0% Rock f 4.9% Others 23.8%	$M_Z = 3.5$ $\sigma_1 = 0.6$ $SK_I = 0.1$	Storm deposits, below normal wave base, lower shoreface
<i>Fl</i>	Very fine to medium plane laminated sandstones	Plane laminations, low angled cross laminations, Horizontal bedding showing colour variations, horizontal and vertical traces	Shoestring	Quartz 73.6% Feldspar 0.7% Rock f 8.1% Others 17.6%	$M_Z = 3.3$ $\sigma_1 = 0.6$ $SK_I = 0.1$	Lower shoreface, low energy
<i>Fm</i>	Mudstones and shales	Bioturbation, plane laminations, tabular silt beds, horizontal trace fossils	Tabular			Offshore-transition

**Table 10:** Summary of the characteristic features of the Palaeogene sediments in and around Botsa

## References

- Acharyya, S. (1982): Structural framework and tectonic evolution of the Eastern Himalaya. *Himalayan Geology*, v.10, pp.412-439.
- Acharyya, S. (1986): Cenozoic plate motion creating the eastern Himalayas and Indo-Burmese ranges around the northern corner of India. In: *Ophiolites and Indian Plate Margins* (Eds. N.C. Ghose and S. Vardarajan), Patna, pp.146-161.
- Acharyya, S. (1990): Pan-Indian Gondwana Plate break up and evolution of the northern and eastern collision margins of the Indian Plate. *Jour. Him. Geol.*, v.1, pp.75-91.
- Acharyya, S. (2007): Evolution of the Himalayan Palaeogene foreland basins, influence of its litho-packet on the formation of thrust related domes and windows in the Eastern Himalayas - A review. *Jour. Asian Sci.*, v.31, pp.1-17.
- Acharyya, S.; Roy, D.K. and Mitra, N.D. (1986): Stratigraphy and Palaeontology of the Naga Hills ophiolite belt. In: *Geology of Nagaland Ophiolite* (Ed. D.B. Ghosh), *Comm. Vol. Mem. Geol. Sur. India*, v.119, pp.64-75.
- Agarwal, O.P. (1985): Geology & geochemistry of the mafic-ultramafic complex of Indo-Burman ranges between Meluri and Awankhoo, Phek district, Nagaland, India. Unpublished Ph.D. thesis, Patna University, Patna.
- Agarwal, O.P. and Ghose, N.C. (1986): Geology and stratigraphy of Naga Ophiolite between Meluri and Awankho, Phek District, Nagaland, India. In: *Ophiolites and Indian Plate Margins* (Eds. N.C. Ghose and S. Vardharajan), pp.163-195.
- Allen, J.R.L. (1966): Note on the use of Plaster of Paris in flow visualization and some geological applications. *Journal of Fluid Mechanics*, v.25, pp.331-335.
- Allen, J.R.L. (1967): Depth indicators of clastic sequences. *Marine Geology*, v.5, pp.429-446.
- Allen, J.R.L. (1982): Simple models for the shape and symmetry of tidal sand waves: dynamically stable symmetrical equilibrium forms. *Marine Geology*, v.48, pp.51-73.
- Allen, R.; Najman, Y.; Carter, A.; Barfod, D.; Bickle, M.J.; Chapman, H.J.; Garzanti, E.; Vezzoli, G.; Ando, S. and Parrish, R.R. (2008): Provenance of the Tertiary sedimentary rocks of the Indo-Burman Ranges, Burma-Burma arc or Himalayan derived? *Jour. Geol. Soc. London*, v.165, pp.1045-1057.
- Banerjee, R.K. (1979): Disang shale, its stratigraphy, sedimentary history and basin configuration in northeastern India and Burma. *Q. Jour. Geol. Min. Metal. Soc. India*, v.51, pp.144-152.

- Basu, A.; Young, S.W.; Suttner, L.J.; James, W.C. and Mack, G.H. (1975): Re-evaluation of the use of undulatory extinction and poly-crystallinity in detrital quartz for provenance interpretation. *Jour. Sed. Petrol.*, v.45, pp.873-882.
- Bendella, M. and Mehadjji, A.O. (2014): Depositional environment and Ichnology (Nereites ichnofacies) of the Late Devonian Sahara region (SW Algeria). *Arabian Journal of Geosciences*, v.8, pp.5303-5316.
- Bhandari, L.L.; Fuloria, B.C. and Sastri, V.V. (1973): Stratigraphy of Assam Valley. *Bull. Am. Assoc. of Petrol. Geol.*, v.57(4), pp.642-654.
- Bhatia, M.R. (1983): Plate tectonics and geochemical composition of sandstones. *The Jour. of Geol.*, v.91(6), pp.611-627.
- Bhatia, M.R. and Crook, K.A.W. (1986): Trace element characteristics of grawackes and tectonic setting discrimination of sedimentary basins. *Contrib. Mineral. Petrol.*, v.92, pp.181-193.
- Billings, E. (1862): New species of fossils from different parts of the Lower, Middle and Upper Silurian rocks of Canada. In: *Palaeozoic Fossils, Geological Survey of Canada Adv Sheet*, v.1(1861-65), pp.96-168.
- Biswas, S.K.; Bhasin, A. L. and Ram, J. (1994): Classification of Indian sedimentary basins in the framework of plate tectonics. In: *Biswas S.K. (Ed.), Proc. Second Seminar on Petroliferous basins of India*. KDM institute of Petroleum Exploration, Dehradun 1, pp.1-46.
- Bjorkum, P.A. and Gjelsvik, N. (1988): An isochemical model for formation of authigenic kaolinite, K-feldspar and illite in sediments. *Jour. Sed. Petrol.*, v.58, pp.506-511.
- Blatt, H. and Christie, J.M. (1963): Undulatory extinction in quartz of igneous and metamorphic rocks and its significance in provenance studies of sedimentary rocks. *Jour. Sed. Research*, v.33(3), pp.559-579.
- Blatt, H.; Middleton, G. and Murray, R. (1980): *Origin of Sedimentary Rocks*. Prentice Hall Inc., Englewood Cliffs, New Jersey. 782p.
- Boggs, S. Jr. (2012): *Petrography of Sedimentary Rocks*, 2nd Edition, Cambridge University Press. 600p.
- Boles, J.R. (1982): Active albitization of plagioclase, Gulf Coast tertiary. *Amer. Jour. Sci.*, v.282, pp.165-180.
- Borak, B. and Friedman, G.M. (1981): Textures of sandstones and carbonate rocks in the world's deepest wells (in excess of 30000 ft or 9.1 km): Anadarko Basin, Oklahoma. *Sedimentary Geology*, v.29, pp.133-151.



- Bromley, R.G. and Ekdale, A.A. (1984): Chondrites: a trace fossil indicator of anoxia in sediments. *Science*, v.224, pp.872–874.
- Brongniart, A.T. (1828): In: *Historic des végétaux fossils, ou recherché botaniques et géologiquessur les végétaux renfermés dans les diverses couches du globe* (Eds. G. Dufour and E. d'Ocagne), Paris, v.1, pp.1–136.
- Brunnschweiler, R. (1966): On the geology of Indo-Burman Ranges. *Jour. Geol. Soc. Australia*, v.13, pp.137-194.
- Burley, S.D.; Kantorowicz, J.D. and Waugh, B. (1985): Clastic diagenesis. In: *Sedimentology: Recent and Applied Aspects* (Eds. P. Brenchley and B.P.B. Williams), *Spec. Publ. Geol. Soc. London, Blackwell Scientific Pub., Oxford*, v.18, pp.189-226.
- Carozzi, A.V. (1960): Microscopic Sedimentary Petrography. *Wiley, New York-London*. 485p.
- Casshyap, S.M. and Khan, Z.A. (1982): Paleohydrology of Permian Gondwana streams in Bokaro basin, Bihar. *Jour. Geol. Soc. India*, v.23, pp.419–430.
- Chakravarti, D.K. and Banerjee, R.M. (1988): Evolution of Kohima Synclinorium – A reappraisal. *GSI 115 pts 2 & 4*.
- Chappell, J. (1967): Recognizing fossil strand lines from grain-size analysis. *Jour. Sed. Research*, v.37(1), pp.157–165.
- Chattopadhyay B.; Venkataramana P.; Roy D. K.; Bhattacharyya S. and Ghosh S. (1983): Geology of Naga Hills ophiolites. *Rec Geol Surv India*, v.112(2), pp.59–115.
- Chaudhary, A.R. (1993): Textural parameters of the Nagthat sediments of the Chakarata Hills, Kumaun Himalayas. *Ind. Jour. Earth Sci.*, v.20(3&4), pp.119-125.
- Collinson, J.D. and Thompson, D.B. (1994): Sedimentary Structures. *CBS Publishers, New Delhi*. 198p.
- Condie, K.C. (1967): Geochemistry of early Precambrian greywacke from Wyoming. *Geochem. Cosmochim. Acta.*, v.321, pp.2136-2147.
- Conner, C.W. and Frem, J.C. (1966): Precision on linear and aerial measurements in estimating grain size. *Jour. Sediment. Petro.*, v.36, pp.397-402.
- Conolly, J.R. (1965): The occurrence of polycrystallinity and undulatory extinction in quartz in sandstones. *Jour. Sediment. Petrol.*, v.35, pp.116-135.
- Crook, K.A.W. (1974): Lithofacies and geotectonics: the significance of compositional variations in flysch arenites (graywackes). In: *Modern and Ancient Geosynclinal Sedimentation* (Eds. R.H. Dott and R.H. Shaver), *SEPM sepc. Pub.*, v.19, pp.304-310.

- Curry, J.R. (1960): Sediments and history of the Holocene transgression, continental shelf, Gulf of Mexico. In: *Recent Sediments, NW Gulf of Mexico* (Ed. R.L. Miller), pp.175-203.
- Dam, G. (1990): Palaeoenvironmental significance of trace fossil from the shallow marine Lower Jurassic Neill Klintner Formation, East Greenland. *Palaeogeography, Palaeoclimatology, Palaeoecology*, v.79, pp.221–248.
- Dapples, E.C. (1979): Diagenesis of sandstones. In: *Diagenesis in Sediments and Sedimentary Rocks* (Eds. G. Larsen and G.V. Chilingar), Elsevier, pp.31-97.
- Dasgupta, A.B. (1977): Geology of Assam-Arakan region. *Quart. Jour. Min. Met. Soc. India*, v.49, pp.1-50.
- Davis, D.K. and Ethridge, R.G. (1975): Sandstone composition and depositional environments. *Bull. Amer. Assoc. Petrol. Geol.*, v.59, pp.239-264.
- Demircan, H. (2008): Trace fossil associations and palaeoenvironmental interpretation of the late Eocene units (SW-Thrace). *Bulletin of the Mineral Research and Exploration*, v.136, pp.29–47.
- Desikachar, S.V. (1974): A review of the tectonic and geologic history of the Eastern India in terms of Plate Tectonic Theory. *Jour. Geol. Soc. India*, v.15(2), pp.137-149.
- Directorate of Geology & Mining (1978): Status of Geological Work and Mineral Discoveries in Nagaland, *Miscellaneous Report (unpub)*.
- Directorate of Geology & Mining (2008): Geological map of Nagaland. Directorate of Geology and Mining, Govt. of Nagaland, Dimapur. *Technical publication. No. 28. DGM/FS, 2008*.
- Dickinson, W.R. (1970): Interpreting detrital modes of greywacke and arkose. *Jour. Sed. Petrol.*, v.40, pp.695-707.
- Dickinson, W.R. (1982): Composition of sandstones in circum-pacific subduction complexes and fore arc basins. *AAPG Bull.*, v.66, pp.121-137.
- Dickinson, W.R. and Rich, E.I. (1972): Petrologic intervals and petrofacies in the Great Valley sequence, Sacramento Valley, California. *Geol. Soc. Amer. Bull.*, v.83, pp.3007-3024.
- Dickinson, W.R. and Suczek, C.A. (1979): Plate tectonics and sandstone composition. *Amer. Assoc. Petrol. Geol. Bull.*, v.63, pp.2164-2182.
- Dickinson, W.R.; Beard, L.S.; Brakenridge, G.R.; Erjave, J.L.; Ferguson, R.C.; Inman, K.F. and Ryberg, P.P. (1983): Provenance of North American Phanerozoic sandstones in relation to tectonic setting. *Geol. Soc. Amer. Bull.*, v.94, pp.222-235.
- Dickinson, W.R. and Valloni, R. (1980): Plate settings and provenance of sands in modern ocean basins. *Geology*, v.8, pp.82-86.

- Dott, R.H. Jr. (1964): Wacke, graywacke and matrix- what approach to immature sandstone classification? *Journal of Sedimentary Petrology*, v.34(3), pp.625-632.
- Dott, R.H. Jr. and Bourgeois, J. (1982): Hummocky stratification: significance of its variable bedding sequences. *Geol. Soc. Amer. Bull.*, v.93, pp.663–680.
- Duane, D.B. (1964): Significance of skewness in recent sediments, western Pamlico Sound, North Carolina. *Jour. Sed. Petrol.*, v.34(4), pp.864–874.
- Dutton, S.P. and Diggs, T.N. (1990): Of quartz cementation in the Lower Cretaceous Travis Peak Formation, East Texas History. *Jour. Sed. Petrol.*, v.60, pp.191-202.
- Einsele, G. and Seilacher, A. (1982): Cyclic and Event Stratification. *Springer-Verlag Inc., Berlin*. 536p
- Ekdale, A.A.; Bromley, R.G. and Pemberton, G.S. (1984): Ichnology: The Use of Trace Fossils in Sedimentology and Stratigraphy, *Short Courses 15, Society of Economic Paleontologists and Mineralogists*.
- Elliot, T (1991): Siliclastic shorelines: In sedimentary environment and facies (Ed-H.G. Reading). 2<sup>nd</sup> edition. *Blackwell Scientific Publication*, pp.155-188.
- Evans, P. (1932): Tertiary succession in Assam. *Trans. Min. Geol. Inst.*, v. 27(3), pp.155-260.
- Folk, R.L. (1951): Stages of textural maturity in sedimentary rocks. *Jour. Sediment. Petrol.*, v.21, pp.127-130.
- Folk, R.L. (1966): A review of grain size parameters. *Sedimentology*, v.6, pp.73-93.
- Folk, R.L. (1974): Petrology of Sedimentary Rocks. *Hemphill Publishing Co., Austin, Texas*. 170p.
- Folk, R.L. (1980): Petrology of Sedimentary Rock. *Hemphill Publishing Co., Austin, Texas*. 182p.
- Folk, R.L. and Ward, W.C. (1957): Brazos River bar: a study in the significance of grain size parameters. *Jour. Sediment. Petrol.*, v.27, pp.3-26.
- Frey, R.W.; Curran, H.A. and Pemberton, S.G. (1984): Trace making activities of crabs and their environmental significance: the ichnogenus *Psilonichnus*. *Jour. Paleon.*, v.56(2), pp.333-350.
- Frey, R.W.; Pemberton, S.G. and Saunders, T.D.A. (1990): Ichnofacies and bathymetry: a passive relationship. *Jour. Paleon.*, v.64, pp.155-158.
- Friedman, G.M. (1961): Distinction between dune, beach and river sands from textural characteristics. *Jour. Sediment. Petrol.*, v.36, pp.514-529.
- Friedman, G.M. (1962): On sorting, sorting coefficient and the log normality of the grain size distribution of sandstones. *Jour. Geol.*, v.70, pp.737-753.

- Friedman, G.M. (1967): Dynamic processes and statistical parameters compared for size frequency distribution of beach and river sands. *Jour. Sediment. Petrol.*, v.37, pp.327-354.
- Friedman, G.M. and Sanders, J.E. (1978): Principles of Sedimentology. *Wiley, New York*. 792p.
- Fürsich, F.T. (1975): Trace fossils as environmental indicators in the Corallian of England and Normandy. *Lethaia*, v.8, pp.151–172.
- Ganju, J. L.; Khar, B. M. and Chaturvedi, J. G. (1986): Geology and Hydrocarbon prospects of Naga Hill, south of 27 degree latitude. Bulletin. Oil and Natural Gas Commission, v.23(2), pp.129-145.
- Geological Survey of India (1975): *Progress Report for Field Session 1974-75 (unpub)*.
- Geological Survey of India (1988): GSI, Toposheet No. 83 K/1, 23.01.88. Kohima and Wokha Districts.
- Geological Survey of India (1989): Recent advances in the study of Tertiary Stratigraphy of North-Eastern India-A critical resume. *GSI Special Publication No. 23*, GSI North Eastern Region.
- Geological Survey of India (2011): Geology and Mineral resources of Manipur, Mizoram, Nagaland and Tripura. Geological Survey of India, Miscellaneous Publication, No. 30, Part IV, v.1, (Part-2).
- Ghose, N. C.; Agarwal, O. P. and Singh, R. N. (1986): Geochemistry of the Ophiolite Belt of Nagaland, N.E. India. In: Ghose NC, Varadarajan S (eds) Ophiolites and Indian Plate margin. Sumna Publishers, Patna, pp 241-294.
- Ghose, N. C.; Agarwal, O. P. and Chatterjee, N. (2010): A Geological and mineralogical study of eclogite and glaucophane schists in the Naga Hills Ophiolite, Northeast India. *Island Arc*, v.19, pp.336–356.
- Ghosh, S.K. and Chatterjee, B.K. (1994): Depositional mechanism as revealed from grain size measures of the Palaeoproterozoic Kolhan siliclastics, Keonjhar district, Orissa, India. *Sediment. Geol.*, v.89, pp.181-196.
- Goldring, R. (1965): Sediments into rock. *New Scientist*, v.26, pp.863-865.
- Griffiths, J.C. (1967): Scientific Methods in Analysis of Sediments. *McGraw-Hill, New York*. 508p.
- Grim, R.E. (1968): Clay Mineralogy, *2nd Edition, McGraw-Hill, New York*. 596p.
- Haentzschel, W. (1975): Treatise on invertebrate paleontology. In: *Part W, Miscellanea (Ed. C. Teichert)*, *Geol. Soc. Amer. and Univ. Kansas Press*, pp.38-122.
- Hall, J. (1843): Geology of New York, Part 4. Survey of the Fourth Geological District: *Carroll and Cook, Albany*. 525p.

- Hall, J. (1847): Palaeontology of New York. *C. Van Benthuyzen, Albany*, v.1, pp.1–338.
- Harms, J.C.; Sutheren, J.B.; Spearing, D.R. and Walker, R.G. (1975): Depositional Environments as Interpreted from Primary Sedimentary Structures and Stratification Sequences, *Society of Economic Palaeontologists and Mineralogists, Short course 2*. 161p.
- Harris, S. A. (1958): Differentiation of various Egyptian aeolian microenvironments by mechanical composition. *Jour. Sed. Petrol.*, v.28, pp.164-174.
- Hayes, M.O. (1975): Morphology of sand accumulation in estuaries - an introduction to the symposium. In: *Estuarine Research v.II, Geol. and Engg.* (Ed. L.E. Cronin), *Academic Press, London*, pp.3-22.
- Heald, M.T. and Lorese, R.E. (1974): Inference of coating on quartz cementation. *Jour. Sed. Pet.*, v.44, pp.1269-1274.
- Heinberg, C. and Birkelund, T. (1984): Trace fossil assemblage and basin evolution of the Verdekluft Formation (Middle Jurassic, Central East Greenland). *Journal of Paleontology*, v.58, pp.362–397.
- Herron, M.M. (1988): Geochemical classification of terrigenous sands and shales from core or log data. *Jour. Sed. Petrol.*, v.58, pp.820-829.
- Heward, A.P. (1981): A review of wave dominated clastic shoreline deposits. *Earth Science Reviews*, v.17, pp.223-276.
- Hill, P. R., Meulé, S. and Longuépée, H. (2003): Combined -Flow processes and sedimentary structures on the shoreface of the wave-dominated Grande-Rivière-de-la-Baleine Delta. *Journal of Sedimentary Research*, v.73(2), pp. 217-226.
- Howard, J.D. (1972): Trace fossils as criteria for recognizing shorelines in stratigraphic record. In: *Recognition of Sedimentary Environments* (Eds. J. K. Rigby and W. M. K. Hambil), *Society of Economic Palaeontologists and Mineralogists Spec. Publ. No. 16*, pp.215–25.
- Hubert, J. F. (1962): A Zircon-Tourmaline-Rutile maturity index and independence of heavy mineral assemblage with gross composition and texture of sandstones. *Journal of Sedimentary Petrology*, v.32(3), pp.440-450.
- Hubert, J.F. and Hyde, M.G. (1982): Sheet flow deposits of graded beds and mudstones on an alluvial sandflat playa system, Upper Triassic Blomidon Red Beds, St. Mary's Bay, Nova Scotia. *Sedimentology*, v.29, pp.437-475.

- Imchen, W.; Thong, G.T. and Pongen, T. (2014): Provenance, tectonic setting and age of the sediments of the Upper Disang Formation in Phek District, Nagaland. *Jour. Asian Earth Sciences*, v.88, pp.11-27.
- Ingersoll, R.V. (1974): Surface textures of first cycle quartz sand grains. *Jour. Sediment. Petrol.*, v.44, pp.151-157.
- Ingersoll, R.V. and Suczek, C.A. (1979): Petrology and provenance of Neogene sand from Nicobar and Bengal fans, DSDP sites 211 and 218. *Jour. Sediment. Petrol.*, v.49, pp.1217-1228.
- Jacquet, J.M. and Varnet, J.P. (1976): Moment and graphic size parameters in the sediments of Lake Geneva, Switzerland. *Jour. Sediment. Petrol.*, v.46, pp.305-312.
- James, U.P. (1879): Description of new species of fossils and remarks on some others from the Lower and Upper Silurian rocks of Ohio. *The Palaeontologist*, v.3, pp.17-24.
- James, W.C. and Oaks, R.Q. Jr. (1977): Petrology of the Kinnikinic quartzite (Middle Ordovician), East Central Idaho. *Jour. Sediment. Petrol.*, v.47, pp.1491-1511.
- Johnson, H.D. and Baldwin, C.T. (1986): Shallow siliciclastic seas. In: *Sedimentary Environments and Facies* (Ed. H.G. Reading), 2nd edition, Blackwell Scientific Pub., Oxford, pp.229-282.
- Johnson, M.A. and Stride, A.H. (1969): Geological significance of North Sea and transport rates. *Nature*, v.224, pp.1016-1017.
- Kakul, Z. (1968): Origin, development and chemical classification of early Palaeozoic sandstone of central Bohemia. *Proc. Int. Geo. Cong.*, pp.61-72.
- Khalo, A. and Pandey, N. (2018): Palaeoenvironmental significance of ichnofossils assemblages from the Palaeogene sediments of Inner Fold Belt, Naga Hills, NE India. *Jour. Geo. Soc. India*, v.91, pp.201-208.
- Kichu, A.M.; Srivastava, S.K. and Khesoh, K. (2018): Trace fossils from Oligocene Barail Sediments in and around Jotsoma, Kohima, Nagaland - implications of palaeoenvironment. *Jour. Palaen. Soc. India*, v.63(2), pp.197-202.
- Kim, J.Y. (2008): A unique occurrence of *Lockeia* from the Yeongheung Formation (Middle Ordovician), Yeongweol, Korea. *Historical Biology*, v.3(3), pp.219-225.
- Knaust, D. (2017): Observations on the ichnofauna of the Polish Carpathians. In: *Trace Fossils* (Eds. T.P. Crimes and J.C. Harper), Liverpool: Seel House Press, pp.283-322.
- Korsch, R.J. (1984): Sandstone composition from the New England orogen, Eastern Australia - implications for tectonic settings. *Jour. Sed. Petrol.*, v.51, pp.212-220.



- Krinsley, D.H. and Doornkamp, J.C. (1973): Atlas of Quartz Sand Surface Textures, *Cambridge University Press*. 90p.
- Krumbein, W.C. and Pettijohn, F.J. (1938): Manual of Sedimentary Petrography. *Appleton Century Crofts, New York*, 549 p.
- Ksiazkiewics, M. (1970): Observations on the ichnofauna of the Polish Carpathians. In: *Trace Fossils 10 da* (Eds. T.P. Crimes and J.C. Harper), *Geological Journal Special Issue*, v.3, pp.283–322.
- Kumar, R. and Naik, G.C. (2006): Late Eocene to early Oligocene depositional system in Assam Shelf, *6th International Conference & Exposition on Petroleum Geophysics, Kolkata, 2006*, pp.904-910.
- Lakhar, A.C. and Hazarika, I.M. (2000): Significance of grain size parameters in environmental interpretation of the Tipam Sandstones, Jaipur area, Dibrugarh District, Assam. *Jour. Ind. Assoc. Sedimentologists*, v.19(1-2), pp.69-78.
- Lambiase, J.J. (1982): Turbulance and the generation of grain size distribution (Abst.), *11th International Congress on Sedimentology, Hamilton*, pp.80-81.
- LeMaitre, R.W. (1976): The chemical variability of some common igneous rocks. *Jour. Petrol.*, v.17, pp.589-637.
- LeBlanc, R.J. (1972): Geometry of sandstone reservoir bodies. In: *Underground Waste Management and Environmental Implications* (Ed. T.D. Cook), *Am. Assoc. Petrol. Geo. Mem.*, v.18, pp.133-187.
- Leeder, M.R. (1982): Sedimentology, *George Allen and Unwin, London*. 344p.
- MacEachern, J.A.; Pemberton, S.G.; Gingras, M.K. and Bann, K.L. (2007): The ichnofacies paradigm: A fifty year retrospective. In: *Trace fossils: Concepts, Problems, Prospects* (Ed. W. Miller), *Amsterdam: Elsevier*, pp. 52–77.
- Mack G.H. (1984): Exceptions to the relationship between plate tectonics and sandstone composition. *Journal Sedimentary Petrology*, v.54, pp.212-220
- Mahendar, K. and Banerji, R.K. (1989): Textural study and depositional environment of sand grains from rocks of Jaisalmer Formation, Jaisalmer District, Rajasthan, India. *Jour. Geol. Soc. India*, v.33(3), pp.228-242.
- Mallet, F.R. (1876): On the coal fields of Naga Hills bordering the Lakhimpur and Sibsagar Distict, Assam. *Jour. Geol. Survey of India*, v.12(2), pp.286.

- Marzolf, J.E. (1976): Sand grain frosting and quartz overgrowth examined by SEM - the Najavo Sandstone, Utah. *Jour. Sediment. Petrol.*, v.46, pp.906-912.
- Mason, C.C. and Folk, R.L. (1958): Differentiation of beach, dune and eolian flat environments by size analysis, Mustang Islands, Texas. *Jour. Sediments. Petrol.*, v.28, pp.211-226.
- Mathur, L.P. and Evans, P. (1964): Oil in India, *Int. Geol. Congress, 22<sup>nd</sup> Session, New Delhi, India.* 85p.
- McBride, E. F. (1963): A classification of common sandstones. *Journal of Sedimentary Research*, v.33 (3), pp. 664–669.
- McBride, E.F. (1985): Diagenetic processes that effect provenance determination in sandstones. In: *Provenance of Arenites* (Ed. G.C. Zuffa), *Dordrecht:Reidel*, pp.95-113.
- McLennan, S.M.; Hemming, S.; McDaniel, D.K. and Hanson, G.N. (1993): Geochemical approaches to sedimentation, provenance and tectonics. *Geol. Soc. Amer. Spl. Paper*, v.284, pp.21-40.
- McLennan, S.M. (1989): REE in sedimentary rocks - influence of provenance and sedimentary processes. In: *Geochemistry and Mineralogy of REE* (Eds. B.R. Lipin and G.A. McKey), *Min. Soc. Am., Washington.* 348p.
- Miall, A.D. (1990): Hierarchies of architectural units in clastic rocks and their relationships to sedimentation rate. In: *The Three Dimensional Facies Architecture of Terrigenous Clastic Sediments* (Eds. A.D. Miall and Tyler), *Soc. Econ. Palaeo. and Mineralogist.*
- Middleton, G.V. (1976): Hydraulic interpretation of sand size distributions. *Jour. Geol.*, v.84, pp.405-426.
- Mishra, D. and Tiwari, R.N. (2005): Provenance study of siliciclastic sediments, Jhura Dome, Kachchh, Gujarat. *Jour. Geol. Soc. India*, v.65 (6), pp.703-714.
- Mishra, U.K. (1983): Palaeontological studies of Disang and Barail sediments in a part of Manipur East district. Geological Survey of India Unpublished Progress Report.
- Mishra, U K. (2016): A note on the reappraisal of Disang-Barail sediments of Manipur and Nagaland. In Srivastava, S. K. (Ed.), *Recent trends in earth science research with special reference to NE India. Today's and Tomorrow publisher, New Delhi*, pp137-143.
- Moiola, R.J. and Weiser, D. (1968): Textural parameter – an evaluation. *Jour. Sediment. Petrol.*, v.38, pp.45-53.

- Morad, S.; Bergan, M.; Knarud, R. and Nystuen, J.P. (1990): Albitization of detrital plagioclase in Triassic reservoir sandstones from the Snorre Field, Norwegian North Sea. *Jour. Sediment. Petrol.*, v.60, pp.411-425.
- Moss, A.J. (1972): Bed load sediments. *Sedimentology*, v.18, pp.159-219.
- Myrow, P.M. (1995): *Thalassinoides* and the enigma of Early Palaeozoic open-framework burrow systems. *Palaios*, v.10, pp.58–74.
- Naik, G.C. (1994): Subsurface Geology and Tectono-Sedimentary Evolution of Pre-Miocene Sediments of Upper Assam, India, *PhD thesis submitted to ISM, Dhanbad* (unpub).
- Naik, G.C. (1998): Tectonostratigraphic Evolution and Paleogeographic Reconstruction of NE India, *Proc. Indo-German Workshop on Border Strandology Magnetostratigraphy Pilot Project, Calcutta*.
- Naik, G.C.; Padhy, P.K. and Mishra, J. (1991): Hydrocarbon Exploration and Related Geo-Scientific Problems in Northeast India, *Proc. Regional Symposium on Hydrocarbon Deposits in Northeast India, Gauhati, Assam*, pp.175-195.
- Nandi, D.R. (2000): Tectonic evolution of North Eastern India and adjoining area with special emphasis on contemporary geodynamics. *Indian Jour. Geol.*, v.72(3), pp.175-195.
- Nandi, D.R. (2017): Geodynamics of Northeastern India and the Adjoining Region, Guwahati, India, *Scientific Book Centre*. 272p.
- Nichols, G. (2009): Sedimentology and Stratigraphy. *Wiley-Blackwell Publication.*, London, Second Edition.335 p.
- Okada, H. (1971): Classification of sandstone - analysis and proposal. *Jour. Geol.*, v.79, pp.509:525.
- Pandey, N. and Srivastava, S.K. (1998): A preliminary report on Disang-Barail Transition, NW of Kohima, Nagaland (Abst.), *Workshop on Geodynamics and Natural Resources of NE India, Dibrugarh*, p.24.
- Paranjape, A.R.; Kulkarni, K.G. and Gurav, S.S. (2013): Significance of *Lockeia* and associated trace fossils from the Bada Bagh Member, Jaisalmer Formation, Rajasthan. *Journal of Earth System Science*, v.122, pp.1359–1371.
- Passega, R. (1957): Textures as characteristics of clastic deposition. *Bull. Am. Assoc. Petrol. Geol.*, v.41, pp.1952-1984.
- Passega, R. (1964): Grain size representation by CM patterns as a geological tool. *Jour. Sediment. Petrol.*, v.34, pp.830-847.

- Passega, R. (1977): Significance of CM diagrams of sediments deposited by suspensions. *Sedimentology*, v.24, pp.723-733.
- Passega, R. and Benarjee, R. (1969): Grain size image of clastic deposits. *Sedimentology*, v.13, pp.233-252.
- Patel, S. J. and Desai, B. G. (2009): Animal-sediment relationship of the crustaceans and polychaetes in the intertidal zone around Mandvi, Gulf of Kachchh, Western India. *Jour. Geol. Soc. India*, v.74, pp.233–259
- Pemberton, S. G. and MacEachern, J. A. (1995): The sequence stratigraphy significance of trace fossils: examples from the Cretaceous foreland basin of Alberta, Canada. In: *Sequence Stratigraphy of Foreland Basin Deposits: Outcrop and Subsurface Examples from the Cretaceous of North America, Memoirs 64* (Eds. Van Wagoner J.C. and Bertram G.), American Association of Petroleum Geologists, Tulsa, Oklahoma. pp.429-475.
- Pemberton, S.G.; Spila, M.; Pulham, A.J.; Saunders, T.; Robbins, D. and Sinclair, I.K. (2001): Ichnology and Sedimentology of Shallow to Marginal Marine Systems, Calgary. *Geological Association of Canada, Short Course 15*. 343p.
- Pemberton, S.G.; Frey, R.W.; Ranger, M.J. and MacEachern, J.A. (1992): The conceptual framework of ichnology. In: Applications of Ichnology to Petroleum Exploration, a Core Workshop (SEPM Core Workshop) (Ed. S.G. Pemberton), *Society for Sedimentary Geology*, v.17, pp.1–28.
- Pettijohn, F.J. (1975): Sedimentary Rocks, 3<sup>rd</sup> edition, *Harper and Row*. 614p.
- Pettijohn, F.J.; Potter, P.E. and Siever, R. (1972): Sand and Sandstones, *Springer-Verlag*, New York, 617p.
- Pettijohn, F.J., Potter, P.E. and Siever, R. (1973): Sand and Sandstones. *Springer Verlag*, New York, 617p.
- Pettijohn, F.J.; Potter, P.E. and Siever, R. (1987): Sand and Sandstone. 2<sup>nd</sup> Edition, *Springer-Verlag*, New York, 553 p.
- Pitman, E.D. (1972): Diagenesis of quartz in sandstone as revealed by SEM. *Jour. Sed. Petrol.*, v.42, pp.507-519.
- Potter, P.E. and Pettijohn, F.J. (1977): Palaeocurrents and Basin Analysis, *Springer- Verlag, New York*. 425p.
- Potter, P.E. (1978a): Significance and origin of big rivers. *Jour. Geol.*, v.86, pp.13-33.
- Potter, P.E. (1978b): Petrology and chemistry of modern big rivers. *Jour. Geol.*, v.86, pp.423-449.

- Prothero, R.D. and Schwab, F. (2004): *Sedimentary Geology: An Introduction to Sedimentary Rocks and Stratigraphy*, 2<sup>nd</sup> edition, *W.H. Freeman and Company, New York*. 557p.
- Quatrefages, M. A. DE (1849): Note Sur la *Scolicia prisca* (A. Deq.), annelid fossil de la craie. *Ann. Sci. Nat. Ser. 3 Zoologie.*, v.12, pp. 265-266.
- RangaRao, A. (1983): Geology and hydrocarbon potential of a part of Assam-Arakan Basin and its adjacent region. *Petroleum Asia Jour.*, pp.127-158.
- RangaRao, A. (1986): North-West Himalayan Foothills: Its Stratigraphical Record and Tectonic Phases. *Bulletin ONGC*, v.23, pp.107-128
- Reading, H.G. (1978): *Sedimentary Environment and Facies*, Elsevier, North Holland, New York. 464p.
- Reading, H.G. (1986): *Sedimentary Environment and Facies*, Elsevier, North Holland, New York. 464p.
- Reading, H. G. (1991): The classification of deep-sea depositional systems by sediment calibre and feeder systems. *Quarterly Jour. of the Geological Soc. of London*, v.148, pp.427-430.
- Reading H.G. and Levell, B. K. (1996): Controls on the sedimentary record. In: Reading, H. G. (ed) *Sedimentary Environments: Processes, Facies and Stratigraphy*. 3<sup>rd</sup> edition. *Blackwell Science Oxford*, pp.5-35
- Reineck, H.E. and Singh, I.B. (1980): *Depositional Sedimentary Environments*. Springer-Verlag, New York. 547p.
- Reith, A. (1932): Neue Fundespongeliomorpher Fucoiden aus dem Jura Schwabens. *Geologische und Palaeontologische Abhandlungen*, v.19, pp.257–294.
- Roser, B.P. and Korsch, R.J. (1986): Determination of tectonic setting of sandstone-mudstone suites using SiO<sub>2</sub> content and Na<sub>2</sub>O/K<sub>2</sub>O ratio. *Jour. Geol.*, v.49, pp.635-650.
- Sagoe, K.O. and Visser, G.S. (1977): Population breaks in grain size distribution of sand– a theoretical model. *Jour. Sediment. Petrol.*, v.47, pp.285-310.
- Sahu, B.K. (1964): Depositional mechanism from size analysis of clastic sediments. *Jour. Sediment. Petrol.*, v.34, pp.73-83.
- Sahu, B.K. (1983): Multigroup discrimination of depositional environments using size discrimination statistics. *Ind. Jour. Earth Sci.*, v.10, pp.20-29.
- Sarmah, R. N. (1989): Clay minerals in Disang–Barail groups of sediments from Kohima, Nagaland. *Bull. Ind. Geol. Assoc.*, v.22, pp.107–111.

- Savrda, C.E. and Bottjer, D.J. (1986): Trace-fossil model for reconstruction of palaeo-oxygenation in bottom waters. *Geology*, v.14, pp.3–6.
- Schlirf, M. (2003): Palaeocological significance of Late Jurassic trace fossils from the Boulonnais, France. *Acta Geologica Polonica*, v.53, pp.123–142.
- Schwab, F.L. (1975): Framework mineralogy and chemical composition of continental margin-type sandstone. *Geology*, v.3, pp.487-490.
- Seilacher, A. (1967): Bathymetry of trace fossils. *Marine Geology*, v.5, pp.413-428.
- Sielacher, A. (1990): Paleozoic trace fossils. In: R. Said (Ed.), *The Geology of Egypt*. Rotterdam (A. A. Balkeman), pp.649-670.
- Selley, R.C. (1968): A classification of palaeocurrent models. *Jour. Geol.*, v.76, pp.349-368.
- Selley, R.C. (1970): *Ancient Sedimentary Environments*, Chapman and Hall, London. 273p.
- Selley, R.C. (1976): Subsurface environmental analysis of North Sea sediments. *Bull.Am. Assoc. Petrol. Geol.*, v.60, pp.184-195.
- Sema, L. and Pandey, N. (2016): Model composition and tectonic provenance of Palaeogene Disang-Barail Transitional sediments in parts of Kohima Synclinorium, Nagaland, India. In: *Recent Trends in Earth Science Research with Special Reference to NE India* (Ed. S.K. Srivastava), Today and Tomorrow's Printers and Publishers, New Delhi, India, pp.89-108.
- Sema, L. (2003): Lithofacies Analysis and Depositional Environment of the Palaeogene Sediments, South of Kohima Town, Ph.D thesis submitted to Nagaland University, Kohima (*unpub*). 96p.
- Sengupta, S.M. (1982): Interpretation of log probability graphs of grain sizes in the light of experimental studies (Abst.), *11th International Congress on Sedimentology*, Hamilton, 81p.
- Sengupta, S.M. (1994): *Introduction to Sedimentology*, Oxford and IBH Publishing Co. 314p.
- Sevon, W.D. (1966): Distinction of New Zealand beach, dune and river sands by their grain size distribution characteristics, New Zealand. *Jour. Geol. and Geophys.*, v.19, pp.212- 223.
- Selley, R.C. (2000): *Applied Sedimentology*, 2<sup>nd</sup> edition, Academic Press, New York, NY. 523p.
- Seilacher, A. (1990): Paleozoic trace fossils. In: Said R (ed) *The Geology of Egypt*. Balkema, Rotterdam, pp. 649-670.
- Singh, B.P. and Srivastava, A.K. (2011): Storm activities during the sedimentation of late Palaeocene-middle Eocene Subathu Formation, western Himalayan foreland basin, N. India. *Jour. Geol. Soc. India*, v.77, pp.130–136.



- Singh, B.P.; Pawar, J.S. and Karlupia, S.K. (2004): Dense mineral data from the north western Himalayas foreland sedimentary rocks and recent sediments - evaluation of the hinterland. *Jour. Asian Earth Sci.*, v.23, pp.23-25.
- Singh, R.H.; Rodriguez-Tovar, F.J. and Ibotombi, S. (2008): Trace fossils of the Upper Eocene-Lower Oligocene Transition of the Manipur, Indo-Myanmar ranges (North-east India). *Turkish Journal of Earth Sciences*, v.17, pp.821–834.
- Skilbeck, C. G. and Cawood, P. A. (1994): Provenance history of a Carboniferous Gondwana margin forearc basin, New England Fold Belt, eastern Australia: modal and geochemical constraints. *Sedimentary Geology*. Issues 1–2, v.93, pp.107-133.
- Smith, R. (1966): Grain size measurement in thin section and in grain mount, *Jour. Sediment. Petrol.*, v.36, pp.841-843.
- Srivastava, S.K. and Pandey, N. (2001): Palaeoenvironmental reconstruction of Palaeogene Disang-Barail Transitional Sequences, NW of Kohima, Nagaland, NE India (Abst.), *Seminar on Contribution to Himalayan Geology, Dehra Dun*, p.7.
- Srivastava, S.K. (2002): Facies Architecture and Depositional Model for Palaeogene Disang-Barail Transition, North West of Kohima, Nagaland, *Ph.D thesis submitted to Nagaland University, Kohima (unpub)*.
- Srivastava, S.K.; Pandey, N. and Srivastava, V. (2004): Tectono-sedimentary evolution of Disang-Barail Transition, NW of Kohima, Nagaland, India. *Himalayan Geology*, v.25(2), pp.121-128.
- Srivastava, S.K. and Pandey, N. (2005): Depositional mechanism of Palaeogene sediments at Disang-Barail Transition, NW of Kohima, Nagaland, India. *Jour. Pal. Soc. India*, v.50(1), pp.135-140.
- Srivastava, S.K. and Pandey, N. (2008): Palaeoenvironmental reconstruction of Disang- Barail Transition using grain size parameters in Nagaland. *Nagaland Univ. Res. Jour.*, v.5, pp.164-176.
- Srivastava, S.K. and Pandey, N. (2011): Search for provenance of Oligocene Barail sandstones in and around Jotsoma, Kohima, Nagaland. *Jour. Geol. Soc. India*, v.77, pp.433-442.
- Srivastava, S.K.; Liba, B. and Chuzo, V. (2017): Lithofacies analysis of the Palaeogene sediments in parts of Kohima Synclinorium, Nagaland, India: implications for the depositional environment. *Him. Geol.*, v.38(1), pp.30-37.
- Srivastava, S.K. and Kesen, K. (2018): Tectonic-sedimentary evolution of Laisong sandstones exposed in and around Pherima, Dimapur, Nagaland. *Jour. Applied Geochem.*, v.19(4), pp.471-479.

- Srivastava, S.K.; Laskar, J.; Kreditsu, V. and Awomi, L. (2018): Petrography and major element geochemistry of Palaeogene sandstones, south of Kohima town, Nagaland. *Jour. Applied Geochem.*, v.20(1), pp.41-49.
- Srivastava, S.K. and Kichu, A.M. (2021): Mineral assemblages and tectono-provenance of the Oligocene Barail sandstones in parts of Naga Hills of the Assam-Arakan Orogenic Belt, North-east India. *Geol. Jour.*, v.57(2), pp.801-817.
- Stauffer, P.H. (1966): Thin section size analysis – a further note. *Sedimentology*, v.7, pp.261- 263.
- Stewart, H.B. Jr. (1958): Sedimentary reflections of depositional environments in San Miguel Lagoon, Baja California, Mexico. *Amer. Assoc. Petrol. Geol. Bull.*, v.2, pp.2567-2618.
- Suczek, C.A. and Ingersoll, R.V. (1985): Petrology and provenance of Cenozoic sandform in the Indus Cone and Arabian Basin (DSDP sites 221, 222, 224). *Jour. Sed. Petrol.*, v.55, pp.340-346.
- Sudan, C.S.; Singh, B.P. and Sharma, U.K. (2002): Ichnofacies of the Murree Group in Jammu area and their ecological implications during late Palaeogene in the NW Himalaya. *Jour. Geol. Soc. India*, v.60, pp.547–557.
- Surdam, R.C. and Boles, R.J. (1979): Diagenesis of Volcanic Sandstones (*Eds. P.A. Scholle and P.R. Schluger*).
- Surdam, R.C.; Crosse, L.J.; Hagen, E.S. and Heasler, H.P. (1989): Organic inorganic interactions and sandstone diagenesis. *Amer. Asso. Petrol. Geol. Bull.*, v.73, pp.1-23.
- Suttner, L.J. (1974): Sedimentary petrographic provinces. In: *Paleogeographic Provinces and Provinciality* (*Ed. C.A. Ross*), *Society for Sedimentary Geology, Tulsa*, pp.75-84.
- Suttner, L.J.; Basu, A. and Mack, G.H. (1981): Climate and the origin of quartz arenites. *Jour. Sed. Petrol.*, v.51, pp.1235-1246.
- Suttner, L.J. and Dutta, P.K. (1986): Alluvial sandstone composition and palaeoclimate framework mineralogy. *Jour. Sed. Petrol.*, v.56, pp.329-345.
- Swan, D.; Clague, J.J and Luternauer, L.J. (1978): Grain size statistics II - Evaluation of grouped moment measures. *Jour. Sed. Pet.*, v.49(2), pp.487-500.
- Swift, D.J.P. (1969): Inner shelf sedimentation: processes and products. In: *The New Concepts of Continental Margin Sedimentation - Application to the Geological Records* (*Ed. D.J. Stanley*), *Am. Geol. Instt., Washington*, pp.DS.5-1.
- Swift, D.J.P.; Stanley, D.J. and Curray, J.R. (1971): Relict sediments on continental shelf - a reconsideration. *Jour. Geol.*, v.79, pp.322-346.

- Tanner, W.F. (1964): Modification of sediment size distributions. *Jour. Sediment. Petrol.*, v.34, pp.156-164.
- Tchoumatchenco, P. and Uchman, A. (2001): The oldest deep-sea Ophiomorpha and Scolicia and associated trace fossils from the Upper Jurassic–Lower Cretaceous deep-water turbidite deposits of SW Bulgaria. *Palaeogeography, Palaeoclimatology, Palaeoecology*, v.169, pp.85–99.
- Textoris, D.A. (1971): Grain size measurement in thin section. In: *Procedures in Sedimentary Petrology* (Ed. R.E. Craver), Wiley, New York, pp.95-108.
- Thong, G.T. (1993): Sedimentological Studies of the Palaeogene Sandstones Around Botsa, Kohima District, Nagaland. *Ph.D. thesis submitted to North Eastern Hill University (unpub)*.
- Thong, G.T. (2001): Clay minerals in the Disang sediments of Botsa, Kohima District, Nagaland. *Bulletin of Pure & Applied Sciences*, v.20, pp.67–70.
- Thong, G.T. and Rao, B.V. (2006): Geochemical investigations of the Disang sandstones of Botsa, Nagaland, NE India. *Jour. Geol. Soc. India*, v.68, pp.715–722.
- Tiwari, R.P.; Rajkonwar, C.; Lalchawimawii; Malsawma, P.L.J.; Ralte, V.Z. and Patel, S.J. (2011): Trace fossils from Bhuban Formation, Surma Group (Lower to Middle Miocene) of Mizoram, India and their palaeoenvironmental significance. *Jour. Earth Syst. Sci.*, v.120, pp.1127–1143.
- Torell, O.M. (1870): Suecana Formations, Cambridge. *Lunds University Arsskr.*, v.2, pp.1–14.
- Tortosa, A.; Palomares, M. and Arribas, J. (1991): Quartz grain types in Holocene deposits from the Spanish central system - some problems in provenance and analysis. In: *Developments in Sedimentary Studies* (Eds. A.C. Morton, S.P. Todd and P.D.W. Haughton), *Geol. Soc. Amer. Special Pub., Bath, UK*, v.57, pp.447-454.
- Towe, K.M. (1962): Clay mineral diagenesis as a possible source of silica cement in sedimentary rocks. *Jour. Sediment. Petrol.*, v.32, pp.26-28.
- Tucker, R.W. and Vacher, H.L. (1980): Effectiveness of discriminating beach, dune and river sands by moments and the cumulative weight percentages. *Jour. Sed. Pet.*, v.50, pp.165-172.
- Tucker, R.W. (1989): *Techniques in Sedimentology*. Blackwell Scientific Publications, Oxford, London.
- Tucker, R.W. (1993): Carbonate diagenesis and sequence stratigraphy. In: *Sedimentology Review* (Ed. W.P. Wright), v.1, pp.51-72.
- Uchman, A. (1998): Taxonomy and ethology of flysch trace fossils: a revision of the Marian Książkiewicz collection and studies of complementary material. *Annales. Societatis Geologorum Poloniae*, v.68, pp.105–218.

- Uchman, A. and GaŹdzicki, A. (2006): New trace fossils from the La Meseta Formation (Eocene) of Seymour Island, Antarctica. *Polish Polar Research*, v.27, pp.153–170.
- Uddin, A. and Lundberg, N. (1998a): Unroofing history of the Eastern Himalayas and the Indo-Burman Ranges: heavy mineral study of the Cenozoic sediments from the Bengal Basin, Bangladesh. *Jour. Sediment. Research*, v.68(3), pp.465-472.
- Uddin, A. and Lundberg, N. (1998b): Cenozoic history of Himalayan-Bengal system: Bangladesh. *Bull. Geol. Soc. Amer.*, v.110(4), pp.497-511.
- Uddin, A., Kumar, P. and Sarma, J.N. (2007): Early orogenic history of the Eastern Himalayas: Compositional studies on Palaeogene Sandstones from Assam, North-East India. *International Geology Review*, v.49, pp.798-810.
- Vineetha, P. R.; Thong, G. T and Aier, I. (2008): Identification, distribution, and significance of clay minerals in the Disang shale of Kohima, Nagaland. In: Proceedings of the National Seminar on Geology & Energy Resources of NE India: Progress and Perspectives. *Nagaland University Research Journal, Special Publication*, pp.24-32
- Visher, G.S. (1965): Fluvial processes as interpreted from ancient and recent fluvial deposits. In: *Primary Sedimentary Structures and Their Hydrodynamic Interpretation* (Ed. G.V. Middleton), *Soc. Econ. Palaeont. Mineral Sp. Pub.*, v.12, pp.265.
- Visher, G.S. (1969): Grain size distribution and depositional processes. *Jour. Sed. Pet.*, v.39(3), pp.1074-1106.
- Visher, G.S. (1970): Fluvial processes as interpreted from ancient and recent fluvial deposits. *Soc. Econ. Palaeont. Mineralogy Sp. Pub.*, v.12, pp.116-132.
- Walker, R. and James, N. (1992): Facies Models: Response to Sea Level Change. *Geol. Asso. Canada*. 407p.
- Walker, T.R. (1974): Formation of red beds in moist tropical climate - a hypothesis. *Geol. Soc. Amer. Bull.*, v.85, pp.633-638.
- Walker, T. R. (1984): Diagenetic albitization of potassium feldspars in arkosic sandstones. *Journal of Sedimentary Petrology*, v.54, pp.3-16.
- Walther, J. (1894): Einleitung in die Geologic Alshistosische Wisenschaft, *Jena Verlag Von Gustav Fischer*, v.3, 1055p.
- Walton, E.K.; Stephens, W.E. and Shawa, M.S. (1980): Reading segmented grain-size curves. *Geol. Mag.*, v.117, pp.517-524.

- Weller, S. (1899): Kinderhook faunal studies: the fauna of the vermicular sandstone of the Northview, Webster County, Missouri, *Transactions of the Academy of Science of St. Louis*, v.9, pp.9-51.
- Wentworth, C.K. (1922): A scale of grade and class terms for sediments. *Jour. Geol.*, v.30, pp.377-392.
- Zuffa, G.G. (1980): Hybrid arenites: their composition and classification. *Jour. Sedimentary Research*, v.50(1), pp.21-29.

## Document Information

Analyzed document	CHAPTERS_FOR_PLAG.docx (D144250030)
Submitted	2022-09-17 08:06:00
Submitted by	S K Srivastava
Submitter email	sksrivastava@nagalanduniversity.ac.in
Similarity	6%
Analysis address	sksrivastava.naga@analysis.arkund.com

## Sources included in the report

SA	<b>Assam University, Silchar / Pandey_Nag.pdf</b> Document Pandey_Nag.pdf (D47611140) Submitted by: arun2929@gmail.com Receiver: arun2929.aus@analysis.arkund.com	8
SA	<b>Assam University, Silchar / Thesis Final C.pdf</b> Document Thesis Final C.pdf (D47313681) Submitted by: profnpandey@gmail.com Receiver: apurbajyoti.aus@analysis.arkund.com	12
W	URL: <a href="https://www.researchgate.net/publication/354408286_Disang_and_Barail_Sediments_their_Contact_and_Palaeodepositional_Environment_along_Tuli-Merangkong-Mokokchung_Area_of_Mokokchung_District_Nagaland_North_East_India_with_Reference_to_Diverse_Palynofoss">https://www.researchgate.net/publication/354408286_Disang_and_Barail_Sediments_their_Contact_and_Palaeodepositional_Environment_along_Tuli-Merangkong-Mokokchung_Area_of_Mokokchung_District_Nagaland_North_East_India_with_Reference_to_Diverse_Palynofoss</a> Fetched: 2022-05-01 11:58:37	2
W	URL: <a href="https://www.kohima.nagalanduniversity.ac.in/geo_pub">https://www.kohima.nagalanduniversity.ac.in/geo_pub</a> Fetched: 2022-05-01 11:30:32	1
SA	<b>Nagaland University, Kohima / Palaeoenvironmental Significance of Trace fossils from the Palaeogene sediment1.docx</b> Document Palaeoenvironmental Significance of Trace fossils from the Palaeogene sediment1.docx (D72956212) Submitted by: sksrivastava@nagalanduniversity.ac.in Receiver: sksrivastava.naga@analysis.arkund.com	2
SA	<b>Assam University, Silchar / THESIS.pdf</b> Document THESIS.pdf (D50118322) Submitted by: apurbajyoti@gmail.com Receiver: apurbajyoti.aus@analysis.arkund.com	16
SA	<b>Dibrugarh University, Dibrugarh / PhD Thesis Manash Pratim Gogoi Dibrugarh University.docx</b> Document PhD Thesis_Manash Pratim Gogoi_Dibrugarh University.docx (D131254905) Submitted by: pradipborgohain@dibru.ac.in Receiver: pradipborgohain.dibru@analysis.arkund.com	5
J	<b>08_chapter_2.pdf</b> URL: 21a1ebb5-511c-4c6a-aaef-969b525b264d Fetched: 2022-08-20 09:51:36	2
SA	<b>Gujarat University, Ahmedabad / Rahul G. Gayakvad Ch-06.pdf</b> Document Rahul G. Gayakvad Ch-06.pdf (D113229934) Submitted by: antiplagcheck@yahoo.com Receiver: antiplagcheck.gujuni@analysis.arkund.com	1
SA	<b>Assam University, Silchar / Thesis-Meghali.pdf</b> Document Thesis-Meghali.pdf (D64713687) Submitted by: profnpandey@gmail.com Receiver: profnpandey.aus@analysis.arkund.com	6
W	URL: <a href="https://www.researchgate.net/publication/330967402_Trace_fossils_from_oligocene_barail_sediments_in_and_around_jotsoma_Kohima_Nagaland">https://www.researchgate.net/publication/330967402_Trace_fossils_from_oligocene_barail_sediments_in_and_around_jotsoma_Kohima_Nagaland</a> Fetched: 2021-09-23 08:49:21	1
SA	<b>Assam University, Silchar / thesis 1-8.pdf</b> Document thesis 1-8.pdf (D50445626) Submitted by: profnpandey@gmail.com Receiver: kalloltalukdar.aus@analysis.arkund.com	2
J	<b>16_published_papers.pdf</b> URL: dabad141-fd50-4ca7-b905-344d9e9751f8 Fetched: 2022-08-20 09:51:44	1
SA	<b>University of Delhi, New Delhi / Lakshmirani Devi Thesis.pdf</b> Document Lakshmirani Devi Thesis.pdf (D123743472) Submitted by: saburisahni@yahoo.co.in Receiver: saburisahni.du@analysis.arkund.com	1

## Entire Document